Investigation of the IcsA-mediated *Shigella flexneri* hyper-adherence

Jilong Qin

M.Sc. (Biotechnology) (Adelaide)

M.Sc. (Biotechnology) (Canberra)

B.Eng. (Bioengineering) (Chengdu)

THE UNIVERSITY of ADELAIDE

Submitted for the Degree of Doctor of Philosophy

Research Centre of Infectious Diseases

Department of Molecular and Biomedical Sciences

School of Biological Sciences

The University of Adelaide

Adelaide, South Australia, Australia

March 2020

Declaration

I certify that this work contains no material which has been accepted for the award of any other degree or diploma in my name in any university or other tertiary institution and, to the best of my knowledge and belief, contains no material previously published or written by another person, except where due reference has been made in the text. In addition, I certify that no part of this work will, in the future, be used in a submission in my name for any other degree or diploma in any university or other tertiary institution without the prior approval of the University of Adelaide and where applicable, any partner institution responsible for the joint award of this degree.

The author acknowledges that copyright of published works contained within this thesis resides with the copyright holder(s) of those works.

I give permission for the digital version of my thesis to be made available on the web, via the University's digital research repository, the Library Search and also through web search engines, unless permission has been granted by the University to restrict access for a period of time.

I acknowledge the support I have received for my research through the provision of an Australian Government Research Training Program Scholarship.

Jilong Qin

November 2019

Abstract

Shigella species cause bacillary dysentery, especially among young individuals. Shigellae target the human colon for invasion; however, the initial adhesion mechanism is poorly understood. The *Shigella* surface localised protein IcsA, in addition to its role in actin-based motility (ABM) intracellularly, acts as a host cell adhesin through unknown mechanism(s). In this thesis, the role of IcsA in cell adherence was confirmed by using purified $IcsA^{53\text{-}740}$ protein to show blocking of *Shigella* adherence and direct binding to host cells. A specific region (residues 138 to 148) in IcsA's functional domain was found to be required for the IcsA mediated adherence, but not for polar localisation and actin-based motility. The purified mutant protein $IcsA^{53\text{-}740(\Delta 138\text{-}148)}$ was found to no longer block *S. flexneri* adherence and had reduced ability to interact with host molecules. Additionally, *S. flexneri* expressing $IcsA^{\Delta 138\text{-}148}$ was found with significant defect in both cell adhesion and invasion. This may provide useful information for designing therapeutics for *Shigella* infection. The conformational change of IcsA's functional domain which is associated with its adhesin activity was also explored. Through limited proteolysis assay, it was found that the $IcsA^{\Delta 138\text{-}148}$ was unable to adapt the conformation associated with the hyper-adherent phenotype. The purified IcsA passenger domain was found to have an intramolecular interaction which might be a consequence of IcsA's conformational change. Identification of HeLa cell receptors for IcsA was also attempted. Mass spec data found that non-muscle myosin heavy chain IIA and IIB might be the potential host binding partners for IcsA. Using a myosin IIA deficient cell line COS-7, *S. flexneri* was still found to be hyper-adherent, and the use of the anti-myosin IIA antibody also failed to reduce *Shigella* adherence. Far Western blotting indicated that myosin IIA is the only one of several IcsA interacting molecule. The DOC induced hyper-adherence of *S. flexneri* was also characterised. It was found that DOC triggers the release of IpaD into culture supernatant and promotes the IcsA self-association activity that might be responsible for the IcsA-dependent biofilm formation. Overall, this work provides further clues and expands our understanding of the adhesin function of IcsA, the potential molecular mechanism of IcsA's conformational change, and the potential receptor for the *Shigella* adhesion mediated by IcsA.

Acknowledgements

Foremost, I would like to acknowledge my supervisor Associated Professor Renato Morona. Thank you for believing in me and taking me as a PhD student in your laboratory. You have taught me a lot in both bacteriology and English. I appreciate your lenience on mistakes that I have made during my PhD and your wisdom in helping me to fix them. You have shaped me on the way of thinking as a genuine scientist, which always stimulates my enthusiasm towards sciences. I particularly thank you for spending your valuable time during my manuscript and thesis writing, and your critical comments on them which, in my point of view, improved the quality of my work significantly.

I would also like to acknowledge the University of Adelaide for providing me with an international scholarship from the beginning of PhD candidature.

I thank all the past and present Morona lab members including Dr. Elizabath Tran, Dr. Matthew Doyle, Dr. Min Teh, Dr. Zuleeza Ahmad, Dr. Alistair Standish, Mr. Vincenzo Leo and Mr. Nicholas Maczuga. Thank you all for being together with me during my candidature here in Adelaide, Australia. Especially Liz for teaching, demonstrating and sharing the techniques, methods, ticks and tips with me. I also thank Matt on the preliminary work he did on the development of the IcsA purification protocol prior to the beginning of my PhD, which gives my project an opportunity to develop. I would also like to acknowledge my PhD buddies Zuza, Chenzleo and Polazn for building a scientific environment in our writing area.

I thank the lab members from McDevitt Lab, especially Dr. Victoria Pederick in teaching me the techniques in protein purification and characterisation. I also thank Ms. Erin Brazel in helping me on protein work, and Tim from McColl's lab in demonstrating FACS techniques.

I thank Dr. Antonio Focareta for introducing me to my supervisor Ren, without your reference, I would never join a fantastic lab like this.

I also thank my life partner, soul mate and lovely wife, Yue, in supporting me pursuing a PhD degree both financially and physically. We have all experienced hard times in our lives, but I feel the most fortunate to have you fighting aside me.

Lastly but not the least, I thank my mum and dad in supporting me unconditionally, as always. I know I would not achieve anything without your endless love and support. You all have been doing excellent in parenting and I feel the luckiest to be your son. I also thank my sister for taking care of my parents during my studying overseas, this means a lot to me and I would never pay off the debts that I owe you.

Thesis Style and Layout

This thesis is submitted in the style of a “Combination of conventional and publication formats”. As such, the result chapters were prepared in the format of both publications (Chapter 4&5) and traditional results chapter (Chapter 6&7). In Chapter 1, the studies and research in the field of this work was summarised and research gaps were identified as aims for studying in this work. In Chapter 2, methods and materials used in this work were outlined in detail.

As for publication purposes, Chapter 4 and 5 were presented as per the requirement of the journal, which included all the information that will be submitted for publication. Author contributions for each publication are stated in the Statement of Authorship section. For Chapter 6 and 7, methods and materials used are outlined in Chapter 2 and are cross-referenced. Each result chapter has a discussion section to explore the underlying meaning of the work. Chapter 7 draws conclusions of the outcomes and significance of this study, and points out the future research directions.

Abbreviations

~	approximately
%	percentage
×g	times g force
°C	Celsius degree
aa	amino acid
ABM	actin-based motility
Amp	ampicillin
Arp2/3	actin related protein 2/3
BAM	barrel assembly machinery
bp	base pairs
BSA	bovine serum albumin
Cml	chloramphenicol
co-IP	co-immunoprecipitation
C-terminal	carboxyl terminal
DMEM	Dulbecco's modified eagle medium
DNA	deoxyribonucleic acid
dNTP	deoxynucleoside triphosphate
DOC	deoxycholate
DSP	dithiobis[succinimidylpropionate]
DTT	dithiothreitol
EDTA	ethylene diamine tetra-acetic acid
FAE	follicular associated epithelium
FCS	fetal calf serum
FLAG	DYKDDDK peptide sequence
FRT	FLP recognition target
GST	glutathione S-transferase
h; min; s	hour(s); minute(s); second(s)
His_6	histamine×6 tag
hNE	human neutrophil elastase
i	insertion site
IFN-γ	gamma interferon
IL	interleukin
IM	inner membrane
Ipa	Invasion plasmid antigens
IPTG	isopropyl-β-D-thiogalactopyranoside
Kan	kanamycin
kb	kilobase pairs
kDa	kiloDaltons
L	litres
LB	Lysogeny Broth

LPS	lipopolysaccharide
M; mM	molar; millimolar
mA	milli-amps
mAb	monoclonal antibody
M-cell	membranous epithelial cells
MEM	modified eagles medium
mg; ml; mm	milligram(s); millilitre(s); millimetre(s)
MQ	MilliQ
MW	molecular weight
MWCO	molecular weight cut off
Ni	nickel
N-terminal	amino terminal
N-WASP	neural Wiskott-Aldrich syndrome protein
Oag	O-antigen
OD_{600}	optical density of 600 nm
OM	outer membrane
pAbs	polyclonal antibodies
PBS	phosphate buffered saline
PCR	polymerase chain reaction
PMBN	polymyxin B nanopeptide
PMN	polymorphonuclear
PMSF	phenylmethanesulfonylfluoride
PP	periplasm
R	resistance
RBS	ribosomal binding site
Rha	rhamnose
RT	room temperature
S/N; Sup	supernatant
SDS	sodium dodecyl sulphate
SDS-PAGE	SDS polyacrylamide gel electrophoresis
SEM	standard error mean
Sm	streptomycin
Sp	spectinomycin
ss	signal sequence
T3SS	type three secretion system
TBE	tris-borate-EDTA
TBS	tris buffered saline
TCA	trichloroacetic acid
Tet	tetracycline
Tris	tris (hydroxymethyl) aminomethane
U	units
Und-PP	undecaprenyl pyrophosphate
UV	ultraviolet

V	volt(s)
v/v	volume per volume
VP	virulence plasmid
w/v	weight per volume
WCL	whole cell lysate
WM	whole membrane
WT	wild type
X-Gal	5'-bromo-4-chloro-3-indolyl-β-D-galactopyranoside
β-ME	β-mercaptoethanol
Δ	deletion
µg; µl; µM	microgram(s); microliter(s); micromolar(s)

Contents

Chapter One

INTRODUCTION

Chapter 1: Introduction

1.1. *Shigella*

Shigella are the causative agents for bacterial dysentery or shigellosis in humans worldwide. This disease often manifests with symptoms including severe abdominal pain, fever, bloody and mucoid stools and watery diarrhea that results from intestinal dysfunction (Butler *et al.*, 1986). Due to the low infectious dose of *Shigella*, which is as few as 10 organisms (Bennish, 1991), they are relatively easy to transmit either person to person or directly via contaminated food and water. *Shigella* alone accounted for over 200,000 deaths in 2016 and was the second leading cause of diarrheal mortality (Khalil *et al.*, 2018). Although shigellosis is typically mild and self-limited for older adults, in children under 5 years of age (Kotloff *et al.*, 2013) and malnourished and immunocompromised people, infections can be more frequent and severe, such as in the case of HIV-coinfection (Lam & Bunce, 2015).

Shigella are Gram-negative, non-motile bacteria belonging to the family of *Enterobacteriacae* and are genetically related to enteroinvasive *E. coli* (EIEC) (Van den Beld & Reubsaet, 2012, Zuo *et al.*, 2013, Ud-Din & Wahid, 2014). This genus comprises four species (serogroups), namely *S. dysenteriae* (A), *S. flexneri* (B), *S. boydii* (C) and *S. sonnei* (D) (Niyogi, 2005). These four species can be further divided into serotypes according to their lipopolysaccharides (LPS) structure (Levine *et al.*, 2007). In *Shigella* species, virulence is conferred by multiple factors encoded by a ~200 kb virulence plasmid (VP), which is essential for infection initiation and invasion (Sansonetti, 2001, Schroeder & Hilbi, 2008).

S. flexneri 2a is the most frequently isolated serotype among all the *Shigella* species worldwide (Levine *et al.*, 2007). However, it is being replaced by *S. sonnei* in many western countries (Holt *et al.*, 2013, Qiu *et al.*, 2015). The current treatment for shigellosis relies on rehydration therapy and antibiotics, however multiple antibiotic resistance has emerged in *Shigella* species (Barry *et al.*, 2013, Khaghani *et al.*, 2014, Qu *et al.*, 2014, Cui *et al.*, 2015), making the development of an effective vaccine more important. Despite many vaccine candidates being under assessment to different degrees (Mani *et al.*, 2016), there is no vaccine available to protect from infection. Due to the serotype-specific immunity

(DeLaine *et al.*, 2016) acquired after *Shigella* infection (Rasolofo-Razanamparany *et al.*, 2001), vaccines that are made using a single attenuated live strain only protect from homologous *Shigella* serotypes (Ferreccio *et al.*, 1991). Together with the issue of side effects, low efficacy, and lack of suitable animal models, this has made vaccine development problematic. To design novel treatments and preventions of *Shigella* infection, it is crucial to understand the nature of *Shigella* pathogenesis.

1.2. Pathogenesis

Humans (Speelman *et al.*, 1984, Anand *et al.*, 1986) and rhesus monkeys (Good *et al.*, 1969) are the only two natural reservoirs of *Shigella*. In studies on human patients (Speelman *et al.*, 1984, Anand *et al.*, 1986) and healthy volunteers (Levine *et al.*, 1973), lesions were found exclusively in the colon with the increased severity towards the distal direction and the most severe damage in the rectosigmoid area (Speelman *et al.*, 1984). *Shigella* infection lesions found in these studies were: cell infiltration of the mucosa area by lymphocytes, disorganisation of crypts, goblet cell depletion, micro-ulcers and flattened surfaces in epithelial layers (Levine *et al.*, 1973, Anand *et al.*, 1986, Mathan & Mathan, 1986). These features are similar to those described in *Shigella* infections in monkeys (Formal *et al.*, 1966, Takeuchi *et al.*, 1975, Takeuchi, 1982) where lesions were reported in the colon while not in the small intestine. It was also found that apart from the mucosal invasions found in colon which result in dysentery, the small intestine, specifically jejunum, was also impaired resulting in diarrhea symptoms but with little or no invasion (Rout *et al.*, 1975). This impaired secretion by the jejunum is due to the release of ShET enterotoxins by *Shigella* in the small intestine (Levine *et al.*, 2007). Little has been known for the species specificity of *Shigella*, yet as *Shigella* preferably invade the colon rather than the small intestine, it is therefore important to distinguish the differences between the colon and the small intestine (Figure 1.1).

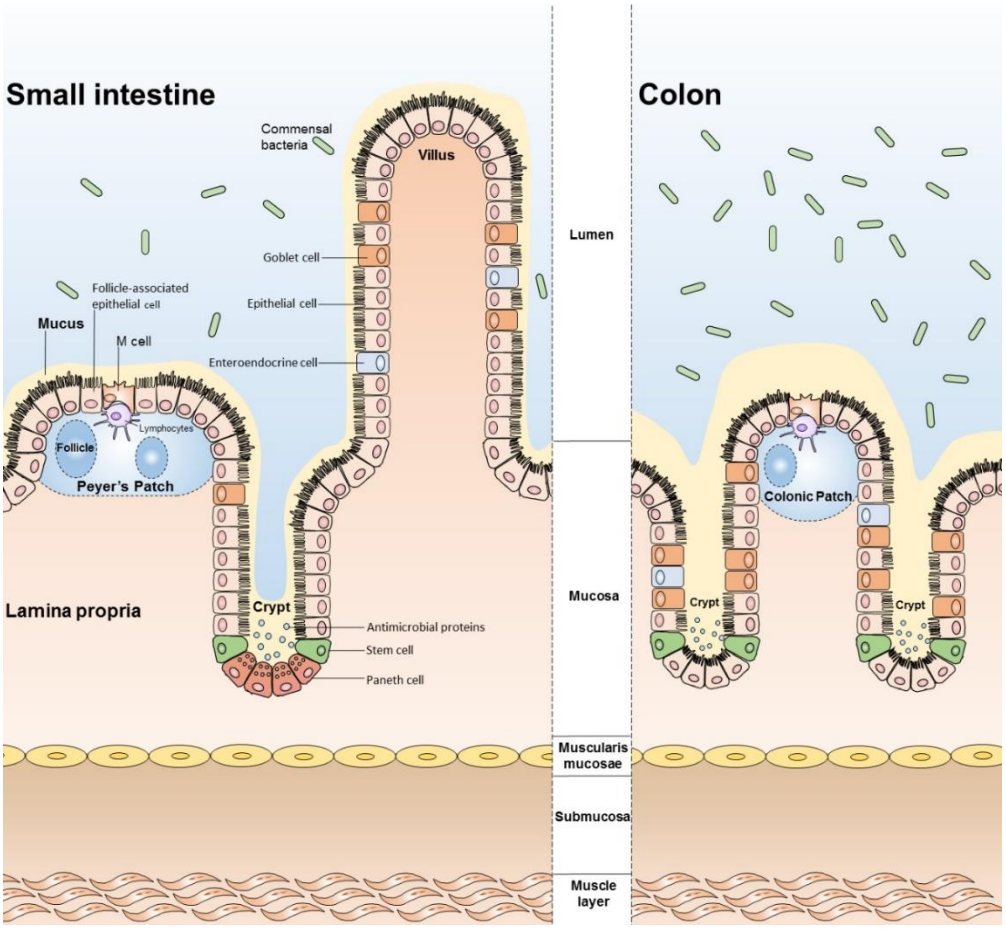

Figure 1.1. Atonamy of intestinal mucosa

Small intestine and colon have distinct structures. In the small intestine, epithelial cells derived from stem cells in crypts and migrate upwards to form villi (Potten & Loeffler, 1990, Barker et al., 2007), which increase the surface area of intestine. These stem cells also give rise to Paneth cells (Cheng et al., 1969) that secrete antimicrobial proteins and are located at bottom of crypts; goblet cells (Merzel & Leblond, 1969, Cairnie, 1970) that produce mucins to form mucus, separating the epithelial cells from commensal bacteria presented in gut lumen; and enteroendocrine cells which function in hormone secretion (Gunawardene et al., 2011). Under the epithelial layers, there are lymphoid follicles of gut-associated lymphoid tissues (GALT) including Peyer's patches and isolated lymphoid follicles. M cells are found predominantly in dome-associated crypts in Peyer's patches (Gebert et al., 1999). M cells are highly specialised for antigen and pathogenic microorganism sampling, and have unique morphological features with reduced glycocalyx and microvilli on the surface (Mabbott et al., 2013). In the colon, epithelial cells derived from stem cells from crypts does not form villi, thus have a relatively flat surface compared to the small intestine. Paneth cells are rare and goblet cells are relatively more abundant. M cells can be identified in colonic patches (Fujimura et al., 1992) which is the Peyer's patches equivalent GALT in the colon.

1.2.1 Acid resistance

One of the reasons why the infectious dosage of *Shigella* is low might be due to its high acid resistance. It has been known that *Shigella* can survive in acid conditions (pH 2.5) for more than 2 hours independent to the large virulence plasmid (Gorden & Small, 1993). However, it is interesting that as reported, *Shigella* surviving acid challenge were unable to invade epithelial cells, yet the ability can be restored by growing at neutral pH for 4 hours (Gorden & Small, 1993). Moreover, the virulence plasmid, which is required for invasion, actually reduces the ability to survive in acid environments (Niu *et al.*, 2017). It can be speculated that *Shigella* might have different repertoires to deal with different environmental conditions. Indeed, it was found that *Shigella* required the alternative Sigma factor RpoS for its acid resistance (Small *et al.*, 1994). Further research revealed that certain genes, *gadC* and *hdeAB*, that contribute to the acid resistance were regulated by RpoS under acidic conditions (Waterman & Small, 1996). GadC is an antiporter that belongs to the glutamate-dependent acid resistance system (Jennison & Verma, 2007), and HdeA, HdeB, HdeC and HdeD are periplasmic chaperones and major acid resistance proteins (Foster, 2004). Moreover, it has also been found that an RNA binding protein Hfq coordinates the expression of acid resistance genes including *hdeA*, *hdeB*, *hdeD*, *gadA* and *gadB*, and T3SS genes in response to the acid environment (Yang *et al.*, 2015). Apart from the regulatory pathways that *Shigella* use to survive the acid environments, the surface component lipopolysaccharides (LPS) is also implicated in the acid resistance (Martinic *et al.*, 2011), particularly the polymerised sugar components.

1.2.2 Mucus layer penetration

To establish shigellosis and causes tissue damage, *Shigella* needs to firstly gain access to colonic epithelial cells, however *Shigella* would initially encounter the mucus layer which is a host innate defense system. The mucus layer consists of mucins, which are glycoproteins produced and secreted by goblet cells. The mucus layer in colon can be separated into outer layer and inner layer. The outer layer is softer and associated with commensal bacteria, and can be easily removed by intestinal movement, whereas the inner layer is thicker and free of bacteria (McGuckin *et al.*, 2011). The mucus layer also contains antimicrobial peptides, defensins and cathelicidins produced and secreted by enterocytes

(McGuckin *et al.*, 2011). Mover, mucins are also indispensable for the epithelial inflammation response triggered by the *Shigella* infection (Nutten *et al.*, 2002).

Shigella does not have flagella, hence it has limited motility in the gut lumen, and it lacks classic adhesins which would aid colonization. To date little has been known in regard to how *Shigella* deal with the mucus layer. However, several studies have implicated the potential strategies that *Shigella* might exploit to colonize and penetrate the mucus layer. It has been reported that the serine protease Pic expressed by *Shigella* and enteroaggregative *E.coli* (EAEC) was able to bind to mucin substrates (Gutierrez-Jimenez *et al.*, 2008). Moreover, by using polarized human intestinal cells, *Shigella* was also found to manipulate the expression, secretion and post-translation modification of mucins, which forms a gel-like matrix and favors the bacteria entry to the epithelial cells (Sperandio *et al.*, 2013). The binding of the mucin to *Shigella* might be specific as *Shigella* only recognizes few hosts. Indeed, mucus composition in different species is different (Podolsky *et al.*, 1986). It has been found that certain serotypes of *Shigella* strains can be agglutinated by Guinea pig mucus, and their invasion to HeLa cells can also be inhibited by the mucus from Guinea pigs, while not by monkey mucus (Dinari *et al.*, 1986). It can be speculated that a specific interaction between *Shigella* and human mucins exist, which facilitates the colonization and subsequent bacterial penetration of the mucus layers. Indeed, the adherence of *Shigella* to Guinea pig mucus can be inhibited by either carbohydrates or *Shigella* LPS (Izhar *et al.*, 1982), which indicated a carbohydrate interactions between the pathogen and hosts. However, in humans, it has been reported that *Shigella* dysenteriae adheres to colonic mucin rather small intestinal mucin (Sudha *et al.*, 2001), and that adherence cannot be inhibited by monosaccharides from mucins, suggesting that the potential receptors might be a glycoprotein. It still needs intensive studies to elucidate the mechanism that *Shigella* uses to adhere and across the mucus barrier.

1.2.3 Epithelial layer invasion

After *Shigella* bacteria cross the mucus barrier, it has to invade the epithelial cells in order to replicate and exert its virulence in the host, causing subsequent inflammatory responses and devastating tissue damage. However, the lining of the epithelial cells consist of polarized enterocytes that have microvilli structures facing the lumen and are sealed by

tight junctions, making it hard for *Shigella* to colonise and penetrate. Therefore, understanding the strategies *Shigella* exploit to cross this barrier may have important clinical value in understanding how to combat the disease.

1.2.3.1 M cell entry pathway

Due to ethical and financial consideration, it is difficult to study the early pathogenesis of shigellosis in humans at a cellular and molecular level. However, with several established animal models and *in vitro* human cancer cell lines, knowledge of *Shigella* infection, especially of the host immune response and inflammatory process respect, is partially elucidated. In the rabbit ligated ileal loop model, Shigellae takes advantage of M cells found within follicle-associated epithelium (FAE) in Peyer's patches (Bernardini *et al.*, 1989, Wassef *et al.*, 1989, Sansonetti *et al.*, 1996) to penetrate epithelial layers (Figure 1.2, A). In the murine macrophage cell line (Zychlinsky *et al.*, 1992), rabbit ligated ileal loop model (Zychlinsky *et al.*, 1996) and human *ex vivo* cells (Senerovic *et al.*, 2012), *Shigella* induces pyroptosis of macrophages after having been engulfed. Using *in vitro* cultured cells, *Shigella* was found to be able to lyse the phagocytic vacuoles with the aid of the type three secretion system (T3SS) (High *et al.*, 1992, Du *et al.*, 2016). Upon pyroptosis, inflammatory IL-1β and IL18 are released to the submucosa when studied in the mouse lung infection model (Sansonetti *et al.*, 2000). This also leads to the release of *Shigella* bacteria into the lamina propria which gain access to the basolateral side of epithelial cells, where they can invade. In addition, using *in vitro* human cell lines (Philpott *et al.*, 2000, Girardin *et al.*, 2001) and mouse models (Singer & Sansonetti, 2004), LPS and peptidoglycan presented by internalised *Shigella* can activate host cell nuclear factor-κB (NF-κB), which then activates the transcription of IL-8. The release of cytokines IL1β, IL18 and IL8 results in amplified inflammatory response and massive tissue destruction.

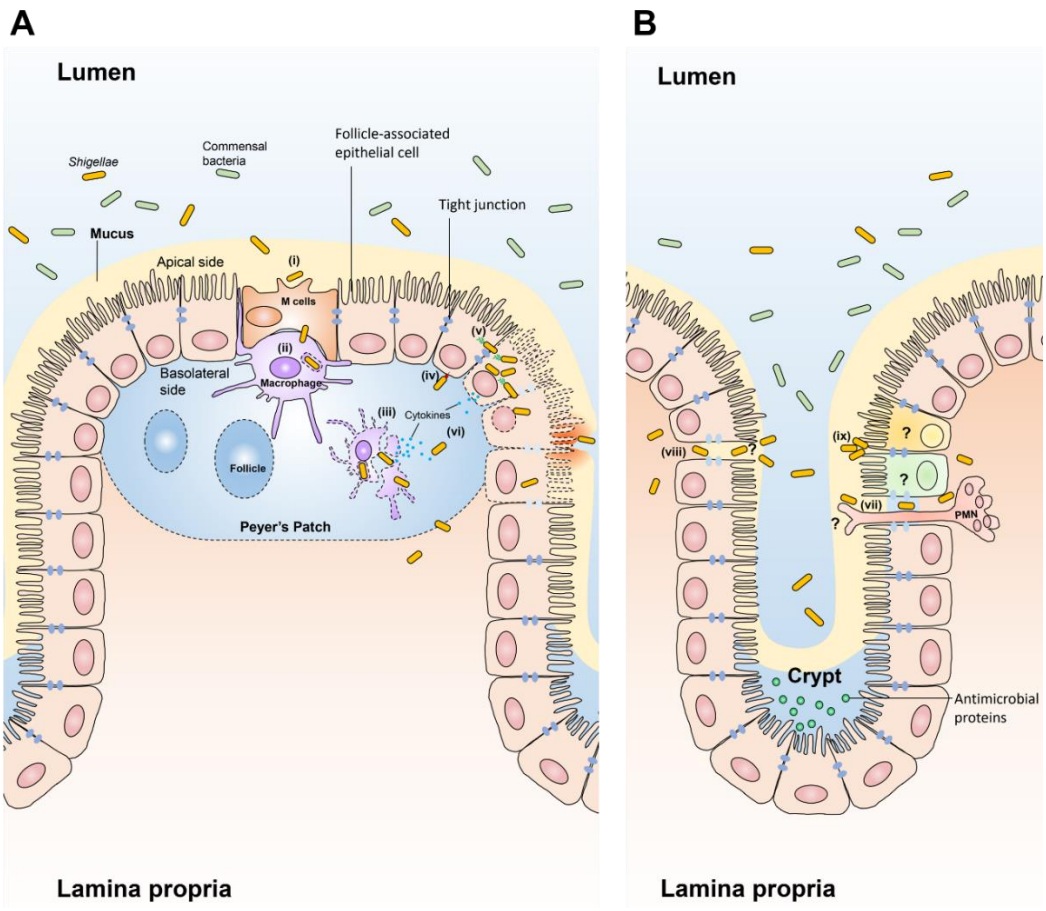

Figure 1.2. Models for *Shigella* penetration of the epithelial barrier.

The colonic epithelium layer is a single layer of polarized epithelial cells with apical and basolateral surfaces. Tight junctions are intracellular structures which form a barrier to control intracellular diffusion of components between epithelial cell's apical and basolateral membrane domains (Shin *et al.*, 2006). **(A)** *Shigella* penetrate the epithelial barrier by M cells. This is based on the rabbit small intestine model, and *in vitro* cell line models (Schroeder & Hilbi, 2008), **(i)** *Shigella* utilise M cells to penetrate epithelial barrier. **(ii)** *Shigella* are delivered into residential macrophages via transcytosis. **(iii)** *Shigella* escape by inducing pyroptosis of macrophages. **(iv)** *Shigella* are able to invade epithelium cells from the basolateral side, aided by its T3SS. **(v)** *Shigella* can spread to adjacent cells via actin based motility. **(vi)** The death of macrophages and infection of epithelium cells results in the release of cytokines, amplifying inflammatory reactions. **(B)** *Shigella* penetrate the epithelial barrier by the para-cellular space. **(vii)** *Shigella* triggers PMN cells to disrupt tight junctions between epithelial cells and use the para-cellular space to penetrate the epithelial barrier. **(viii)** *Shigella* actively disrupts tight junction between epithelial cells to gain access to the mucosa. **(ix)** *Shigella* was found targeting upper third of the colonic crypts, however the cell type(s) is unknown.

1.2.3.2 Paracellular entry pathway

While Wassef *et al.* (1989) have reported the initial entry of *Shigella* to mucosa is through M cells, this is not entirely convincing because the discovery of this mechanism used a rabbit small intestine model, while the actual infection site in humans is in the colon. *Shigella* do not require Peyer's patches and M cells to establish infections in both mouse-human intestinal xenograft (Zhang *et al.*, 2001) and in the *ex vivo* human colon model (Coron *et al.*, 2009). To date, there is no M cell-entry mechanism reported in humans nor in rhesus monkeys studies, and whether M cells in human colonic patches (Fujimura *et al.*, 1992) have the same function as in rabbit small intestines and whether they can be utilised by *Shigella* remains unknown. However, *Shigella* may have other entry sites. According to Mounier *et al.* (1992), *Shigella* was imaged binding to intercellular junctions of host cells and inefficient in invading polarised Caco-2 cells (human colonic cancer cell line) from the apical side compared that from the basolateral side. Histological studies on patient rectal biopsies frequently identified bacteria in para-cellular spaces (Mathan & Mathan, 1986). These results suggest that *Shigella* can gain access to mucosa through a para-cellular pathway. Using an *in vitro* human colonic cancer cell line (T84 cells), Perdomo *et al.* (1994a) demonstrated that *Shigella* on the apical side of monolayer is able to promote PMN cells migrating from basolateral side towards apical side and disrupt the barrier formed by the polarised monolayer (Figure 1.2, B-vii). In addition, in a rabbit model, Sansonetti *et al.* (1999) demonstrated that in the presence of IL8 which was released by epithelial cells, PMN cells were recruited to disrupt the epithelial barrier, though the exact mechanism is still controversial (McCormick *et al.*, 1998). One possible pathway showed by Sakaguchi *et al.* (2002) is that *Shigella* has the ability to interact with and penetrate the tight junctional seal to gain access to the basolateral side where it invades T84 monolayer cells (Figure 1.2, B-viii). In addition, *Shigella flexneri* disrupts the tight junction of Caco-2 cell monolayers independent of pro-inflammatory IL-8 (Fiorentino *et al.*, 2014). These results indicate that *Shigella* can penetrate the epithelial layers by the disruption of the tight junctions, yet the exact mechanism also remains unknown.

1.2.3.3 Apical infection pathway

Apart from the para-cellular pathway, internalisation of *Shigella* is also observed when adding bacteria apically to Caco-2 cell lines (Wells *et al.*, 1998, Mathias *et al.*, 2013, Longet *et al.*, 2014), suggesting an alternative route to penetrate epithelial layers. However, it worth mentioning that in these experiments, bacteria were either incubated with Caco-2 cells overnight where a transepithelial electrical resistance (TEER, which represents the integrity of cell monolayer) drop was observed (Mathias *et al.*, 2013, Longet *et al.*, 2014), or centrifuged to promote the contact of bacteria and cells (Wells *et al.*, 1998). Therefore, it is still unknown whether *Shigella* can directly infect and enter epithelial cells apically. More studies on apical infection are needed to confirm this pathway.

Recently, *Shigella* were found targeting crypts in both the Guinea pig colon and human *ex vivo* specimens by bioimage analysis (Arena *et al.*, 2015), which is consistent with the observations in patient biopsy where damage was found predominantly in the upper third of crypts (Figure 1.2, B-ix) (Mathan & Mathan, 1986). Colonic crypts have epithelial stem cells that can proliferate and differentiate to different cell types, such as epithelial cells, enteroendocrine cells and goblet cells, all of which are important in maintaining the colonic health (Abdul Khalek *et al.*, 2010). Moreover, the upper third of crypts might have M cells that are derived from the follicle-associated epithelial cells before they migrate and mature in lymphoid follicles. As reported by Tahoun *et al.* (2012), M cells can be derived from follicle-associated epithelial cells upon the contact with pathogen. However, the targeted cell type in colonic crypts and the mechanism of cell targeting in humans by *Shigella* are completely unexplored.

1.3. *Shigella* pathogenesis models

1.3.1 Immortal cell lines

The majority of research on the interactions between *Shigella* and host have relied on immortal cell lines such as HeLa (human cervix epithelial cells), Intestine-407 (human embryonic intestinal cells contaminated with HeLa cells), T84 (human colonic epithelial cells), HT-29 (human colonic epithelial cells) and Caco-2 (human colonic

epithelial cells). Using these cell lines, studies were able to demonstrate the successful adherence and invasion, therefore they have become useful tools to investigate *Shigella* virulence factors at the cellular and molecular level. HeLa cells and Intestine-407 cells are useful for assessing invasion ability, and cell to cell spread of *Shigella* by plaque formation, as well as the adherent characteristics of different *Shigella* strains (Koestler *et al.*, 2018b). Caco-2 and T84, as they are derived from human colonic tissue and can form polarized colonic epithelial cells, are useful in assessing the efficiency of *Shigella* invasion and adhesion from different sides (Mounier *et al.*, 1992), i.e. apical and basolateral side (Figure 1.3). It is also helpful in investigating the host pathogen interactions at the molecular level. Using T84 cells, it was found that *Shigella* was able to manipulate the expression of tight junction proteins via dephosphorylation independent to their invasion machinery (Sakaguchi *et al.*, 2002). Further research on this demonstrated that *Shigella* secrete serine protease A (SepA) to disrupt the tight junctions by causing a decrease in active LIM kinase 1, a negative regulator of cofilin which leads to the remodeling of actin and the opening of tight junctions (Maldonado-Contreras *et al.*, 2017).

Although these cells are derived from human source, they have altered physiology and expression profile compared to their normal human counterparts, therefore they do not fully represent the intestinal epithelial cells. Besides, as they are all single cell type, they lack the complexity which a multicellular system can provide, hence they have limited ability to represent the disease progression and unable to elucidate the initially infected cell type. Moreover, when using these cells, it often requires either long infection time with large number of bacteria or centrifugation to promote contact between bacteria and host cells. Furthermore, Caco-2 and HT-29 cells have multiple cell subtypes (Lievin-Le Moal & Servin, 2013) which is likely to give variable results.

1.3.2 Animal models

When trying to understand the initial infection process of shigellosis and the cell type that *Shigella* utilizes for its entry, as well as establishing a model for the assessment of *Shigella* vaccine candidates, animal models are often exploited (Table 1.1).

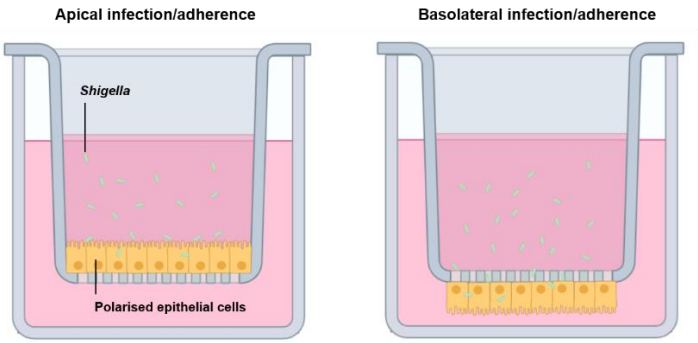

Figure 1.3. Polarised epithelial infection and adherence system.

Tissue cultured polarised epithelial cell system for the investigation of *Shigella* adherence and infection from apical (left) and basolateral (right) sides. Colonic immortal cells grow on the surface of the transwell which hold a 0.4 µm (basolateral) or 0.2 µm (apical) microporous membrane and sit in the 24-well plate. Depend on the side they grow, they can expose either apical or basolateral side to the bacteria which can be added into the transwell. The confluence of the cell layer is measured by the transepithelial electrical resistance (TEER).

Table 1.1. Summary of *Shigella* animal models.

Animal models	References
Rabbits	
Ligated ileal loop model	(Arm *et al.*, 1965, Wassef *et al.*, 1989)
Cecal ligation model	(Rabbani *et al.*, 1995)
Oral infection model	(Etheridge *et al.*, 1996)
Guinea pigs	
Oral infection model	(Formal *et al.*, 1958)
Sereny test model	(Sereny, 1959, Sansonetti *et al.*, 1983)
Intrarectal infection model	(Shim *et al.*, 2007)
Cecal ligation model	(Barman *et al.*, 2011)
Mice	
Intranasally infection model	(Voino-Yasenetsky & Voino-Yasenetskaya, 1962, Mallett *et al.*, 1993)
New-born mouse intragastrical infection model	(Fernandez *et al.*, 2003, Fernandez *et al.*, 2008)
Intraperitoneal infection model	(Yang *et al.*, 2014)
Human intestinal xenograft model	(Seydel *et al.*, 1997)
Antibiotic treated oral infection model	(Medeiros *et al.*, 2019)
Other models	
Monkey model	(Kent *et al.*, 1967, Takeuchi *et al.*, 1968, Rout *et al.*, 1975, Takeuchi *et al.*, 1975, Takeuchi, 1982, Formal *et al.*, 1984, Oaks *et al.*, 1986, Karnell *et al.*, 1993, Gardner & Luciw, 2008, Shipley *et al.*, 2010, Gregory *et al.*, 2014, Islam *et al.*, 2014)
Pig model	(Maurelli *et al.*, 1998)
Chicken model	(Shi *et al.*, 2014)
C. elegans model	(Burton *et al.*, 2006, George *et al.*, 2014)
Zebrafish model	(Mostowy *et al.*, 2013)

1.3.2.1 Rabbit models

The most successful model that demonstrated the potential pathogenesis of *Shigella* is the ligated rabbit ileal loop model (Arm *et al.*, 1965), by which it was found that M cells are the entry site of *Shigella* (Wassef *et al.*, 1989). However, in this study, ileal loop was used instead of the large intestine section, which is the natural infection site in humans. Besides, large number of bacteria were inoculated and made contact directly to Peyer's Patch-rich sections, and both pathogenic and non-pathogenic strains were taken up by M cells, which may not truly represent the natural disease progression. Although rabbit can be infected in the colon, it again requires the administration of large amount of bacteria and the manipulations of the intestines, where bacteria was directly injected into the proximal colon after been ligated to the distal cecum (Rabbani *et al.*, 1995). Rabbits can be orally infected with *Shigella*, yet it required starving and preconditioning of the animal (Etheridge *et al.*, 1996). More importantly, although the histological analysis of the lesion was the same as that in other hosts, the primary infection site is restrained in the ileum, suggesting an intrinsic difference to its natural host, humans.

1.3.2.2 Guinea pig models

The Guinea pig is one of the oldest animal models used in obtaining knowledge about *Shigella* pathogenesis. By starving and preconditioning of the animal, orally administrated *Shigella* successfully caused disease symptoms and tissue destruction in guinea pigs (Formal *et al.*, 1958). Similar to shigellosis in the humans, lesions were restrained in the colon rather the small intestine, yet it was not as diffused as observed in patients. Guinea pig models seems to be superior in studying *Shigella* adherence, as it was found to be the most efficient host for bacteria to adhere among rats, rabbits and hamsters (Izhar *et al.*, 1982). In addition, the adherence of *Shigella* in the colon was found significantly higher than that in the small intestine, with increasing adherence rate towards the distal end, which closely correlated to the observations in humans where lesions were predominantly found in the colon with the increasing severity towards the distal end of the colon (Formal *et al.*, 1958). Another widely used purpose of the Guinea pig is to assess the virulence of *Shigella* strains, known as the Sereny test (Sereny, 1959), where *Shigella* strains were inoculated into Guinea pig eyes, and the conjunctivitis and keratitis was observed in animals

infected with virulent strains (Sansonetti *et al.*, 1983). In addition, through intrarectal administration of *Shigella* strains, Guinea pigs can be infected and not only displayed the symptoms of weight loss, fever, severe damage to the colonic mucosa as observed in humans, but also the inflammatory response was similar to shigellosis (Shim *et al.*, 2007). Further analysis in this model revealed the colonic crypts are the favored entry site for *Shigella* (Arena *et al.*, 2015). Again, this model bypasses the proximal colon, which is the targeted site by *Shigella* in humans. In another Guinea pig model, *Shigella* was administrated in the proximal colon after the ileocecal junction was tied, which also produced acute inflammatory response and colonic tissue damage (Barman *et al.*, 2011). However, this model failed to develop severe diarrhea and the severity of the disease was mitigated after 3 to 4 days. Although these Guinea pig models closely resemble the pathogenesis of shigellosis, they either involve animal starvation or preconditioning, which could potentially alter the normal intestinal flora and contributing to the observed results.

1.3.2.3 Mouse models

One of the early developed mouse models was the mouse pneumonia model, where *Shigella* was inoculated intranasally to determine bacterial virulence (Voino-Yasenetsky & Voino-Yasenetskaya, 1962, Mallett *et al.*, 1993), but this model was only useful in assessing the virulence of the attenuated live *Shigella* vaccines and exploring the inflammatory responses, hence it had limited relevance in terms of exploring pathogenesis. Adult mice cannot easily be orally, intragastrically or intrarectally infected by *Shigella*. The possible explanation of the difficulty in establishing shigellosis in adult mice might be the proportion of polymorphonuclear neutrophils (PMNs) in mouse blood is far less than that of in humans, representing 10-25% and 50-70% respectively (Mestas & Hughes, 2004), as PMNs play an important role during *Shigella* infection. Besides, mice do not express IL-8 which recruits PMNs (Singer & Sansonetti, 2004), which was thought to be responsible for the massive inflammatory response and the disruption of epithelial barrier, dampening the tissue destruction in humans. Because of this, the newborn mouse was exploited as a model (Fernandez *et al.*, 2003), where *Shigella* was administrated intragastrically, and was able to elicit an acute immune response. However, the tissue damage described in the literature was restrained in the small intestine. It is still unknown why newborn mice can be easily infected

by *Shigella*, yet one might speculate that the immaturity of the newborn mice might affect the ability to control the inflammatory response (Liechty *et al.*, 1993). Moreover, as the newborn mice infected by *Shigella* developed small intestine lesions similar to human colonic lesions, it is reasonable to investigate the transcriptomic differences in mice growing for different days. Indeed, expression of certain genes specific for Paneth cells accounts for the limited disease progressing in adult mice, suggesting the importance of Paneth cells in combating shigellosis in humans (Fernandez *et al.*, 2008). Nevertheless, it has been reported recently that mice can be orally infected with *Shigella flexneri* 2a after the treatment of antibiotics (Medeiros *et al.*, 2019), with the infection found in the colon and been promoted by the zinc deficiency. In addition, by intraperitoneal injection of *Shigella flexneri* 2a, adult mice were found having bacillary dysentery, with observations of invasion and colonization of the bacterial pathogen in the colon (Yang *et al.*, 2014). Another mouse model that was developed is the mouse-human intestinal xenograft model (Seydel *et al.*, 1997), where human colonic tissue was grafted into the subscapular region of mice to assess the immune response elicited by *Shigella* infection (Zhang *et al.*, 2001). This model has limitations in investigation the dissemination of the bacteria, yet demonstrated the ability of *Shigella* to invade human colonic tissue in the absence of M cells.

1.3.2.4 Other animal models

Since primates were reported naturally infected with *Shigella* (Banish et al., 1993), it has been recognized as a natural host and used to examined the tissue lesions at a morphological and histological level, or used to assess vaccine candidates (Labrec *et al.*, 1964, Kent *et al.*, 1967, Takeuchi *et al.*, 1968, Rout *et al.*, 1975, Takeuchi, 1982, Formal *et al.*, 1984, Karnell *et al.*, 1993, Shipley *et al.*, 2010, Gregory *et al.*, 2014). In these models, *Shigella* were experimentally administrated via oral route or intragastric route (Islam *et al.*, 2014). The symptoms, immune responses and tissue damages closely resemble the human shigellosis, but it is costly and strictly restrained by ethics regulation.

Pigs have also been experimentally infected with *Shigella* via the oral route (Maurelli *et al.*, 1998). However, they failed to elicit an inflammating response and failed to penetrate colonic cells. Therefore, it has little value in investigating the pathogenesis of *Shigella*.

Chickens have been reported with shigellosis, with the symptoms of bloody and mucoid diarrhea. Because of this, chickens were intraperitoneally injected with *Shigella* isolated from human, and invasion were observed in intestinal mucosa. However, bacteria internalization was only observed in the jejunum and ileum, rather in the duodenum, cecum, or rectum (Shi *et al.*, 2014), suggesting that chickens are not appropriate to represent shigellosis in humans.

Caenorhabditis elegans were also exploited as a *Shigella* infection model (Burton *et al.*, 2006). The research into the interactions between *Caenorhabditis elegans* and the pathogen revealed that *Shigella* was able to induce a cytopathological changes in the host and disrupt the host iron homeostasis, making the host more susceptible to the infection (George *et al.*, 2014). Through proteomic analysis, a *Shigella* periplasmic enzyme, AnsB, which has been reported to be immunogenic, was found to contribute to bacterial adherence.(Jennison *et al.*, 2006).

Apart from chickens, pigs and worms, infection of zebrafish have also been used as a model to study the host-pathogen interactions (Mostowy *et al.*, 2013), but this model is not suitable for investigation of the pathogenicity of *Shigella*, rather it provided information in host innate immune response after the infection.

Humans and monkeys are the only natural reservoir for *Shigella*, while rabbits, guinea pig, mice, and other animals are non-susceptible to the natural infections. To study the pathogenesis in these animal models requires a variety of manipulation including starvation, administration of antimicrobial reagents, toxic reagents, acid neutralization treatments and even opiates. Some are even involve surgery to bypass the small intestine, or infection directly from distal end of the colon. These heavy manipulations on animal subjects would alter the natural microflora and represent artificial infection cases, which has limitations in deciphering the pathogenesis as occurs in the naturally susceptible hosts.

1.3.3 Human biopsies and organoids model

As far as the host specificity of shigellosis is concerned, experimental material from humans seems to be more suitable for the study of the pathogenesis. Human *ex vivo* colon specimens were used to examine the primary infection site targeted by *Shigella*

(Coron *et al.*, 2009, Arena *et al.*, 2015), where specimens were taken from the patients undergoing surgery, and immediately infected by *Shigella*, flowed by immunohistochemical analysis. Although it might be helpful in gaining the understanding of how human colonic cells react to the infection of *Shigella* in the cellular and molecular level, it is limited in explaining the process of spread of bacteria and the immune response elicited by the infection, as they lack of an underlining tissue and blood circulation which also contributes to the disease progression.

A recently developed human model is human intestinal enteroids, being theoretically advantageous in investigating *Shigella* invasion processes. These enteroids are derived from LGR5+ stem cells, which are originally isolated from human colonic crypts and subsequently differentiated to different enterocytes including epithelial cells, goblet cells, Paneth cells and enteroendocrine cells (Barker *et al.*, 2007, Wells & Spence, 2014, Bartfeld & Clevers, 2015, VanDussen *et al.*, 2015). They have been used to investigate the interactions between human tissues and a variety of bacteria including: *Salmonella* (Zhang *et al.*, 2014, Forbester *et al.*, 2015, Wilson *et al.*, 2015), *Helicobacter* (McCracken *et al.*, 2014, Bartfeld *et al.*, 2015), and recently, *Shigella* (Koestler *et al.*, 2019, Ranganathan *et al.*, 2019). In *Shigella* infection, it was found that *Shigella* was able to invade more efficiently from the basolateral side of the epithelial cells compared to that of from the apical side (Koestler *et al.*, 2019, Ranganathan *et al.*, 2019), consistent to that reported from the tissue cultured cells (Mounier *et al.*, 1992). When enteroids were made to differentiate to M cells, apical infection of *Shigella* was increased by 10-fold, suggesting that M cells does contribute to the uptake of pathogen and facilitate *Shigella* across the epithelial barrier (Ranganathan *et al.*, 2019). However, it can still be argued that M cells are not as abundant in the colon as in the small intestine (Bowcutt *et al.*, 2014), and the fact that *Shigella* is unable to invade the small intestinal epithelial suggesting that M cells might not be the primary targeted site for the entry. Enteroids also have limitations in capturing the interactions between the pathogen and immune system, gut fluid and flora. Therefore, enteroids have limitations with respects to deciphering aspects of pathogenesis.

1.4. *Shigella* cell adhesion

For pathogenesis, adhesion of bacteria to host cells is crucial for establishing early infection, allowing bacteria to contact with specific host cells and initiate subsequent infection. A variety of bacterial adhesins have been identified and reviewed (Chahales & Thanassi, 2015), including pili, curli, and some autotransporters such as Ag43, FdeC and pertactin. It is still unclear as to what molecular and mechanism *Shigella* utilises to adhere to the host cells and to initiate infection, as until recently there are no well characterised adhesins in *Shigella*. However, several host molecules and bacterial surface molecules were recently reported to promote adhesion of *Shigella* bacteria to host cells.

1.4.1 Host molecules enhanced adherence.

It has been reported that neutrophils are required for effective *Shigella* invasion of epithelial cells (Perdomo *et al.*, 1994a), and are recruited early in infection (Perdomo *et al.*, 1994b). Further studies found that these recruited neutrophils can degranulate and release antimicrobial proteins which were then exploited by *Shigella* to enhance their adherence and invasion to epithelial cells, by potentially binding to the bacterial surface (Eilers *et al.*, 2010). Recently, human enteric α-defensin 5 (HD5) that is secreted by intestinal Paneth cells was found to promote *Shigella* adherence and invasion in a variety of *in vivo* models including the Guinea pig Sereny test model, the Guinea pig intrarectal infection model and a mouse ligated ileal and colonic model (Xu *et al.*, 2018). HD5 was also found binding to *Shigella* surface molecules to mediate the adherence and invasion to epithelial cells *in vitro* (Xu *et al.*, 2018). However, the exact mechanism of this remains unknown.

1.4.2 LPS

One of the bacterial surface molecules found to promote adhesion is lipopolysaccharide (LPS), which is an important bacterial virulence factor (Trent *et al.*, 2006), and is known to be involved in the adherence of many bacteria (Jacques, 1996). Fully assembled LPS can be divided into three units: 1) an outer membrane embedded Lipid A, 2) a core sugar component, and 3) a repeated O-antigen glycan subunit of various lengths.

Shigella that are devoid of O-antigen units are called rough LPS strains, while those with the presence of O-antigen units, are called smooth LPS strains (Figure 1.4).

The diversity of the O-antigen also plays a role in *Shigella* virulence and host immune avoidance. It has been reported that the glucosylated O-antigen on LPS might adapt a helical structure compared with the unglucosylated LPS, making the LPS molecules shorter, and hence allowing more exposure of the T3SS (West *et al.*, 2005). Moreover, LPS has been implicated in pathogen-host interactions in many bacterial species, and been reviewed by Jacques (1996). In *Shigella*, it has been found that isogenic LPS preparation inhibits the adherence of bacteria to Guinea pig intestinal cells (Izhar *et al.*, 1982) and human cancer cells (Day *et al.*, 2015). This inhibition can also be achieved by glycans from human cells (Day *et al.*, 2015). Moreover, LPS-specific secretory IgA (Boullier *et al.*, 2009) and anti-O antigen antibody (Chowers *et al.*, 2007) can reduce invasion and *Shigella* induced inflammatory reactions. Recently, purified polysaccharides of *Shigella* showed specific binding to human small intestinal sections and glycan arrays, and can inhibit adherence to T84 cells (Day et al., 2015). Collectively, these studies indicate a role of LPS O-antigen in adherence of Shigella to host cells.

1.4.3 The SSO1327 multivalent adhesion molecule

Recently, through sequence comparison, a putative protein SSO1327 (around 120 kDa) encoded by the chromosome near the *ipaH* pathogenicity island was found in *Shigella sonnei* as an ortholog of the well characterized multivalent adhesion molecules in *V. parahaemolyticus* (VP1611) (Mahmoud *et al.*, 2016). This protein has been predicted with seven mammalian cell entry domains and can be also found in *S. boydii* (SB01249), *S. flexneri* (SF1391) and *S. dysenteriae* (SDY1985) although in most *S. flexneri*, it encodes for a truncated protein. Mutations in this protein in *Shigella sonnei* lead to decreased adherence and invasion in the *Galleria mellonella* larvae infection model, demonstrating a role of SSO1327 in contributing to *Shigella* adhesion. However the effect of its other othologs in other *Shigella* species needs to be investigated as well.

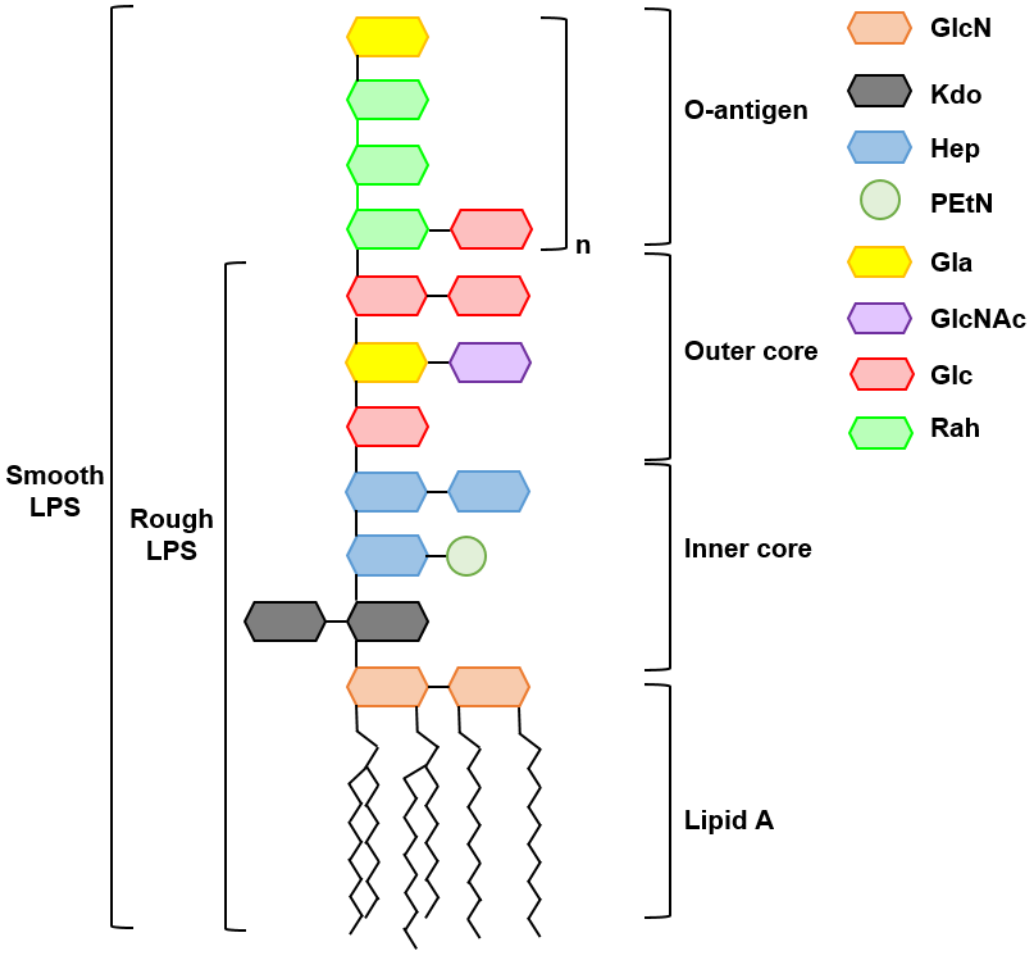

Figure 1.4. Schematic representation of *Shigella* LPS structure.

The matured LPS molecules (shown as of *Shigella flexneri* 2a) can be separated into three parts including lipid A, core sugar (inner and outer core), and the O-antigen repeating units. LPS having the full length O-antigen repeating units is called smooth LPS, while the LPS devoid of O-antigen is called rough LPS. GlcN: glucosamine; Kdo: 3-deoxy-D-mannooct-2-ulosonic acid; Hep: L-glycero-D-manno-heptose phosphate; PEtN: O-phosphoryl-ethanolamine; Gla: D-galactose; Glc: D-glucose; GlcNAc: N-acetyl-D-glucosamine; Rha: L-rhamnose.

1.4.4 Type III secretion system (T3SS)

Another surface component that has been found essential to establish early infection is the type III secretion system (T3SS). The T3SS exists in a wide range of Gram-negative bacterial pathogens and symbionts, and is comprised of more than 20 proteins, which form the entire T3SS apparatus across the bacterial inner and outer membrane, namely the injectisome (Deng *et al.*, 2017). The injectisome can be divided into three parts according to their cellular locations, which are 1) the peripheral cytoplasmic components including the ATPase complex and the cytoplasmic ring (C ring), which are responsible for protein secretion, sorting and unfolding; 2) the basal body consisted of proteins that are highly oligomerized spanning across the inner and outer membrane, through which the effector proteins are secreted; and 3) the extracellular components including the hollow needle and the tip complex, which is responsible for the delivery of effector proteins to the host cytoplasm. Proteins involved in the assembly of the T3SS and their function were reviewed and summarized by (Deng *et al.*, 2017). In *Shigella*, this system is encoded by the *ipa-mxi-spa* locus of the large virulence plasmid (VP).

1.4.4.1 Membrane targeting of T3SS

The T3SS extracellular needle contains IpaB, IpaC and IpaD (Veenendaal *et al.*, 2007). Specifically, IpaB and IpaC are hydrophobic proteins and were thought to be assembled onto the needle with the help of IpaD, and are inserted into host cell membranes to form a channel for delivery of effector proteins (Blocker *et al.*, 1999, Veenendaal *et al.*, 2007). These effector proteins are involved in the subversion of host cell processes to facilitate *Shigella* invasion, and their functions are reviewed by Belotserkovsky and Sansonetti (2018). It has been shown that IpaB, IpaC and IpaD proteins can interact with host receptor $\alpha_5\beta_1$ integrin (Watarai *et al.*, 1996), and IpaB interacts with CD44 (Skoudy *et al.*, 2000, Lafont *et al.*, 2002) and host cell membrane component cholesterol (Hayward *et al.*, 2005), initiating the invasion process to host cells. However, these two host membrane receptors are thought to be located at the basolateral surface of the polarized epithelial cells (Neame & Isacke, 1993, Lee & Streuli, 2014), and those Ipa proteins are not directly contributing to the cell adhesion (Menard *et al.*, 1993), questioning their role in the initial adherence of *Shigella* to the apical surface of the host lumen. Nevertheless, the apical

infection of the intestinal epithelial layers could be attributed to the interaction between host filopodia and T3SS (Carayol & Nhieu, 2013). Recently, *Shigella* effector protein IpaA was found binding to host focal adhesion protein talin to stabilize the adhesion of *Shigella* to host cell filopodia and facilitates the capture of the bacteria (Valencia-Gallardo *et al.*, 2019). IpaA proteins has previously been reported binding to another focal adhesion protein vinculin (Tran Van Nhieu *et al.*, 1997, Bourdet-Sicard *et al.*, 1999), through which it increased the association between vinculin and F-actin and subsequently depolymerized the actin filaments. Clearly, it suggests that IpaA contributes to the filopodial capture of *Shigella* by host cells, yet prior to this, it requires the activation of T3SS and close contact between the pathogen and host cells.

1.4.4.2 T3SS as a host sensing system

T3SS is thought to react to the environmental stimuli, specifically, the gut environment, to modulate cell surface components and trigger increased adherence and invasion. Indeed, when switched from anaerobic environment to the epithelial barrier where O_2 can be detected, the expression of T3SS regulators was changed in *Shigella* to activate the T3SS, allowing efficient invasion (Marteyn *et al.*, 2010). *Shigella* also regulates its virulence in response to conditions such as temperature (Maurelli *et al.*, 1984) and osmolarity (Bernardini *et al.*, 1990). Studies comparing the difference in expression of *Shigella* proteins between intracellular and extracellular also revealed some changes in the expression and the secretion of T3SS effector proteins (Headley & Payne, 1990, Pieper *et al.*, 2013). This further suggests that *Shigella* has evolved into a well host adapted pathogen that can utilize a sophisticated system to sense the host environment facilitating its colonization and invasion.

1.4.4.3 T3SS activation by bile

The natural infectious dose of *Shigella* in humans is as low as 10 organisms (Bennish, 1991), in contrast, infection of the tissue culture cells requires a large number of organisms and often involves spinoculation (Koestler *et al.*, 2018b). One might speculate that it might be that in the gut environment, there are factors that can stimulate the bacteria towards their virulence activated form which is more efficient in adherence and invasion. One factor that *Shigella* would encounter in human gut is bile salt. Bile salt has been reported

as a signaling trigger to regulate the expression of virulence factors during the infection in other bacterial species including *Salmonella typhimurium* (Prouty & Gunn, 2000, Prouty *et al.*, 2004) and *Vibrio* (Gupta & Chowdhury, 1997, Schuhmacher & Klose, 1999, Krukonis & DiRita, 2003), and was reviewed by Begley *et al.* (2005). In a *Shigella* study, a bile salt deoxycholate (DOC), among other related compounds, were reported to significantly increase the ability of *Shigella* adhesion and invasion of tissue culture cells (Pope *et al.*, 1995). DOC is a secondary bile acid which is mainly produced by microbial reactions in the human large intestine (Ridlon *et al.*, 2006). This coincide with the observations that *Shigella* preferably invade colon. In addition, DOC does not directly enhance the *Shigella* adhesion and invasion, it requires bacterial growth (Pope *et al.*, 1995). Therefore, it can be speculated that DOC might act as a stimulus that activates a signal transduction cascade that leads to the expression of virulence factors, priming for cell invasion. This may also partially explain the observations in the patients with shigellosis, where severity of tissue damage increases towards the distal colon (Speelman *et al.*, 1984). When bacteria travel along the colon towards the distal end, they are continuously exposed to DOC, which would allow them to produce and secrete effectors such as Ipa proteins and surface localize adhesins for more efficient cell adhesion and invasion when they reach the rectum.

1.4.4.4 DOC induced adhesins

As DOC plays such an important role in activating *Shigella* adherence, one might hypothesize that adhesins might be involved in this. Indeed, it has been demonstrated that the T3SS is indirectly required for the DOC enhanced attachment (Faherty *et al.*, 2012), and analysis of the change of global expression of *Shigella* proteins at the transcriptional level in the presence of DOC revealed two potential adhesins, OspE1 and OspE2 proteins. The expression of OspE1 and OspE2 was induced by DOC, and which was subsequently secreted by T3SS and localized on the bacterial membrane (Faherty *et al.*, 2012) (Figure 1.5). Clearly, these data suggest that DOC acts on T3SS to activate an unknown signal transduction cascade to modulate the expression of virulence factors.

To date, little has been known for this signal transduction process, yet the fact that the exposure of bacteria to DOC leads to an increased secretion of effector proteins into bacterial culture supernatant gives a clue. The secretion of effector proteins is through

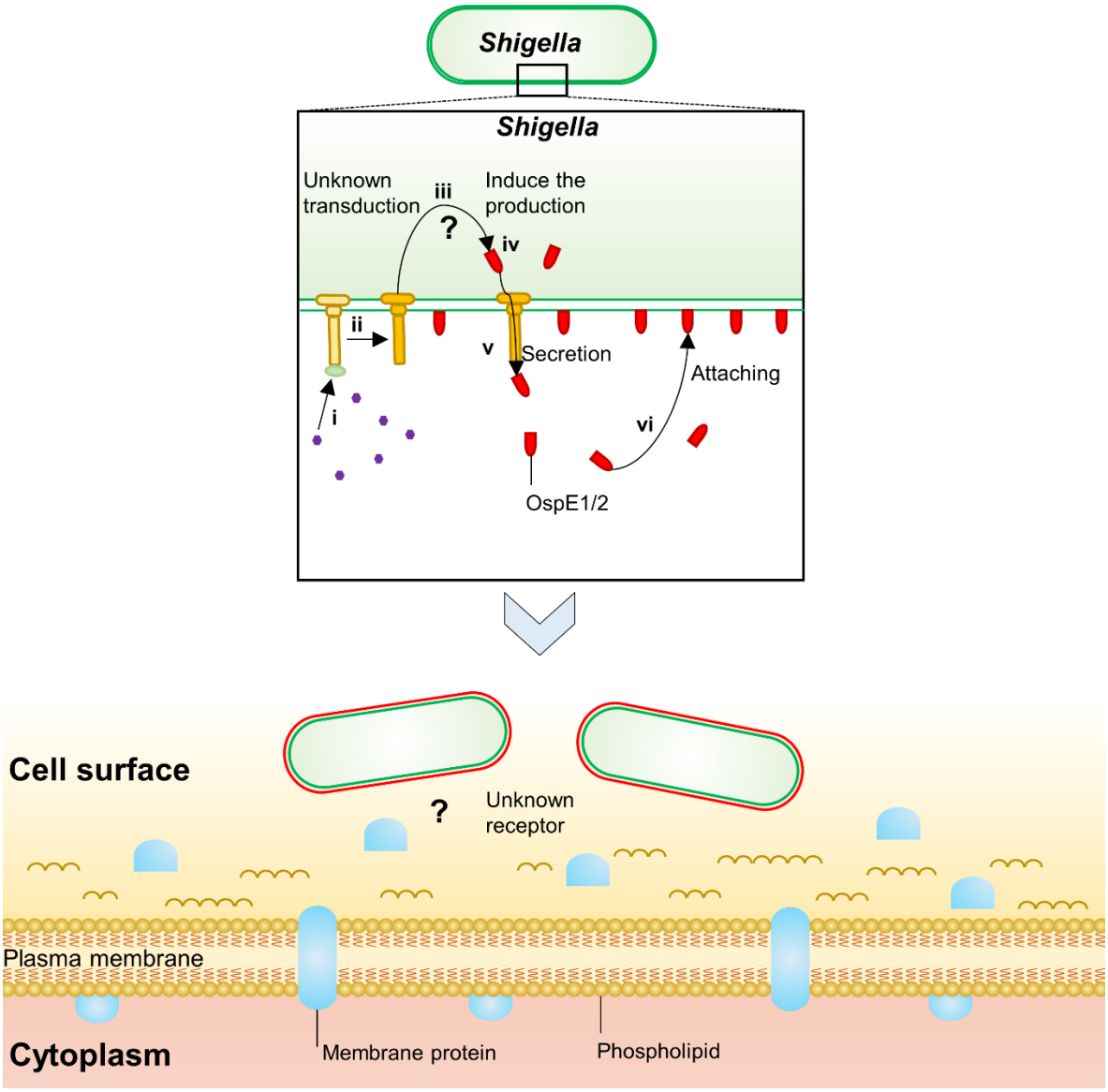

Figure 1.5. Deoxycholate induced *Shigella* adherence.

In the human gut, *Shigella* encounters bile salt DOC. **i)** DOC binds to the protein IpaD which reside on the needle tip of the T3SS. **ii)** This binding leads to the activation of T3SS. Activated T3SS then undergo **iii)** an unknown transduction, which leads to i**v)** the increased expression of adhesins OspE1/2, and **v)** their subsequent secretion via T3SS. The secreted OspE1/2 then **vi)** bind back to the surface of *Shigella* and function as adhesins to mediate the adherence of *Shigell*a to gut epithelial cells.

the induction of the T3SS (Menard *et al.*, 1994), particularly the needle-resident proteins IpaB and IpaD. IpaD is thought to be located at the needle tip of T3SS and prevents leakage and secretion of effectors through the T3SS (Roehrich *et al.*, 2013). While the initial localization of IpaB is controversial, some conclude that it is absent from the needle tip and can be recruited upon contact between DOC and bacteria surface (Olive *et al.*, 2007, Stensrud *et al.*, 2008), whereas others claimed that IpaB is a part of needle complex residing at the needle tip (Veenendaal *et al.*, 2007, Cheung *et al.*, 2015, Murillo *et al.*, 2016). Nevertheless, it has been reported that DOC can directly bind to IpaD, causing a conformational change to the protein that subsequently leads to the activation of T3SS (Stensrud *et al.*, 2008, Barta *et al.*, 2012). When the flexible region that is responsible for the conformational change was mutated, *Shigella* no longer had an increased adherence, presumably due to the inability to respond to the binding of DOC (Bernard *et al.*, 2017), by potentially affecting the interaction with IpaB (Kaur *et al.*, 2016).

How exactly the initial contact between IpaD and DOC, and the subsequent altered interaction between IpaD and IpaB which then leads to an increased bacterial adhesion and invasion remains to be investigated. As IpaB and IpaD were thought to be important in regulating the activity of T3SS, by knocking out *ipaB* or *ipaD*, *S. flexneri* was found to be hyper-adherent to host cells (Menard *et al.*, 1993). Surprisingly, under this simulated activation event (Brotcke-Zumsteg *et al.*, 2014), the surface presented autotransporter IcsA was found to play a crucial role in the hyper-adherence phenotype, which uncovered a long missing *Shigella* adhesin.

1.5. IcsA protein

Intra-/inter-cellular spread protein A (IcsA) or large virulence plasmid encoded virulence protein G (VirG) was first found in *S. flexneri*, where a *Tn5* insertion in the large virulence plasmid made the mutant avirulent, and while maintaining the ability to invade the host cell, it was unable to escape the initial infected cells and spread intercellularly (Makino *et al.*, 1986). Mutations in *icsA* also lead to attenuated virulence in both animal and human studies (Sansonetti *et al.*, 1991, Kotloff *et al.*, 1996), demonstrating the indispensable role of IcsA in *Shigella* pathogenesis.

1.5.1 The biosynthesis of IcsA

IcsA contains an N-terminal domain ($IcsA_{1-52}$), which is responsible for its secretion; a passenger domain ($IcsA_{53-740,}$ or IcsAα), which is responsible for its biological function; a β-barrel domain ($IcsA_{813-1102}$ or IcsAβ), which is a pore forming structure inserted in the outer membrane and is responsible in the translocation of the passenger; and an unstructured linker region ($IcsA_{741-812}$) that connects the passenger with β-barrel (Figure 1.6). The maturation of IcsA starts with the translocation of the nascent peptides across the inner membrane via Sec machinery. IcsA then exists in the periplasmic compartment and this transit state is stabilized by periplasmic folding factors DegP, SkP and SurA (Purdy *et al.*, 2007). The β-barrel domain of IcsA is then thought to be assembled by a complex known as the β-barrel assembly machinery (BAM) complex (Hagan *et al.*, 2011), which folds the IcsA β-barrel domain into the outer membrane and transports the passenger domain across the outer membrane. The maturated IcsA passenger protein can either remain on the surface of the bacteria or be cleaved off by a specific serine protease IcsP (SopA), which cleaves IcsAα on lateral region of the bacteria (Shere *et al.*, 1997, Tran *et al.*, 2013). IcsA requires other membrane proteins for its proper localization on outer membrane, as deletion of the cytoplasmic membrane protein insertase YidC abolished the proper IcsA localization (Gray *et al.*, 2014). Recently, it has been found that the intracellular expression of IcsA is depend on the presence of formate (Koestler *et al.*, 2018a), which is a byproduct produced by metabolizing host cytosolic carbon.

1.5.2 The polar distribution of IcsA

IcsA preferably displayed at the old pole of the bacterium (Charles *et al.*, 2001). Mutagenesis studies suggested a region within IcsA played an important role in this polar distribution ($IcsA_{506-620}$) (Doyle *et al.*, 2015a). Apart from IcsA itself, it has been reported that the periplasmic region of FtsQ and RpoS are also involved in the IcsA polar distribution (Fixen *et al.*, 2012), yet the fundamental mechanism remains to be discovered. Recently, it has been found that IcsA can interact with cardiolipin, which is preferably located at the bacteria pole due to its biochemical characteristics (Rossi *et al.*, 2017). Although it provided a model that by interacting with cardiolipin, IcsA is directed to the pole of the bacteria, it did not satisfactorily explain the unipolar distribution of IcsA, specifically,

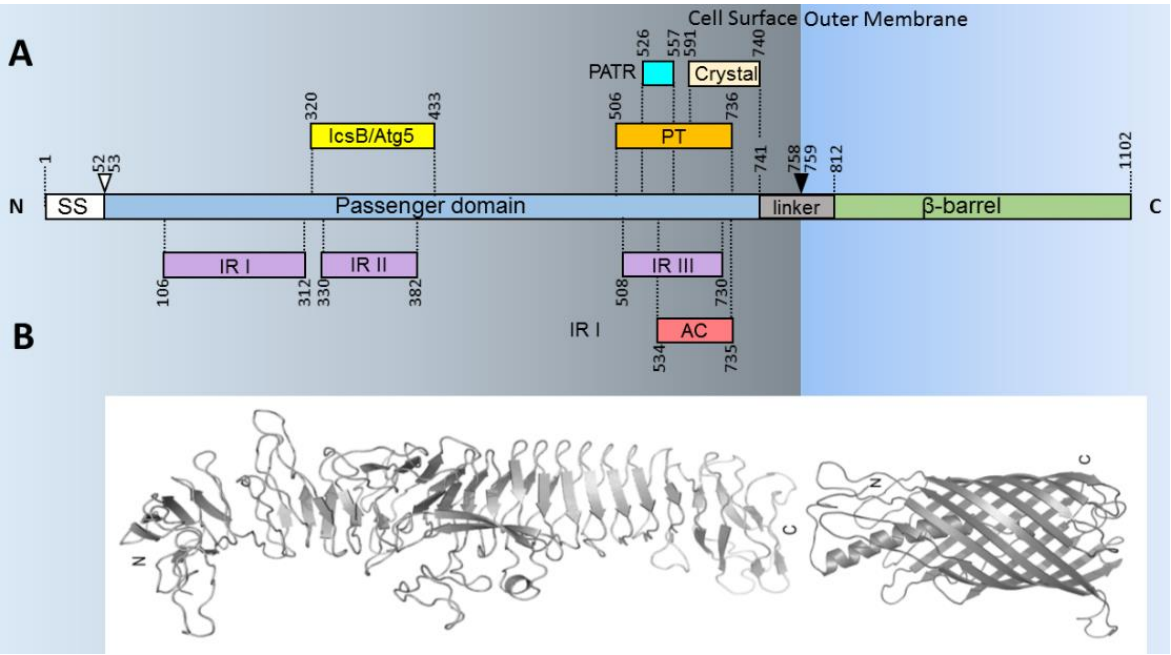

Figure 1.6. Structure of IcsA protein.

A) Schematic structure of IcsA protein and its primary features. IcsA protein comprises an N-terminal signal sequence (SS, white, $IcsA_{1-52}$) for its secretion, a passenger domain (blue, $IcsA_{53-740}$) for its function, a β-barrel domain (green, $IcsA_{812-1102}$) for passenger translocation, and a linker region (grey, $IcsA_{741-812}$) that connects passenger to barrel. The mature IcsA beyond the bacterial surface is cleaved by IcsP at $IcsA_{758}$ (dark arrow). At the C terminus end of the passenger, there is a polar targeting region (PT, orange, $IcsA_{506-736}$) that responsible for IcsA asymmetric distribution. Interacting regions (IR) of passenger to N-WASP protein (purple, $IcsA_{185-312}$, $IcsA_{330-382}$, and $IcsA_{508-730}$). $IcsA_{320-433}$ (yellow) is targeted by host cell autophagy protein Atg5, and masked by IcsB. The putative autochaperone (pink, $IcsA_{534-735}$) (May *et al.*, 2012) and passenger-associated transport repeat (PATR, light blue, $IcsA_{526-557}$) (Doyle *et al.*, 2015b) were conserved structures in ATs and identified in IcsA passenger. The stable core (light yellow, $IcsA_{591-740}$) of passenger was crystallised and the 3D structure is available (Kuhnel & Diezmann, 2011). **B)** I-TASSER predicted IcsA passenger structure and predicted β-barrel structure.

the localization on the old pole rather the septum forming pole. This polar distribution is further maintained by the asymmetrically distributed IcsP, which cleaves IcsA passenger off the bacterial surface on the septum forming pole (Tran *et al.*, 2013). However, IcsP does not determine the polarity of IcsA, as knocking out IcsP did not abolish the polarity of IcsA completely (Tran *et al.*, 2015).

1.5.3 Actin based motility

The polar distribution of IcsA results in the accumulation of F-actin at the pole of the bacterium, which is essential in performing actin based motility (ABM) (Bernardini *et al.*, 1989). IcsA is essential and sufficient for ABM in that mutations in *icsA* mutants did not develop comet tails; *E. coli* expressing IcsA were able to form actin tails and demonstrate ABM; and inert particles coated with IcsA demonstrated ABM (Goldberg & Theriot, 1995). The ABM is achieved by the binding of three interacting regions (IRI, IRII and IRIII) on IcsA passenger to Neural Wiskott-Aldrich syndrome protein (N-WASP), which in turn recruits Arp2/3 complex, resulting in the polymerization of actin in the host cell cytosol (Suzuki & Sasakawa, 1998, Egile *et al.*, 1999, Teh & Morona, 2013). The efficient spread of *Shigella* in the epithelial lining was reported through targeting a tricellular junction protein, tricellulin, and was aided by phosphoinositide 3-kinase, clathrin, Epsin-1 and Dynamin-2 (Fukumatsu *et al.*, 2012, Lum & Morona, 2014a).

Apart from IcsA itself, other molecules are also involved in the intercellular spread process. It has been known that *Shigella* have dysregulated LPS chain length will affect the spread of bacterial between host cell, and it was through a masking effect on IcsA (Morona *et al.*, 2003). Deletion of a periplasmic protein, Apyrase or PhoN2, which is located at the same pole to IcsA (Scribano *et al.*, 2014), resulted in *Shigella* generating smaller plaques in cell monolayers (Santapaola *et al.*, 2006), while deletion of an outer membrane protein OmpA made *Shigella* unable to generating plaques (Ambrosi *et al.*, 2012). In both cases, IcsA expression is not altered and can form actin comet tails, yet the distribution of IcsA is affected. Further research on PhoN2 failed to show interaction between the PhoN2 and IcsA, but revealed an interaction between PhoN2 and OmpA (Scribano *et al.*, 2014, Scribano *et al.*, 2016). However, to date, it is still unknown how these proteins are implicated in affecting the function of IcsA.

1.5.4 IcsA is a target of autophagy

While IcsA does not require the T3SS to be secreted onto the surface of the bacteria, it is masked by a T3SS secreted effector protein IcsB binding to an area of passenger domain ($IcsA_{320-433}$) (Kayath *et al.*, 2010), and this region is otherwise important in binding to an autophagic response system protein Atg5 (Ogawa *et al.*, 2005), resulting in the escape of intracellular *Shigella* from autophagy. This indicates the interaction between T3SS and IcsA, demonstrating a potential regulation of IcsA activity by the T3SS.

1.5.5 The autotransporters

Sequence analysis of the mutations revealed that IcsA has the characteristics of an autotransporter (Lett *et al.*, 1989). IcsA is classified as a type Va autotransporter, and belongs to the AIDA autotransporter family. Members of this family including some well characterised autotransporters AIDA-1 (Benz & Schmidt, 1992), Ag43 (Henderson & Owen, 1999), TibA (Lindenthal & Elsinghorst, 1999), which all play important roles in bacterial adherence.

Type Va autotransporters are proteins with a conserved β-barrel structure that inserts into the outer membrane and a passenger domain, which is secreted to the surface of the bacteria and determines the function of the protein (Leyton *et al.*, 2012). Pertactin, which functions as an adhesin mediating the interactions of *Bordetella pertussis* to human respiratory epithelial cells, is the first autotransporter for which the structure of the passenger domain was solved (Emsley *et al.*, 1996). Following which, the structure of Antigen 43 (Ag43) (Heras *et al.*, 2014), which is responsible for the biofilm formation of uropathogenic *E. coli*; Hbp (Otto *et al.*, 2005), which is a heme binding protein from pathogenic *E. coli*; Pet (Domingo Meza-Aguilar *et al.*, 2014), which is a cytoskeleton-altering toxin from pathogenic *E. coli*; TibA (Lu *et al.*, 2014), which mediates the adherence of enterotoxigenic *E. coli* to a variety of human cells; VacA (Gangwer *et al.*, 2007), which is a toxin from *Helicobacter pylori*; IgA1 protease (Johnson *et al.*, 2009), which is a protease from *Haemophilus influenzae* and is responsible for the degradation of immunoglobulin A1; and Hap (Meng *et al.*, 2011), which is an adhesin from *Haemophilus influenzae*; were all solved. Although the passenger domains of these proteins are different in their sequences and

functions, they adapt similar structures, which is characterized as extended triangular β-helices formed by multiple β-sheets. While the full-length structure of IcsA passenger domain remains to be solved, structures of several regions have been solved ($IcsA_{591-740}$ and $IcsA_{419-758}$). Similar to the above autotransporters, IcsA passenger domain also folds into a prism-like 3D structure (Figure 1.7) (Kuhnel & Diezmann, 2011, Leupold *et al.*, 2017). The overall architecture of the protein adapts an L shape (Mauricio *et al.*, 2017), similar to the structure of Ag43 (Heras *et al.*, 2014), which was reported to have a self-association ability. IcsA has also been found to have self-association ability (May *et al.*, 2012), although the exact outcomes of this self-association has not yet been fully elucidated.

1.5.6 IcsA is recognized as an adhesin

Despite IcsA being known to be important in both ABM and inducing host autophagy process in the absence of IcsB, it has been found to act as an adhesin. Brotcke-Zumsteg *et al.* (2014) reported that *S. flexneri* lacking IpaB and IpaD hyper-adhere to the host cells via their pole, indicating a potential role of IcsA in this process, since IcsA has a polar localisation. Indeed, deleting IcsA in these mutant stains abolished polar adhesion and reduced adherence to host cells. This decreased adhesion was also observed by Mahmoud *et al.* (2016) using an *icsA* knockout *Shigella sonnei*. IcsA is also involved in the human enteric α-defensin 5 enhanced *Shigella* adherence and invasion (Xu *et al.*, 2018). Moreover, IcsA was able to promote adhesion of an *E. coli* B strain, and the protease cleavage pattern of IcsA in adhesive and non-adhesive strains was different (Brotcke-Zumsteg *et al.*, 2014). Random insertions (May & Morona, 2008) (5 aa) on two sites (i148 and i386) of IcsA passenger abolished the hyper-adherence phenotype in *S. flexneri ΔipaB* and *S. flexneri ΔipaD*. Hence these studies suggested that IcsA functions as an adhesin in a certain conformation, and several amino acids or regions might act in adherence in a cooperative manner. Using a limited proteolysis assay, IcsA was found to have different conformations in the hyper-adherent strains compared to the wild type *Shigella*, and this conformational change seems to be related to the increased adherence, since it can be observed when expressing IcsA in *E. coli*. This implies that in *Shigella*, IcsA adherence activity is tightly regulated by a factor, since *Shigella* lacking the T3SS components do not have an IcsA-dependent hyper-adherence, while in *E. coli*, IcsA can promote adherence by itself. In addition, the bile salt sodium

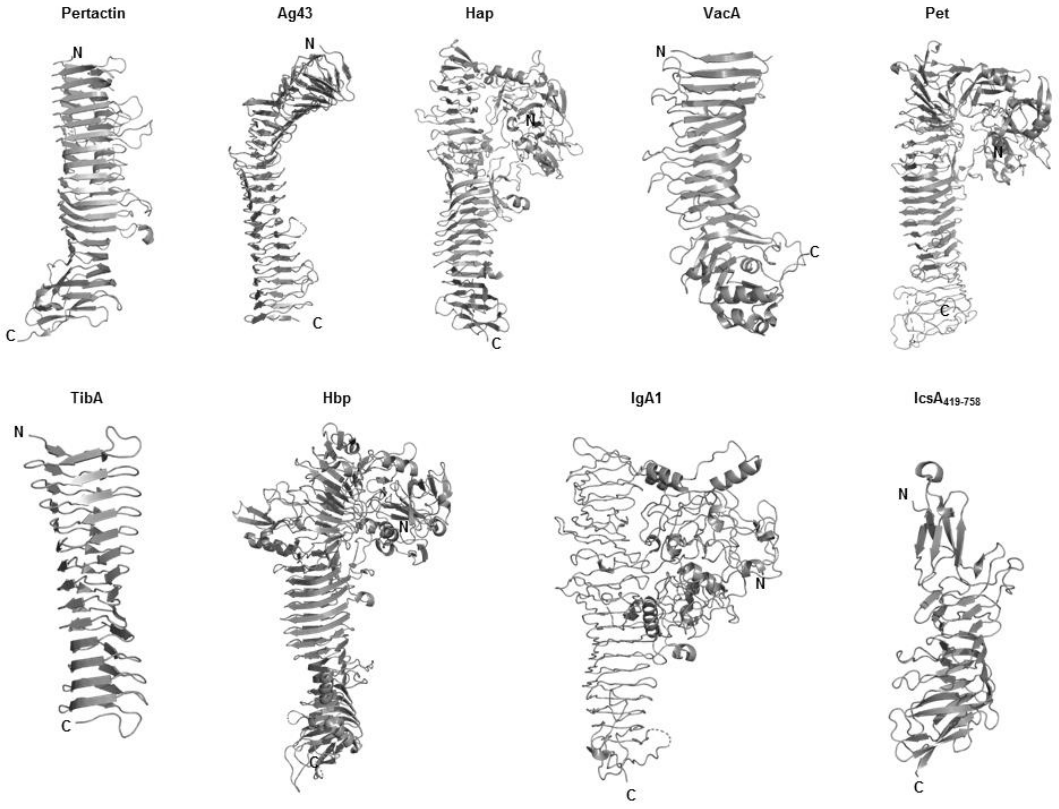

Figure 1.7. Autotransporters with solved structures

Ribbon representation of solved autotransporter structures including Pertactin (*B. pertussis*, 1DAB), Ag43 (*E. coli*, 4KH3), Hap (*H. influenzae*, 3SYJ), VacA (*H. pylori*, 2QV3), Pet (*E. coli*, 4OM9), TibA (*E. coli*, 4Q1Q), Hbp (*E. coli*, 1WXR), IgA1 (*H. influenzae*, 3H09), partial IcsA passenger domain $IcsA_{419\text{-}758}$ (*Shigella*, 5KE1). All the structures were acquired from the protein database (PDB) with their file number shown in the bracket.

deoxycholate (DOC) was also found to induce a hyper-adherence phenotype in *S. flexneri* in both an IcsA- and T3SS-dependent manner (Brotcke-Zumsteg *et al.*, 2014). Though the exact mechanism of DOC, IpaB and IpaD deficiency induced hyper-adherence in *S. flexneri* is unknown, IcsA was found essential and sufficient to promote the adhesion to host cells.

1.6. Research Plan

As described above, understanding how *Shigella* initially attaches to host cells which leads to subsequent colonization and invasion is a key step in understanding *Shigella* pathogenesis. Therefore, investigating the mechanism of IcsA-dependent adhesion (Brotcke-Zumsteg *et al.*, 2014) will expand our knowledge of shigellosis, and contribute to therapeutic intervention and strategies.

This leads to the question as to what parts of IcsA are functioning in adhesion to host cells, what host cell type of IcsA is targeting, and what is the cellular receptor(s) of IcsA. Moreover, as IcsA completely conserved in all *Shigella* species, and immunogenic in *Shigella* infected patients (Oaks *et al.*, 1986), it is therefore important to investigate its adhesion function as this will contribute to understanding early steps in pathogenesis of the whole genus.

1.7. Aims/Objectives of the project

1.7.1 Aim 1: To investigate the regions in IcsA involved in the adherence

- To construct the hyper-adherent stains *S. flexneri* 2a *ΔipaD* and *S. flexneri* 2a *ΔipaDΔicsA*, and to examine their ability in adherence
- To demonstrate the interactions between IcsA and host cell surface
- To screen the regions which are essential for IcsA adherence with an IcsA insertion mutant library
- To purify IcsA passenger in a stable and soluble form
- To investigate the molecular basis of IcsA adherence regions

1.7.2 Aim 2: To investigate the conformations of IcsA involved in the adherence

- To purify IcsA passenger in a native form
- To investigate the role of the IcsA adhesin region in the adhesin associated conformation

1.7.3 Aim 3: To identify the cellular targets and receptors for IcsA.

- To identify the receptors for IcsA on HeLa cells
- To validate the interactions between the putative receptor(s) and IcsA passenger protein

1.7.4 Aim 4: To characterise IcsA in the hyper-adherence phenotype induced by DOC

- To investigate how IpaD and IcsA was affected in the DOC treated *S. flexneri*
- To investigate the conformations of IcsA in the DOC induced hyper-adherent *S. flexneri*

Chapter Two

MATERIALS AND METHODS

Chapter 2: Methods and Materials

2.1. Bacterial strains and plasmids maintenance

2.1.1 Bacteria strains

Bacteria strains involved in this work are listed in Appendix A: Bacterial strains, and all the strains were stored at -80 °C in storage media (Section 2.1.3.3). Whenever required, bacteria were streaked out on a solid medium plate with appropriate selection additives.

2.1.2 Plasmids

Plasmids used in this work were listed in Appendix B: Plasmids. Unless specified, all the plasmids were maintained in *E. coli* DH5α.

2.1.3 Bacterial growth media

2.1.3.1 Solidified growth media

Strains were grown on Tryptic Soy (TS) agar [15 g/L agar (Becton, Dickinson and Co.; BD), 30 g/L TSB soybean-casein digest (BD)], or on Lysogeny broth (LB) (Bertani, 2004) agar [10 g/L tryptone (BD), 5 g/L yeast extract (BD), 5 g/L NaCl, 15 g/L agar].

2.1.3.2 Liquid growth media

Strains were streaked out on solidified media and a single colony was picked to inoculate an LB broth [10 g/L tryptone (BD), 5 g/L yeast extract (BD), 5 g/L NaCl]. Bacterial growth phase was measured by optical absorbance at 600 nm (OD_{600}), where the reading of 0.4-0.8 was considered as bacteria growing at mid- exponential phase.

2.1.3.3 Storage media

Strains grown on solidified media were recovered and resuspended in 1 mL storage media [10 g/L peptone (BD), 30% (v/v) glycerol] and immediately stored at -80 °C.

2.2. Mammalian cell lines and culture conditions

2.2.1 Mammalian cell lines

Cell lines used in this thesis were HeLa cells (human cervical epithelial adenocarcinoma cells, ATCC CRM-CCL-2), and COS-7 cells (grivet kidney fibroblast cells, ATCC CRL-1651).

2.2.2 Cell line culture conditions and maintenance

All cells were maintained in the medium recommended by the manufacture; (Eagle's Minimum Essential Medium (MEM) for HeLa cells, Dulbecco's modified Eagle's medium (DMEM) for COS-7 cells and supplemented with 5% (v/v) fetal calf serum (FCS), 4 mM glutamine, 100 U/mL penicillin and 100 U/mL streptomycin. All the cells were cultured at 37 °C with 5% carbon dioxide (CO_2).

When growing in 75 cm^2 culture flask and reaching over 80% confluence, cells were washed with phosphate-buffered saline (PBS) to remove all traces of serum that contains trypsin inhibitor and then dispersed by adding 2 to 3 mL of 0.25% (w/v) Trypsin-0.53 mM ethylenediaminetetraacetic acid (EDTA) solution and incubating at 37 °C for 10 min. Trypsinised cells were then resuspended in culture medium and subcultured into 75 cm^2 culture flask with appropriate subculture ratio (1:10 for both HeLa and COS-7 cells).

2.2.3 Cell line storage

Cells were stored in corresponding medium supplemented with 5% (v/v) dimethyl sulfoxide (DMSO) at -80 °C or in liquid nitrogen.

2.3. Antibodies and antibiotics

2.3.1 Antibodies and antisera

Antibodies used in this thesis were rabbit anti-IcsA polyclonal antibodies (pAbs), in-house made, (Van Den Bosch *et al.*, 1997), mouse anti-His_6 monoclonal antibody (mAb, Genscript), mouse anti-DYKDDDDK (anti-FLAG) mAb (Genscript), rabbit anti-Myosin IIA pAbs (Sigma), rabbit anti-Myosin IIB pAbs (Sigma), mouse anti-IpaD pAbs

(gifted by Prof. Nikolai Petrovsky, Flinders University). For Western immunoblotting, horse radish peroxidase (HRP) conjugated goat anti-rabbit or goat anti-mouse secondary antibodies (KPL) were used. For immunofluorescence microscopy, donkey anti-mouse AlexaFluor 488 or donkey anti-rabbit AlexaFluor 488 secondary antibodies (Life Technologies) were used.

2.3.2 Antibiotics and additives

For selection and plasmid maintenance, antibiotics were added to bacterial growth medium as appropriate: ampicillin at 100 µg/mL, kanamycin at 50 µg/mL, tetracycline at 10 µg/mL, chloramphenicol at 25 µg/mL, gentamycin at 40 µg/mL, and spectinomycin at 100 µg/mL. For screening virulence plasmid carrying *Shigella* strains, Congo red (Sigma) dye was supplemented to TS agar at the concentration of 0.01% (w/v). *Shigella* strains harboring virulence plasmid will develop red colonies at 37 °C as the result of binding of Congo red dye to the hydrophobic virulence factors encoded by the virulence plasmid. For blue-white colony screening with strains harboring pGEM-T Easy (Promega) plasmid, LB agar were supplemented with 0.5 mM Isopropyl β-D-1-thiogalactopyranoside (IPTG) and 20 µg/mL 5-bromo-4-chloro-3-indolyl-β-D-galactopyranoside (X-gal). When expressing protein controlled by a P_{BAD} promoter, glucose at 0.2% (w/v) was added to suppress expression and L-arabinose at 0.2% (v/w) was added to induce expression.

2.4. DNA technique

2.4.1 DNA preparation

2.4.1.1 Chromosomal DNA extraction

For bacterial chromosomal DNA extraction, bacteria were cultured in 10 mL LB broth for 16 h, harvested by centrifugation (4500×g, 7 min) and resuspended in 3 mL 0.85% (w/v) saline by vortexing. Proteins were removed by mixing with 3 mL Tris-equilibrated phenol (pH 7.5) followed by centrifugation (4500×g, 7 min). The aqueous layer containing DNA was then collected and DNA was precipitated by adding 3 mL of cold 100% isopropanol and incubated at -20 °C. The precipitated DNA was then collected and washed with 70% (v/v) ethanol and dissolved in Milli-Q (MQ) water, and stored at -20 °C.

2.4.1.2 Plasmid Isolation

Plasmid DNA was isolated from bacterial cultures (LB, 10 mL) grown for 16 h using QIAprep Spin Miniprep kit (Qiagen) as per manufacture's protocol. All plasmids were eluted in MQ water and stored at -20 °C.

2.4.1.3 Crude bacterial DNA preparation

When used for colony PCR screening purposes, bacterial DNA sample were prepared by resuspending single colonies of bacteria in 100 µL of MQ water and heated at 100 °C for 5 min. Crude bacterial DNA preparation were then obtained by centrifugation (16,250×g, 1 min).

2.4.1.4 DNA fragment purification

For DNA fragments amplified by polymerase chain reaction (PCR) or generated by restriction endonuclease enzyme digestion, purification was performed by using the GFX PCR DNA and Gel Band Purification Kit (GE Healthcare) as per manufacture's protocol. All DNA was eluted in MQ water and stored at -20 °C.

For DNA fragments amplified by PCR and used for *in vivo* genetic engineering, PCR products were precipitated by adding NaCl to a final concentration of 0.5 M and ethanol to a final concentration of 75% (v/v), followed by an incubation on ice for 20 min. The DNA fragments were then recovered by centrifugation (16,100 ×g), washed with 75% (v/v) ethanol, and air dried at room temperature. The fragments were then solubilised in 50 µL of MQ water and kept on ice before use.

2.4.1.5 Oligonucleotides

All oligonucleotides [Appendix C: Oligonucleotides] were ordered from Integrated DNA Technologies (IDT), resuspended in MQ water at the concentration of 100 µM for storage at -20 °C, and further diluted in MQ to 10 µM before use in PCR at 0.5-2 µM.

2.4.1.6 DNA quantitation

DNA was quantified using a NanoDrop 2000c Spectrophotometer (Thermo Scientific) by measuring the absorption at 260 nm. A ratio of the absorbance at 260 nm to the absorbance at 280 nm ($A_{260/280}$) around 1.8 was considered as a pure DNA preparation.

2.4.1.7 DNA sequencing

Sample was prepared by adding oligonucleotides at the final concentration of 0.8 µM to 600-1500 ng of purified DNA template to a total volume of 12 µL. The samples were sequenced by the Australia Genome Research Facility (AGRF) sequencing service.

2.4.2 DNA manipulation

2.4.2.1 Restriction endonuclease digestion

DNA was digested using appropriate restriction endonucleases purchased from New England Biolabs (NEB) and used per manufacture's protocol with supplied buffer. Following digestion, enzymes were heat inactivated where possible or otherwise removed by using the GFX PCR DNA and Gel Band Purification Kit (GE Healthcare).

2.4.2.2 DNA phosphorylation

To prepare the PCR amplified DNA for ligation, DNA fragments were 5' phosphorylated using T4 polynucleotide kinase (PNK, NEB), according to manufacturer's protocol.

2.4.2.3 DNA ligation

Ligation of linear DNA fragments was performed using T4 DNA ligase (NEB) according to supplier's protocol. Samples were incubated at 16 °C for 2 h or at 4 °C overnight to maximise the yield of product.

For ligating fragments into pGEMT-Easy, fragments were polyadenylated according to manufactures' protocol (Promega), and ligated into pGEMT-Easy as above.

2.4.2.4 Polymerase chain reaction (PCR)

PCR reactions were prepared according to supplier's protocol (NEB). Deoxynucleic triphosphates (dNTPs) were purchased from Sigma. All the reactions were conducted in an Eppendorf Mastercycler Gradient thermocycler. The reaction conditions were as per supplier's (NEB) recommendations. Primer annealing temperature was calculated using the Tm Calculator tool supplied by NEB (https://tmcalculator.neb.com), where primer's Tm exceeding 72 °C, the annealing step was skipped, and two-step PCR reaction were performed instead.

For screening purposes, Taq polymerase (NEB) was used to amplify DNA fragments with appropriate oligonucleotides. For cloning purposes, Q5 high fidelity polymerase (NEB) was used instead.

2.4.2.5 Electrophoretic separation of DNA and visualization

For DNA size analysis and fragments separation, DNA sample was mixed with DNA loading dye [1 mg/mL bromophenol blue, 20% (v/v) glycerol, 0.1 mg/mL RNase] at the ratio of 1:9. Samples were separated with 1, 1.5 or 2% (w/v) agarose TBE [70 mM Tris, 20 mM boric acid, 1 mM EDTA] gel containing RedSafe nucleic staining solution (iNtRON Biotechnology) at 20,000× dilution. Size marker used were SPP1 phage DNA digested by EcoRI and made in house (sizes (kb): 8.51, 7.35, 6.11, 4.84, 3.59, 2.81, 1.95, 1.86, 1.51, 1.39, 1.16, 0.98, 0.72, 0.48, 0.36, and 0.09). Gels were electrophoresed at 120V for 30 min and visualised using a GelDoc XR system (Biorad).

2.4.3 Inverse PCR deletion, addition and substitution

For in-frame deletion of protein coding regions within plasmids, oligonucleotide primers were designed to target the adjacent sequences of the region to be deleted in opposite direction. The entire plasmid was PCR amplified (Section 2.4.2.4), phosphorylated (Section 2.4.2.2) and ligated (Section 2.4.2.3).

For in-frame addition or substitution, primers were designed to target the adjacent sequences of the desired region in opposite direction, and the sequences encoding the addition or substitution were incorporated at the 5' end of each primer. The entire plasmid

was PCR amplified (Section 2.4.2.4), phosphorylated (Section 2.4.2.2) and ligated (Section 2.4.2.3).

2.4.4 PCR coupled with Restriction enzyme cloning

For generating expression constructs, the protein coding sequence was PCR amplified (Section 2.4.2.4) using oligonucleotides flanked with appropriate restriction enzyme recognition sequences and 5 random nucleotides overhang at 5' end for efficient binding of restriction endonuclease enzymes. Amplicons were then digested with appropriate restriction endonuclease enzymes (Section 2.4.2.1) and ligated (Section 2.4.2.3) to the Multi-cloning site (MCS) of the plasmid vector digested with the same enzymes.

2.4.5 Overlap extension PCR

For in-frame addition of affinity tags, a pair of hybrid oligonucleotide primers were designed containing complementary sequence to both the desired insert and the adjacent sequences to the target site. These primers were used to PCR amplify (Section 2.4.2.4) fragments containing full insert flanked with over 50 base pairs (bp) sequences homologous to the adjacent region of the targeted site. The fragment was then used as a mega-primer to perform a secondary PCR (Section 2.4.2.4) with the target plasmid to generate a nicked hybrid vector. The parental plasmid was eliminated by DpnI treatment (Section 2.4.2.1), leaving the final construct ready for transformation.

2.4.6 Site-directed mutagenesis with degenerated primers

Random single amino acid substitutions were performed using the QuickChange Lighting Site-directed Mutagenesis kit (Aglient Technologies) according to manufacturer's protocol. Primers were designed using the primer design tool supplied by the manufacturer (https://www.genomics.agilent.com/primerDesignProgram.jsp).

2.5. Gene cloning

2.5.1 Bacterial competent cells preparation

2.5.1.1 Chemical competent cells

Bacterial cells from 16 h incubation at 37 °C with aeration were diluted 1 in 20 in 10 mL broth and incubated at 37 °C to an OD_{600} of 0.5. Bacterial cells were then collected by centrifugation (4,500 ×g, 4 °C, 7 min) and sequentially washed by precooled 0.1 M $MgCl_2$, 0.1 M $CaCl_2$. Bacterial cells were then resuspended in 0.1 M $CaCl_2$ solution containing 15% (v/v) glycerol, and stored at -80 °C.

2.5.1.2 Super competent *Shigella* bacterial cells

For smooth *Shigella* strains and strains used for recovering constructs that were of low yield, and to ensure a high transformation efficiency, bacterial strains were prepared differently (Inoue *et al.*, 1990). Briefly, bacteria were grown overnight at 37 °C for approximately 8 h to reach stationary growth phase, and then were diluted in 250 mL of SOB medium [20 g/L tryptone [BD], 5 g/L yeast extract [BD] and 0.5 g/L NaCl, 2.5 mM KCl, 10 mM $MgCl_2$, pH 7.0] in different ratios; 1:10, 1:20 and 1:50. Cultures were then incubated at 18 °C for 16 h with vigorous shaking (250-300 rpm). The bacterial culture that has the OD_{600} reading closest to but under 0.55 were then continued to grow to OD_{600} reading of 0.55. Bacterial cells were then collected by centrifugation (4,500 ×g, 4 °C, 10 min), and washed with 80 mL of precooled transformation buffer [55 mM $MnCl_2$, 15 mM $CaCl_2$, 250 mM KCl, 10 mM PIPES, pH 6.7], followed by centrifugation as above. The bacterial pellet was then resuspended in 20 mL of ice cold transformation buffer, and 1.5 mL of DMSO was added and 100 µL aliquots were stored at -80 °C.

2.5.1.3 Electrocompetent cells

Bacterial cell culture (10 mL) grown to an OD_{600} of 0.5 after subcultured from an 16 h culture were collected by centrifugation (4,500 ×g, 4 °C, 7 min), washed twice with 10 mL ice cold MQ water, and resuspended in 200 µL of 10% (v/v) glycerol, and stored at -80 °C.

2.5.2 Transformation

2.5.2.1 Heat shock

Chemical competent cells (100 µL) thawed on ice were mixed with 2-10 µL of purified DNA and left on ice for 20 min. Bacterial cells were then heat shocked at 37 °C for 3 min or 42 °C for 90 s, and immediately return on ice for another 5 min. The mixture was then supplemented with 900 µL of SOC medium [SOB with 20 mM glucose] and incubated at 37 °C (or 30 °C if harboring a temperature sensitive plasmid) for 30-90 min before spreading on LB agar selection plates. Plates were then incubated at appropriate temperature for 16 h to recover transformants.

2.5.2.2 Electroporation

Electrocompetent bacterial cells (100 µL) thawed on ice were mixed with 2-10 µL of purified DNA in a sterile electroporation cuvette (0.2 cm gap, BioRad) and incubated on ice for 5 min. Bacterial cells were then electroporated (BioRad Gene Pulser, 2.5 kV, 25 µF, Capacitance extender 960 µF, Pulse Controller 200 Ω) and supplemented with 900 µL SOC medium. The mixture was incubated at 37 °C (or 30 °C if harboring a temperature sensitive plasmid for 30-90 min) before spreading on LB agar selection plates. Plates were then incubated at the appropriate temperature for 16 h to recover transformants.

2.6. *In vivo* genetic engineering

Bacterial *in vivo* genetic engineering was performed using the λ Red mutagenesis as described by (Datsenko & Wanner, 2000). Briefly, primers were designed to PCR amplify the *frt-kan-frt* cassette from pKD13 or pKD4 plasmid with 50 bp nucleotides homologous to the adjacent region of the target gene. Ten PCR reactions were combined and the amplicons were purified and eluted to a total volume of 50 µL (Section 2.4.1.4). The parental plasmid was eliminated by DpnI digestion (Section 2.4.2.1). Strains to be mutated harbouring a plasmid pKD46 were grown at 30 °C in the presence of 0.2% (v/v) arabinose and made electrocompetent. The purified PCR amplicon was then electroporated into 100 µL of the competent cells. The transformants that grew at 37 °C were then patched onto LB agar containing ampicillin and appropriate antibiotics, respectively, to confirm the loss of

pKD46 and the incorporation of the resistance cassette. The successful replacement of target gene with the resistance gene cassette was then confirmed by PCR. In order to avoid any polar effect, a plasmid, pCP20, carrying yeast FLP recombinase recognising *frt* sequences was then electroporated in the mutant. Transformants were recovered by using LB agar containing ampicillin and grown at 30 °C. Colonies were picked and inoculated in 10 mL LB broth grown at 30 °C for 16 h and incubated at 42 °C for another 3 h. Cultures were diluted and spread on an LB agar plate and incubated at 37 °C for 16 h. The loss of pCP20 and the resistance gene cassette was then confirmed by patching colonies onto LB agar with or without chloramphenicol antibiotics. Mutants were confirmed by PCR (Section 2.4.2.4) with the appropriate primers and DNA sequencing (Section 2.4.1.7).

2.7. Protein techniques

2.7.1 Bacterial whole cell sample preparation

Bacterial whole cell lysates were prepared by collecting 5×10^8 cells grown at mid-exponential phase (OD_{600} of 0.4-0.8) by centrifugation (16,250 ×g, 1 min). The pellet was then resuspended in 100 µL of 2× SDS-PAGE buffer [80 mM Tris, 2% (w/v) SDS, 10% (v/v) glycerol, 0.0006% (w/v) bromophenol blue, 0.1 M DTT] (Lugtenberg *et al.*, 1975) and heated at 100 °C for 5-10 min.

2.7.2 TCA precipitation of secreted protein samples

When analysing protein secreted by bacterial strains, bacteria were grown for 18 h in 10 mL LB broth, and the culture supernatant was recovered by centrifugation (16,250 ×g, 5 min, 4 °C), followed by filtration through a membrane (0.45 µm pore size) to exclude bacterial cells. The filtered culture supernatant was then cooled on ice and protein was precipitated by adding 10% (v/v) Trichloroacetic acid (TCA) and incubation on ice for 20 min. Protein was then collected by centrifugation (16,250 ×g, 5 min, 4 °C), washed twice by 500 µL of ice cold acetone and centrifuged as above. The protein pellet was then air dried and resuspended in 2× SDS-PAGE buffer and heated at 100 °C for 5-10 min.

For protein filaments secreted by *S. flexneri ΔipaD*, filaments were washed three times with 1 mL of PBS and dissolved in 500 µL of 2× SDS-PAGE buffer and heated at 100 °C for 5-10 min.

2.7.3 IcsA protein purification

2.7.3.1 IcsA protein purification from inclusion bodies (IB)

For IcsA passenger purification from IB, an 18 h cultured *E. coli* TOP10 [pMDBAD::$his_{12\times}$-$IcsA^{53\text{-}740}$] was inoculated 1 in 1000 into 8 L of auto-induction Terrific Broth medium [22 g/L Bacto Tryptone (BD), 11 g/L Bacto yeast extract (BD), 2.94 g/L NH_4Cl, 2.2 mM $MgSO_4$, 5.5% (v/v) glycerol, 1.157 g/L KH_2PO_4, 6.27 g/L K_2HPO_4] containing a mixture of glucose and arabinose in the ratio of 0.1%:0.3% (w/v) and incubated at 37 °C 18 h with aeration (200 rpm). Bacterial cells were harvested by centrifugation (10,000 ×g, 10 min) and lysed by cell disruptor (30 kpsi, Constant Cell Disruption System, Constant System Ltd) in 250 mL of TN buffer [50 mM Tris pH 7.0, 150 mM NaCl] containing four EDTA-free protease inhibitor tablets (Roche). The IBs were recovered by centrifugation of the cell lysate (20,000 ×g, 10 min), and pre-cleaned by 120 mL of detergent wash buffer [50 mM Tris, 1M NaCl, 2% (v/v) Triton X-100, 4 mM DDM and 2% (w/v) DOC, pH 8.0] to exclude membranes fractions. IcsA passenger protein from IB was then washed twice with 120 mL of TN buffer, and solubilised in 50 mL of protein solubilisation buffer [8 M urea, 50 mM NaCl, 50 mM Tris, 10 mM imidazole, pH 8.0], followed by centrifugation (185,000 ×g, 1 h). Solubilised IcsA passenger protein was loaded on a 5 mL His-trap column (GE healthcare, #17524801), washed and eluted by increasing concentration (10 mM to 500 mM in 45 mL) of imidazole by using an ÄKTAprime plus (GE healthcare).

2.7.3.2 Supernatant secreted IcsA protein purification

For secreted IcsA passenger purification, an 18 h cultured *E. coli* C43(DE3) [pCDF-Duet::$IcsA^{54::FLAG\times3}$-IcsP] (JQRM115) was subcultured 1 in 20 into 6 L of LB broth supplemented with 1 mM IPTG, and incubated at 30 °C for 16 h. The bacterial culture was then collected by centrifugation (10,000 ×g, 10 min, 4 °C) and filtered by a Nalgene Rapid-Flow Filter (0.2 µm asymmetric Polyethersulfone (aPES) membrane, Thermo Fisher Scientific). Proteins in the filtered culture supernatant were then concentrated and exchanged

into 50 mL of TBS buffer [50 mM Tris, 150 mM NaCl, pH 7.5] using a Vivaflow 200 (30,000 MWCO PES membrane, Sartorius). Concentrated protein was then loaded onto a TBS pre-equilibrated polypropylene column (Thermo Scientific) prepacked with 2 mL of anti-DYKDDDDK G1 affinity resin (GenScript, #L00432). The column was washed by TBS three times, and protein was then eluted in 10 mL of acidic elution buffer [0.1 M glycine, pH 3.0]. The pH of eluates was then adjusted to 7.0 by Tris buffer (1 M Tris, pH 9.0). Protein was then concentrated into 1 mL by Vivaspin 6 column (10 kDa MWCO, GE healthcare, #14VS0608) via centrifugation (4,000×g, 10 min, 4 °C).

2.7.4 Protein purification by size exclusion chromatography (SEC)

Proteins purified by affinity purification were further cleaned by SEC on a Superdex^{TM} 200 increase column 10/300 GL (GE Healthcare, #28990944) using an ÄTKA pure system (GE Healthcare). Elution fractions were concentrated using Vivaspin 6 (10 kDa molecular weight cut off, MWCO, GE Healthcare). Gel filtration markers Kit (29 kDa, 66 kDa, 150 kDa, 200 kDa, 443 kDa, 669 kDa and 2000 kDa; Sigma, #SLBN3608V) were used to calculate the apparent molecular size of purified proteins.

2.7.5 Protein dialysis

Protein was loaded and sealed in a buffer pre-equilibrated dialysis tube (CelluSep T4, MWCO 12-14 kDa, CelluSep, #1430-25) and incubated in 4 L of desired dialysis buffer for at least 18 h with stirring (150 rpm) at room temperature or 4 °C.

2.7.6 Affinity purification of anti-IcsA pAbs

Rabbit anti-IcsA pAbs were purified from antisera acquired as described in Van Den Bosch *et al.* (1997). Briefly, purified IcsA proteins were separated by a self-cast SDS-PAGE gel and transferred onto a nitrocellulose membrane (BioRad, #1620112). Membrane that contains IcsA protein was then excised and blocked with 10 mL of 5% (w/v) skim milk in PBS for 20 min. Membrane was then washed with 10 mL of PBS and incubated with 10 mL of 10% (v/v) rabbit antisera in PBS for 4 h. Non-specifically bound antibodies were then washed off by 10 mL of PBS. Anti-IcsA pAbs were then eluted from the membrane using 700 µL 0.2 M glycine pH 2.0. The eluate was then dialysed against PBS (Section 2.7.5) for 18 h at 4 °C and 700 µL 100% glycerol were added and stored at -20 °C.

2.7.7 Protein quantification

Protein preparations were quantified by performing a protein assay using bicinchoninic acid as per manufacture's protocol (Pierce BCA protein assay kit, Thermo Scientific). Optical absorption was taken by a microplate Spectrophotometer (PowerWave XS2, BioTek).

For quantitation of pure protein at high concentration (>200 µg/mL), protein sample was quantified using a NanoDrop 1000 Spectrophotometer (ThermoFisher Scientific). Protein concentration was then calculated using a protein concentration calculator tool (AAT Bioquest®, https://www.aatbio.com/tools/calculate-protein-concentration) based on the absorbance reading at 280 nm and the calculated protein extinction coefficient.

2.7.8 Chemical crosslinking

2.7.8.1 *In vivo* chemical crosslinking of IcsA

In vivo chemical crosslinking of IcsA was done as described by May *et al.* (2012). Briefly, *Shigella* grown to mid-exponential phase (OD_{600} of 0.4-0.6) were collected (1×10^9 cells), washed with PBS three times and resuspended in 1 mL crosslinking buffer [0.2 mM DSP (Sigma, #D3669) in PBS, pH 7.0] and incubated at room temperature for 1 h. The reaction was quenched by 20 mM Tris pH 7.0 and incubated for another 15 min. Bacteria were then harvested via centrifugation (16,000 ×g, 1 min) and resuspended in 1 mL sonication buffer [PBS, 1 mM PMSF] and sonicated (Sonifier 450, Branson) on ice at the output power 4 for four 40% cycles with the microtip. The sonicate was centrifuged (4,000×g, 10 min, 4°C) to exclude unbroken cells. The isolated sonicate was then ultracentrifuged (108,000 ×g, 30 min, 4°C, Beckman Optima™ MAX-XP Ultracentrifuge) and the resulting pellet was resuspended in 2× PAGE buffer [4% (w/v) SDS, 20% (v/v) glycerol, 0.01% (w/v) bromophenol blue and 100 mM Tris HCl]. Alternatively, SDS-PAGE samples were reduced by adding 10 mM DTT.

2.7.8.2 Chemical crosslinking of purified IcsA

Purified IcsA passenger protein (0.38 mg/mL) was dialysed against PBS (Section 2.7.5) for 18 h at 4°C. DSP (50 mM) was then added to the dialysed protein to a final concentration of 0.1 mM, 1 mM and 10 mM respectively and incubated for 30 min at room temperature. Protein samples were then resuspended in 2× PAGE buffer.

2.7.9 Protein electrophoresis

2.7.9.1 SDS-polyacrylamide gel electrophoresis (PAGE)

For protein separation by molecular weight, protein containing sample resuspended in an equal volume of 2× SDS-PAGE sample buffer [4% (w/v) SDS, 20% (v/v) glycerol, 200 mM DTT, 0.01% (w/v) bromophenol blue and 100 mM Tris HCl] was heated at 100 °C for 5-10 min and loaded on self-cast SDS-PAGE gel [375 mM Tris pH 8.5, 0.1% (w/v) SDS, 0.05% (w/v) ammonium persulfate (APS) 0.05% (v/v) Tetramethylethylenediamine (TEMED, Sigma), 7.5-20% acrylamide/bis (BioRad)] using Mini-Protean system III (BioRad). For high resolution separation, protein sample was loaded on a pre-cast 4-12% gradient SDS-PAGE (Thermo Scientific) or an AnykDa gel (BioRad, #4569033). Running buffer consist of 25 mM Tris pH 8.3, 200 mM glycine, and 0.1% (w/v) SDS. Gels were electrophoresed at 100-200 V for 1 h. Seeblue Plus2 molecular marker (198 kDa, 98 kDa, 62 kDa, 49 kDa, 38 kDa, 28 kDa, 17 kDa, 14 kDa, 6 kDa and 3 kDa; Invitrogen, #LC5925), Novex Sharp pre-stained protein standard marker (260 kDa, 160 kDa, 110 kDa, 80 kDa, 60 kDa, 50 kDa, 40 kDa, 30 kDa, 20 kDa, 15 kDa, 10 kDa and 3.5 kDa; Invitrogen, #LC5800), or BenchMark^{TM} pre-strained protein ladder marker (190 kDa, 120 kDa, 85 kDa, 60 kDa, 50 kDa, 40 kDa, 25 kDa, 20 kDa, 15 kDa, and 10 kDa; Invitrogen, #10748010) were used to determine the molecular size of proteins.

2.7.9.2 Native-PAGE

For analysing the oligomeric states of the purified IcsA proteins, proteins were resuspended in Native sample buffer 2× [62.5 mM Tris-HCl pH 6.8, 25% (v/v) glycerol, 1% (w/v) bromophenol blue] at the ratio of 1:1, and directly loaded onto a self-cast Native gel [315 mM Tris-HCl pH 8.5, 0.1% (w/v) APS, 6-15% acrylamide/bis] without prior heating.

Running buffer consist of 25 mM Tris-HCl pH 8.5, and 192 mM glycine. Gels were electrophoresed at 200 V for 0.5-1 h at 4 °C. NativeMark Unstained (1236 kDa, 1048 kDa, 720 kDa, 480 kDa, 242 kDa, 146 kDa, 66 kDa and 20 kDa; Invitrogen, #LC0725) was used to estimate the molecular size of proteins.

2.7.10 Protein visualisation by staining

2.7.10.1 Coomassie Blue staining

Proteins separated by electrophoresis were stained with Coomassie blue staining solution [0.01% (w/v) Coomassie blue G250 (Sigma), 10% (v/v) acetic acid, 50% (v/v) methanol] at room temperature with shaking overnight. Gels were destained with repeated washes of destain solution [10% (v/v) acetic acid, 50% (v/v) methanol]. Images was acquired by an electronic scanner (HP).

2.7.10.2 Colloidal Blue Staining

For proteins that were either at low concentration or for the proteins recovered by immunoprecipitation for mass spectrometry analysis, gels were stained with Colloidal Blue Staining Kit (ThermoFisher Scientific) as per manufacture's protocol.

2.7.11 Western Immunoblotting

2.7.11.1 Western transfer

Proteins separated by electrophoresis were transferred to nitrocellulose membrane (NitroBind, pure nitrocellulose, 0.45 µm, GR Water & Process Technologies) using Trans-Blot® Turbo™ transfer system (BioRad) with Trans-Blot Turbo transfer buffer (BioRad, # 1704271). For proteins that are large in size (>150 kDa), transfer was done by using Trans-Blot Electrophoretic Transfer Cells (BioRad) at 400 mA for 1 h with an ice block in the transfer buffer [25 mM Tris-HCl, 200 mM glycine, 5% (v/v) methanol].

2.7.11.2 Ponceau S staining

For proteins that had been transferred to a nitrocellulose membrane, Ponceau S staining was performed by incubating the membrane with 5 mL of ponceau S staining

solution (0.1% (w/v) Ponceau S (Sigma), 5% (v/v) glacial acetic acid) for 1 min and rinsing with MQ water.

2.7.11.3 Western immunoblotting

The membrane was blocked with TTBS buffer [16 mM Tris-HCl, 120 mM NaCl, 0.05% (v/v) Tween-20 (Sigma)] with 5% (w/v) of skim milk for 1 h before incubation with primary antibodies (Section 2.3.1) in TTBS with 5% (w/v) of skim milk for 18 h. The membrane was then washed with TTBS three times (5 min each) and incubated with HPR conjugated secondary antibodies (Section 2.3.1) in TTBS with 5% (w/v) of skim milk for 2 h. The membrane was then washed three times with TTBS and once with TBS [16 mM Tris-HCl, 120 mM NaCl], followed by the incubation with Chemiluminescent substrate (Sigma, # WBKLS0500) for 5 min. Imaged were then acquired by using a BioRad GelDoc XR+.

2.7.11.4 Colony immunoblotting

Screening for either the successful generation of expression constructs or the addition of affinity tags was performed as follow. Colonies that recovered from transformation were picked and patched directly onto a nitrocellulose membrane. The membrane was then blocked with 5% (w/v) BSA in PBS for 20 min at room temperature. Membrane was then sequentially incubated with 10% (w/v) SDS; 0.5 M NaOH, 1.5 M NaCl; 0.5 M Tris pH 7.5, 1.5 M NaCl, and 2×SSC buffer [0.3 M NaCl, 0.03 M sodium citrate, pH 7.0] for 5 min each. The membrane was then re-blocked with 5% BSA in PBS for 20 min and was subjected to Western immunoblotting (Section 2.7.11.3).

2.7.11.5 Far Western immunoblotting

For far Western immunoblotting, the membrane on which proteins were transferred was blocked by 5% (w/v) skim milk in TTBS buffer and incubated with 0.28 nM IcsA passenger protein in 1 mL of TTBS with 5% (w/v) skim milk for 18 h at 4 °C. Membrane was then washed with TBS three times and interaction between IcsA passenger protein and host cell proteins was detected with the anti-IcsA antibody (1:1000) (Section 2.7.11.3).

2.7.12 Protein refolding buffer screening and refolding by dialysis

Purified IcsA passenger protein (~2 mg/mL) (Section 2.7.3.1) was diluted 1:20 into 200 µL base buffer (50 mM NaCl, 50 mM Tris, pH 8) with different screening ingredients and/or conditions including 10% (v/v) glycerol, 1.5 M NaCl, 1% (v/v) NP-40, 0.5 M urea, 10 mM DTT, 1% (w/v) glycine, 100 mM $MgCl_2$ or 50 mM Tris, pH 7.0. The mixtures were incubated 16 h at 4 °C, and ultracentrifuged (108,000 ×g, 30 min, 4°C, Beckman Optima^{TM} MAX-XP Ultracentrifuge) to separate the insoluble and soluble fractions. Both insoluble and soluble fractions were electrophoresed into a 12% SDS-PAGE gel (Section 2.7.9.1), transferred onto nitrocellulose membrane (Section 2.7.11.1), and stained with Ponceau S (Section 2.7.11.2). Conditions that yielded the least aggregation were then used for refolding by dialysis (Section 2.7.5).

2.7.13 Proteolysis assays

Proteolysis assays were done as described by May and Morona (2008) with modifications. Basically, a 500 µL of refolded IcsA passenger protein (1.35 mg/mL) was incubated with human neutrophil elastase (hNE) (0.33 µM) (Elastin Products Company) for up to 2 h at 37 °C. Aliquots (50 µL) were taken at different time points (0 min, 5 min, 10 min, 15 min, 30 min, 45 min, 60 min, and 90 min) and immediately mixed with an equal volume of 2× SDS-PAGE buffer and heated at 100 °C for 10 min, and then analysed by a 12% SDS-PAGE (Section 2.7.9.1) and stained with Coomassie Blue G250 (Section 2.7.10.1).

For hNE accessibility of IcsA, *S. flexneri* grown to the mid-exponential phase were collected (1×10^9 cells) and washed with 1 mL of PBS three times. Bacteria were then resuspended into 500 µL of PBS and incubated with hNE (0.33 µM) (Elastin Products Company) for up to 90 min. Aliquots (50 µL) were taken at different time points (0 min, 5 min, 10 min, 15 min, 30 min, 45 min, 60 min, and 90 min) and immediately resuspended with equal volume of 2× SDS-PAGE buffer and heated at 100 °C for 10 min. Alternatively, Aliquots (50 µL) taken at different time points were separated into whole cell fraction and digestion supernatant via centrifugation (13,200×g, 1 min, 4 °C). Samples were then mixed with 50 µL of 2× SDS-PAGE buffer and heated at 100 °C for 10 min.

For hNE digestions performed on the growth inhibited *S. flexneri*. Bacteria grown to the mid-exponential phase (OD_{600} of 0.4-0.6) were centrifuged (13,200 ×g, 1 min 25 °C) and resuspended in 10 mL LB broth with 25 µg/mL of chloramphenicol and incubated for 30 min at 37 °C, and the inhibition of the bacterial growth was confirmed by reading the OD_{600}. DOC at 2.5 mM was then added and the bacterial cultures were then incubated at 37 °C for another 2 h before being digested with hNE (0.33 µM) in the presence of chloramphenicol.

2.7.14 Mammalian cell line whole cell sample preparation

Mammalian cells that were grown to confluence on a 100 mm dish were recovered either by cell scraper or trypsin digestion (Section 2.2.2), and washed with PBS followed by centrifugation (4,000 ×g, 5 min, 4 °C). Pellets were lysed using 1 mL of RIPA buffer [25 mM Tris-HCl, 150 mM NaCl, 1% (v/v) NP-40, 0.5% (w/v) deoxycholate, 0.1% (w/v) SDS, 1 mM Na_3VO_4, 1 mM phenylmethylsulfonyl fluoride (PMSF), 10 µg/mL leupeptin] supplemented with 1 mg/mL of DNase I (Sigma) as described previously (Suzuki et al., 1998). Lysates were then ultracentrifuged (108,000 ×g, 30 min, 4°C, Beckman Optima™ MAX-XP Ultracentrifuge) and mixed with the same volume of sample buffer, incubated at 95 °C for 10 min before electrophoresing into 4-12% gradient SDS-PAGE gel (ThermoFisher Scientific, #NP0322PK2) and then transferring onto a nitrocellulose membrane (Section 2.7.11.1) for subsequent analysis.

2.7.15 Fractionation of HeLa cells and sample preparation

Cell fractionation was done as described by Laarmann and Schmidt (2003). Briefly, HeLa cells grown to confluence on a 100 mm dish were into 10 mL of PBS containing 1 mM Pefabloc® (Sigma, #PEFBSC-RO) and 10 µg/mL leupeptin (Sigma, #L2884) and sonicated (Sonifier 450, Branson) on ice at the output power 4 for four 40% cycles with the microtip. The unbroken cells were excluded from the sonicate via centrifugation (4,000×g, 10 min, 4°C). The isolated sonicate was then ultracentrifuged (108,000 ×g, 30 min, 4°C, Beckman Optima™ MAX-XP Ultracentrifuge). Supernatant was isolated as cytosolic fraction and the pellet was then washed with 1 mL of PBS before being resuspended in 1 mL buffer containing 0.1 M Na_2CO_3/1 M NaCl (pH 11) and incubated on

ice for 30 min. The solubilised membrane was then ultracentrifuged (108,000 ×g, 30 min, 4°C, Beckman Optima^{TM} MAX-XP Ultracentrifuge), and resulting a membrane associated fraction in the supernatant and the integral membrane fraction in the pellet. The pellet was then washed using 1 mL of 2% (w/v) CHAPS in sonication buffer and ultracentrifuged again (108,000 ×g, 30 min, 4°C), resulting in the detergent resistant integral membrane fraction in the pellet. All fractions were solubilised in 2× SDS-PAGE sample buffer and incubated at 95 °C for 10 min before electrophoresing into 4-12% gradient SDS-PAGE (Section 2.7.9.1) and transferred onto a nitrocellulose membrane (Section 2.7.11.1).

2.7.16 Protein fluorescent probe generation

One hundred µL of purified IcsA passenger protein (28 µM) (Section 2.7.3.1) and BSA protein (28 µM) (Sigma) were incubated with DyLight 594 Maleimide (50 µM) (ThermoFisher) for 18 h at room temperature. Excessive dye was quenched by reacting with β-mercaptoethanol (2-ME) (1 mM), and subsequently dialysed against 4 L determined dialysis buffer (Section 2.7.12) to remove 2-ME. Successful labelling was visualised in SDS-PAGE (Section 2.7.9.1) via imaging with a BioRad GelDoc XR+.

2.7.17 Immunoprecipitation (IP) of IcsA

For immunoprecipitation (IP) by IcsA passenger protein, HeLa cells grown confluent on four 100 mm culture dishes were recovered by cell scraper and washed with 10 mL of PBS. Cells were then lysed in 1 mL of cell solubilization buffer [50 mM sodium phosphate, pH 7.4, 150 mM NaCl, 1 mM EDTA, 1 mM EGTA, 10% (v/v) glycerol, 0.025% (w/v) NaN_3 (Sigma), 10 µg/mL leupeptin (Sigma), 1 µ/mL aprotinin (Sigma), 1 mM Pefabloc (Sigma), 0.125 U/mL α_2-macroglobulin (Roche), 2% (w/v) CHAPS (Roche)] and incubated for 30 min at 4 °C with rotation. Unlysed cells were then spun down (4,000 ×g, 4 °C, 10 min) and the lysate was then split into two samples (600 µL each). The lysate was then precleaned with 30 µL protein A resin (Genscript, #L00210) by incubation for 30 min at 4 °C with rotation. Both samples were then adjusted to 1.2 mL with TSA buffer [50 mM Tris-HCl pH 7.4, 100 mM NaCl, 0.02% (w/v) NaN_3], 20 µL of IcsA passenger protein (28 µM) was then added to the lysate and incubated for 2 h at 4 °C with rotation. For mock pull down, 20 µL protein refolding buffer was added and incubated in the same way. To pull down IcsA-target

protein complexes, 20 µL of anti-IcsA antibody or anti-His_6 antibody and 40 µL of protein A resin were added to both IcsA and mock pull down reactions and incubated for another 2 h at 4 °C with rotation. Resins were then recovered by centrifugation (1,000 ×g, 4 °C, 1 min), and washed sequentially by 1 mL TSA buffer; TSA buffer containing 0.1% (w/v) CHAPS; TSA buffer containing 0.1% (v/v) CHAPS and 250 mM NaCl; and finally TSA buffer again. Protein A resins were then mixed with 30 µL of SDS-PAGE sample buffer and heated at 100 °C for 5 min before loading onto a 4-12% SDS-PAGE gel.

2.7.18 Protein pull down assay

2.7.18.1 N-WASP pull down of IcsA

For N-WASP pull down experiments, approximately 60 µg mini-N-WASP-GST protein purified as described previously (Papayannopoulos *et al.*, 2005) was mixed with either 12.5 µg $IcsA^{53\text{-}740}$ or $IcsA^{\Delta 138\text{-}148}$, and incubated with 200 µl glutathione Sepharose™ 4B (GE Healthcare, # 17075601) resin overnight at 4 °C. For mock pull down, approximately 60 µg GST protein was mixed with 12.5 µg $IcsA^{53\text{-}740}$ and processed as above. Resins were washed sequentially with PBS; PBS containing 1 mM DTT; PBS containing 0.1% (v/v) NP-40; and PBS for three times each. Protein was eluted in 50 µL PBS containing 20 mM reduced glutathione (Sigma). Samples were solubilised in SDS-PAGE sample buffer and subjected to SDS-PAGE (Section 2.7.9.1) and Western immunoblotting (Section 2.7.11.3).

2.7.18.2 IcsA pull down N-WASP

For IcsA pull down N-WASP experiments, approximately 60 µg mini-N-WASP-his protein purified as described previously (Papayannopoulos *et al.*, 2005) was mixed with either 38 µg IcsA , and incubated with 100 µL of anti-DYKDDDDK G1 affinity resin (GenScript, #L00432) resin overnight at 4 °C. For mock pull down, 60 µg mini-N-WASP-his protein was mixed with 100 µL of anti-DYKDDDDK G1 affinity resin and processed as above. Resins were washed 5 times with 1 mL TBS and beads were resuspended in 50 µL of 2× SDS-PAGE buffer and heated to 100 °C. Samples were then subjected to SDS-PAGE (Section 2.7.9.1) and Western immunoblotting (Section 2.7.11.3).

2.7.19 Mass spectrometry (MS)

2.7.19.1 MS for IcsA-interacting protein identification

For IcsA receptor identification via mass spectrometry, samples from IP (Section 2.7.17) were separated by SDS-PAGE (Section 2.7.9.1) and stained by Colloidal Blue (Section 2.7.10.2). Unique proteins from the IcsA pull down sample compared to mock pull down, and having the same apparent molecular weight that been visualised in far Western immunoblotting, were excised and sent for protein identification via liquid chromatography electrospray ionization tandem mass spectrometry (Nano-LC-ESI-MS/MS, Adelaide Proteomics Centre). The same mass position regions in the mock pull down sample were also excised and analysed in the same way to determine background protein contamination. Unique peptides identified from IcsA pull down was then searched against the non-redundant human Uniport database to identify IcsA interacting proteins.

2.7.20 IcsA structure prediction

The predicted IcsA structure was acquired by using an online protein prediction tool Iterative Threading ASSEmbly Refinement (I-TASSER) (Zhang, 2008).

2.8. LPS methods

2.8.1 LPS sample preparation

Bacteria strains grown 18 h at 37 °C were subcultured 1:20 in LB broth and incubated at 37 °C for another 4 h with shaking (200 rpm). Bacteria cells were then collected (1×10^9 cells) by centrifugation (16,250 ×g, 1 min) and resuspended in 50 µL of LPS lysing buffer [2% (w/v) SDS, 0.1% (w/v) bromophenol blue, 4% (v/v) 2-ME, 10% (v/v) glycerol, 0.66 M Tris-HCl, pH 7.6]. After an incubation at 100 °C for 5-10 min, 10 µL of proteinase K (2.5 mg/mL) was added and samples were then incubated at 56 °C for 4 h allowing complete digestion of proteins. Samples were then stored at -20 °C.

2.8.2 Silver staining of LPS

2.8.2.1 LPS SDS-PAGE

For separation of LPS molecules in samples, samples were diluted 1:4 in LPS lysis buffer and heated at 100 ℃ for 5 min before loading onto a self-cast SDS-PAGE gels (Section 2.7.9.1) except all solutions were made in MQ water. LPS were then electrophoresed at 12 mA for 16 h.

2.8.2.2 LPS silver staining

For LPS silver staining, PAGE gels were fixed in fixing solution [5% (v/v) glacial acetic acid, 40% (v/v) ethanol] for 2.5 h, oxidized for 5 min with oxidizing solution [5% (v/v) glacial acetic acid, 40% (v/v) ethanol, 0.7% (w/v) periodic acid], washed 4 times with MQ water for 15 min each, stained for 10 min with staining solution [1.33% (v/v) NH_3OH, 0.08% (w/v) NaOH, 0.67% (w/v) $AgNO_3$] and washed 5 times with MQ water as above. Staining was developed in pre-warmed (42 ℃) developing solution [0.005% (w/v) citric acid, 0.037% (v/v) formaldehyde], and stopped by using stropping solution [4% (v/v) glacial acetic acid]. The image was then acquired using an electronic scanner (HP).

2.8.3 LPS depletion and regeneration

LPS depletion and regeneration were done as described previously (Teh *et al.*, 2012). Briefly, *Shigella* bacteria grown for 16 h were subcultured 1 in 20 into 10 mL of LB and grown to an OD_{600} of 0.5 at 37 ℃ before further dilution 1:20 into 10 mL of LB in the presence of 3 μg/ml polymyxin B nonapeptide (PBMN, Sigma) and 5 μg/ml tunicamycin (Sigma), and incubated for another 3 h at 37 ℃ to deplete the LPS O antigen. Bacterial cultures were then centrifuged (4,000×g, 10 min), washed twice with 10 mL of fresh LB to remove PMBN and tunicamycin, and further diluted 1:20 into 10 mL of LB for another 3 h incubation at 37 ℃ to regenerate LPS O antigen. *Shigella* bacteria with either depleted LPS O antigen or regenerated LPS O antigen were prepared into LPS sample (Section 2.8.1) and analysed via LPS SDS-PAGE (Section 2.8.2.1) and LPS silver staining (Section 2.8.2.2) or subjected to proteolysis assays (Section 2.7.13).

2.9. Tissue culture techniques

2.9.1 Bacterial adherence assay

Bacterial adherence assays were performed as described by Brotcke-Zumsteg *et al*. (2014) with modifications. Briefly, HeLa cells and COS-7 cells seeded at 4.5 $\times 10^5$/well a day before the assay and grown to confluence in 24-well plates, were washed with 1 mL of PBS three times, replenished with 200 µL of culture medium devoid of antibiotics. *S. flexneri* 2a strains grown to the mid-exponential phase were collected (4.5×10^8 cells), washed with 1 mL of PBS three times, and replenished with 1 mL of culture medium devoid of antibiotics. A 100 µL of bacteria suspension was then added onto monolayers to reach the multiplicity of infection (MOI) of 100:1. The 24-well plates were centrifuged (500 ×g, 5 min) and incubated for 15 min. Unbound *Shigella* bacteria were removed by washing three times with 1 mL of PBS, and monolayers were lysed using 500 µL of 0.1% (v/v) Triton X-100 at 37 °C for 10 min. A 20 µL of monolayer lysate containing *Shigella* bacteria were then used to prepare serial dilution in 200 µL each to up to 10^{-4} in triplicate, and a 20 µL of each dilution triplicate were doted on an agar plate containing appropriate antibiotics. Plates were then incubated at 37 °C for 16 h, and the average number of the colonies from dilution triplicate was used.

2.9.2 Bacterial adherence blocking assay

2.9.2.1 Adherence blocking assays using purified IcsA

HeLa cells seeded at 4.5×10^5/well a day before assay and grown to confluence in 24-well plates were washed by 1 mL of PBS three times, then replenished with 200 µL of culture medium devoid of antibiotics. A 100 µL of IcsA passenger protein at different concentrations (2.5 µM, 1.25 µM, 250 nM and 25 nM), along with 100 µL of culture medium washed *S. flexneri* 2a strains (Section 2.9.1) were added onto monolayers at the multiplicity of infection (MOI) of 100:1. A 100 µL of protein dialysis buffer (Section 2.7.12) with or without BSA protein at the concentration of 2.5 µM were used as controls. Samples were then subjected to bacterial adherence assays (Section 2.9.1).

2.9.2.2 Adherence blocking assays using antibodies

HeLa cells seeded at 4.5×10^5/well a day before assay and grown to confluence in 24-well plates were washed by 1 mL of PBS three times, then replenished with 200 µL of culture medium devoid of antibiotics. Bacteria were washed with 1 mL PBS and replenished in 900 µL of culture medium, mixed with 100 µL of rabbit anti-IcsA pAbs (3.125 µg/mL and 0.3125 µg/mL in PBS), mouse anti-Myosin II-A antibodies (15 µg/mL, 1.5 µg/mL and 0.15 µg/mL in PBS), mouse anti-Myosin II-B antibodies (15 µg/mL, 1.5 µg/mL and 0.15 µg/mL in PBS) or rabbit pre-immune serum (concentration of IgG 100 µg/mL), and incubated for 15 min at room temperature. A mixture of 100 µL of bacteria with antibodies were then added onto cell monolayers at the MOI of 100 and incubated for another 15 min at 37 °C with 5% CO_2 to allow bacteria passive settling. Samples were then subjected to bacterial adherence assays (Section 2.9.1)

2.9.3 Invasion assay

Bacterial invasion assays were performed as described by Brotcke-Zumsteg *et al.* (2014) with modifications. Briefly, HeLa cells seeded at 4.5×10^5/well a day before the assay and grown to confluence in 24-well plates, were washed with 1 mL of PBS three times, replenished with 200 µL of culture medium devoid of antibiotics. *Shigella* grown to an OD_{600} of 0.4-0.6 in the presence of DOC (2.5 mM) were collected (4.5×10^8 cells), washed with 1 mL of PBS three times, and replenished with 1 mL of culture medium devoid of antibiotics. A 100 µL of bacteria suspension was then added onto monolayers to reach the multiplicity of infection (MOI) of 100:1, and the 24-well plates were incubated at 37 °C. Gentamycin (40 µg/mL) was added after 45 min post infection and HeLa monolayers were incubated for another 45 min. The monolayers were then washed three times with 1 mL of PBS, and were lysed using 500 µL of 0.1% (v/v) Triton X-100 at 37 °C for 10 min. The intracellular *Shigella* bacteria were enumerated by serial dilution plating onto LB agar (Section 2.9.1).

2.9.4 Statistical analysis

The statistical analysis on *Shigella* adherence and invasion assays was performed using GraphPad Prism 8.0.0. Data were normalised against the relevant controls and significance was calculated using either a student *t* test or one-way ANOVA followed by

Dunnett's multiple comparisons test against the controls based on at least two independent experiments.

2.9.5 Plaque assay

Bacterial plaque formation assay was done as described previously (Tran *et al.,* 2015). In general, HeLa cells or COS-7 cells seeded at 2×10^6 cells/well a day before assay and grown to confluence in 6-well plates were washed by 2 mL of PBS three times. *S. flexneri* 2a strains grown to the mid-exponential phase were collected (6×10^8 cells), washed with 1 mL of PBS three times, and replenished with 1 mL of culture medium devoid of antibiotics. Washed bacteria were then diluted 1 in 1000 in PBS, and a 250 µL of the diluted bacteria preparation was added onto each monolayer, and incubated in MEM at 37 °C with 5% CO_2. After 90 min post-infection, a 5 mL of first overlay (5% (v/v) FCS, 0.5% (w/v) agarose, 20 µg/mL Gentamicin, in DMEM) was added and incubated at 37 °C with 5% CO_2. After 48 h post-infection, a 5 mL of a second overlay (5% (v/v) FCS, 20 µg/mL Gentamicin, 0.5% (w/v) agarose, 3 mg/mL, 0.1% (w/v) Neutral Red (Gibco BRL) in DMEM) was added and plaque formation was observed 6–8 h later. Plaque size was measured using MetaMorph V7.5.

2.10. Microscopy techniques

2.10.1 Fluorescence Microscopy

2.10.1.1 Staining with fluorescent IcsA protein probe

To visualise the binding of IcsA to host cell surfaces, confluent HeLa monolayers grown on glass slides in 24-well plates were fixed with 200 µL of 3.7% (v/v) formaldehyde in PBS. Monolayers were then washed with 1 mL of PBS, quenched with 200 µL of 50 mM NH_4Cl for 10 min, washed with 1 mL of PBS, and incubated with 50 µL of IcsA-Dylight 594 (2.8 µM) or BSA-Dylight 594 (2.8 µM) probes in PBS containing 10% (v/v) FCS for 2 h at room temperature. Monolayers were then washed with 1 mL of PBS, permeabilised with 100 µL of 0.1% (v/v) Triton X-100 in PBS. The cytoskeleton was stained by 50 µL of AlexaFluor 488 phalloidin (Invitrogen) diluted to 1:100 in PBS containing 10 % (v/v) FCS, and DNA was stained using 50 µL of 10 µg/mL DAPI for 1 min, and washed 1

mL of PBS again. Samples were then mounted with 6 µL of 20% Mowiol 4–88 (Calbiochem), 4 mg/mL p-phenylenediamine, and visualised by an Olympus IX-70 microscope driven by MetaMorph software (Version 7.5) using a ×100 oil immersion objective, or an Olympus confocal laser scanning microscope FV3000 driven by FV31S-SW Fluoview software (V2.3.1.163) with a ×100 oil immersion objective.

2.10.1.2 Immunofluorescence (IF) staining of bacterial surface antigen

For surface immunostaining of the bacterial strains, bacteria were grown to mid-exponential phase (OD_{600} of 0.5) and collected (10^8 cells) by centrifugation (16,250 ×g, 1 min). Cells were then washed with 1 mL of PBS once and fixed in 1 mL of 3.7% (v/v) formaldehyde solution in PBS at room temperature for 20 min. Fixed cells were then washed twice with 1 mL of PBS and resuspended in 100 µL of PBS. Fixed bacteria (5 µL) were then centrifuged (500 ×g, 5 min) onto 10 mm round cover slips (in 24-well plate) precoated with 200 µL of 10% (v/v) poly-L-lysine (Sigma).

Bacteria were then incubated with 50 µL of appropriate primary antibodies at appropriate concentration (generally 1:100) in PBS containing 10% (v/v) FCS for 2 h at room temperature. Bacteria were then washed twice with 1 mL of PBS and incubated with 50 µL of AlexaFluor 488 conjugated secondary antibody in PBS containing 10% (v/v) FCS. Coverslips were then washed with 1 mL of PBS twice and mounted on microscope slides (Section 2.10.1.1). Images were acquired using an Olympus IX-70 microscope driven by Metamorph software (Version 7.5) using a ×100 oil immersion objective.

Chapter Three

ARTICLE 1:

The virulence domain of *Shigella* IcsA contains a subregion with specific host cell adhesion function

Jilong Qin, Matthew Thomas Doyle, Elizabeth Ngoc Hoa Tran and Renato Morona

Chapter 3: The virulence domain of *Shigella* IcsA contains a subregion with specific host cell adhesion function

3.1. Statement of Authorship

Title of paper	The virulence domain of *Shigella* IcsA contains a subregion with specific host cell adhesion function
Status	Published (Jan, 2020)
Authors.*Journal*	Qin, J., Doyle, MT., Tran EN. & Morona R. *PlosOne*

Principal author

Principal author	Jilong Qin		
Contribution	Conducted all experiments; analysed all results, constructed all figures, tables, supplementary information, wrote the manuscript		
Overall (%)	90		
Certification	This paper reports on original research I conducted during the period of my Higher Degree by Research candidature and is not subject to any obligations or contractual agreements with a third party that would constrain its inclusion in this thesis. I am the primary author of this paper.		
Signature		Date	2/12/19

Co-author contributions

By signing the Statement of Authorship, each author certifies that:

i. the candidate's stated contribution to the publication is accurate (as detailed above);

ii. permission is granted for the candidate in include the publication in the thesis; and

iii. the sum of all co-author contributions is equal to 100% less the candidate's stated contribution.

Author	Matthew Thomas Doyle		
Contribution	Designed and constructed the expression plasmid and strains for IcsA$^{53-740}$ purification; provided methods for IcsA$^{53-740}$ purification from IBs; Conducted preliminary trails in IcsA refolding. Critical manuscript editing.		
Signature		Date	2/12/19

Author	Elizabeth Ngoc Hoa Tran		
Contribution	Supervised adherence assays and invasion assays, Critical manuscript editing.		
Signature		Date	2/12/19

Author	Renato Morona		
Contribution	Supervised development of work; provided laboratory and materials; analysed data with principal author, evaluated and edited manuscript; acted as corresponding author.		
Signature		Date	2/12/19

3.2. Article abstract

Shigella species cause bacillary dysentery, especially among young individuals. Shigellae target the human colon for invasion; however, the initial adhesion mechanism is poorly understood. The *Shigella* surface protein IcsA, in addition to its role in actin-based motility, acts as a host cell adhesin through unknown mechanism(s). Here we confirmed the role of IcsA in cell adhesion and defined the region required for IcsA adhesin activity. Purified IcsA passenger domain was able block *S. flexneri* adherence and was also used as a molecular probe that recognised multiple components from host cells. The region within IcsA's functional passenger domain (aa 138-148) was identified by mutagenesis. Upon the deletion of this region, the purified IcsA$^{\Delta 138\text{-}148}$ was found to no longer block *S. flexneri* adherence and had reduced ability to interact with host molecules. Furthermore, *S. flexneri* expressing IcsA$^{\Delta 138\text{-}148}$ was found to be significantly defective in both cell adherence and invasion. Taken together, our data identify an adherence region within the IcsA functional domain and provides useful information for designing therapeutics for *Shigella* infection.

3.3. Article introduction

Shigellae are Gram-negative bacteria that cause severe bloody diarrhoea in humans (Speelman *et al.*, 1984) and rhesus monkeys (Good *et al.*, 1969). Shigellosis is life threating to children under 4 years of age (Kotloff *et al.*, 2018) and is a growing health problem in developed countries due to decreased susceptibility to antibiotics (Kozyreva *et al.*, 2016). *Shigella* spp. are primate specific pathogens that target the colon (Speelman *et al.*, 1984, Anand *et al.*, 1986) and it has been demonstrated in the rabbit ligated ileum model (Wassef *et al.*, 1989), and *in vitro* colonoids (Ranganathan *et al.*, 2019), that *Shigella* can be taken up by M cells. However, *Shigella* has been reported to target the human colonic crypts where M cells were not present (Arena *et al.*, 2015), strongly indicating that an alternative route of entry exists. Indeed, the mechanisms by which *Shigella* species initially adhere to host cells, a prerequisite for subsequent invasion and establishing infection, remains poorly understood.

A role in host cell adhesion has been recently revealed for the essential surface displayed virulence factor IcsA (Brotcke-Zumsteg *et al.*, 2014). IcsA is 100% conserved in *Shigella* species and is a member of the secreted autotransporter (AT) superfamily. IcsA contains a signal sequence (aa 1-52) at its N-terminus for secretion across the inner membrane; a passenger domain (aa 53-740) which confers its function; a β-barrel domain (aa 813-1102) which is responsible for passenger domain translocation across the outer membrane; and an unstructured linker region (aa 741-812) that connects the passenger with the β-barrel. IcsA also belongs to the AIDA subfamily with members that are well characterised adhesins, such as AIDA-I and Ag43, both of which are known to have β-helix passenger structures (Emsley *et al.*, 1996, Charbonneau *et al.*, 2009, Heras *et al.*, 2014). The IcsA passenger also possesses these β-helix structures (Kuhnel & Diezmann, 2011, Doyle *et al.*, 2015a, Doyle *et al.*, 2015b, Leupold *et al.*, 2017). IcsA has been well studied with respect to its function in actin based motility (ABM) (Goldberg *et al.*, 1993, Goldberg & Theriot, 1995), where polarly distributed IcsA recruits host N-WASP protein (Suzuki & Sasakawa, 1998, Suzuki *et al.*, 2002, Teh & Morona, 2013), resulting in the subsequent polymerisation of host cell actin at one pole of the bacterium to facilitate bacterial inter- and intracellular motility (Egile *et al.*, 1999). Recently, IcsA has been found contributing to *S. flexneri* biofilm

formation in the presence of bile salt deoxycholate (DOC) by promoting cell-to-cell contact and aggregative bacterial growth (Koseoglu *et al.*, 2019). Besides ABM and biofilm formation, however, knockouts of the type 3 secretion tip complex proteins IpaD or IpaB in *Shigella flexneri* result in polar adhesion to host cells in an IcsA-dependent manner (Brotcke-Zumsteg *et al.*, 2014). IcsA was also found to contribute to DOC induced hyper-adherence, and expressing IcsA in *E. coli* promotes adherence to host cells, confirming that IcsA is sufficient to promote bacterial adherence (Brotcke-Zumsteg *et al.*, 2014). While IcsA's expression level and cellular distribution is not altered in the hyper-adherent *Shigella* compared to the wild type strain, data suggest that the conformation of IcsA is different in hyper-adherent strains (Brotcke-Zumsteg *et al.*, 2014).

In this study, the direct role of IcsA in *Shigella*-host-cell adherence was demonstrated via adherence inhibition with purified IcsA passenger domain, and adherence blocking with anti-IcsA antibodies. Fluorescently labelled IcsA passenger was also able to bind to host cell surfaces. Indirect probing with purified IcsA passenger protein recognised several host molecules through far Western blotting. Through screening of an IcsA 5 aa insertion library (May & Morona, 2008), the region responsible for adhesin activity was identified and characterised.

3.4. Article materials and methods

3.4.1 Ethics statement

The anti-GST antibody and anti-IcsA antibody were produced under the National Health and Medical Research Council (NHMRC) Australian Code of Practice for the Care and Use of Animals for Scientific Purposes, and was approved by the University of Adelaide Animal Ethics Committee (S-2012-90). Bacterial adherence and invasion assays were performed under the National Statement of Ethical Conduct in Human Research 2018, and was approved by Human Research Ethics Committee (HREC H-2016-091).

3.4.2 Bacterial strains and tissue culture

The bacterial strains used in this study are listed in S1 Table. For adherence assays, bacterial strains were streaked onto Tryptic Soy Agar with 0.2% (w/v) Congo Red, and after incubation at 37 °C overnight, red colonies were selected and incubated in Lysogeny broth (LB) overnight with appropriate antibiotics (tetracycline, 10 $\mu g\,ml^{-1}$; kanamycin, 50 $\mu g\,ml^{-1}$; chloramphenicol, 25 $\mu g\,ml^{-1}$ and ampicillin, 100 $\mu g\,ml^{-1}$). For all assays, overnight bacterial cultures were subcultured (1:20) in the presence or absence of 2.5 mM sodium deoxycholate and grown to a mid-exponential phase (OD_{600} reading of 0.6-0.8) before use.

HeLa cells were maintained and grown in minimal essential medium (MEM) supplemented with L-glutamine, 10% (v/v) fetal calf serum (FCS), and penicillin/streptomycin. Cell cultures were maintained at 37 °C with 5% CO_2 for growth. The day prior to the bacterial adherence assay and invasion assay, or for microscopy, HeLa cells were seeded at 4.5×10^5/well into 24-well plates or onto glass coverslips respectively. For plaque assays, HeLa cells were seeded into 6-well plates and were allowed to grow confluent.

3.4.3 Mutagenesis and DNA manipulation

S. flexneri 2a *ΔipaD* or *ΔipaB* strains were generated using the λ red mutagenesis method as described previously (Datsenko & Wanner, 2000). Briefly, primers (S2 Table) were designed to PCR amplify the kanamycin cassette flanked with 50 bp of the

start and end coding sequences of IpaD or IpaB. The fragments were then electroporated into WT *S. flexneri* 2457T or a *ΔicsA* knockout strain to generate *ΔipaD/ΔipaB* or *ΔipaDΔicsA/ΔipaDΔicsA* mutant strains. The kanamycin cassette was then eliminated by the introduction of pCP20 to avoid potential polar effects.

Site-directed mutagenesis was performed on pIcsA plasmid (May & Morona, 2008) using the QuikChange II® system (Agilent) as per the manufacturers protocol. The primers used are listed in S2 Table.

For alanine scanning of the amino region 138 to 148 in the IcsA passenger domain, codons of each amino acid were substituted with a codon of alanine and changed via inverse PCR with the primers listed in S2 Table.

The hyper-adherent mutant library was generated by transforming plasmids from the IcsA 5 aa insertion library (May & Morona, 2008) into *S. flexneri* 2a *ΔipaDΔicsA* via chemical transformation as described by Sambrook and Russell (2006).

For IcsA production, the IcsA passenger sequence from amino acid 53 to 740 was amplified using primers MD80/81 (S2 Table) from pIcsA, and cloned into the pBADhisB vector (Invitrogen) between the XhoI and KpnI sites, resulting in pBADhisB::IcsA$^{53\text{-}740}$. The vector was then optimised for purification by inverse PCR to replace the His×6 tag with a N-terminus fused His×12 tag, resulting in pMDBAD::IcsA$^{53\text{-}740}$. For the IcsA$^{\Delta 138\text{-}148}$ production, the coding sequence of amino acids 138 to 148 in the IcsA passenger domain was deleted via inverse PCR, resulting in pMDBAD::IcsA$^{53\text{-}740/\Delta 138\text{-}148}$.

3.4.4 Protein purification and refolding

For IcsA passenger domain production, an overnight culture of *E. coli* TOP10 transformed with pMDBAD::IcsA$^{53\text{-}740}$ was sub-cultured 1 in 1000 into auto-induction 2 L Terrific Broth medium (Tartoff & Hobbs, 1987) that contained a mixture of glucose and arabinose in the ratio of 0.1%:0.3% (w/v), and incubated at 37 °C overnight. Cells were then harvested by centrifugation (10,000 ×g, 10 min), resuspended in 80 ml TBS [50 mM Tris, 150 mM NaCl, pH 7.0] and lysed using a cell disruptor (30 kpsi, Constant Systems Ltd) in the presence of two EDTA-free protease inhibitor tablets (Roche). Inclusion bodies (IBs) were recovered by centrifugation of the cell lysates (20,000 ×g, 10 min), and

pre-cleaned by detergent wash [50 mM Tris, 1 M NaCl, 2% (v/v) Triton X-100, 4 mM DDM and 2% (w/v) DOC, pH 8.0] to exclude membrane fractions. IcsA passenger protein from the IBs was then solubilised in 50 ml protein solubilisation buffer [8 M urea, 50 mM NaCl, 50 mM Tris, 10 mM imidazole, pH 8] for 2 h, followed by centrifugation (185,000 ×g, 1 hr). Solubilised IcsA passenger protein was then loaded on a His-trap column, washed and eluted with increasing concentration of imidazole. IcsA passenger protein was then further purified through an HiLoad 16/600 Superdex 200pg column (GE Healthcare) and eluted fractions containing purified protein were confirmed by SDS-PAGE. IcsA passenger domain-containing fractions were then pooled and subjected to refolding.

Purified IcsA passenger protein was diluted 1:20 into base buffer [50 mM NaCl, 50 mM Tris, pH 8.0] with different screening ingredients or conditions including 10% (v/v) glycerol, 1.5 M NaCl, 1% (v/v) NP-40, 0.5 M urea, 10 mM DTT, 1% (w/v) glycine, 100 mM $MgCl_2$ or pH 7.0. The mixtures were then incubated for 16 h at 4 °C, and ultracentrifuged (185,000 ×g, 30 min) to separate the insoluble and soluble fractions. Samples of both insoluble and soluble fractions were compared by electrophoresis into a 12% polyacrylamide SDS-PAGE gel and subjected to Western transfer and Ponceau S staining. Conditions that yielded the least aggregation were then used, and the purified IcsA passenger protein was refolded by dialysing against optimised buffer [0.5 M urea, 10% (v/v) glycerol, 50 mM NaCl and 50 mM Tris-HCl pH 7.0] at room temperature for 48 h. Dialysed IcsA passenger protein was then ultracentrifuged (185,000 ×g, 1 h) and the resulting supernatant was quantified using the protein BCA assay (Thermo Fisher) and stored at -80 °C. With this protocol a yield of IcsA of approximately 10 mg protein was obtained from a 2 L overnight culture.

3.4.5 Proteinase accessibility assay

Proteinase accessibility assay was performed as described by May and Morona (2008) with modifications. Refolded IcsA passenger protein was incubated with Human Neutrophil Elastase (hNE, EPC Elastin Products) in dialysis buffer at the molecular ratio of 1000:1 at 37 °C for 1.5 h. Aliquots were taken at different time points (0 min, 5 min, 10 min, 15 min, 30 min, 45 min, 60 min and 90 min) and immediately resuspended with an equal volume of SDS-PAGE sample buffer (Lugtenberg *et al.*, 1975) followed by incubation

at 100 °C for 10 min. A sample of IcsA passenger protein was also heated at 65 °C for 15 min, cooled to room temperature, and digested as above to serve as a control. Fractions taken from different time points were then analysed by SDS-PAGE and stained with Coomassie blue G250 (Sigma).

3.4.6 Fluorescent labelling

For protein labelling, refolded IcsA passenger protein (that has three cysteine residues available for labelling with Dylight 594 maleimide), mutant IcsA passenger protein ($IcsA^{\Delta 138\text{-}148}$), or bovine serum albumin (BSA) protein (Sigma) were incubated with DyLight594 maleimide (Thermo Fisher) at the molecular ratio of 1:2 overnight at room temperature, and subsequently dialysed against dialysis buffer to remove excessive dye. Successfully labelled protein was analysed via SDS-PAGE and the fluorescence was confirmed using a ChemiDoc imaging system (BioRad).

IcsA immunofluorescent labelling on bacterial surfaces was performed as described previously (May *et al.*, 2012). Briefly, *Shigella* grown to an OD_{600} of 0.5 was collected and fixed in PBS containing 3.7% (v/v) formaldehyde and centrifuged onto poly-L-lysine-coated coverslips. Bacteria was then incubated with 50 µl of rabbit anti-IcsA antibody (1:100) for 1 h, washed with PBS, and labelled with 50 µl of Alexa 488-conjugated donkey anti-rabbit antibody (1:100) for another 1 h. Samples were then mounted with 20% (v/v) Mowiol 4–88 (Calbiochem), 4 mg ml^{-1} *p*-phenylenediamine, and imaged with an Olympus fluorescent microscope (IX-70).

3.4.7 SDS-PAGE and Western blotting

For SDS-PAGE, samples were resuspended in an equal volume of 2× SDS-PAGE sample buffer (Lugtenberg *et al.*, 1975), and immediately heated at 100 °C for 10 min. A total of 20 µl from each sample was then electrophoresed on Any kD^{TM} gels (BioRad) or hand-cast 12% SDS acrylamide (BioRad) gels. For Western immunoblotting, samples were then transferred onto a nitrocellulose membrane, blocked with TBST [TBS, 0.05% (v/v) Tween-20] containing 5% (w/v) skim milk, and incubated with rabbit anti-IcsA antibody (Van Den Bosch *et al.*, 1997), rabbit anti-GST antibody (in house made), or mouse anti-His_6 antibody (Genscript) for 4 h. The membrane was then washed with TBST and incubated with

HRP-conjugated goat anti-mouse antibody (Biomediq DPC) or HRP-conjugated goat anti-rabbit antibody (Biomediq DPC) for 1 h. The membrane was then washed with TBS and incubated with Chemiluminescence Substrate (Sigma) for 5 min. Chemiluminescence was detected using a ChemiDoc imaging system (BioRad).

3.4.8 Confocal microscopy

To visualise the binding of IcsA to host cell surfaces, fluorescently labelled wild type IcsA passenger protein (2.8 µM), IcsA$^{\Delta 138\text{-}148}$ protein (2.8 µM) or BSA protein (5 µM) were added onto confluent HeLa cell monolayers grown on coverslips in 24-well trays and incubated at 37 °C with 5% CO_2 for 15 min followed by washing with PBS. Monolayers were then fixed with 3.7% (v/v) formaldehyde in PBS, washed with PBS, incubated with 1% (v/v) Triton in PBS for 10 min, and then stained with AlexaFluor 488 phalloidin (Invitrogen) diluted to 1:100 in PBS containing 10 % (v/v) FCS. Monolayers were then washed with PBS and DNA was stained using 10 µg ml^{-1} DAPI for 1 min, followed by another PBS wash. Coverslips were then mounted with 20% (v/v) Mowiol 4–88 (Calbiochem), 4 mg ml^{-1} *p*-phenylenediamine, and imaged with an Olympus confocal laser scanning microscope (FV3000).

3.4.9 Adherence, invasion and plaque formation assays

For whole cell adherence assays, *Shigella* grown to an OD_{600} of 0.4-0.6 were collected, washed with MEM, and inoculated to HeLa cell monolayers at the MOI of 100. Centrifugation (500 ×g, 5 min) was used as outlined in the results. After 15 min of incubation, HeLa cell monolayers were washed with PBS and lysed using PBS containing 0.1% (v/v) Triton X-100 at 37 °C for 10 min. The remaining *Shigella* bacteria were enumerated by serial dilution plating onto LB agar.

For invasion assays, *Shigella* grown to an OD_{600} of 0.4-0.6 in the presence of DOC were used to infect HeLa cell monolayer at the MOI of 100. Gentamycin (40 µg ml^{-1}) was added after 45 min post infection and HeLa monolayers were incubated for another 45 min before being lysed and treated as above.

Plaque formation was performed as described previously (May *et al.*, 2012). Briefly, HeLa cells grown to confluency in six-well trays were washed with PBS and

Dulbecco's modified Eagle's medium (DMEM) sequentially before infection with of *Shigella* (1.25 $\times 10^5$ cfu) grown to an OD_{600} of 0.5. At 90 min post infection, an overlay [DMEM, 5% (v/v) FCS, 20 μg ml^{-1} gentamycin, 0.5% (w/v) agarose was added to each well. The second overlay containing 0.1% (w/v) Neutral Red was added at 48 h post infection and images of plaques were taken after another 2 h incubation.

3.4.10 Adherence blocking assays using purified IcsA or anti-IcsA antibody

For both adherence blocking assays, HeLa cells grown to confluence were washed with PBS, and replenished with culture medium devoid of antibiotics. For the IcsA adherence blocking assays, IcsA passenger protein at different concentrations (2.5 μM, 1.25 μM, 250 nM and 25 nM) along with *S. flexneri* 2a strains were added onto monolayers at the multiplicity of infection (MOI) of 100:1. After an incubation of 15 min at 37 °C with 5% CO_2, samples were centrifuged (500 ×g, 5 min) and incubated for another 15 min as above.

For the antibody adherence blocking assays, bacteria were washed with PBS and replenished in the culture medium (as above) and incubated with either rabbit anti-IcsA pAbs (3.125 μg/ml and 0.3125 μg/ml) or rabbit pre-immune serum (concentration of IgG 100 μg/ml) for 15 min. Bacteria with antibodies were then added onto cell monolayers at the MOI of 100 and incubated for another 15 min at 37 °C with 5% CO_2. For both assays, unbound *Shigella* bacteria were washed three times with PBS, and monolayers were lysed using 0.1% (v/v) Triton X-100 at 37 °C for 10 min. The remaining *Shigella* bacteria were enumerated by serial dilution plating onto LB agar.

3.4.11 Statistical analysis

The statistical analysis on *Shigella* adherence and invasion assays was performed using GraphPad Prism 8.0.0. Data was normalised against the relevant control and significance was calculated using either a student *t* test or one-way ANOVA followed by Dunnett's multiple comparisons test against the control.

3.4.12 Protein lysates, cell fractionation and far Western blotting

HeLa cells grown to confluence on 100 mm dishes (approximately 8.8×10^8 cells) were recovered either by using a cell scraper or trypsin digestion, and washed with

PBS followed by centrifugation (4,000 ×g, 5 min, 4 °C). Pellets were lysed using RIPA buffer [25 mM Tris-HCl, 150 mM NaCl, 1% (v/v) NP-40, 0.5% (w/v) deoxycholate, 0.1% (w/v) SDS, 1 mM Na_3VO_4, 1 mM phenylmethylsulfonyl fluoride (PMSF), 10 µg/ml leupeptin] as described previously (Suzuki *et al.*, 1998). Lysates were then ultracentrifuged (185,000 ×g, 30 min, 4 °C) and resuspended in the same volume of SDS-PAGE sample buffer, incubated at 95 °C for 10 min, then electrophoresed into a 4-12% gradient SDS-PAGE gel (Thermo Fisher) and transferred onto a nitrocellulose membrane.

Cell fractionation was performed as described by Laarmann and Schmidt (2003). Briefly, HeLa cells were scraped from the 100 mm dishes into PBS containing 1 mM Pefabloc and 10 µg ml^{-1} leupeptin, and then sonicated on ice. The sonicated mix was then ultracentrifuged (108,000 ×g, 30 min, 4°C). The supernatant was isolated as the cytosolic fraction and the pellet was washed with PBS before resuspension in buffer containing 0.1 M Na_2CO_3/1 M NaCl (pH 11) and incubated on ice for 30 min. The extracted membrane lysate was then ultracentrifuged as above, resulting in a membrane associated fraction in the supernatant and the integral membrane fraction in the pellet. The pellet was solubilised in 2% (w/v) CHAPS in sonication buffer, and ultracentrifuged again, resulting in the detergent resistant integral membrane fraction in the pellet. All fractions were solubilised in SDS-PAGE sample buffer incubated at 95 °C for 10 min, then electrophoresed into a 4-12% gradient SDS-PAGE gel (Thermo Fisher), and transferred onto a nitrocellulose membrane.

For far Western blotting, the membrane was blocked in 5% (w/v) skim milk in TBST [50 mM Tris, pH 7.0, 150 mM NaCl, 0.1% Tween 20] and incubated with 12.5 µg $IcsA^{53\text{-}740}$ or $IcsA^{\Delta 138\text{-}148}$ in TBST with 5% (w/v) skim milk overnight at 4 °C. The membrane was then washed with TBS three times and the interaction between $IcsA^{53\text{-}740}$ or $IcsA^{\Delta 138\text{-}148}$ and host cell proteins was detected with the anti-IcsA antibody as above.

3.4.13 N-WASP pull down

For N-WASP pull down experiments, approximately 60 µg mini-N-WASP-GST protein purified as described previously (Papayannopoulos *et al.*, 2005) was mixed with either 12.5 µg $IcsA^{53\text{-}740}$ or $IcsA^{53\text{-}740(\Delta 138\text{-}148)}$, and incubated with 200 µl glutathione Sepharose™ 4B (GE Healthcare) resin overnight at 4 °C. $IcsA^{53\text{-}740}$ and $IcsA^{53\text{-}740(\Delta 138\text{-}148)}$ were mixed with or without GST, incubated with glutathione Sepharose™ 4B (GE

Healthcare) resin and served as controls. Resins were washed sequentially with PBS; PBS containing 1 mM DTT; PBS containing 0.1% (v/v) NP-40; and PBS for three times each. Protein was eluted in 50 µl PBS containing 20 mM reduced glutathione.

3.4.14 IcsA structure prediction

The structure of IcsA passenger was acquired using I-TASSER (Roy *et al.*, 2010) and analysed using Chimera (Pettersen *et al.*, 2004).

3.5. Article results

3.5.1 Purification of IcsA passenger protein and refolding

In order to validate the role of IcsA in *Shigella* adherence *in vitro*, the IcsA passenger domain (53-740) without the previously described unstructured region (741-758) (Kuhnel & Diezmann, 2011) was expressed from a pBAD vector with an N-terminal His×12 tag for purification (Fig S1 A). $IcsA^{53-740}$ was purified from urea solubilised inclusion bodies via nickel affinity purification. Fractions containing $IcsA^{53-740}$ were pooled and further purified by size exclusion chromatography (Fig S1 B) and refolded via dialysis. This purification strategy has significant advantages including high yields and reduced endogenous degradation of the autotransporter passenger domain, a type of domain family that is notoriously difficult to purify in a stable and soluble state.

Since human neutrophil elastase (hNE) has been reported to specifically target *Shigella* surface virulence factors (Weinrauch *et al.*, 2002) and has previously been used to assess the conformation and folding of IcsA (Brotcke-Zumsteg *et al.*, 2014), we conducted hNE digestions on the purified $IcsA^{53-740}$ to assess the success of refolding. The purified $IcsA^{53-740}$ showed several resistant fragments, with sizes of approximately 70 kDa, 60 kD, 40 kDa, 12 kDa and 5 kDa (Fig S1 D), suggesting that the protein has a compact structure which is resistant to hNE proteolysis. Heat denaturation at 65 °C for 5 min resulted in $IcsA^{53-740}$ becoming susceptible to hNE, with complete digestion into fragments less than 15 kDa within the first 5 min (Fig S1 E). In addition, the refolded $IcsA^{53-740}$ was able to interact with mini-N-WASP protein (Fig S2). Together, these data suggest that the purified $IcsA^{53-740}$ was successfully refolded and was functional after purification from inclusion bodies.

3.5.2 Adherence of hyper-adhesion *Shigella* mutants is highly IcsA dependent

While previous data strongly indicated that IcsA has adhesin activity (Brotcke-Zumsteg *et al.*, 2014), this has not been directly demonstrated. We hypothesised that the passenger domain of IcsA directly binds specifically to host cell surface factors in a way that pre-treatment of host cells with purified $IcsA^{53-740}$ would block the adherence of

subsequently added *S. flexneri*. As expected, an *ΔipaD* mutant strain exhibited an increased adherence phenotype to HeLa cells compared to wild type *S. flexneri* (Fig 1A). This increase in adherence is dependent on the presence of IcsA because deletion of IcsA abolished the hyper-adherence (Fig 1A). More importantly, addition of the purified $IcsA^{53-740}$, but not the dialysis buffer or BSA protein, was able to inhibit the adherence of the *ΔipaD* mutant to HeLa cells in a dose dependent manner (Fig 1A). This inhibition was also confirmed for a hyper-adherent *ΔipaB* mutant (Fig S3). Moreover, these data also confirmed that the purified $IcsA^{53-740}$ protein was folded in a functional conformation. To confirm that endogenous IcsA on the bacterial surface has a direct contribution to the adherence observed for the *ΔipaD* mutant, an adherence blocking assay using polyclonal anti-IcsA antibodies was also conducted (Fig 1B). It was found that pre-treatment of bacteria with anti-IcsA antibodies, but not the rabbit pre-immune serum, was able to significantly block the adherence of the *ΔipaD* mutant to host cells (Fig 1B). Collectively, these data confirmed a direct role of IcsA in the *S. flexneri* hyper-adherence activity exhibited by *ΔipaD* and *ΔipaB* mutants.

3.5.3 IcsA binds specifically to the host cells

Evidence was next generated to determine whether that the IcsA passenger domain binds specifically to host cell molecules as potential receptors for adherence. The purified $IcsA^{53-740}$ was fluorescently labelled by reacting with DL^{594} maleimide (Fig 2A). BSA protein labelled with DL^{594} was used as a control (Fig 2A). Unlike the control BSA-DL^{594}, $IcsA^{53-740}$- DL^{594} was detected on the surface of the HeLa cells (Fig 2B). To investigate whether the interaction between $IcsA^{53-740}$ and the HeLa cell surface was specified by a host cell displayed factor, trypsin treated, or untreated HeLa cells lysates were subjected to far Western blotting with $IcsA^{53-740}$ protein (Fig 3A). Two trypsin sensitive molecules (~60 kDa and >200 kDa) were recognised by $IcsA^{53-740}$ protein (Fig 3A). The anti-IcsA antibody showed no cross reaction to the HeLa cell lysate (Fig 3A). To further validate the cell surface location of these IcsA targets, HeLa cells were fractionated (Fig 3B), and subjected to far Western blotting with purified $IcsA^{53-740}$. IcsA interacting components from integral membrane fractions (Fig 3B, lane 4) were detected and two of which were corresponding in size (>200 kDa and ~60 kDa) to the trypsin sensitive molecules from whole cell lysate (Fig 3A). Apart from these two molecules, we also detected bands at ~25 kDa and

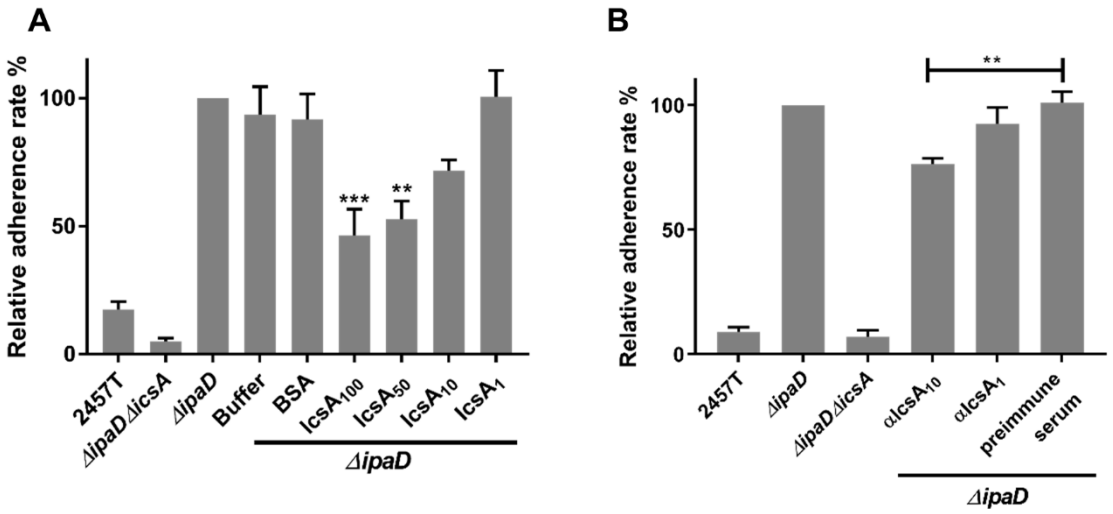

Fig 1. Inhibition of the IcsA-mediated adherence by purified IcsA passenger protein and anti-IcsA antibodies.

A. IcsA adherence blocking assay. *Shigella* grown to an OD_{600} of 0.5 were collected and used to infect HeLa cell monolayer at the MOI of 100. Purified $IcsA^{53\text{-}740}$ protein at the concentration of 2.5 μM ($IcsA_{100}$), 1.25 μM ($IcsA_{50}$), 250 nM ($IcsA_{10}$) and 25 nM ($IcsA_1$) were applied at the same time. Refolding buffer and BSA at the concentration of 2.8 μM were used as negative controls. After 15 min incubation, the cell monolayers were washed and lysed. Lysates were serial diluted before dotting on an agar plate for enumeration. Data are normalised against *ΔipaD* (defined as 100%) and are the mean with SEM of three independent experiments. Significance was calculated using one-way ANOVA followed by Dunnett's multiple comparisons test against *ΔipaD*, and *p* values are as follows: **, $p<0.01$; ***, $p<0.001$. **B.** Antibody adherence blocking assay. *Shigella* grown to an OD_{600} of 0.5 were collected and incubated with 3.125 μg/ml (αIcsA10), 0.3125 μg/ml (αIcsA1) of anti-IcsA antibodies or rabbit pre-immune serum with 100 μg/ml IgG for 15 min before infecting HeLa cell monolayers at the MOI of 100. After an extend 15 min incubation, cell monolayers were treated as in A. Data are normalised against the *ΔipaD* (defined as 100%) and are the mean with SEM of three independent experiments. Significance was calculated using a student *t* test, and *p* values are as follows: **, $p<0.01$.

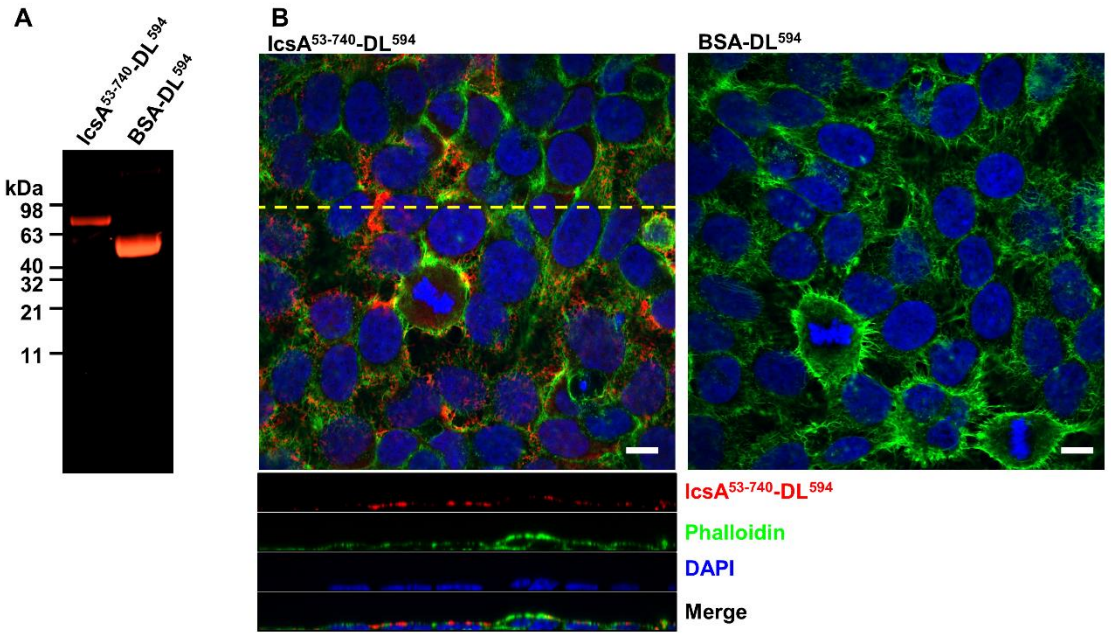

Fig 2. IcsA binds to the surface of HeLa cells.

A. Fluorescent labelling of IcsA$^{53\text{-}740}$. IcsA$^{53\text{-}740}$ protein and BSA protein were reacted with DL^{594} maleimide overnight and dialysed against protein solubilisation buffer. Labelled fluorescent protein probes were detected at the 650 nm after SDS-PAGE. **B.** IcsA$^{53\text{-}740}$-DL^{594} labelled HeLa cells. IcsA$^{53\text{-}740}$-DL^{594} at the concentration of 2.8 μM was applied to cells for 15 min. Samples were then permeabilised and stained with phalloidin and DAPI sequentially. Images were acquired by confocal microscopy with the orthogonal view (position as shown by the dashed yellow line) of a z stack shown below. Cells were stained in the same way with BSA-DL^{594}at 28 μM as a negative control. Scale bars = 10 μm.

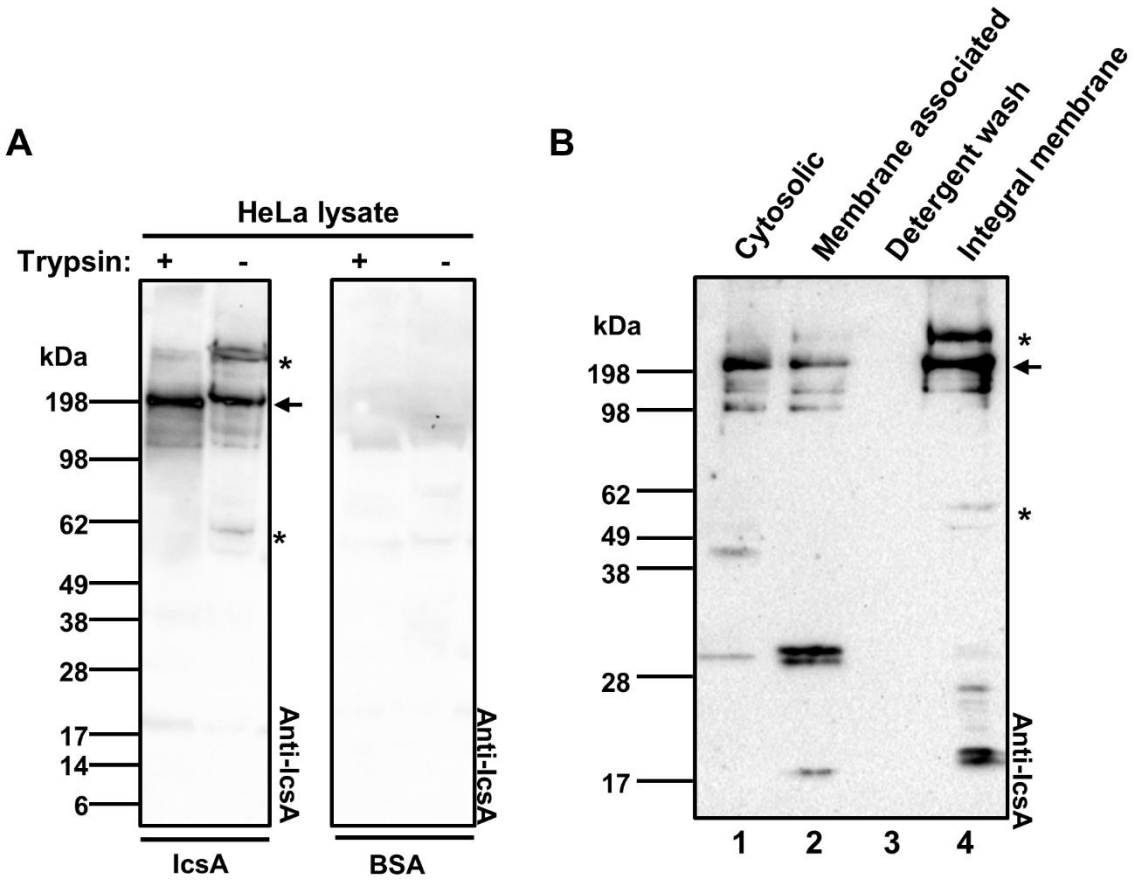

Fig 3. Interactions between IcsA passenger protein and host cell molecules.

A. Far Western blotting of HeLa cell lysates with IcsA$^{53\text{-}740}$. Confluent HeLa cells were recovered either by trypsinisation or cell scraper and lysed by RIPA buffer. Lysates were then separated by SDS-PAGE, transferred onto a nitrocellulose membrane, and probed with IcsA$^{53\text{-}740}$ passenger protein or BSA as a negative control. Membranes were subsequently probed with anti-IcsA antibody. **B.** Far Western blotting of HeLa cell fractions with IcsA$^{53\text{-}740}$. HeLa cells were lysed and cytosolic and membrane fractions were isolated. All fractions were subjected to far Western blotting, as in A.

20 kDa that interacted with IcsA$^{53-740}$ (Fig 3B lane 4). A molecule at ~ 200 kDa was detected across the all fractions (Fig 3B, lane 1, 2 & 4). These data suggest that the interactions between the IcsA$^{53-740}$ passenger domain and the host cell surface is specific and complex.

3.5.4 IcsA amino acid region 138-148 is required for adhesion

To identify functional regions required in adhesin activity, we utilised our previously generated plasmid collection that express IcsA mutants harbouring 5 amino acid insertions across the passenger domain (May & Morona, 2008) to screen for defects in *S. flexneri* adherence. These plasmids were introduced into *S. flexneri ΔipaDΔicsA* and transformants were used in adherence assays with HeLa cells. In a preliminary experiment attempting to repeat the result of Brotcke-Zumsteg *et al.* (2014), the IcsA^{i148} mutant but not the IcsA^{i386} mutant had an adherence defect (Fig S4 A). The screening was then focused on the N-terminus of IcsA passenger domain and three sites (i138, i140 and i148) were found to result in mutated IcsA protein having significant defect in adherence activity (Fig S4 B). To further investigate this region (138-148), the amino acids from 138 to 148 were each substituted for alanine and the resulting mutants were screened via HeLa adherence assays (Fig S4 C). However, none of these mutants conferred a significant defect in adherence indicating that a larger region, rather than individual residues, drives host receptor interactions. Subsequently, the adjacent amino acids to the i138, i140 and i148 insertion sites (138 and 139, 140 and 141, and 148 and 149 respectively) were randomly substituted and screened for the defects in adherence. Two IcsA mutants (IcsA^{I138P} and IcsA$^{Q148C/G149N}$) were found to cause complete loss of IcsA adherence function (Fig 4A). A deletion spanning this region (IcsA$^{\Delta 138-148}$), was likewise defective in adherence (Fig 4B). To rule out any confounding effects caused by centrifugation, adherence assays were also performed with passive settling of bacteria (Fig 4C). Compared to the point mutants IcsA^{I138P} and IcsA$^{Q148C/G149N}$, the deletion mutant (IcsA$^{\Delta 138-148}$) was found to have the greatest defect in adherence (Fig 4C).

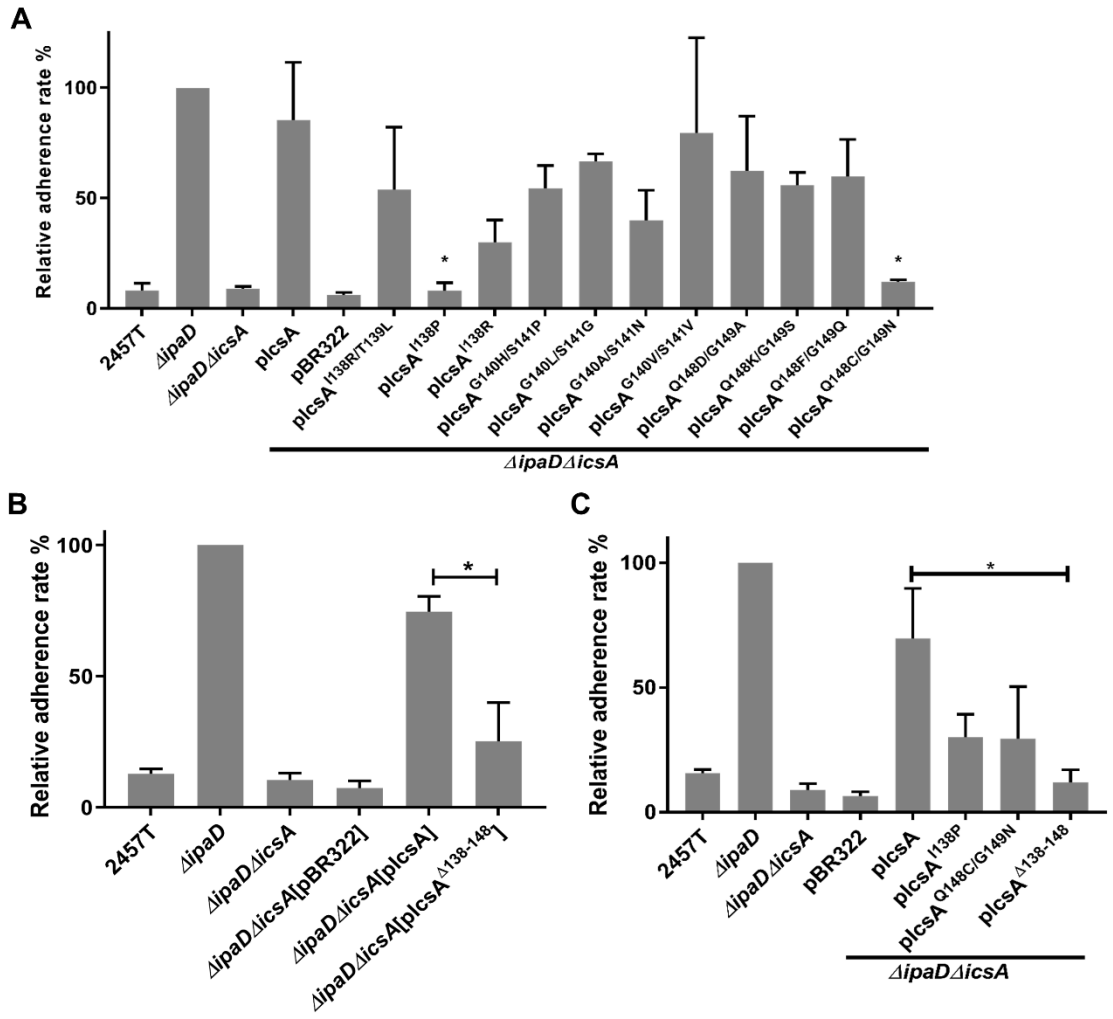

Fig 4. Identification of IcsA adherence function regions.

A. Screening for adherence related regions using IcsA point mutants and adherence assays. Mid-exponential phase *S. flexneri* were collected and used to infect HeLa cell monolayers at a MOI of 100 for 15 min. Monolayers were washed, lysed, and lysates were serial diluted before spotting on an agar plate for enumeration. Data are normalised against *ΔipaD* (defined as 100%) and are the mean with SEM of three independent experiments. Significance was calculated using one-way ANOVA followed by Dunnett's multiple comparisons test against *ΔipaDΔicsA*[pIcsA], and *p* values are as follows: *, $p<0.05$. **B.** Adherence assay of the IcsA$^{\Delta 138\text{-}148}$ mutant. Significance was calculated using a student *t* test, and *p* values are as follows: *, $p<0.05$. **C.** Adherence assay of IcsA adherent defective mutants. Adherence assays were performed as above with passive settling of bacteria. Significance was calculated using a student *t* test, and *p* values are as follows: *, $p<0.05$.

The adherence functional region 138 to 148 is within the glycine repeat region (May & Morona, 2008), thus deletion of this region might affect IcsA biogenesis and/or its ABM function. To test this, the expression, polar localisation, and ABM function of IcsA$^{\Delta 138\text{-}148}$ were confirmed by Western blotting (Fig S5 A), immunofluorescent staining (Fig S5 B), and plaque formation (Fig S5 C) respectively. There was no difference in IcsA expression level, its surface localisation, and the size of plaques formed, between IcsA and IcsA$^{\Delta 138\text{-}148}$. This rules out any major defects in IcsA biogenesis and ABM function for this mutant.

To validate that IcsA$^{\Delta 138\text{-}148}$ has a defect in adherence *in vitro*, IcsA$^{53\text{-}740(\Delta 138\text{-}148)}$ was expressed, purified, and refolded in an equivalent manner to IcsA$^{53\text{-}740}$. Refolded IcsA$^{53\text{-}740(\Delta 138\text{-}148)}$ was able to interact with mini-N-WASP protein *in vitro* (Fig S2), confirming that the region 138-148 is not essential for IcsA's ABM function, and that purified IcsA$^{53\text{-}740(\Delta 138\text{-}148)}$ protein was functional. However, relative to IcsA$^{53\text{-}740}$, IcsA$^{53\text{-}740(\Delta 138\text{-}148)}$ was unable to block the adherence of *S. flexneri ΔipaD* (Fig 5A). Moreover, in far Western blotting of HeLa cell lysates, unlike IcsA$^{53\text{-}740}$, IcsA$^{53\text{-}740(\Delta 138\text{-}148)}$ had greatly reduced interaction with host molecules (Fig 5B), given that the deletion of 138-148 did not affect the recognition via anti-IcsA antibody (Fig S2). Fluorescently labelled IcsA$^{53\text{-}740(\Delta 138\text{-}148)}$ (Fig 6A) was prepared and used to label HeLa cells, but no staining was detected (Fig 6C). These data further supporting the notion that residues 138 to 148 affect IcsA's adhesin function.

In the human gut, *Shigella* virulence is activated by, among other stimuli, bile salt components such as DOC (Pope *et al.*, 1995).The impact of the aa 138-148 region on DOC induced hyper-adherence was investigated. As expected, DOC at the physiological concentration 2.5 mM was able to enhance the adherence of *Shigella* significantly (Fig 7A). However, the IcsA$^{\Delta 138\text{-}148}$ mutant displayed a significant defect in the DOC enhanced adherence (Fig 7A), which again confirmed that the region from 138-148 is required for the IcsA-mediated adherence. Moreover, invasion of HeLa cells by *S. flexneri ΔicsA* complemented with IcsA$^{\Delta 138\text{-}148}$ to HeLa cells was also significantly attenuated (Fig 7B), indicating that the IcsA-mediated adherence is required for *Shigella* invasion.

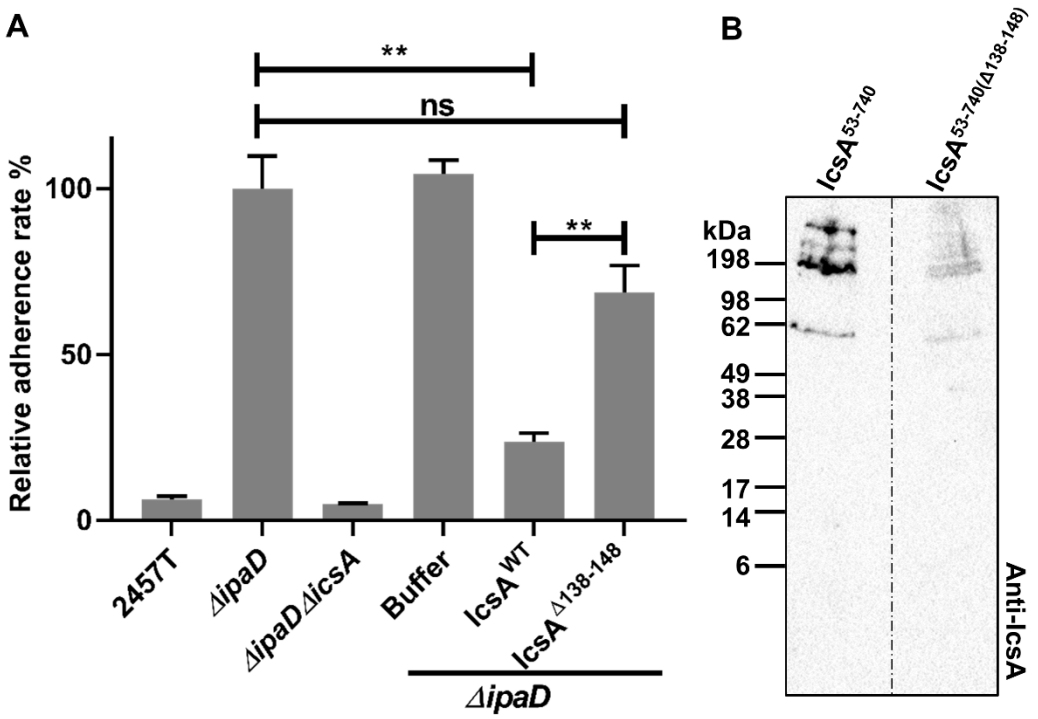

Fig 5. Confirmation of the IcsA adherence related region 138-148.

A. IcsA adherence blocking assay. *Shigella* grown to an OD_{600} of 0.5 were collected and used to infect HeLa cell monolayer at the MOI of 100. Purified wild type ($IcsA^{53\text{-}740}$) or mutant ($IcsA^{53\text{-}740(\Delta 138\text{-}148)}$) IcsA passenger protein at the concentration of 1.25 μM were applied at the same time. Refolding buffer was used as a negative control. After 15 min incubation, the cell monolayers were washed and lysed. Lysates were serial diluted before dotting on an agar plate for enumeration. Data are normalised against the mean of *ΔipaD* (defined as 100%) and are the mean with SEM of three independent experiments. Significance was calculated using a student *t* test, and *p* values are as follows: **, $p<0.01$. **B.** Far Western blotting of HeLa cell lysates with wild type ($IcsA^{53\text{-}740}$) or mutant ($IcsA^{53\text{-}740(\Delta 138\text{-}148)}$) IcsA passenger protein. HeLa cells grown on 100 mm dish were recovered either by trypsin or cell scraper, and lysed by RIPA buffer. Lysates were then separated by 12% SDS-PAGE, transferred onto a nitrocellulose membrane, and probed by either $IcsA^{53\text{-}740}$ or mutant $IcsA^{53\text{-}740(\Delta 138\text{-}148)}$ protein (12.5 μg) overnight at 4 °C. The membrane was then washed by TBST and subjected to Western blotting with anti-IcsA antibody. Note that B contains two membranes (indicated by the dashed line) that were incubated with antibodies and imaged together.

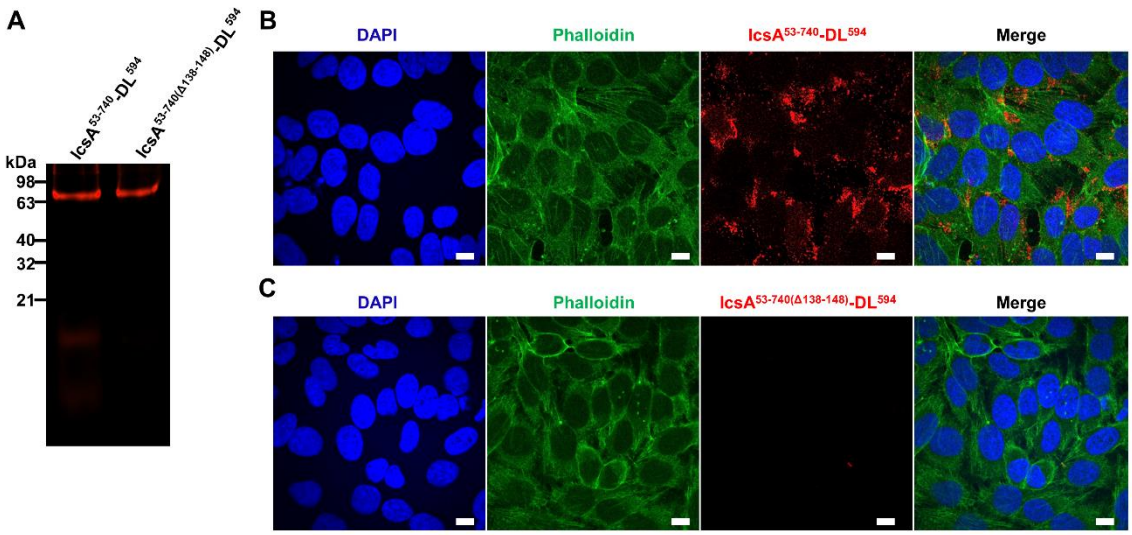

Fig 6. IcsAΔ138-148 lacks the binding ability to HeLa cells.

A. Fluorescent labelling of IcsA$^{53\text{-}740}$ and IcsA$^{53\text{-}740(\Delta 138\text{-}148)}$. IcsA$^{53\text{-}740}$and IcsA$^{53\text{-}740(\Delta 138\text{-}148)}$ were reacted with DL^{594} maleimide overnight and dialysed against protein solubilisation buffer. Labelled fluorescent protein probes were detected at the 650 nm after SDS-PAGE. **B.** IcsA$^{53\text{-}740}$ protein labelled HeLa cells. IcsA$^{53\text{-}740}$-DL^{594} at the concentration of 1.5 μM was applied in the assay. After an incubation of 15 min with HeLa monolayers, samples were then permeabilised and stained with phalloidin and DAPI sequentially. Image was acquired by confocal microscopy. **C.** IcsA$^{53\text{-}740(\Delta 138\text{-}148)}$ protein labelled HeLa cells. IcsA$^{53\text{-}740(\Delta 138\text{-}148)}$-DL^{594} at the concentration of 1.5 μM was applied in the assay and samples were treated the same as in A. Scale bars = 10 μm.

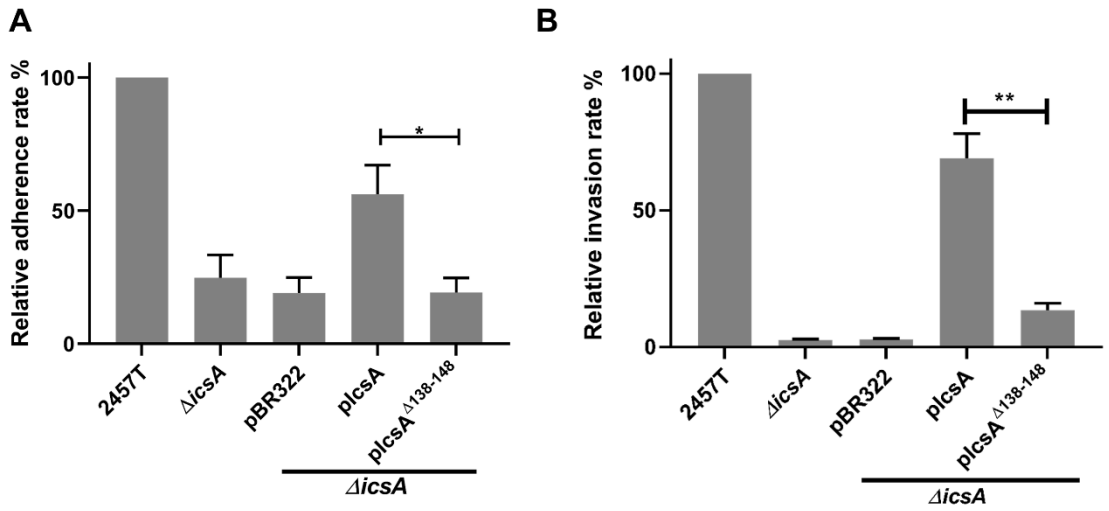

Fig 7. The adherence region IcsA 138-148 is required for *Shigella* adhesion and invasion during DOC stimulation.

A. Adherence assay. *Shigella* grown to an OD_{600} of 0.5 in the presence of 2.5 mM DOC were collected and used to infect HeLa cell monolayer at the MOI of 100. After 15 min incubation, the cell monolayers were washed and lysed. Lysates were serial diluted before dotting on an agar plate for enumeration. Data are normalised against 2457T (defined as 100%) and are the mean with SEM of three independent experiments. **B.** Invasion assay. *Shigella* grown to an OD_{600} of 0.5 in the presence of 2.5 mM DOC were collected and used to infect HeLa cell monolayer at the MOI of 100. At the 45 min post-infection, gentamicin was added and incubated with the cell monolayers for another 45 min. Cell monolayers were then treated as in A. Significance was calculated using a student *t* test, and *p* values are as follows: *, $p<0.05$; **, $p<0.01$.

3.6. Article discussion

In this work we have generated evidence that IcsA directly contributes to adherence of *Shigella* species to host cells. We were able to block the hyper-adherence phenotype of *S. flexneri ΔipaD* strains using either purified IcsA$^{53\text{-}740}$ passenger domain or anti-IcsA antibody. Purified IcsA$^{53\text{-}740}$ was able to bind host cell surfaces and recognised a multitude of host cell molecules. In addition, IcsA residues 138-148 were shown to be critical for adhesin function and purified IcsA$^{53\text{-}740(\Delta 138\text{-}148)}$ could no longer block *Shigella* adherence to host cells and was unable to recognise host cell molecules via far Western immunoblotting.

IcsA does not have detectable adherence activity in wild-type *S. flexneri* unless exposed to environmental stimuli (such as DOC) (Pope *et al.*, 1995), or via activation of the T3SS (Brotcke-Zumsteg *et al.*, 2014). IcsA adherence activity is strongly associated to a conformational change as detected by proteinase accessibility (Brotcke-Zumsteg *et al.*, 2014). Nevertheless, in *E. coli*, heterogeneously expressed IcsA can promote bacterial adherence to host cells (Brotcke-Zumsteg *et al.*, 2014), presumably because the conformation, stimuli, folding, or modification of IcsA is different to that of the *S. flexneri*. Indeed, through hNE digestion analysis on our refolded IcsA$^{53\text{-}740}$, we detected a resistant fragment of ~40 kD similarly to that reported previously for the hNE digestion of IcsA on intact *S. flexneri* bacteria (Brotcke-Zumsteg *et al.*, 2014), where a fragment around 40 kDa was more resistant to degradation by hNE in those strains with increased IcsA-mediated adherence. It is plausible that in *Shigella*, IcsA's function in adherence is carefully downregulated by some mechanism governed by the T3SS before it encounters an environmental cue, such as DOC, whereas in *E. coli*, lack of such a regulating system allows IcsA to exert its adherence function constitutively.

The purified and refolded IcsA$^{53\text{-}740}$ passenger domain retains its activity as a *Shigella* adhesin. Due to this, pre-incubation of the HeLa cells with purified IcsA$^{53\text{-}740}$protein blocks the adherence of *S. flexneri ΔipaD* and *ΔipaB* strain. The minimum IcsA concentration in our experiments showing significant adherence blocking was 1.25 µM, which is approximately 10,000 times to the IcsA molecules expressed per input bacteria, assuming that each bacterium expresses approximately 4,000 IcsA molecules on the surface (Magdalena & Goldberg, 2002). This is likely because purified IcsA$^{53\text{-}740}$ must bind to many

host cell receptors to block adherence. Indeed, comparable concentrations of antigens were also used to block virus entry (Tiwari *et al.*, 2011) and bacteria adherence (Rose *et al.*, 2008) to host cells. This is also supported by both the fluorescent labelling of HeLa cell surface and the far Western immunoblotting with purified $IcsA^{53-740}$, indicating a specific and complex interaction between IcsA and host cells. It was not surprising that $IcsA^{53-740}$ recognised other molecules from both cytosolic and membrane associated fractions, as IcsA is known to interact with cytosolic molecules responsible for actin based motility (Teh & Morona, 2013) and is recognised by host cell autophagic systems (Ogawa *et al.*, 2005). In our antibody blocking assay, the anti-IcsA antibody at 3.125 µg/ml blocked the *Shigella* adherence significantly, which is comparable to the concentrations of antibodies used in other studies (Amerighi *et al.*, 2016, Zhao *et al.*, 2018, Perez-Zsolt *et al.*, 2019). Given that our data support a model where IcsA may recognise multiple receptors on host cells, and that anti-IcsA antibodies were able to neutralise *Shigella* adherence *in vitro*, this strongly suggests that the IcsA passenger domain has excellent vaccine potential.

The previous study using our IcsA insertion library found insertions at sites 148 and 386 affected IcsA-mediated *Shigella* adherence (Brotcke-Zumsteg *et al.*, 2014). However, in the present study i138, i140, and i148, but not i386, were found to result in decreased IcsA-mediated adherence. The discrepancy at the site 386 is possibly due to the differences in the screening system. In the previous study (Brotcke-Zumsteg *et al.*, 2014), IcsA mutants with normal ABM function and defects in DOC-enhanced *Shigella* invasion were selected, whereas in this study, the adherence region was screened directly by assessing the adherence of *Shigella* IcsA insertion mutants to HeLa cells. While alanine scanning mutagenesis of the region 138-148 showed no significant defect in adherence, it is likely that the entire region 138-148 is required for multiple contacts between IcsA and host cell receptors such that the overall interface stability between IcsA and receptor cannot be significantly reduced by any single alanine substitution. Nevertheless, site-directed mutagenesis on the IcsAi-adjacent amino acids revealed substitution mutants (I138P and Q148C/G149N) that resulted in significant defects in adherence. Moreover, deletion of the entire region (138-148) in the IcsA passenger domain also reproduced the defect of the 5aa insertions, and was much more severe compared to the double mutants.

We speculate that this 138-148 IcsA region is involved in host cell receptor binding events. Indeed, in a predicted IcsA passenger structure (Fig S6), the predicted β-rung harbouring aa 138-148 is smaller than the adjacent β-helixes and generates a groove in the IcsA passenger domain that might function as a putative receptor binding cleft. The Q148C found next to another cysteine (C130) in space located on the adjacent β-strand in the β-helix potentially allows the formation of a disulfide bond that might obstruct this binding cleft. Furthermore, purified mutant IcsA$^{53\text{-}740(\Delta 138\text{-}148)}$ passenger domain was unable to block adherence and showed reduced interactions to host cell components further supporting our speculations that this region might be a binding cleft for host receptors. Even DOC-stimulated hyper-adherence of *S. flexneri* expressing mutant IcsA (IcsA$^{\Delta 138\text{-}148}$) consistently showed a defect in adherence and host cell invasion. IcsA has established functional roles in binding of host cell cytosolic factors to nucleate ABM, and the IcsA passenger domain can also accommodate further functions in adhesion via a specific binding region. Therefore, IcsA is a truly multifunctional virulence factor providing an avenue for *Shigella* to quickly respond to the pathogenic niche for adhesion, invasion, and spreading (Koseoglu & Agaisse, 2019).

3.7. Funding statement

We gratefully acknowledge the University of Adelaide for awarding a Faculty of Science Postgraduate Scholarship to J.Q.

3.8. Article references

1. Speelman P, Kabir I, Islam M. Distribution and spread of colonic lesions in shigellosis: a colonoscopic study. J Infect Dis. 1984;150(6):899-903. Epub 1984/12/01. doi: 10.1093/infdis/150.6.899. PubMed PMID: 6501931.
2. Good RC, May BD, Kawatomari T. Enteric pathogens in monkeys. J Bacteriol. 1969;97(3):1048-55. Epub 1969/03/01. PubMed PMID: 4180466; PubMed Central PMCID: PMCPMC249813.
3. Kotloff KL, Riddle MS, Platts-Mills JA, Pavlinac P, Zaidi AKM. Shigellosis. Lancet. 2018;391(10122):801-12. Epub 2017/12/20. doi: 10.1016/S0140-6736(17)33296-8. PubMed PMID: 29254859.
4. Kozyreva VK, Jospin G, Greninger AL, Watt JP, Eisen JA, Chaturvedi V. Recent outbreaks of shigellosis in California caused by two distinct populations of *Shigella sonnei* with either increased virulence or fluoroquinolone resistance. Msphere. 2016;1(6). Epub 2016/12/29. doi: 10.1128/mSphere.00344-16. PubMed PMID: 28028547; PubMed Central PMCID: PMCPMC5177732.
5. Anand BS, Malhotra V, Bhattacharya SK, Datta P, Datta D, Sen D, et al. Rectal histology in acute bacillary dysentery. Gastroenterology. 1986;90(3):654-60. Epub 1986/03/01. doi: 10.1016/0016-5085(86)91120-0. PubMed PMID: 3510937.
6. Wassef JS, Keren DF, Mailloux JL. Role of M cells in initial antigen uptake and in ulcer formation in the rabbit intestinal loop model of shigellosis. Infect Immun. 1989;57(3):858-63. Epub 1989/03/01. PubMed PMID: 2645214; PubMed Central PMCID: PMCPMC313189.

7. Ranganathan S, Doucet M, Grassel CL, Delaine-Elias B, Zachos NC, Barry EM. Evaluating *Shigella flexneri* pathogenesis in the human enteroid model. Infect Immun. 2019;87(4). Epub 2019/01/16. doi: 10.1128/IAI.00740-18. PubMed PMID: 30642900; PubMed Central PMCID: PMCPMC6434113.
8. Arena ET, Campbell-Valois FX, Tinevez JY, Nigro G, Sachse M, Moya-Nilges M, et al. Bioimage analysis of *Shigella* infection reveals targeting of colonic crypts. Proc Natl Acad Sci U S A. 2015;112(25):E3282-90. Epub 2015/06/10. doi: 10.1073/pnas.1509091112. PubMed PMID: 26056271; PubMed Central PMCID: PMCPMC4485126.
9. Brotcke-Zumsteg A, Goosmann C, Brinkmann V, Morona R, Zychlinsky A. IcsA is a *Shigella flexneri* adhesin regulated by the type III secretion system and required for pathogenesis. Cell Host Microbe. 2014;15(4):435-45.
10. Emsley P, Charles IG, Fairweather NF, Isaacs NW. Structure of *Bordetella pertussis* virulence factor P.69 pertactin. Nature. 1996;381(6577):90-2. Epub 1996/05/02. doi: 10.1038/381090a0. PubMed PMID: 8609998.
11. Charbonneau ME, Janvore J, Mourez M. Autoprocessing of the *Escherichia coli* AIDA-I autotransporter: a new mechanism involving acidic residues in the junction region. J Biol Chem. 2009;284(25):17340-51. Epub 2009/04/29. doi: 10.1074/jbc.M109.010108. PubMed PMID: 19398552; PubMed Central PMCID: PMCPMC2719369.
12. Heras B, Totsika M, Peters KM, Paxman JJ, Gee CL, Jarrott RJ, et al. The antigen 43 structure reveals a molecular Velcro-like mechanism of autotransporter-mediated bacterial clumping. Proc Natl Acad Sci U S A. 2014;111(1):457-62. Epub 2013/12/18.

doi: 10.1073/pnas.1311592111. PubMed PMID: 24335802; PubMed Central PMCID: PMCPMC3890832.

13. Doyle MT, Tran EN, Morona R. The passenger-associated transport repeat promotes virulence factor secretion efficiency and delineates a distinct autotransporter subtype. Mol Microbiol. 2015;97(2):315-29. Epub 2015/04/15. doi: 10.1111/mmi.13027. PubMed PMID: 25869731.
14. Doyle MT, Grabowicz M, Morona R. A small conserved motif supports polarity augmentation of *Shigella flexneri* IcsA. Microbiology. 2015;161(11):2087-97. Epub 2015/09/01. doi: 10.1099/mic.0.000165. PubMed PMID: 26315462.
15. Kuhnel K, Diezmann D. Crystal structure of the autochaperone region from the *Shigella flexneri* autotransporter IcsA. J Bacteriol. 2011;193(8):2042-5. Epub 2011/02/22. doi: 10.1128/JB.00790-10. PubMed PMID: 21335457; PubMed Central PMCID: PMCPMC3133035.
16. Leupold S, Busing P, Mas PJ, Hart DJ, Scrima A. Structural insights into the architecture of the *Shigella flexneri* virulence factor IcsA/VirG and motifs involved in polar distribution and secretion. J Struct Biol. 2017;198(1):19-27. Epub 2017/03/08. doi: 10.1016/j.jsb.2017.03.003. PubMed PMID: 28268178.
17. Goldberg MB, Barzu O, Parsot C, Sansonetti PJ. Unipolar localization and ATPase activity of IcsA, a *Shigella flexneri* protein involved in intracellular movement. Infect Agents Dis. 1993;2(4):210-1. Epub 1993/08/01. PubMed PMID: 8173795.
18. Goldberg MB, Theriot JA. *Shigella flexneri* surface protein IcsA is sufficient to direct actin-based motility. Proc Natl Acad Sci U S A. 1995;92(14):6572-6. Epub 1995/07/03.

doi: 10.1073/pnas.92.14.6572. PubMed PMID: 7604035; PubMed Central PMCID: PMCPMC41560.

19. Teh MY, Morona R. Identification of *Shigella flexneri* IcsA residues affecting interaction with N-WASP, and evidence for IcsA-IcsA co-operative interaction. PloS one. 2013;8(2):e55152. Epub 2013/02/14. doi: 10.1371/journal.pone.0055152. PubMed PMID: 23405119; PubMed Central PMCID: PMCPMC3566212.
20. Suzuki T, Sasakawa C. N-WASP is an important protein for the actin-based motility of *Shigella flexneri* in the infected epithelial cells. Jpn J Med Sci Biol. 1998;51 Suppl:S63-8. Epub 1999/04/22. doi: 10.7883/yoken1952.51.supplement1_s63. PubMed PMID: 10211437.
21. Suzuki T, Mimuro H, Suetsugu S, Miki H, Takenawa T, Sasakawa C. Neural Wiskott-Aldrich syndrome protein (N-WASP) is the specific ligand for *Shigella* VirG among the WASP family and determines the host cell type allowing actin-based spreading. Cell Microbiol. 2002;4(4):223-33. Epub 2002/04/16. PubMed PMID: 11952639.
22. Egile C, Loisel TP, Laurent V, Li R, Pantaloni D, Sansonetti PJ, et al. Activation of the CDC42 effector N-WASP by the *Shigella flexneri* IcsA protein promotes actin nucleation by Arp2/3 complex and bacterial actin-based motility. J Cell Biol. 1999;146(6):1319-32. Epub 1999/09/24. doi: 10.1083/jcb.146.6.1319. PubMed PMID: 10491394; PubMed Central PMCID: PMCPMC2156126.
23. Koseoglu VK, Hall CP, Rodriguez-Lopez EM, Agaisse H. The autotransporter IcsA promotes *Shigella flexneri* biofilm formation in the presence of bile salts. Infect Immun. 2019;87(7):e00861-18. Epub 2019/04/17. doi: 10.1128/IAI.00861-18. PubMed PMID: 30988059; PubMed Central PMCID: PMCPMC6589070.

24. May KL, Morona R. Mutagenesis of the *Shigella flexneri* autotransporter IcsA reveals novel functional regions involved in IcsA biogenesis and recruitment of host neural Wiscott-Aldrich syndrome protein. J Bacteriol. 2008;190(13):4666-76. Epub 2008/05/06. doi: 10.1128/JB.00093-08. PubMed PMID: 18456802; PubMed Central PMCID: PMCPMC2446779.
25. Datsenko KA, Wanner BL. One-step inactivation of chromosomal genes in *Escherichia coli* K-12 using PCR products. Proc Natl Acad Sci U S A. 2000;97(12):6640-5. Epub 2000/06/01. doi: 10.1073/pnas.120163297. PubMed PMID: 10829079; PubMed Central PMCID: PMCPMC18686.
26. Sambrook J, Russell DW. The inoue method for preparation and transformation of competent *E. Coli*: "ultra-competent" cells. CSH Protoc. 2006;2006(1). Epub 2006/01/01. doi: 10.1101/pdb.prot3944. PubMed PMID: 22485385.
27. Tartoff KD, Hobbs CA. Improved media for growing plasmid and cosmid clones. Bethesda Research Laboratories Focus. 1987;9(12).
28. Van den Bosch L, Manning PA, Morona R. Regulation of O-antigen chain length is required for *Shigella flexneri* virulence. Mol Microbiol. 1997;23(4):765-75. Epub 1997/02/01. doi: 10.1046/j.1365-2958.1997.2541625.x. PubMed PMID: 9157247.
29. Lugtenberg B, Meijers J, Peters R, van der Hoek P, van Alphen L. Electrophoretic resolution of the 'major outer membrane protein' of *Escherichia coli* K12 into four bands. FEBS Lett. 1975;58(1-2):254-8. doi: 10.1016/0014-5793(75)80272-9.
30. May KL, Grabowicz M, Polyak SW, Morona R. Self-association of the *Shigella flexneri* IcsA autotransporter protein. Microbiology. 2012;158(Pt 7):1874-83. Epub 2012/04/21. doi: 10.1099/mic.0.056465-0. PubMed PMID: 22516224.

31. Suzuki T, Miki H, Takenawa T, Sasakawa C. Neural Wiskott-Aldrich syndrome protein is implicated in the actin-based motility of *Shigella flexneri*. The EMBO journal. 1998;17(10):2767-76. Epub 1998/06/10. doi: 10.1093/emboj/17.10.2767. PubMed PMID: 9582270; PubMed Central PMCID: PMCPMC1170617.
32. Laarmann S, Schmidt MA. The *Escherichia coli* AIDA autotransporter adhesin recognizes an integral membrane glycoprotein as receptor. Microbiology. 2003;149(Pt 7):1871-82. Epub 2003/07/12. doi: 10.1099/mic.0.26264-0. PubMed PMID: 12855737.
33. Papayannopoulos V, Co C, Prehoda KE, Snapper S, Taunton J, Lim WA. A polybasic motif allows N-WASP to act as a sensor of PIP(2) density. Mol Cell. 2005;17(2):181-91. Epub 2005/01/25. doi: 10.1016/j.molcel.2004.11.054. PubMed PMID: 15664188.
34. Roy A, Kucukural A, Zhang Y. I-TASSER: a unified platform for automated protein structure and function prediction. Nat Protoc. 2010;5(4):725-38. Epub 2010/04/03. doi: 10.1038/nprot.2010.5. PubMed PMID: 20360767; PubMed Central PMCID: PMCPMC2849174.
35. Pettersen EF, Goddard TD, Huang CC, Couch GS, Greenblatt DM, Meng EC, et al. UCSF Chimera--a visualization system for exploratory research and analysis. J Comput Chem. 2004;25(13):1605-12. Epub 2004/07/21. doi: 10.1002/jcc.20084. PubMed PMID: 15264254.
36. Weinrauch Y, Drujan D, Shapiro SD, Weiss J, Zychlinsky A. Neutrophil elastase targets virulence factors of enterobacteria. Nature. 2002;417(6884):91-4. Epub 2002/05/23. doi: 10.1038/417091a. PubMed PMID: 12018205.
37. Pope LM, Reed KE, Payne SM. Increased protein secretion and adherence to HeLa cells by *Shigella spp*. following growth in the presence of bile salts. Infect Immun.

1995;63(9):3642-8. Epub 1995/09/01. PubMed PMID: 7642302; PubMed Central PMCID: PMCPMC173505.

38. Magdalena J, Goldberg MB. Quantification of *Shigella* IcsA required for bacterial actin polymerization. Cell Motil Cytoskel. 2002;51(4):187-96. Epub 2002/04/27. doi: 10.1002/cm.10024. PubMed PMID: 11977093.

39. Tiwari V, Liu J, Valyi-Nagy T, Shukla D. Anti-heparan sulfate peptides that block herpes simplex virus infection *in vivo*. J Biol Chem. 2011;286(28):25406-15. Epub 2011/05/21. doi: 10.1074/jbc.M110.201103. PubMed PMID: 21596749; PubMed Central PMCID: PMCPMC3137111.

40. Rose L, Shivshankar P, Hinojosa E, Rodriguez A, Sanchez CJ, Orihuela CJ. Antibodies against PsrP, a novel *Streptococcus pneumoniae* adhesin, block adhesion and protect mice against pneumococcal challenge. J Infect Dis. 2008;198(3):375-83. Epub 2008/05/30. doi: 10.1086/589775. PubMed PMID: 18507531.

41. Ogawa M, Yoshimori T, Suzuki T, Sagara H, Mizushima N, Sasakawa C. Escape of intracellular *Shigella* from autophagy. Science. 2005;307(5710):727-31. Epub 2004/12/04. doi: 10.1126/science.1106036. PubMed PMID: 15576571.

42. Zhao WD, Liu DX, Wei JY, Miao ZW, Zhang K, Su ZK, et al. Caspr1 is a host receptor for meningitis-causing *Escherichia coli*. Nat Commun. 2018;9(1):2296. Epub 2018/06/14. doi: 10.1038/s41467-018-04637-3. PubMed PMID: 29895952; PubMed Central PMCID: PMCPMC5997682.

43. Perez-Zsolt D, Erkizia I, Pino M, Garcia-Gallo M, Martin MT, Benet S, et al. Anti-Siglec-1 antibodies block Ebola viral uptake and decrease cytoplasmic viral entry. Nat

Microbiol. 2019;4(9):1558-70. Epub 2019/06/05. doi: 10.1038/s41564-019-0453-2. PubMed PMID: 31160823.

44. Amerighi F, Valeri M, Donnarumma D, Maccari S, Moschioni M, Taddei A, et al. Identification of a monoclonal antibody against pneumococcal pilus 1 ancillary protein impairing bacterial adhesion to human epithelial cells. J Infect Dis. 2016;213(4):516-22. Epub 2015/09/25. doi: 10.1093/infdis/jiv461. PubMed PMID: 26401026.
45. Koseoglu VK, Agaisse H. Evolutionary perspectives on the moonlighting functions of bacterial factors that support actin-based motility. MBio. 2019;10(4). Epub 2019/08/29. doi: 10.1128/mBio.01520-19. PubMed PMID: 31455648; PubMed Central PMCID: PMCPMC6712393.

3.9. Article supporting information

S1 Table. Strains and Plasmids

Strain or plasmid	Characteristics	Source/reference
Strains		
2457T	Wild type *S. flexneri* 2a	(Van Den Bosch *et al.*, 1997)
RMA2041	2457T*ΔicsA::Tc*^{R}	(Morona & Van Den Bosch, 2003)
RMA2090	2457T*ΔicsA::Tc*^{R}[pIcsA]	(Van den Bosch & Morona, 2003)
JQRM9	2457T*ΔipaD*	This study
JQRM10	2457T*ΔipaB*	This study
JQRM11	2457T*ΔipaDΔicsA::Tc*^{R}	This study
JQRM12	2457T*ΔipaBΔicsA::Tc*^{R}	This study
MDRM190	TOP10[pMDBADIcsA$^{53\text{-}740}$]	This study
JQRM116	TOP10[pMDBAD-*icsA*$^{\Delta 138\text{-}148}$]	This study
Shigella IcsA 5aa insertion collection		
JQRM16	2457T*ΔicsAΔipaD::frt*[pIcsA]	This study
JQRM17	2457T*ΔicsAΔipaD::frt*[pBR322]	This study
JQRM22	2457T*ΔicsAΔipaD::frt*[pIcsA^{i56}]	This study
JQEM23	2457T*ΔicsAΔipaD::frt*[pIcsA^{i81}]	This study
JQRM24	2457T*ΔicsAΔipaD::frt*[pIcsA^{i87}]	This study
JQRM25	2457T*ΔicsAΔipaD::frt*[pIcsA^{i120}]	This study
JQRM26	2457T*ΔicsAΔipaD::frt*[pIcsA^{i122}]	This study
JQRM27	2457T*ΔicsAΔipaD::frt*[pIcsA^{i128}]	This study
JQRM28	2457T*ΔicsAΔipaD::frt*[pIcsA^{i132}]	This study
JQRM29	2457T*ΔicsAΔipaD::frt*[pIcsA^{i137}]	This study
JQRM30	2457T*ΔicsAΔipaD::frt*[pIcsA^{i138}]	This study
JQRM31	2457T*ΔicsAΔipaD::frt*[pIcsA^{i140}]	This study

JQRM32	2457T*ΔicsAΔipaD::frt*[pIcsA^{i148}]	This study
JQRM33	2457T*ΔicsAΔipaD::frt*[pIcsA^{i185}]	This study
JQRM34	2457T*ΔicsAΔipaD::frt*[pIcsA^{i193}]	This study
JQRM35	2457T*ΔicsAΔipaD::frt*[pIcsA^{i219}]	This study
JQRM36	2457T*ΔicsAΔipaD::frt*[pIcsA^{i226}]	This study
JQRM37	2457T*ΔicsAΔipaD::frt*[pIcsA^{i228}]	This study
JQRM38	2457T*ΔicsAΔipaD::frt*[pIcsA^{i230}]	This study
JQRM39	2457T*ΔicsAΔipaD::frt*[pIcsA^{i244}]	This study
JQRM40	2457T*ΔicsAΔipaD::frt*[pIcsA^{i248}]	This study
JQRM41	2457T*ΔicsAΔipaD::frt*[pIcsA^{i268}]	This study
JQRM42	2457T*ΔicsAΔipaD::frt*[pIcsA^{i271}]	This study
JQRM43	2457T*ΔicsAΔipaD::frt*[pIcsA^{i288}]	This study
JQRM44	2457T*ΔicsAΔipaD::frt*[pIcsA^{i292}]	This study
JQRM45	2457T*ΔicsAΔipaD::frt*[pIcsA^{i297}]	This study
JQRM46	2457T*ΔicsAΔipaD::frt*[pIcsA^{i312}]	This study
JQRM47	2457T*ΔicsAΔipaD::frt*[pIcsA^{i314}]	This study
JQRM48	2457T*ΔicsAΔipaD::frt*[pIcsA^{i322}]	This study
JQRM49	2457T*ΔicsAΔipaD::frt*[pIcsA^{i324}]	This study
JQRM50	2457T*ΔicsAΔipaD::frt*[pIcsA^{i326}]	This study
JQRM51	2457T*ΔicsAΔipaD::frt*[pIcsA^{i330a}]	This study
JQRM52	2457T*ΔicsAΔipaD::frt*[pIcsA^{i330b}]	This study
JQRM53	2457T*ΔicsAΔipaD::frt*[pIcsA^{i342}]	This study
JQRM54	2457T*ΔicsAΔipaD::frt*[pIcsA^{i346}]	This study
JQRM55	2457T*ΔicsAΔipaD::frt*[pIcsA^{i369}]	This study
JQRM56	2457T*ΔicsAΔipaD::frt*[pIcsA^{i381}]	This study
JQRM57	2457T*ΔicsAΔipaD::frt*[pIcsA^{i386}]	This study
JQRM58	2457T*ΔicsAΔipaD::frt*[pIcsA^{i456}]	This study
JQRM59	2457T*ΔicsAΔipaD::frt*[pIcsA^{i502}]	This study
JQRM60	2457T*ΔicsAΔipaD::frt*[pIcsA^{i532}]	This study
JQRM61	2457T*ΔicsAΔipaD::frt*[pIcsA^{i563}]	This study
JQRM62	2457T*ΔicsAΔipaD::frt*[pIcsA^{i595}]	This study

JQRM63	2457T*ΔicsAΔipaD::frt*[pIcsA^{i598}]	This study
JQRM64	2457T*ΔicsAΔipaD::frt*[pIcsA^{i633}]	This study
JQRM65	2457T*ΔicsAΔipaD::frt*[pIcsA^{i643}]	This study
JQRM66	2457T*ΔicsAΔipaD::frt*[pIcsA^{i677}]	This study
JQRM67	2457T*ΔicsAΔipaD::frt*[pIcsA^{i716}]	This study
JQRM68	2457T*ΔicsAΔipaD::frt*[pIcsA^{i748}]	This study
	IcsA point mutants	
JQRM85	2457T*ΔicsAΔipaD::frt*[pIcsA$^{I138R/T139L}$]	This study
JQRM86	2457T*ΔicsAΔipaD::frt*[pIcsA$^{I138P/T139T}$]	This study
JQRM94	2457T*ΔicsAΔipaD::frt*[pIcsA$^{I138R/T139T}$]	This study
JQRM96	2457T*ΔicsAΔipaD::frt*[pIcsA$^{G140H/S141P}$]	This study
JQRM98	2457T*ΔicsAΔipaD::frt*[pIcsA$^{G140L/S141G}$]	This study
JQRM101	2457T*ΔicsAΔipaD::frt*[pIcsA$^{G140A/S140N}$]	This study
JQRM102	2457T*ΔicsAΔipaD::frt*[pIcsA$^{G140V/S140V}$]	This study
JQRM106	2457T*ΔicsAΔipaD::frt*[pIcsA$^{Q148D/G149S}$]	This study
JQRM107	2457T*ΔicsAΔipaD::frt*[pIcsA$^{Q148K/G149S}$]	This study
JQRM109	2457T*ΔicsAΔipaD::frt*[pIcsA$^{Q148F/G149Q}$]	This study
JQRM111	2457T*ΔicsAΔipaD::frt*[pIcsA$^{Q148C/G149N}$]	This study
	Alanine scanning	
JQRM141	2457T*ΔicsAΔipaD::frt*[pIcsA^{138A}]	This study
JQRM142	2457T*ΔicsAΔipaD::frt*[pIcsA^{139A}]	This study
JQRM143	2457T*ΔicsAΔipaD::frt*[pIcsA^{140A}]	This study
JQRM144	2457T*ΔicsAΔipaD::frt*[pIcsA^{141A}]	This study
JQRM145	2457T*ΔicsAΔipaD::frt*[pIcsA^{142A}]	This study
JQRM146	2457T*ΔicsAΔipaD::frt*[pIcsA^{143A}]	This study
JQRM147	2457T*ΔicsAΔipaD::frt*[pIcsA^{144A}]	This study
JQRM148	2457T*ΔicsAΔipaD::frt*[pIcsA^{145A}]	This study
JQRM149	2457T*ΔicsAΔipaD::frt*[pIcsA^{146A}]	This study
JQRM150	2457T*ΔicsAΔipaD::frt*[pIcsA^{147A}]	This study
JQRM151	2457T*ΔicsAΔipaD::frt*[pIcsA^{148A}]	This study
JQRM152	2457T*ΔicsAΔipaD::frt*[pIcsA^{149A}]	This study

Plasmids

pMDBADIcsA$^{53-740}$	IcsA$^{53-740}$ expression construct	This study
pIcsA	pBR322 derivatives with CDS of IcsA	(Van den Bosch & Morona, 2003)
pJQ9	pIcsA$^{\Delta 138-148}$ IcsA mutant	This study
pJQ11	pMDBAD::*icsA*$^{53-740/\Delta 138-148}$	This study
pKD46	Lambda red plasmid, Ap^{R}, 30 °C	(Datsenko & Wanner, 2000)
pKD4	Vector containing FRT-flanked *kan*^{R} gene	(Datsenko & Wanner, 2000)
pCP20	FLP recombinase, Ap^{R}, Cm^{R}, 30 °C	(Datsenko & Wanner, 2000)

References

1. Van Den Bosch L, Manning PA, Morona R. 1997. Regulation of O-antigen chain length is required for *Shigella flexneri* virulence. Mol Microbiol 23:765-775.
2. Morona R, Van Den Bosch L. 2003. Multicopy *icsA* is able to suppress the virulence defect caused by *wzz*(SF) mutation in the *Shigella flexneri*. FEMS Microbiol Lett 221:213-219.
3. Van den Bosch L, Morona R. 2003. The actin-based motility defect of a *Shigella flexneri rmlD* rough LPS mutant is not due to loss of IcsA polarity. Microb Pathog 35:11-8.
4. Datsenko KA, Wanner BL. 2000. One-step inactivation of chromosomal genes in *Escherichia coli* K-12 using PCR products. Proc Natl Acad Sci U S A 97:6640-5.

S2 Table Oligonucleotides

Oligos	Sequence[#]	Description
JQ1	TATATCCAAGAGCCATAATAATATATGGCTCTTCCTGTAAGGAAATAACCGTGTAGGCTGGAGCTGCTTC	*ΔipaD* Fwd
JQ2	GCCTTATATAAGAATGTTGGCGCTTGAGTATTATTTACATTATGCATGGCGCACCGCCATGGTCCATATGAATATCCTCC	*ΔipaD* Rev
JQ3	AAAGCACAATCATACTTGGACGCAATTCAGGATATCAAGGAGTAATTATTGTGTAGGCTGGAGCTGCTTC	*ΔipaB* Fwd
JQ4	TATAAAATCTGGGTTGGTTTTGTGTTTTGAATTTCCATAACATTCTCCTTATTTGTAGCCATGGTCCATATGAATATCCTCC	*ΔipaB* Rev
MD80	TTTTTTCTCGAGACTCCTCTTTCGGGTACTCAAG	XhoI $IcsA^{53}$ Fwd
MD81	TTTTTTGGTACCTTATCCATCTGACTAGTTAGATACCAC	KpnI $IcsA^{740}$ Rev
MD85	GGTATGGCTAGCATGACTGGTGG	His_{12} Fwd
MD86	ATGATGATGATGATGATGATGATGATGATGATGATGAGAACCCCCC	His_{12} Rev
JQ27	AATAGTTGTGGCGGTAATGGTGGTGACTCTNNNNNNGGATCTGACTTGTCTATAATCAATCAAGG	Site-directed mutagenesis primer targeting $IcsA_{138-139}$
JQ28	TGTGGCGGTAATGGTGGTGACTCTATTACCNNNNNNGACTTGTCTATAATCAATCAAGGCATG	Site-directed mutagenesis primer targeting $IcsA_{140-141}$
148NNS	ATTACCGGATCTGACTTGTCTATAATCAATNNSNNSATGATTCTTGGTGGTAGCGGCGGTAGCG	Site-directed mutagenesis primer targeting $IcsA_{148-149}$

JQ43	AGAGTCACCACCATTACCG	Universal primer for alanine scanning aa 138-149
JQ44	GCTACCGGATCTGACTTGTCTATAATC	Mutagenesis primer, I138A
JQ45	ATTGCTGGATCTGACTTGTCTATAATCAATCAAG	Mutagenesis primer, T139A
JQ46	ATTACCGCTTCTGACTTGTCTATAATCAATCAAGG	Mutagenesis primer, G140A
JQ47	ATTACCGGAGCTGACTTGTCTATAATCAATCAAGGCATG	Mutagenesis primer, S141A
JQ48	ATTACCGGATCTGCTTTGTCTATAATCAATCAAGGCATGATTC	Mutagenesis primer, D142A
JQ49	ATTACCGGATCTGACGCTTCTATAATCAATCAAGGCATGATTCTTG	Mutagenesis primer, L143A
JQ50	ATTACCGGATCTGACTTGGCTATAATCAATCAAGGCATGATTCTTGG	Mutagenesis primer, S144A
JQ51	ATTACCGGATCTGACTTGTCTGCTATCAATCAAGGCATGATTCTTGG	Mutagenesis primer, I145A
JQ52	ATTACCGGATCTGACTTGTCTATAGCTAATCAAGGCATGATTCTTGGTG	Mutagenesis primer, I146A
JQ53	ATTACCGGATCTGACTTGTCTATAATCGCTCAAGGCATGATTCTTGGTGG	Mutagenesis primer, N147A
JQ54	ATTACCGGATCTGACTTGTCTATAATCAATGCTGGCATGATTCTTGGTGGTAG	Mutagenesis primer, Q148A
JQ55	ATTACCGGATCTGACTTGTCTATAATCAATCAAGCTATGATTCTTGGTGGTAGCGG	Mutagenesis primer, G149A

underlined nucleotides are degenerated nucleotides.

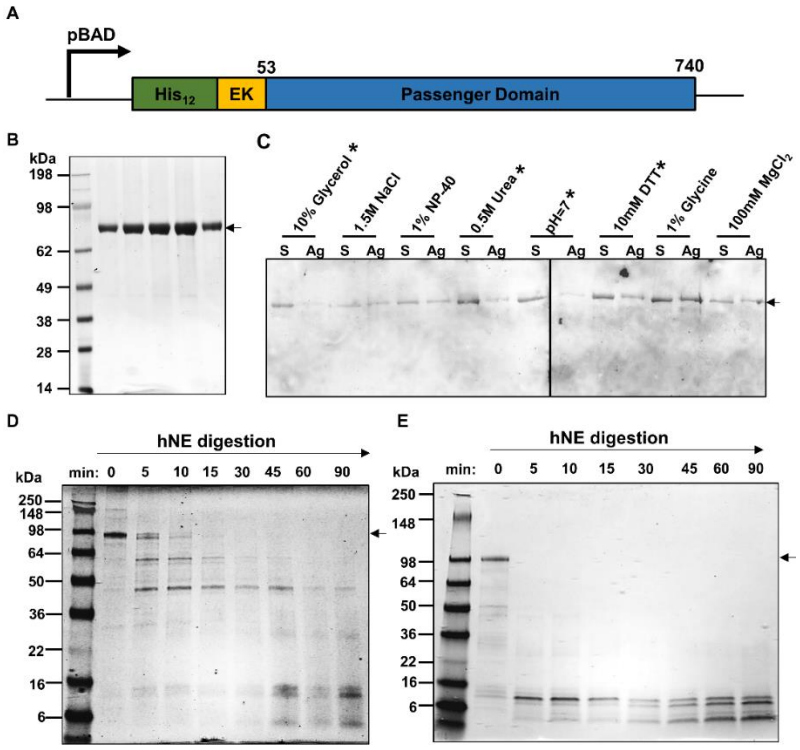

Fig S1. Expression, purification and refolding of the IcsA passenger protein.

A. Schematic representation of IcsA passenger expression construct. IcsA passenger from amino acid 53 to 740 was fused with a His_{12} tag; its expression in *E. coli* Top10 was controlled by the pBAD promoter. EK, enterokinase site. **B.** Coomassie blue staining of purified fractions containing $IcsA^{53-740}$ protein. $IcsA^{53-740}$ protein (indicated by the arrow) was solubilised from inclusion bodies, purified through nickel affinity chromatography and further cleaned by size exclusion gel filtration. Peak fractions were analysed by SDS-PAGE and stained by Coomassie blue. **C.** IcsA passenger refolding buffer screening. $IcsA^{53-740}$protein was diluted 1 in 20 into different buffer solutions (as indicated), and after an incubation of approximately 16 h at 4 °C, solutions were ultracentrifuged, resulting in the soluble fractions in the supernatant (S) and the insoluble fractions in the aggregates (Ag). Both fractions were separated by 12% SDS-PAGE and transferred onto nitrocellulose membrane and stained with Ponceau S. Buffer solutions are all based on 50 mM NaCl, 50 mM Tris, pH 8, unless where stated. **D.** Limited proteolysis of refolded $IcsA^{53-740}$ protein by human neutrophil elastase (hNE). Following purification, $IcsA^{53-740}$ protein was dialysed and digested by hNE in the molecular ratio of 1000:1. Sample from different time points were taken and analysed by Coomassie blue stained SDS-polyacrylamide gel. **E.** Limited proteolysis of heat inactivated $IcsA^{53-740}$ protein by human neutrophil elastase (hNE). Refolded $IcsA^{53-740}$ protein was heated to 65 °C for 15 min and cooled to room temperature before being digested by hNE in the molecular ratio of 1000:1.

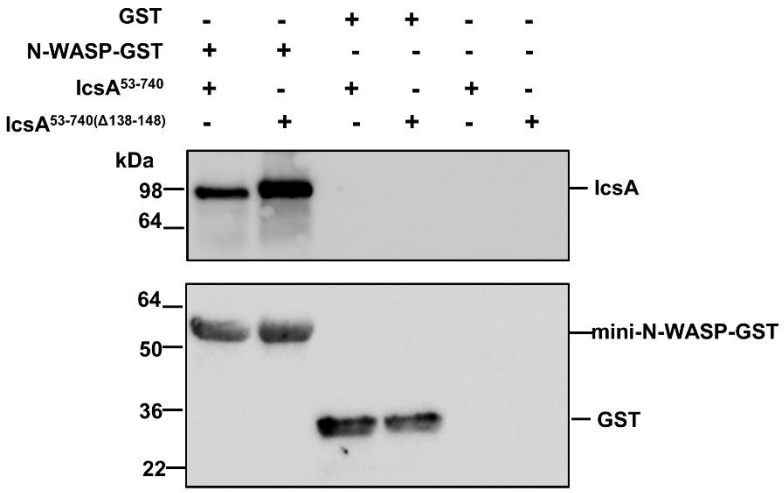

Fig S2. Purified IcsA protein was able to interact with mini-N-WASP.

IcsA$^{53\text{-}740}$ and IcsA$^{53\text{-}740(\Delta 138\text{-}148)}$ were mixed with mini-N-WASP-GST, incubated with glutathione resin overnight. IcsA$^{53\text{-}740}$ and IcsA$^{53\text{-}740(\Delta 138\text{-}148)}$ were mixed with or without GST, incubated with glutathione resin and served as controls. Resin was then washed, and protein was eluted and analysed via a 12% SDS-PAGE gel and Western immunoblotting using anti-IcsA antibody (upper) **or** anti-GST antibody (lower).

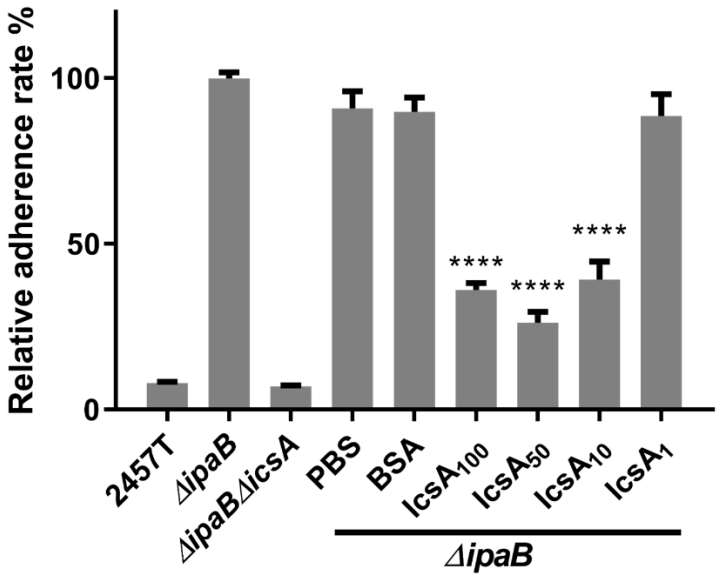

Fig S3. Inhibition of the IcsA-mediated adherence of S. flexneri *ΔipaB* with IcsA passenger protein.

Shigella grown to an OD_{600} of 0.5 were collected and used to infect HeLa cell monolayer at the MOI of 100. Purified $IcsA^{53-740}$ protein at the concentration of 2.5 μM ($IcsA_{100}$), 1.25 μM ($IcsA_{50}$), 250 nM ($IcsA_{10}$) and 25 nM ($IcsA_1$) were applied at the same time. Refolding buffer and BSA at the concentration of 2.8 μM were used as negative controls. After 15 min incubation, the cell monolayers were washed and lysed. Lysates were serial diluted before dotting onto agar plates for enumeration. Data are normalised against the mean of *ΔipaB* (defined as 100%) and are the mean with SEM of four independent experiments. Significance was calculated using one-way ANOVA followed by Dunnett's multiple comparisons test against *ΔipaB*, and *p* values are as follows: ****, $p<0.0001$.

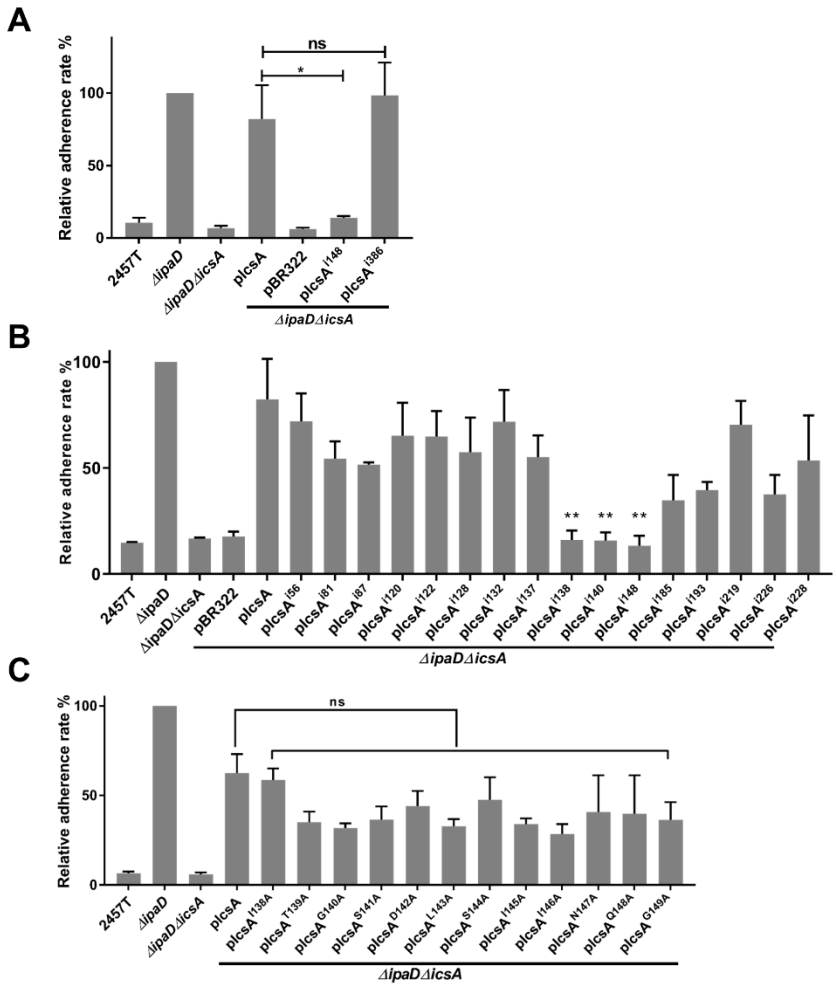

Fig S4. Screening of the IcsA mutants via adherence assays.

A. Screening of the putative adherence defective IcsA mutants via adherence assay. *Shigella ΔipaDΔicsA* expressing the indicated IcsA mutant constructs were grown to an OD_{600} of 0.5 and used to infect HeLa cell monolayer at the MOI of 100. After 15 min infection, the cell monolayers were washed and lysed. Lysates were serial diluted before dotting onto agar plates for enumeration. Data are normalised against *ΔipaD* (defined as 100%) and are the mean with SEM of three independent experiments. Significance was calculated using a student *t* test, and *p* values are as follows: *, $p<0.05$. **B.** Screening of the *Shigella* IcsA 5aa insertion mutants via adherence assays performed as in **A**. Data represent two independent experiments. Significance was calculated using one-way ANOVA followed by Dunnett's multiple comparisons test against *ΔipaDΔicsA*[pIcsA], and *p* values are as follows: **, $p<0.01$. **C.** Alanine scanning of the IcsA adherent region via adherence assays. *Shigella ΔipaDΔicsA* expressing the indicated IcsA mutant constructs were used to infect HeLa cells as in A. Data represent two independent experiments. Experiments and statistical analysis were performed as above. ns: non-significant.

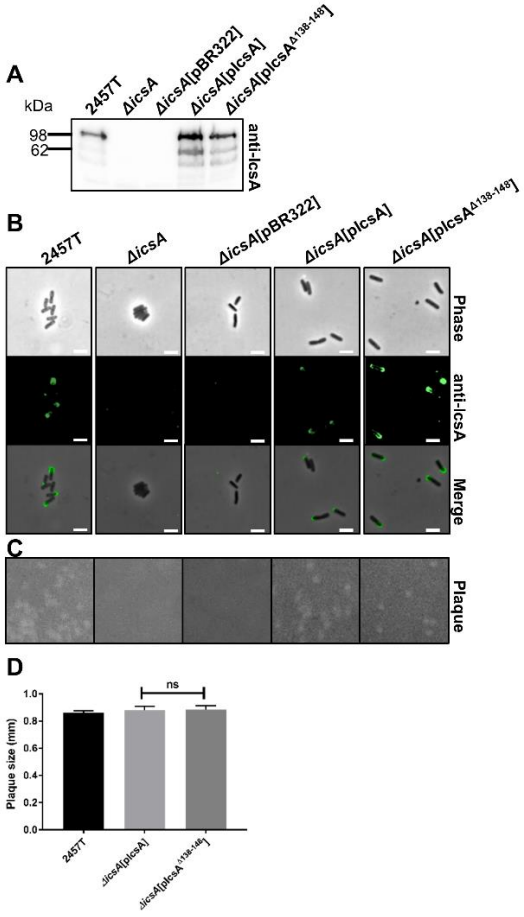

Fig S5. The region 138-148 does not affect IcsA's expression, localization and ABM function.

A. Western immunoblotting of *S. flexneri* 2457T, and *ΔicsA* expressing IcsA or IcsA$^{\Delta 138\text{-}148}$. *Shigella* strains grown to an OD_{600} of 0.5 were collected and analysed via a 12% SDS-PAGE gel and Western immunoblotting with anti-IcsA. **B.** Immunofluorescent staining of IcsA with whole *Shigella* bacteria. Bacteria grown to an OD_{600} of 0.5 were collected and fixed with formaldehyde. IcsA was stained with rabbit anti-IcsA, and Alexa Fluor 488 conjugated donkey anti-rabbit antibodies. Images were acquired using an Olympus epifluorescence microscope (May & Morona, 2008). Scale bar represents 2 µm. **C.** Plaque formation assay with IcsA mutants and their complemented strains. *Shigella* grown to an OD_{600} of 0.5 were collected to infect HeLa cell monolayers. After 1.5 h infection, the extracellular bacteria was killed by adding DMEM supplemented with 0.5% (w/v) agar and 40 µg/ml gentamycin. After 24 h post-infection, a second layer of DMEM medium containing 0.5% (w/v) agar and 0.1% (w/v) Neutral Red was added and images were taken after 72 h post-infection. **D.** Plaque size measurements for plaques formed in **C**. Data were acquired at least from 20 plaques for each strain and significance was calculated using a student *t* test, and p values are as follow: ns, non-significant. Note that *ΔicsA* and *ΔicsA* [pBR322] did not form plaques.

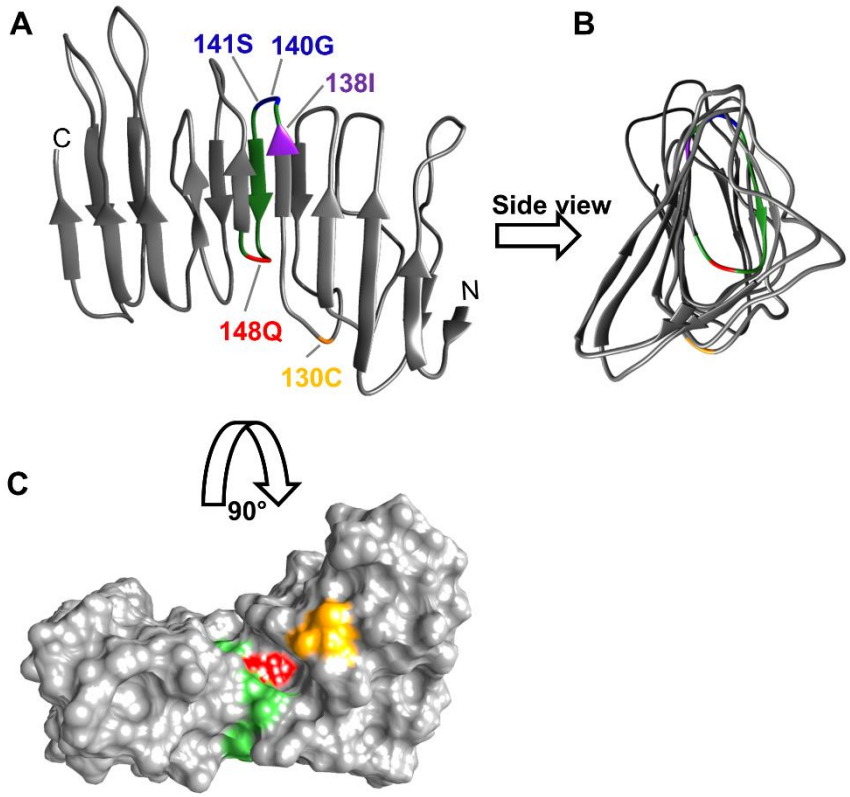

Fig S6. Structural analysis of the amino group substitution sites in the IcsA passenger domain.

A. Predicted structure of IcsA passenger 55-241 shown in ribbon. **B.** Side view of the ribbon structure of $IcsA^{55-241}$. **C.** Surface of the predicted $IcsA^{55-241}$ structure. The structure of the IcsA passenger (55-241) was acquired from Itasser and annotated using Chimera. The amino group adjacent to the insertion sites (i138, i140 and i148) are marked on the structure. The IcsA adherent region is shown in green.

Chapter Four

ARTICLE 2:

The passenger domain of *Shigella flexneri* IcsA has multiple conformations

Jilong Qin and Renato Morona

Chapter 4: The passenger domain of *Shigella flexneri* IcsA has multiple conformations

4.1. Statement of Authorship

Title of paper	The passenger domain of *Shigella flexneri* IcsA has multiple conformations
Status	Unpublished and unsubmitted work written in manuscript style
Authors	Qin, J. & Morona R.

Principal author

Principal author	Jilong Qin		
Contribution	Designed and conducted all experiments; analysed all results, constructed all figures, tables, supplementary information, wrote the manuscript		
Overall (%)	95		
Certification	This paper reports on original research I conducted during the period of my Higher Degree by Research candidature and is not subject to any obligations or contractual agreements with a third party that would constrain its inclusion in this thesis. I am the primary author of this paper.		
Signature		Date	2/12/19

Co-author contributions

By signing the Statement of Authorship, each author certifies that:

i. the candidate's stated contribution to the publication is accurate (as detailed above);

ii. permission is granted for the candidate in include the publication in the thesis; and

iii. the sum of all co-author contributions is equal to 100% less the candidate's stated contribution.

Author	Renato Morona		
Contribution	Supervised development of work; provided laboratory and materials; analysed data with principal author, evaluated and edited manuscript; acted as corresponding author.		
Signature		Date	2/12/19

4.2. Article abstract

Shigella species cause human bacillary dysentery by colonising the colonic mucosa which subsequently aids invasion of the colonic epithelium. IcsA, which has been long recognized for its actin-based motility (ABM) function that promotes cell to cell spread during the infection, also functions as a *Shigella* cell adhesin. IcsA's adhesin activity was proposed to be through a conformational change. This study revealed that the conformational change is dependent on the adhesin region (aa 138-148) and is likely due to an interaction between IcsA's N-terminal and C-terminal regions. Through the purification of IcsA passenger, two IcsA populations were isolated, and one was found to be stabilised via a disulfide bond. We propose that IcsA modulates its structure through a head to tail interaction and a disulfide bond formation stabilises this conformation.

4.3. Article introduction

Shigella spp. are responsible for approximately 100 million episodes of shigellosis and 164,000 death cases annually worldwide, especially among children under the age of 5 (Kotloff *et al.*, 2018). *Shigella* causes diseases in humans by targeting and invading human colonic epithelial cells (Labrec *et al.*, 1964, Mathan & Mathan, 1986), which triggers a massive inflammatory reaction, and causes severe tissue destruction (Perdomo *et al.*, 1994a), resulting in the disease symptoms of blood and mucoid stools. However, the mechanisms of how *Shigella* successfully adheres and colonises the human colon are poorly understood, and the IcsA protein is only one of the few surface molecules that have been reported to contribute to the attachment of *Shigella* to host cells (Brotcke-Zumsteg *et al.*, 2014).

IcsA has long been known for its role in the inter- and intra-cellular spreading (Bernardini *et al.*, 1989, Lett *et al.*, 1989). Inside host cells, IcsA on the old pole of bacteria binds to neural Wiskott–Aldrich Syndrome protein (N-WASP) (Suzuki *et al.*, 1998) and recruits the Arp2/3 complex (Egile *et al.*, 1999), which results in the polymerisation of actin, facilitating the movement of the bacteria. This is known as actin-based motility (ABM). IcsA also functions as an adhesin in the presence of a host environmental clue deoxycholate (DOC) or in IpaB or IpaD null *Shigella* mutants (Brotcke-Zumsteg *et al.*, 2014). It has been suggested that IcsA might possess two different conformations for its different roles (Brotcke-Zumsteg *et al.*, 2014), however the mechanism remains unclear.

In our previous study, IcsA has been confirmed as an adhesin directly contributing to *Shigella* adherence and a region (aa 138-148) that is responsible for IcsA's adhesin role was identified and characterized (Chapter 3). In this study, it was found that the IcsA adhesin region affects conformational change in the IcsA passenger domain. The conformational change is independent to LPS O antigen, and is likely to involve a head to tail interaction of the IcsA passenger domain.

4.4. Article methods and materials

4.4.1 Ethics statement

The anti-IcsA antibody were produced under the National Health and Medical Research Council (NHMRC) Australian Code of Practice for the Care and Use of Animals for Scientific Purposes, and was approved by the University of Adelaide Animal Ethics Committee (S-2012-90).

4.4.2 Bacterial maintenance and culture

Shigella flexneri strains (Table S1) were streaked onto Tryptic Soy Agar with 0.2% (w/v) Congo Red, and after incubation at 37 °C overnight, red colonies were selected and incubated in Lysogeny broth (LB) broth overnight with appropriate antibiotics (tetracycline, 10 μg/ml; kanamycin, 50 μg/ml; chloramphenicol, 25 μg/ml, spectinomycin 50 μg/ml and ampicillin, 100 μg/ml) in the presence or absence of 2.5 mM deoxycholate.

4.4.3 DNA manipulation

For proteinase accessibility assays, the coding sequence of FLAG×3 tag was added at the amino acid (aa) site 737 of the IcsA passenger in either pIcsA (Morona & Van Den Bosch, 2003) or pIcsA$^{\Delta 138\text{-}148}$ (Chapter 3) plasmids using inverse PCR (Fig S1A) with primers listed in Table S2, resulting in pIcsA^{FLAG} and pIcsA$^{FLAG/\Delta 138\text{-}148}$ respectively.

For IcsA passenger (IcsA$^{54::FLAG\times3}$) production, the sequences of *icsA* and *icsP* were PCR amplified from *S. flexneri* 2457T chromosomal DNA, digested with NcoI/SalI and NdeI/KpnI, respectively, and then ligated into the MCS1 and MCS2 of the pCDFDuet-1 (Novagen) plasmid to generate pCDFDuet-1::*icsA*-*icsP*. A FLAG×3 tag was inserted next to aa 54 of IcsA passenger domain via restriction free cloning. Primers (Table S2) were designed to be complement to each other and were used to PCR amplify gene blocks containing the coding sequence FLAG×3 tag flanked with sequence up- and down-stream of the insertion site aa 54 (Fig S1B). Gene blocks were then used as mega primers to PCR clone the FLAG×3 tag into the pCDFDuet-1::*icsA*-*icsP* to generate the co-expression construct pCDFDuet-1::*icsA*$^{54::FLAG}$-*icsP*.

4.4.4 IcsA passenger purification and size exclusion chromatography

For IcsA passenger (IcsA$^{54::FLAG\times3}$) production, pCDFDuet-1::*icsA*$_{54::FLAG\times3}$-*icsP* was introduced into C43(DE3). Bacterial strains were subcultured 1 in 20 into 4 L of LB from 18 h cultures and were grown to an OD_{600} of 0.4-0.6 at 37 °C. Expression of IcsA was then induced with 1 mM isopropyl β-D-1-thiogalactopyranoside (IPTG) and cultures were incubated at 30 °C for 18 h. The culture supernatant was harvested via centrifugation (7,000 ×g, 25 °C, 15 min), and further cleaned by passing through an asymmetric polyethersulfone (aPES) membrane with 0.2 μm pore size (Rapid-flow, Thermo Scientific). Proteins in the filtered culture supernatant were then concentrated and exchanged into 50 ml of TBS buffer [50 mM Tris, 150 mM NaCl, pH 7.5] using a VivaFlow 200 filtration system (Sartorius) with 30,000 MWCO PES membranes. The concentrated protein preparation was then loaded onto a TBS pre-equilibrated polypropylene column (Thermo Scientific) prepacked with 2 mL of anti-FLAG G1 resin (Genescript). The column was washed with TBS, and IcsA passenger was eluted with 10 ml of 100 mM glycine, pH 3.5. IcsA passenger was then concentrated to 500 µl using a Vivaspin 6 with 10 kDa MWCO (GE Healthcare). For size exclusion chromatography analysis, protein was loaded onto a Superdex 200 Increase 10/300 column (GE Healthcare) with TBS buffer, and different protein elution fractions were pooled and concentrated again as above, which yielded ~0.8 mg from 4 L culture supernatant. Sizes were calculated according to the Gel Filtration Makers Kit (for protein molecular weight 29 kDa to 700 kDa, Sigma).

4.4.5 IcsA N-WASP pull down

For IcsA N-WASP pull down experiments, approximately 60 µg mini-N-WASP-his protein purified as described previously (Papayannopoulos *et al.*, 2005) was mixed with either 38 µg IcsA, and incubated with 100 µL of anti-FLAG affinity resin (anti-DYKDDDDK G1 resin, GenScript) resin overnight at 4 °C. For mock pull down, 60 µg mini-N-WASP-his protein was mixed with 100 µL of anti-FLAG affinity resin and processed as above. Resins were washed 5 times with 1 mL TBS and beads were resuspended in 50 µL of 2× SDS PAGE buffer (Lugtenberg *et al.*, 1975) and heated to 100 °C.

4.4.6 Native PAGE, SDS-PAGE and Western immunoblotting

For native PAGE, proteins were mixed with 2× native sample buffer [62.5 mM Tris pH 6.8, 25% (v/v) glycerol, 1% (w/v) bromophenol blue] at the ratio of 1:1, and directly loaded onto a self-cast native gel [315 mM Tris pH 8.5, 0.1% ammonium persulfate (APS), 7% acrylamide/bis]. Proteins were electrophoresed with the running buffer [25 mM Tris pH 8.5, 192 mM glycine]. For SDS-PAGE, proteins were mixed with 2× SDS-PAGE sample buffer and electrophoresed in any-kDa gels (Biorad). Proteins were stained with Coomassie blue G250 (Thermo Scientific).

For Western immunoblotting, proteins from the gel were transferred onto a nitrocellulose membrane, and the membrane was blocked with 5% (v/v) skim milk in TTBS buffer [TBS, 0.1% (v/v) Tween 20], incubated with either mouse anti-FLAG antibody (anti-DYKDDDDK antibody, Genscript), anti-N-WASP antibody (Suzuki *et al.*, 2002) or rabbit anti-IcsA antibody (Van Den Bosch *et al.*, 1997) overnight. The membrane was then washed with TTBS and incubated with either HRP-conjugated goat anti-mouse antibody (Biomediq DPC) or HRP-conjugated goat anti-rabbit antibody (Biomediq DPC) for 1 h. The membrane was then washed with TBS and incubated with Chemiluminescence Substrate (Sigma) for 5 min. Chemiluminescence was detected using a ChemiDoc imaging system (BioRad).

4.4.7 IcsA self-interaction analysis

For IcsA self-interaction analysis, purified protein was mixed with either 100 mM $MgCl_2$ or 10 mM DTT and incubated for 5 min at room temperature and analysed via native PAGE.

4.4.8 Chemical crosslinking

For chemical crosslinking, purified IcsA passenger protein was mixed with 0.1 mM, 1 mM or 10 mM DSP (Sigma) in PBS and incubated at room temperature for 30 min. The reaction was quenched by adding 50 mM Tris (pH 7.0). 10 mM DTT was added to reduce the protein crosslink when required. Samples were mixed with 2× SDS-PAGE sample buffer without β-ME and subjected to SDS-PAGE.

4.4.9 Proteinase accessibility assay

Protein accessibility assay was described previously (Brotcke-Zumsteg *et al.*, 2014). Briefly, *Shigella* strains grown overnight were collected (1×10^9 cells) washed with and resuspended into 1 ml PBS. 33 nM human neutrophil elastase (hNE, Elastin Products) was added and incubated at 37 °C. At the indicated time points in the figure legends, a 100 µl of sample was taken, mixed with 2× SDS-PAGE sample buffer and immediately incubated at 100 °C for 15 min. Alternatively, digestion fractions at the indicated time point were centrifuged (16,000 ×g, 1 min) to give whole bacterial and supernatant fractions, mixed with 2× SDS-PAGE sample buffer and immediately incubated at 100 °C for 15 min. Samples were then subjected to SDS-PAGE and Western immunoblotting with anti-FLAG antibody.

4.4.10 LPS O antigen depletion, regeneration and LPS silver staining

LPS depletion and regeneration were done as described previously (Teh *et al.*, 2012). Briefly, 18 h bacterial cultures were subcultured 1 in 20 into LB and grown to an OD_{600} of 0.5 at 37 °C before further dilution 1:20 into LB in the presence of 3 µg/ml polymyxin B nanopeptide (PBMN, Sigma) and 5 µg/ml tunicamycin (Sigma), and incubated for another 3 h at 37 °C to deplete the LPS O antigen. Bacterial cultures were then centrifuged, washed twice with fresh LB to remove PMBN and tunicamycin, and further diluted 1:20 into LB for another 3 h incubation at 37 °C to regenerate LPS O antigen. Samples were prepared for LPS silver staining and proteinase accessibility assays. LPS silver staining was performed as described previously (Murray *et al.*, 2003). Briefly, *Shigella* strains grown to an OD_{600} of 0.8 were collected (1×10^9 cells), resuspended in 50 µl lysing buffer and incubated with 2.5 µg proteinase K (Invitrogen) overnight at 56 °C. The LPS samples were electrophoresed on an SDS-15 %-PAGE gel, and the gel was stained with silver nitrate and developed with formaldehyde.

4.5. Article results

4.5.1 IcsA's conformational change is independent to LPS O antigen masking

It has been shown that IcsA functions as an adhesin in the hyper-adherent *Shigella flexneri ΔipaD* (Brotcke-Zumsteg *et al.*, 2014), and the authors proposed that an alternative conformation is required for IcsA to be able to promote *Shigella* adherence. This was demonstrated through *in situ* bacterial surface protein digestion with hNE. However, as *Shigella* surface LPS O antigen might have masking effects on IcsA (Morona *et al.*, 2003), which might influence proteinase accessibility of surface presented IcsA, we considered it is important to rule out that the changes in hNE digestion could be attributed to modulation of LPS in the *Shigella flexneri ΔipaD*, such that it might then lead to an altered proteinase accessibility of IcsA (Mattock & Blocker, 2017). To examine the impact of LPS O antigen on the hNE accessibility of IcsA, we also constructed a C-terminus FLAG tagged IcsA^{FLAG} (IcsA$^{737::FLAG\times3}$) which is similar to the previously reported construct (Brotcke-Zumsteg *et al.*, 2014). Upon the assessment of the accessibility of IcsA^{FLAG} produced in *S. flexneri ΔicsA*[pIcsA^{FLAG}] or *ΔicsAΔipaD*[pIcsA^{FLAG}] with depleted O antigen (Fig 1A) to hNE digestion (Fig 1B), it was found that a ~40 kDa fragment from IcsA^{FLAG} produced in the *S. flexneri ΔicsAΔipaD*[pIcsA^{FLAG}] was more resistant to hNE than that expressed in the *S. flexneri ΔicsA*[pIcsA^{FLAG}], which is in accordance with findings reported by Brotcke-Zumsteg *et al.* (2014) using smooth LPS *Shigella*, suggesting that the altered proteinase accessibility is not due to an LPS O antigen masking effect.

4.5.2 Adhesin region of IcsA affects hNE accessibility of C terminal region

We have recently identified a region (aa 138-148) within IcsA passenger affecting IcsA's adhesin function (Chapter 3), and hypothesised that the mutant IcsA$^{\Delta138\text{-}148}$ does not have the altered IpaD dependent hNE accessibility compared to the wild type IcsA (Fig 1B&C). We digested IcsA^{FLAG} (IcsA$^{737::FLAG\times3}$) (Fig 2A&C) and mutant IcsA$^{FLAG/\Delta138\text{-}148}$ (IcsA$^{737::FLAG\times3/\Delta138\text{-}148}$) (Fig 2B&D) produced in *S. flexneri ΔicsA* [pIcsA^{FLAG}] (Fig 2A); *S. flexneri ΔicsAΔipaD* [pIcsA^{FLAG}] (Fig 2C); *S. flexneri ΔicsA* [pIcsA$^{FLAG/\Delta138\text{-}148}$] (Fig 2B); and *S. flexneri ΔicsAΔipaD* [pIcsA$^{FLAG/\Delta138\text{-}148}$] (Fig 2D), respectively, with hNE. Consistent

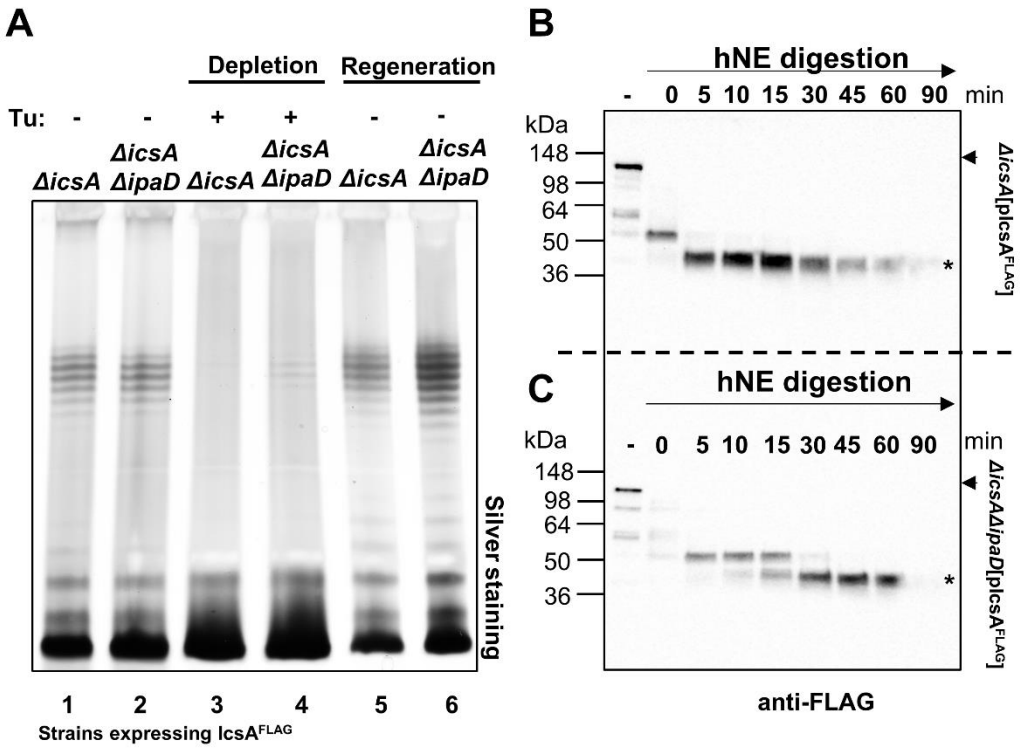

Fig 1. LPS O antigen does not affect the altered hNE accessibility of IcsA.

(A) Silver staining of *Shigella* LPS O antigen depletion. *S. flexneri ΔicsA* [pIcsA^{FLAG}] and *S. flexneri ΔicsAΔipaD* [pIcsA^{FLAG}] expressing IcsA^{FLAG} were treated without (lane 1&2) or with (lane 3&4) tunicamycin/PMBN and were grown for 3 h. *Shigella* treated with tunicamycin/PMBN were then washed and diluted in LB and were grown for another 3 h for LPS O antigen regeneration (lane 5&6). *S. flexneri ΔicsA* [pIcsA^{FLAG}] (A, lane 3) and *S. flexneri ΔicsAΔipaD* [pIcsA^{FLAG}] (A, lane 4) depleted of O antigen by treatment with tunicamycin/PMBN (A lane 3&4) were taken for analysis in B and C, respectively. IcsA^{FLAG} produced from *S. flexneri ΔicsA* [pIcsA^{FLAG}] **(B)** and *S. flexneri ΔicsAΔipaD* [pIcsA^{FLAG}] **(C)** were digested with hNE *in vivo*. Samples were taken at indicated time points and were immunoblotted with anti-FLAG antibody. Arrow indicates full length IcsA, and the hNE resistant fragment (~40 kDa) is indicated by an asterisk. Note that B&C consists two gels and were transferred onto the same membrane.

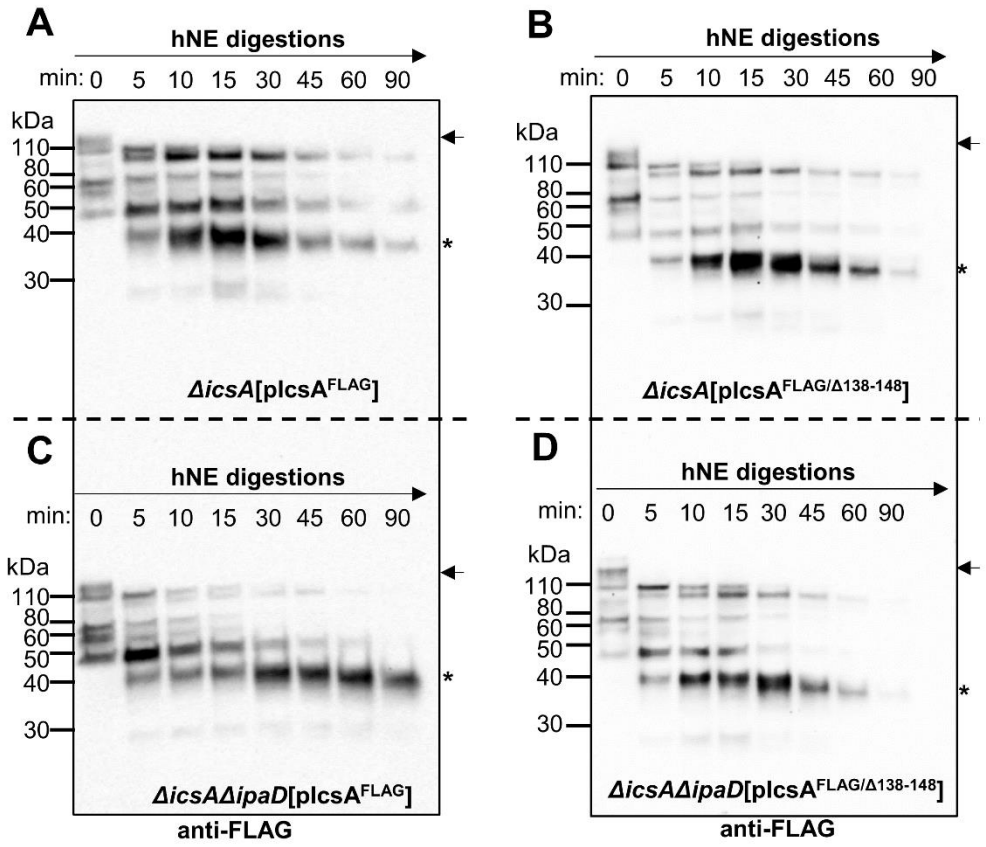

Fig 2. Adherence defective IcsA$^{\Delta 138\text{-}148}$ has an altered hNE accessibility.

S. flexneri ΔicsA [pIcsA^{FLAG}] **(A),** *S. flexneri ΔicsA* [pIcsA$^{FLAG/\Delta 138\text{-}148}$] **(B)**, *S. flexneri ΔicsAΔipaD* [pIcsA^{FLAG}] **(C)**, and *S. flexneri ΔicsAΔipaD* [pIcsA$^{FLAG/\Delta 138\text{-}148}$] **(D)** were digested with hNE *in vivo*. Samples were taken at the indicated time points and were immunoblotted using anti-FLAG. Arrow indicates full length IcsA (~120 kDa), and the hNE resistant fragment (~40 kDa) is indicated by an asterisk. Note that A&C and B&D consists two gels respectively and were transferred onto the same membrane.

with Brotcke-Zumsteg *et al.* (2014), we detected an ~40 kDa IcsA fragment in the hyper-adherent strain *S. flexneri ΔicsAΔipaD* [pIcsA^{FLAG}] (Figure 2C) with increased resistance to hNE digestion compared to that produced in *S. flexneri ΔicsA* [pIcsA^{FLAG}] (Fig 2A). Additionally, the digestion patterns of IcsA^{FLAG} (Fig 2A) and the mutant IcsA$^{FLAG/\Delta 138\text{-}148}$ (Fig 2B) produced in *S. flexneri ΔicsA* [pIcsA^{FLAG}] and *S. flexneri ΔicsA* [pIcsA$^{FLAG/\Delta 138\text{-}148}$] were similar, suggesting that the deletion of the adhesin region did not dramatically alter the structure of IcsA. However, unlike the IcsA^{FLAG} (Fig 2C), the mutant IcsA$^{FLAG/\Delta 138\text{-}148}$ produced in the *S. flexneri ΔicsAΔipaD* [pIcsA$^{FLAG/\Delta 138\text{-}148}$] (Fig 2D) was much less resistant to hNE digestion, suggesting that 138-148 region is required for the wild type IcsA^{FLAG} to have an alternative proteinase accessibility as detected in IcsA^{FLAG} produced in the hyper-adherent *S. flexneri ΔipaD* background.

To further investigate the molecular mechanism of how IcsA alters its conformation for its adhesin role, we took advantage of our FLAG tagged construct to determine the origin of the FLAG×3 tagged 40 kDa fragment from IcsA^{FLAG}. The FLAG×3 tag was engineered to be between the C terminus of IcsA passenger and the β-barrel domain (Fig 3C). To determine whether the detected 40 kDa fragment was actually from the IcsA passenger domain, the digested samples at each time point were separated into whole bacteria and supernatant sub-fractions. We found that the hNE resistant fragment (40 kDa) was cleaved off the bacteria surface in the first 5 min and released into the supernatant (Figure 3B). Therefore, the ~40 kDa hNE resistant fragment is derived from the passenger domain. This were also the case for both IcsA^{FLAG} and the mutant IcsA$^{FLAG/\Delta 138\text{-}148}$ produced by *S. flexneri ΔicsA* [pIcsA^{FLAG}] (Fig S2A), *S. flexneri ΔicsAΔipaD* [pIcsA^{FLAG}] (Fig S2C), *S. flexneri ΔicsA* [pIcsA$^{FLAG/\Delta 138\text{-}148}$] (Fig S2B), and *S. flexneri ΔicsAΔipaD* [pIcsA$^{FLAG/\Delta 138\text{-}148}$] (Fig S2D), respectively. Moreover, at 90 min post-digestion by hNE, the ~40 kDa fragment was predominant only in the sample for *S. flexneri ΔicsAΔipaD* [pIcsA^{FLAG}] (Fig S2C), which again confirmed our hypothesis that the region 138-148 is responsible for the altered proteinase accessibility associated with IcsA's hyper-adherence phenotype in *S. flexneri ΔipaD* background. The β-barrel domain (aa 759-1102) of IcsA is embedded into the membrane and inaccessible to the hNE, hence the cleavage at the C-terminal of the ~40 kDa fragment was between the FLAG×3 and β-barrel domain, which is predicted to be at around

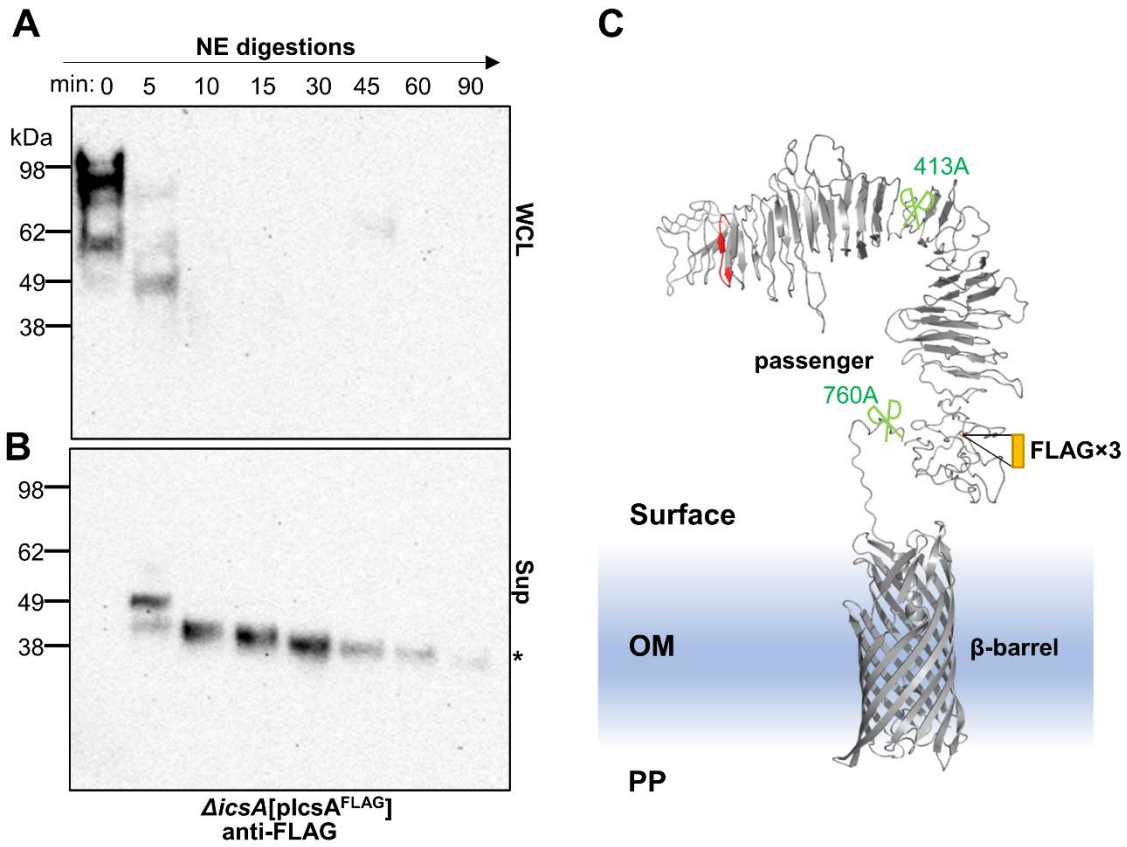

Fig 3. The ~40 kDa hNE resistant fragment is from the C terminal region of IcsA passenger.

S. flexneri ΔicsA [pIcsA^{FLAG}] expressing IcsA^{FLAG} were digested with hNE *in situ*. Samples were taken at the indicated time points and were separated into **(A)** whole cell lysate (WCL) and **(B)** digestion supernatant (Sup), and were immunoblotted with anti-FLAG antibody. The hNE resistant fragment (~40 kDa) is indicated by an asterisk. **(C)** Predicted hNE digestion map. 3D structures of IcsA passenger and β-barrel were acquired from I-TASSER. The predicted hNE cutting sites are indicated by the scissors and the adhesin region (aa 138-148) of IcsA is shown in red. The position of the FLAG×3 is indicated in the orange box.

aa 760, given that hNE preferably cleaves alanine, valine and isoleucine (Weinrauch *et al.*, 2002, Fu *et al.*, 2018). According to the size of the fragment, it can also be estimated that the cleavage at the N-terminal of the ~40 kDa fragment is around aa 413. Clearly, the ~40 kDa fragment does not contain the adhesin region aa 138-148, yet deletion of this region at N-terminal of IcsA passenger affected IcsA's resistance to hNE digestion at the C terminal region (Fig 2). Therefore, we hypothesised that IcsA's N-terminal region may interact with C terminal region (414-760) in the hyper-adherent *S. flexneri ΔipaD,* thereby increasing the resistance of C terminal region to hNE.

4.5.3 Purified IcsA passenger has an intramolecular interaction

To further investigate the potential head to tail interaction of IcsA at a molecular level, we purified IcsA passenger ($IcsA^{54::FLAG\times3}$) from the culture supernatant (Fig 4A) and confirmed its function of interacting with N-WASP protein (Fig S3 A&B). Following size exclusion chromatography, the purified IcsA passenger showed two populations (Fig 4B) which migrated with the apparent molecular size of 249 kDa (Fig 4B, H) and 137 kDa (Fig 4B, L). This was also confirmed by Native PAGE gel (Fig 4D), indicating that IcsA passenger has self-association ability. To further analyse the self-interaction of IcsA, we tested whether these two forms of IcsA were affected by electrostatic interactions (Jekow *et al.*, 1999) using 100 mM $MgCl_2$ or disulfide bond formation using 10 mM DTT (Fig S4). We found that treatment of DTT resulted in a shift in migration of the 137 kD band up to ~146 kDa in the Native PAGE gel (Fig 5A and Fig S4), indicating that the 137 kDa band had a disulfide bond. IcsA adapts an elongated shape (Kuhnel & Diezmann, 2011, Leupold *et al.*, 2017, Mauricio *et al.*, 2017), similar to other bacterial autotransporter adhesins Pertactin (Emsley *et al.*, 1996) and antigen 43 (Heras *et al.*, 2014). Therefore, it was not possible to determine the oligomeric status of these sub-populations using standard protein markers with globular shape. However, when treated to reduce disulfide bonds, the IcsA passenger domain migrated slower in the Native PAGE gel (Fig 5A), suggesting that the disulfide bond forms intramolecularly. IcsA has three cysteines in the passenger domain. One of the cysteines (aa 130) is located near the adhesin region (138-148), and the other two (aa 376 and 380) are closely located in the middle of the passenger. It is likely that the disulfide bond forms between 130 to 376 or 380, thereby causing a dramatic change in gel

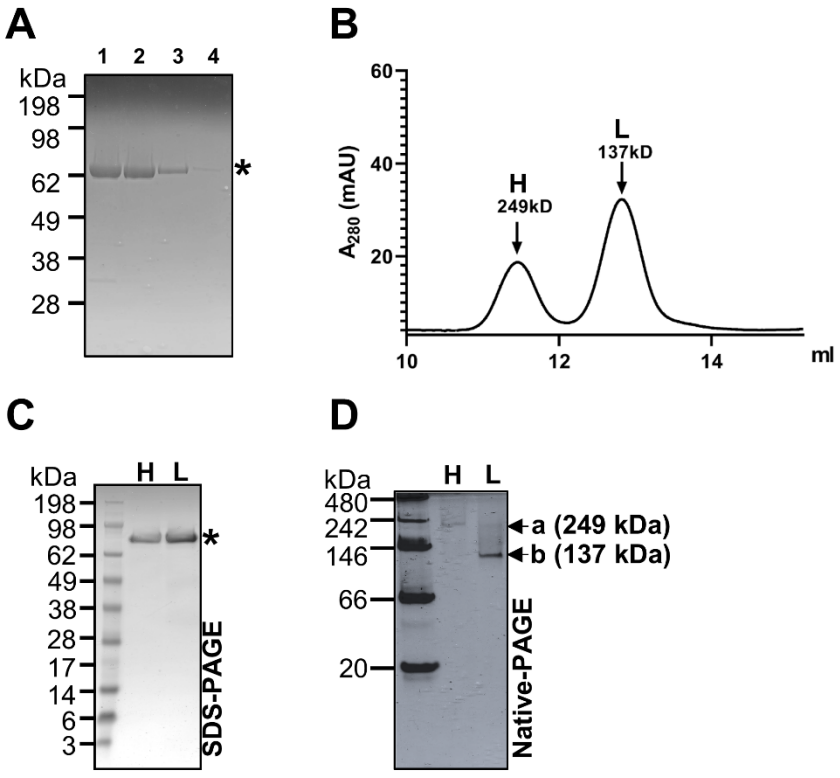

Fig 4. Purification of IcsA passenger protein.

(A) IcsA passenger (IcsA$^{54::FLAG_{\times 3}}$) was purified with FLAG affinity resin, and the eluted fractions (lane 1-4) were analysed by SDS-PAGE. **(B)** Purified IcsA passenger was analysed via size exclusion chromatography, and protein sizes were calculated using protein standard markers. The IcsA populations at the higher (a) apparent molecular weight (249 kD) and the lower (b) apparent molecular weight (137 kDa) were analysed by **(C)** SDS-PAGE and **(D)** Native PAGE. Purified IcsA passenger is indicated by an asterisk.

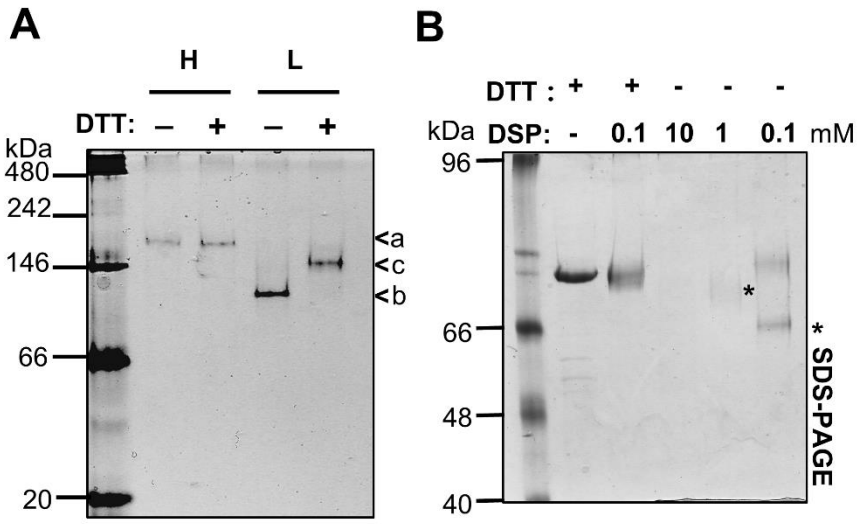

Fig 5. Purified IcsA passenger protein has an intramolecular interaction to promote a disulfide bond formation.

(A) Purified IcsA passenger ($IcsA^{54::FLAG\times3}$) separated by size exclusion chromatography with higher (H) and lower (L) apparent molecular weight were treated with 10 mM DTT. Samples were then analysed via Native PAGE. IcsA with higher apparent molecular weight (a), lower apparent molecular weight (b) and DTT reduced lower apparent molecular weight population (c) were indicated. **(B)** DSP crosslinking of purified IcsA protein. Purified IcsA passenger was treated with DSP at different concentration and analysed by SDS-PAGE. DSP cross-linked IcsA are indicated with asterisks.

mobility, as this would be a result from a head to tail interaction which changes the overall shape of the IcsA molecule. Indeed, we found that when treated with 0.1 mM DSP (Fig 5B), purified IcsA passenger (74 kDa) migrated at ~66 kDa in denaturing conditions (Fig 5B), faster than the migration of un-crosslinked IcsA passenger in the gel. In addition, this migration change is reversible by the treatment of DTT which reduced the disulfide bond in DSP (Fig 5B). Collectively, these data suggested that the purified IcsA passenger has an intramolecular interaction between head to tail which allows a disulfide bond to form. This supports our observations that a head to tail arrangement of IcsA is impacted by the adhesin region.

4.6. Discussion

In this study we found that the IcsA exists in multiple conformations. We found that the alternative conformation of IcsA requires the IcsA adhesin region aa 138-148, as the adhesin defective mutant $IcsA^{\Delta 138\text{-}148}$ did not show altered accessibility to hNE when expressed in *S. flexneri ΔicsAΔipaD* (Fig 2B&D). Furthermore, the hNE resistant $IcsA^{FLAG}$ fragment at ~40 kDa was found to be derived from the C terminus of passenger, which is the region close to the bacterial surface and well separated from the adhesin region (138-148). IcsA passenger had been purified as a monomer previously (Mauricio *et al.*, 2017). Using the similar approach, we isolated IcsA passenger in two forms and found one with an intramolecular interaction which facilitated an intramolecular disulfide bond formation (Fig 5A). This intramolecular interaction was also revealed by DSP crosslinking of the purified IcsA protein (Fig 5B). It has been reported previously that IcsA forms a disulfide bond, which increases the resistance to proteinases (Brandon & Goldberg, 2001). Therefore, it is plausible that the alternative conformation of IcsA associated with adhesin activity might involve in the interaction between the adhesin region and the C terminus region, whereby allowing the C terminal region of IcsA to become more resistant to hNE digestion. Interestingly, in addition to the region 138-148, 5 aa insertion mutation at 386, which is near the other two cysteines (376 and 380), was also reported to affect IcsA's adhesin activity (Brotcke-Zumsteg *et al.*, 2014). It is plausible that a disulfide bond could form between 130 and 376 or 380, as the overall structure of IcsA passenger was found in a "V" shape which has been proposed to form a bridging loop between the central region of the protein to interact with the N-terminal domain (Mauricio *et al.*, 2017).

We speculate that the N-terminal domain of IcsA is flexible which could aid the conformational change, as the C-terminal of the passenger adapts a compact structure (Leupold *et al.*, 2017). In contrast to the N-terminal domain, the C-terminal domain (aa ~414-760) of IcsA passenger is more resistant to hNE (Fig 3B). This region is almost identical to the crystalized IcsA passenger region (419-758) , which was screened out from 18,432 truncated IcsA constructs and was the only one to succeed in crystallization (Leupold *et al.*, 2017).

IcsA has recently been reported to aid *S. flexneri* biofilm formation in the presence of bile salts by promoting bacterial cell to cell contact and aggregative growth (Koseoglu *et al.*, 2019). *E. coli* bacterial clumping was revealed to be mediated via the head to tail interaction of autotransporter antigen 43 (Heras *et al.*, 2014). Therefore, we speculate that this head to tail interaction in IcsA is important for its function as an adhesin that promotes *S. flexner*i adherence and biofilm formation. Here we propose a model (Fig 6) where IcsA changes its conformation through the interaction between the N-terminal domain and its C-terminal domain in the hyper-adherent *S. flexneri* and this interaction also allows the formation of a disulfide bond.

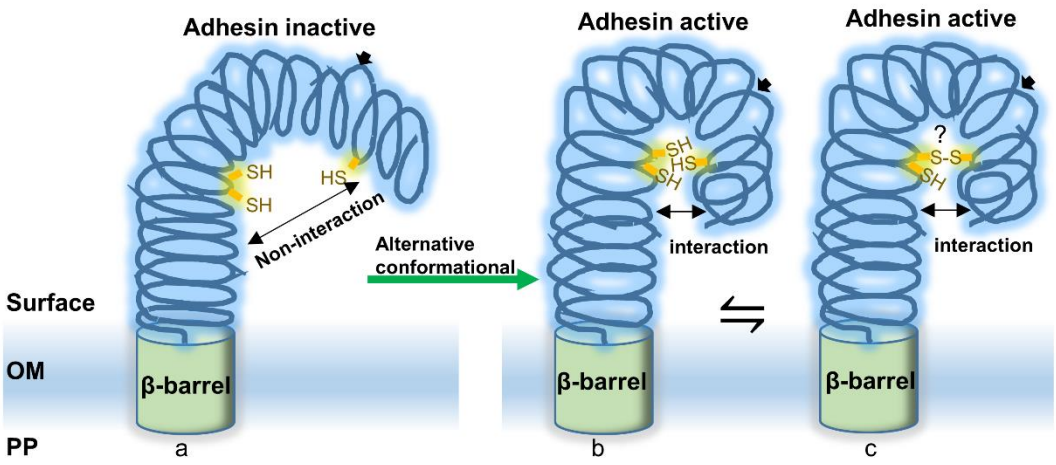

Fig 6. Model of IcsA adapting alternative conformations through an intramolecular interaction.

In the wild type strain grown in standard culture conditions, IcsA passenger is adhesin inactive (a). The N-terminal region does not interact with its C terminal region. When produced in *S. flexneri ΔipaD*, IcsA is adhesin active (b). The N-terminal region interacts with the C terminal region. This interaction allows a disulfide bond formation (c). The adhesin region aa 138-148 is indicated with arrows.

4.7. Article acknowledgement

We gratefully acknowledge the University of Adelaide for awarding a Faculty of Science Postgraduate Scholarship to J.Q.

4.8. Article references

Kotloff, K.L., Riddle, M.S., Platts-Mills, J.A., Pavlinac, P. and Zaidi, A.K.M. (2018). Shigellosis. Lancet 391, 801-812.

Mathan, M.M. and Mathan, V.I. (1986). Ultrastructural pathology of the rectal mucosa in *Shigella dysentery*. Am J Pathol 123, 25-38.

Labrec, E.H., Schneider, H., Magnani, T.J. and Formal, S.B. (1964). Epithelial cell penetration as an essential step in the pathogenesis of bacillary dysentery. J Bacteriol 88, 1503-18.

Perdomo, J.J., Gounon, P. and Sansonetti, P.J. (1994). Polymorphonuclear leukocyte transmigration promotes invasion of colonic epithelial monolayer by *Shigella flexneri*. J Clin Invest 93, 633-43.

Brotcke-Zumsteg, A., Goosmann, C., Brinkmann, V., Morona, R. and Zychlinsky, A. (2014). IcsA is a *Shigella flexneri* adhesin regulated by the type III secretion system and required for pathogenesis. Cell Host Microbe 15, 435-45.

Lett, M.C., Sasakawa, C., Okada, N., Sakai, T., Makino, S., Yamada, M., Komatsu, K. and Yoshikawa, M. (1989). *virG*, a plasmid-coded virulence gene of *Shigella flexneri*: identification of the virG protein and determination of the complete coding sequence. J Bacteriol 171, 353-9.

Bernardini, M.L., Mounier, J., Dhauteville, H., Coquisrondon, M. and Sansonetti, P.J. (1989). Identification of IcsA, a plasmid locus of *Shigella flexneri* that governs bacterial intracellular and intercellular spread through interaction with F-actin. Proc Natl Acad Sci U S A 86, 3867-3871.

Suzuki, T., Miki, H., Takenawa, T. and Sasakawa, C. (1998). Neural Wiskott-Aldrich syndrome protein is implicated in the actin-based motility of *Shigella flexneri*. EMBO J 17, 2767-76.

Egile, C., Loisel, T.P., Laurent, V., Li, R., Pantaloni, D., Sansonetti, P.J. and Carlier, M.F. (1999). Activation of the CDC42 effector N-WASP by the *Shigella flexneri* IcsA protein promotes actin nucleation by Arp2/3 complex and bacterial actin-based motility. J Cell Biol 146, 1319-32.

Morona, R. and Van Den Bosch, L. (2003). Multicopy *icsA* is able to suppress the virulence defect caused by *wzz*(SF) mutation in the *Shigella flexneri*. FEMS Microbiol Lett 221, 213-219.

Papayannopoulos, V., Co, C., Prehoda, K.E., Snapper, S., Taunton, J. and Lim, W.A. (2005). A polybasic motif allows N-WASP to act as a sensor of PIP(2) density. Mol Cell 17, 181-91.

Lugtenberg, B., Meijers, J., Peters, R., van der Hoek, P. and van Alphen, L. (1975). Electrophoretic resolution of the 'major outer membrane protein' of *Escherichia coli* K12 into four bands. FEBS Lett 58, 254-258.

Suzuki, T., Mimuro, H., Suetsugu, S., Miki, H., Takenawa, T. and Sasakawa, C. (2002). Neural Wiskott-Aldrich syndrome protein (N-WASP) is the specific ligand for *Shigella* VirG among the WASP family and determines the host cell type allowing actin-based spreading. Cell Microbiol 4, 223-33.

Van den Bosch, L., Manning, P.A. and Morona, R. (1997). Regulation of O-antigen chain length is required for *Shigella flexneri* virulence. Mol Microbiol 23, 765-75.

Teh, M.Y., Tran, E.N. and Morona, R. (2012). Absence of O antigen suppresses *Shigella flexneri* IcsA autochaperone region mutations. Microbiology 158, 2835-50.

Murray, G.L., Attridge, S.R. and Morona, R. (2003). Regulation of *Salmonella typhimurium* lipopolysaccharide O antigen chain length is required for virulence; identification of FepE as a second Wzz. Mol Microbiol 47, 1395-406.

Morona, R., Daniels, C. and Van Den Bosch, L. (2003). Genetic modulation of *Shigella flexneri* 2a lipopolysaccharide O antigen modal chain length reveals that it has been optimized for virulence. Microbiology 149, 925-39.

Mattock, E. and Blocker, A.J. (2017). How do the virulence factors of *Shigella* work together to cause disease? Front Cell Infect Microbiol 7, 64.

Weinrauch, Y., Drujan, D., Shapiro, S.D., Weiss, J. and Zychlinsky, A. (2002). Neutrophil elastase targets virulence factors of enterobacteria. Nature 417, 91-4.

Fu, Z., Thorpe, M., Akula, S., Chahal, G. and Hellman, L.T. (2018). Extended cleavage specificity of human neutrophil elastase, human proteinase 3, and their distant ortholog clawed frog PR3-three elastases with similar primary but different extended specificities and stability. Front Immunol 9, 2387.

Jekow, P., Behlke, J., Tichelaar, W., Lurz, R., Regalla, M., Hinrichs, W. and Tavares, P. (1999). Effect of the ionic environment on the molecular structure of bacteriophage SPP1 portal protein. Eur J Biochem 264, 724-35.

Mauricio, R.P., Jeffries, C.M., Svergun, D.I. and Deane, J.E. (2017). The *Shigella virulence* factor IcsA relieves N-WASP autoinhibition by displacing the verprolin homology/cofilin/acidic (VCA) domain. J Biol Chem 292, 134-145.

Leupold, S., Busing, P., Mas, P.J., Hart, D.J. and Scrima, A. (2017). Structural insights into the architecture of the *Shigella flexneri* virulence factor IcsA/VirG and motifs involved in polar distribution and secretion. J Struct Biol 198, 19-27.

Kuhnel, K. and Diezmann, D. (2011). Crystal structure of the autochaperone region from the *Shigella flexneri* autotransporter IcsA. J Bacteriol 193, 2042-5.

Emsley, P., Charles, I.G., Fairweather, N.F. and Isaacs, N.W. (1996). Structure of *Bordetella pertussis* virulence factor P.69 pertactin. Nature 381, 90-2.

Heras, B. et al. (2014). The antigen 43 structure reveals a molecular Velcro-like mechanism of autotransporter-mediated bacterial clumping. Proc Natl Acad Sci U S A 111, 457-62.

Brandon, L.D. and Goldberg, M.B. (2001). Periplasmic transit and disulfide bond formation of the autotransporter *Shigella* protein IcsA. J Bacteriol 183, 951-958.

Koseoglu, V.K., Hall, C.P., Rodriguez-Lopez, E.M. and Agaisse, H. (2019). The autotransporter IcsA promotes *Shigella flexneri* biofilm formation in the presence of bile salts. Infect Immun 87, e00861-18.

4.9. Article supporting information

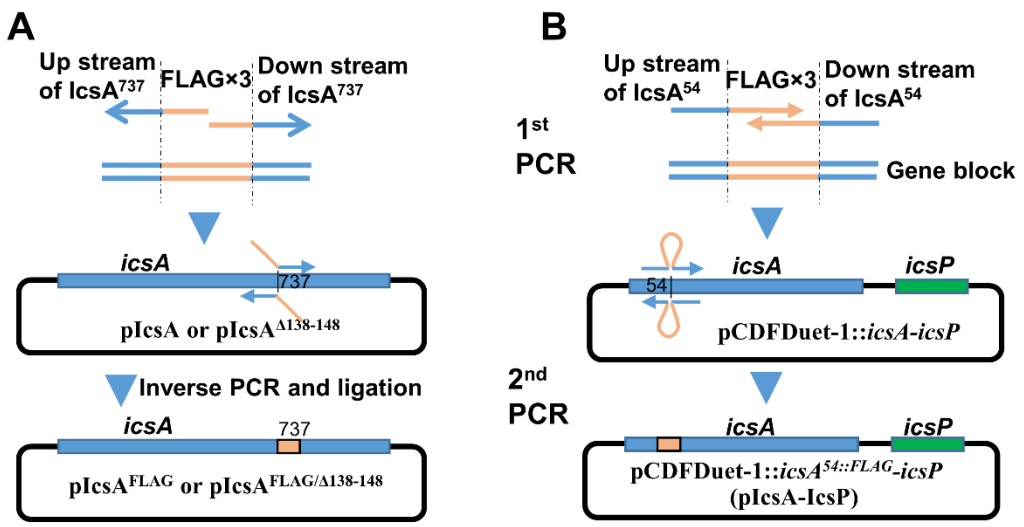

Fig S1. Generation of FLAG-tagged IcsA expression construct.

(A) Generation of pIcsA^{FLAG} and pIcsA$^{\Delta 138\text{-}148/FLAG}$. Primers were designed to target the adjacent sequence to aa 737 with half of the FLAG×3 sequence each and amplify the whole pIcsA or pIcsA$^{\Delta 138\text{-}148}$ plasmid to generate pIcsA^{FLAG} and pIcsA$^{\Delta 138\text{-}148/FLAG}$. **(B)** Construction of FLAG-tagged IcsA plasmid for IcsA passenger (IcsA$^{54::FLAG\times 3}$) purification. Primers were designed to be complementary to each other and were used to PCR amplify (1st PCR) gene blocks containing the coding sequences of FLAG×3 tag and flanked with up- and down-stream sequences to the insertion site at aa 54. Gene blocks were then used as mega primers to PCR clone (2nd PCR) the FLAG×3 tag into the pCDFDuet-1::*icsA-icsP* to generate the co-expression construct pCDFDuet-1::*icsA*$^{54::FLAG\times 3}$*-icsP* (pIcsA-IcsP).

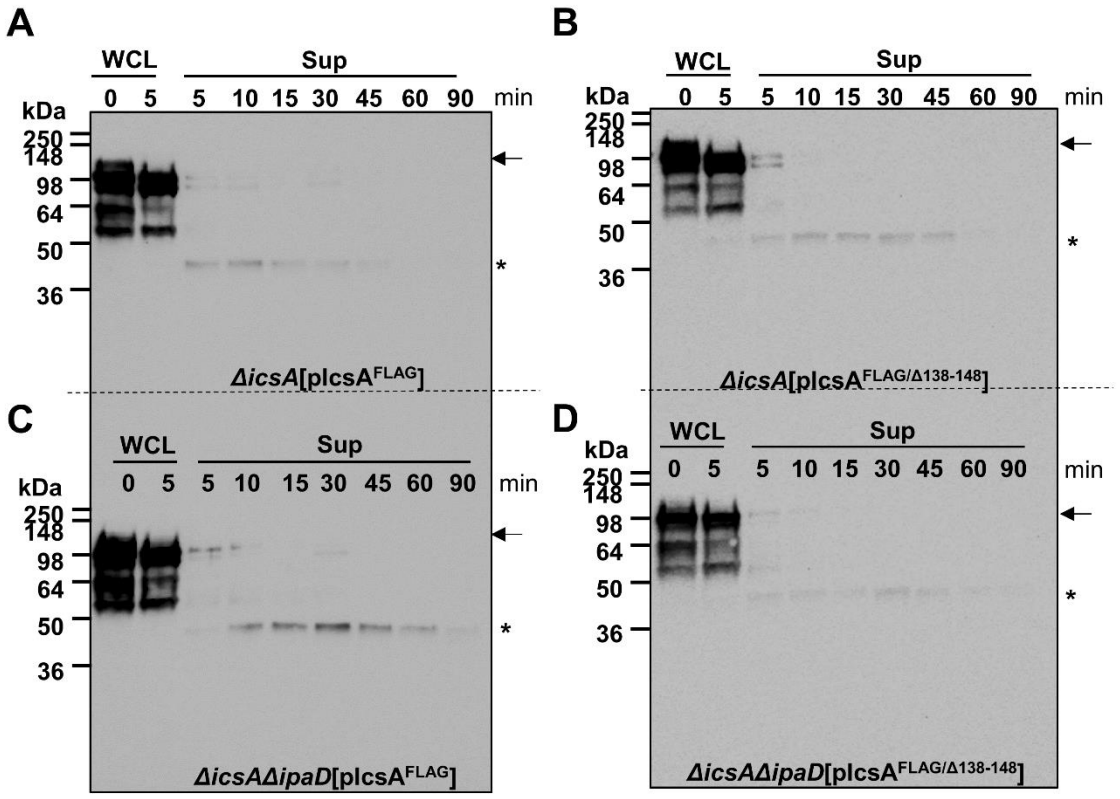

Fig S2. The ~40 kDa hNE resistant fragment is from the C terminal region of IcsA passenger.

S. flexneri ΔicsA [pIcsA^{FLAG}] **(A),** *S. flexneri ΔicsA* [pIcsA$^{FLAG/\Delta 138\text{-}148}$] **(B)**, *S. flexneri ΔicsAΔipaD* [pIcsA^{FLAG}] **(C)**, and *S. flexneri ΔicsAΔipaD* [pIcsA$^{FLAG/\Delta 138\text{-}148}$] **(D)** were digested with hNE *in vivo*. Samples were taken at the indicated time points and were separated into whole cell lysate (WCL) and digestion supernatant (Sup), and were immunoblotted with anti-FLAG antibody. Arrow indicates full length IcsA, and the hNE resistant fragment (~40 kDa) is indicated by an asterisk.

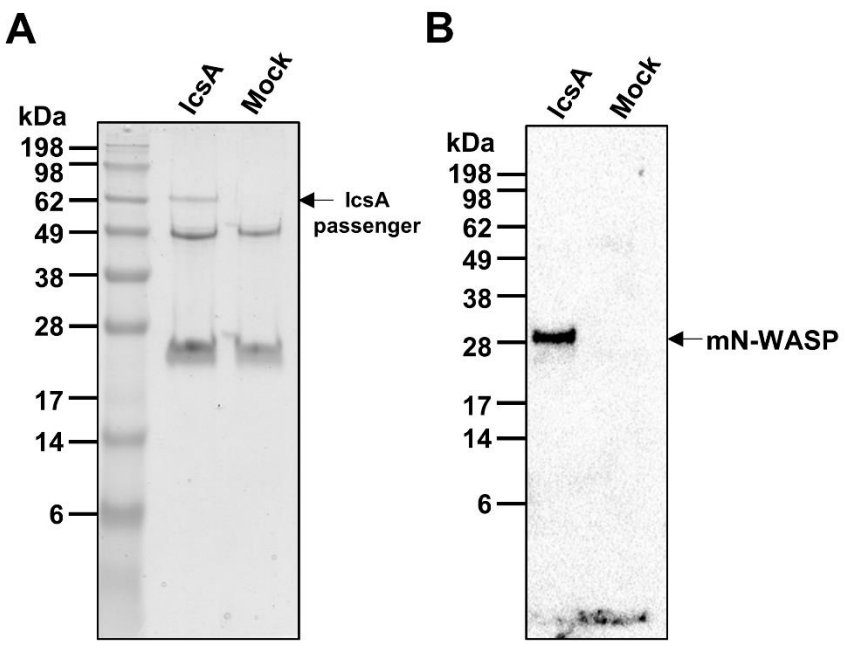

Fig S3. Purified FLAG-tagged IcsA is able to interact with N-WASP.

Purified IcsA passenger ($IcsA^{54::FLAG\times3}$) was mixed with both mN-WASP and FLAG resin, and were incubated for 18 h. For mock pull down, mN-WASP was mixed with FLAG resin only (mock). Resins were washed, and denatured in SDS-PAGE buffer. Samples were analysed via **(A)** SDS-PAGE and **(B)** immunoblotting with anti-N-WASP. The position of IcsA passenger and mN-WASP are indicated.

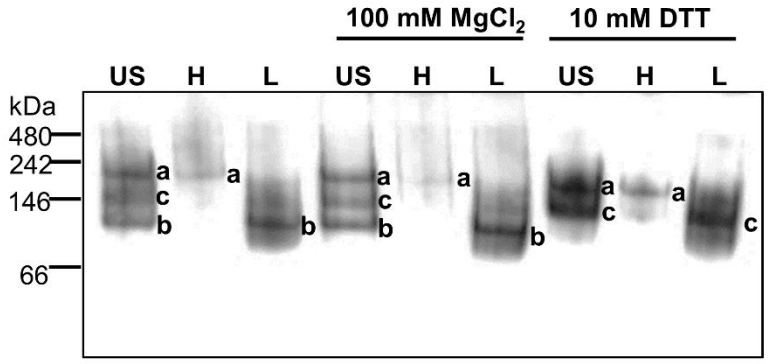

Fig S4. Purified IcsA forms an intramolecular disulfide bond.

Purified IcsA passenger (unseparated, US) and size exclusion chromatography separated IcsA with higher (H) and lower (L) apparent molecular weight were treated with 100 mM $MgCl_2$ and 10 mM DTT. Samples were then analysed via Native PAGE and were immunoblotted with anti-IcsA. IcsA with higher apparent molecular weight (a), lower apparent molecular weight (b) and DTT reduced apparent lower molecular weight population (c) are indicated.

Table S1. Strains and Plasmids

Strain or plasmid	Characteristics	Source/reference
Strains		
2457T	Wild type *S. flexneri* 2a	(Van Den Bosch *et al.*, 1997)
RMA2041	2457T*ΔicsA::Tc*^{R}	(Morona & Van Den Bosch, 2003)
JQRM11	2457T*ΔipaDΔicsA::Tc*^{R}	(Chapter 3)
JQRM115	C43[pCDFDuet-1::*icsA*$^{54::FLAG\times3}$*-icsP*]	This study
JQRM120	*ΔicsA*[pIcsA^{FLAG}]	This study
JQRM121	*ΔicsA*[pIcsA$^{FLAG/\Delta138-148}$]	This study
JQRM122	*ΔipaDΔicsA*[pIcsA^{FLAG}]	This study
JQRM123	*ΔipaDΔicsA*[pIcsA$^{FLAG/\Delta138-148}$]	This study
Plasmids		
pIcsA	pBR322 derivatives with CDS of IcsA	(Van den Bosch & Morona, 2003)
pIcsA$^{\Delta138-148}$	pIcsA$^{\Delta138-148}$ IcsA mutant	(Chapter 3)
pIcsA-IcsP	pCDFDuet-1::*icsA*$^{54::FLAG\times3}$*-icsP*	This study
pIcsA^{FLAG}	pIcsA$^{737::FLAG\times3}$	This study
pIcsA$^{FLAG/\Delta138-148}$	pIcsA$^{737::FLAG\times3/\Delta138-148}$	This study

References

Van Den Bosch, L., Manning, P.A. and Morona, R. (1997). Regulation of O-antigen chain length is required for *Shigella flexneri* virulence. Mol Microbiol 23, 765-775.

Morona, R. and Van Den Bosch, L. (2003). Multicopy *icsA* is able to suppress the virulence defect caused by *wzz*(SF) mutation in the *Shigella flexneri*. FEMS Microbiol Lett 221, 213-219.

Van den Bosch, L. and Morona, R. (2003). The actin-based motility defect of a *Shigella flexneri rmlD* rough LPS mutant is not due to loss of IcsA polarity. Microb Pathog 35, 11-8.

Table S2 Oligonucleotides

Oligos	Sequence[#]	Description
JQ17	CTACGACCATGGCTATGAATCAAATTCACA AATTTTTTTGTAATATGACCC	NcoI-ATG-IcsA
JQ18	CTACGAGTCGACTCAGAAGGTATATTTCAC ACCCAAAATACC	IcsA-SalI
JQ19	CTACGACATATGATGAAATTAAAATTCTTTG TACTTGCAC	NdeI-IcsP
JQ20	CTACGAGGTACCTCAAAAAATATACTTTAT ACCTGCGG	IcsP-KpnI
JQ36	CTCGGGGGGCCAATAGCTTTTGCTACTCCTG ACTACAAAGACCATGACGGTGATTATAAAG ATCATGACATCGATTACAAGGATGACG	IcsA$^{54::FLAG\times3}$ FLAG tag addition
JQ37	TGAAAAATGAAGTTCTTGAGTACCCGAAAG CTTGTCATCGTCATCCTTGTAATCGATGTCA TGATCTTTATAATCACCGTCATGG	IcsA$^{54::FLAG\times3}$ FLAG tag addition
JQ40	CATGACATCGATTACAAGGATGACGATGAC AAGCAGATGGATAATCAAGAATCAAAACA G	IcsA$^{737::FLAG\times3}$ FLAG tag addition
JQ41	ATCTTTATAATCACCGTCATGGTCTTTGTAG TCACTAGTTAGATACCACTTATTGGTATTC	IcsA$^{737::FLAG\times3}$ FLAG tag addition

Chapter Five

ICSA RECEPTOR IDENTIFICATION

Chapter 5: IcsA receptor identification

5.1. Introduction

IcsA has been confirmed as a *S. flexneri* adhesin contributing to the polar attachment of *Shigella* to host cells (Brotcke-Zumsteg *et al.*, 2014), thereby facilitating subsequent invasion. However, the cellular receptors for IcsA have not yet been revealed. Brotcke-Zumsteg *et al.* (2014) suggested that the receptors for IcsA are expressed in multiple cell types, given that the IcsA-dependent hyper-adherence can be demonstrated in HeLa cells, polymorphonuclear leukocytes (PMN) cells, and mouse Bone-marrow-derived macrophage (BMDM) cells. In Chapter 3, the purified IcsA passenger $IcsA^{53-740}$ showed ability to bind to HeLa cell surfaces by interacting with several trypsin sensitive molecules from the membrane fraction, which demonstrated a potential use as a bait protein to investigate the host cellular receptors. The aim of this Chapter was to attempt to use the purified $IcsA^{53-740}$ protein to identify receptors in HeLa cells.

5.2. IcsA receptor identification

To identify the receptors for IcsA, HeLa cells grown to confluence from four 100 mm dishes were lysed and incubated with His-tagged $IcsA^{53-740}$, and the $IcsA^{53-740}$ interacting complexes was immunoprecipitated using protein A resin preloaded with either anti-IcsA or anti-His_6 antibody (Section 2.7.17). Samples were then prepared and electrophoresed in an SDS-PAGE gel as described in Section 2.7.17.

Several HeLa cell molecules with apparent molecular sizes around 15 kDa, 40 kDa, 65 kDa, 180 kDa, 200 kDa and over 200 kDa were pulled down by $IcsA^{53-740}$ (Figure 5.1, lane 2&3) compared to the mock co-immunoprecipitation (co-IP) (Figure 5.1, lane 1). To investigate the cell surface receptors for IcsA, it was decided to select only the bands (Figure 5.1, lane 2&3, a) that correlated to the trypsin sensitive molecules from the HeLa membrane fraction detected via far Western blotting (Section 3.5.3), and these were excised out for mass spectrometry analysis (Section 2.7.19.1). The same region in the mock co-IP (Figure 5.1, lane 1) was excised and analysed by mass spectrometry to determine non-specifically bound proteins.

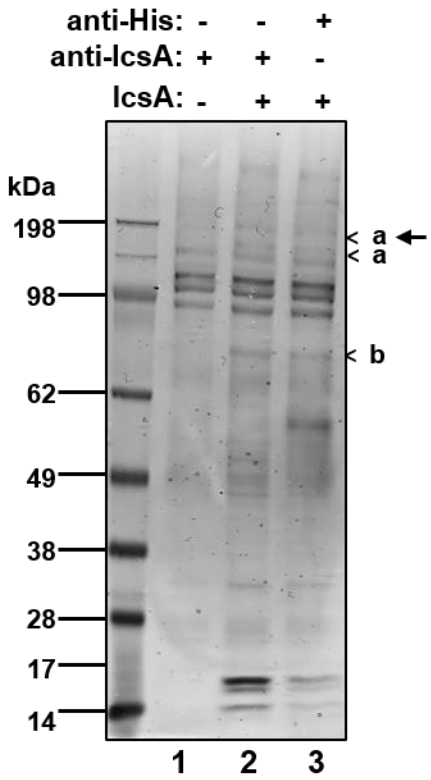

Figure 5.1. Co-immunoprecipitation of IcsA-interacting molecules from HeLa cells.

HeLa cell lysates were incubated with either dialysis buffer (lane 1) or IcsA$^{53-740}$ (lane 2 and 3), and IcsA interacting complexes were precipitated with anti-IcsA (lane 1 and 2) or anti-His_6 (lane 3) (Section 2.7.17), separated by SDS-PAGE (Section 2.7.9.1), and stained with Colloidal blue (Section 2.7.10.2). The IcsA interacting molecules detected in both far Western blotting (Section 3.5.3) and in co-IPs are indicated by an arrow. a: bands excised for MS analysis; b: IcsA$^{53-740}$.

Upon the mass spectrometry analysis of samples (Figure 5.1, a) from both anti-IcsA and anti-His_6 immunoprecipitations, Nonmuscle Myosin Heavy Chain IIA (NM-Myosin IIA, *MYH9*) and NM-Myosin IIA (*MYH10*) (~220 kDa) were identified with unique peptides matched to 31.7% and 23.1% of the sequences, respectively (Table 5.1). These were not present in samples from the mock co-IP. This implicates these proteins as potential host cell surface displayed receptors for the IcsA passenger domain. These co-IP samples were also analysed via Western immunoblotting (Section 2.7.11) with anti-Myosin IIA antibodies. However, Myosin IIA was undetectable in both the co-IPs done with anti-IcsA and anti-His_6 antibodies, but was detected in HeLa cell lysates (see Figure 5.3).

5.3. Investigation of the interaction between IcsA and Myosin IIA/IIB

To investigate whether Myosin IIA and Myosin IIB are the host cell molecules that are recognised by *S. flexneri* IcsA, thereby allowing the attachment of the hyper-adherent *S. flexneri ΔipaD*, anti-Myosin IIA and anti-Myosin IIB antibodies (Section 2.3.1) were used in *Shigella* adherence blocking assays (Section 2.9.2.2).

It was found that neither anti-Myosin IIA nor anti-Myosin IIB antibodies significantly blocked the adherence of *S. flexneri ΔipaD* to HeLa cells (Figure 5.2), although it showed an decrease in adherence rate when treated with 15 μg/ml anti-Myosin IIA antibodies compared to the *S. flexneri ΔipaD* treated with lower concentrations of anti-Myosin IIA.

Since the preincubation of HeLa monolayers with 15 μg/ml of anti-Myosin IIA antibody showed a slight decrease in the adherence of *S. flexneri ΔipaD* (Figure 5.2), the role of Myosin IIA in HeLa cells for *S. flexneri ΔipaD* adherence was investigated in COS-7 cells. COS-7 cells are African Green Monkey kidney cells and do not express Myosin IIA (Bao *et al.*, 2005).

To confirm that COS-7 does not express Myosin IIA, whole cell lysate sample (Section 2.7.14) of both COS-7 cells and HeLa cells were prepared and analysed via Western immunoblotting (Section 2.7.11.3) with anti-Myosin IIA antibodies (Section 2.3.1). Indeed, compared to HeLa cell lysate, anti-Myosin IIA antibody does not recognise any

Table 5.1. Mass spectrometry identified Myosin IIA/IIB unique peptides

Myosin IIA unique peptides (31.7% sequence coverage)				
TDLLLEPYNKYR	VISGVLQLGNIVFKK	INFDVNGYIVGANIETYLLEK	VSHLLGINVTDFTR	ALELDSNLYR
RQAQQERDELADEIANSSGK	IAQLEEQLDNETKER	IAQLEEQLDNETK	MQQNIQELEEQLEEEESAR	YEILTPNSIPK
TVGQLYKEQLAK	KLEEEQIILEDQNCK	KVEAQLQELQVK	QAQQERDELADEIANSSGK	KVIQYLAYVASSHK
QKHSQAVEELAEQLEQTKR	HSQAVEELAEQLEQTK	KLVWVPSDK	SMEAEMIQLQEELAAAER	LQVELDNVTGLLSQSDSK
LVWVPSDK	IAEFTTNLTEEEEKSK	QRYEILTPNSIPK	ALEEAMEQKAELER	ITDVIIGFQACCR
LEEEQIILEDQNCK	ELESQISELQEDLESER	LKDVLLQVDDERR	KANLQIDQINTDLNLER	IMGIPEEEQMGLLR
AKQTLENERGELANEVK	VISGVLQLGNIVFK	ELEDATETADAMNR	RGDLPFVVPR	VIQYLAYVASSHK
LEVNLQAMK	KRHEMPPHIYAITDTAYR	KKVEAQLQELQVK	KLEGDSTDLSDQIAELQAQIAELK	LTEMETLQSQLMAEK
VVFQEFR	HSQAVEELAEQLEQTKR	NLPIYSEEIVEMYK	VEAQLQELQVK	DFSALESQLQDTQELLQEENR
IAEFTTNLTEEEEK	HEMPPHIYAITDTAYR	LQQELDDLLVDLDHQR	IAQLEEELEEEQGNTELINDR	ANLQIDQINTDLNLER
SGFEPASLKEEVGEEAIVELVENGKK	RHEMPPHIYAITDTAYR	NFINNPLAQADWAAK	TDLLLEPYNK	
Myosin IIB unique peptides (23.1% sequence coverage)				
VVSSVLQFGNISFKK	RHAEQERDELADEITNSASGK	ALEEALEAKEEFER	YEILTPNAIPK	ITDIIIFFQAVCR
IVFQEFR	KVDDDLGTIESLEEAK	LQQELDDLTVDLDHQR	QRYEILTPNAIPK	KKVDDDLGTIESLEEAK
LLKDAEALSQR	TTLQVDTLNAELAAER	INFDVTGYIVGANIETYLLEK	ELEAELEDER	ELDDATEANEGLSR
IGQLEEQLEQEAKER	KQELEEILHDLESR	HAEQERDELADEITNSASGK	HATALEELSEQLEQAK	SDLLLEGFNNYR
QEEELQAKDEELLK	DAEALSQRLEEK	QLLQANPILESFGNAK	ALELDPNLYR	VIQYLAHVASSHK
VVSSVLQFGNISFK	EQADFAVEALAK	HATALEELSEQLEQAKR	IGQLEEQLEQEAK	LQNELDNVSTLLEEAEKK
QVLALQSQLADTKK	ELQAQIAELQEDFESEK	IAECSSQLAEEEEKAK	NKQEVMISDLEER	IVGLDQVTGMTETAFGSAYK
DAASLESQLQDTQELLQEETR	SLEAEILQLQEELASSER	QVLALQSQLADTK		
Peptides shared by Myosin IIA and IIB				
ADFCIIHYAGK	KFDQLLAEEK	FDQLLAEEK	TQLEELEDELQATEDAK	AGKLDPHLVLDQLR
LDPHLVLDQLR	QLLQANPILEAFGNAK	EDQSILCTGESGAGK	LQQLFNHTMFILEQEEYQR	AGVLAHLEEERDLK
AGVLAHLEEER				

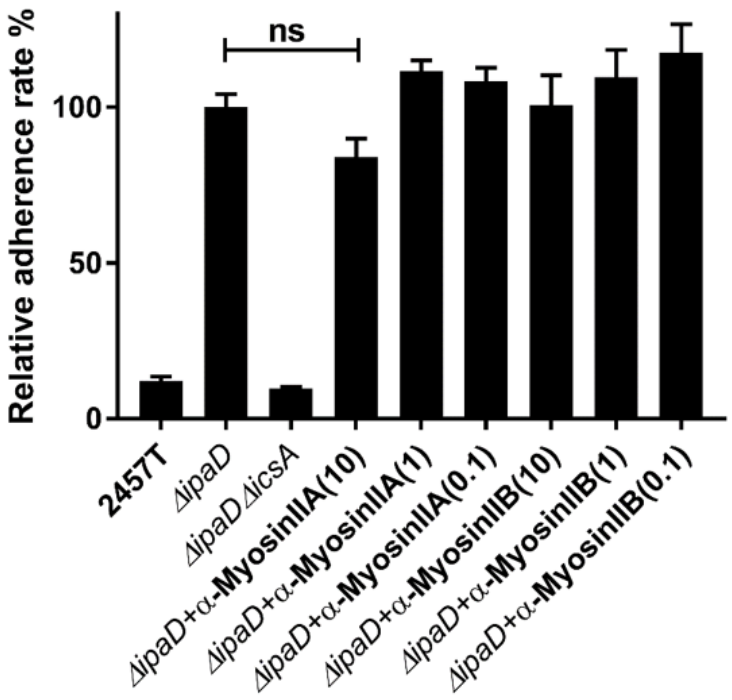

Figure 5.2. *Shigella* adherence blocking assay by anti-Myosin IIA and anti-Myosin IIB

Antibody adherence blocking assay. HeLa cells grown to confluence were incubated with either anti-Myosin IIA or anti-Myosin IIB at the concentrations of 15 μg/ml (10), 1.5 μg/ml (1), and 0.15 μg/ml (0.1) for 15 min. *Shigella* grown to an OD_{600} of 0.5 were collected and infected HeLa cell monolayers at the MOI of 100. After an extended 15 min incubation, cell monolayers were washed with PBS and lysed in PBS containing 1% (v/v) Triton X-100 before serial dilution plating on LB agar plates (Section 2.9.2.2). Data is normalised against the mean of *ΔipaD* (defined as 100%) and is the mean with SEM of three independent experiments. Significance was calculated (Section 2.9.4) using a student *t* test, and *p* values are as follows: ns, non-significant.

molecules from COS-7 cell lysate (Figure 5.3), which confirmed the absence of Myosin IIA in COS-7 cells.

To assess the IcsA-dependent adherence of *S. flexneri ΔipaD* in the absence of Myosin IIA, COS-7 cells grown to confluence were used to perform *Shigella* adherence assays (Section 2.9.1) with WT *Shigella flexneri* 2a (2457T), *S. flexneri ΔipaD, S. flexneri ΔipaDΔicsA, S. flexneri ΔipaDΔicsA* [pIcsA], and *S. flexneri ΔipaDΔicsA* [pBR322]. It was found that the expression of IcsA in *S. flexneri ΔipaDΔicsA* [pIcsA] significantly increased the adherence to COS-7 cells compared to that in *S. flexneri ΔipaDΔicsA* [pBR322] (Figure 5.4). This suggested that although Myosin IIA was absent in COS-7 cells, *S. flexneri ΔipaD* was still able to adhere to cells. Furthermore, both the adherence levels of *S. flexneri ΔipaD* and *S. flexneri ΔipaDΔicsA* [pIcsA] were not significantly different between HeLa cells and COS-7 cells (Figure 5.4). Collectively, this indicated that there might be other IcsA receptors existing in COS-7 cells.

To assess whether COS-7 cells express molecules that can be recognised by IcsA, COS-7 cells were lysed (Section 2.7.14) and analysed via far Western blotting (Section 2.7.11.5) with both purified $IcsA^{53\text{-}740}$ (Figure 5.5, lane 1&2) and the adherence defective mutant $IcsA^{53\text{-}740(\Delta 138\text{-}148)}$ (Figure 5.5, lane 3&4). A HeLa cell lysate was used as a control (Figure 5.5, lane 1&3).

As expected, unlike the purified mutant $IcsA^{53\text{-}740(\Delta 138\text{-}148)}$ (Figure 5.5, lane 3), $IcsA^{53\text{-}740}$ (Figure 5.5, lane 1) was able to recognise molecules from HeLa cells. However, there are molecules from COS-7 cells recognised by $IcsA^{53\text{-}740}$ (Figure 5.5, lane 2) but not by $IcsA^{53\text{-}740(\Delta 138\text{-}148)}$ (Figure 5.5, lane 4), which indicated that other IcsA-interacting molecules are present in COS-7 that contribute to the IcsA-dependent adherence observed for *S. flexneri ΔipaD* (Figure 5.4).

Myosin IIA has been reported to be essential for *S. flexneri* spread intercellularly in HeLa cells (Lum & Morona, 2014b). Therefore, to test whether this is also the case in COS-7 cells, *S. flexneri* WT (2457T), *S. flexneri ΔicsA* [pBR322], and *S. flexneri ΔicsA* [pIcsA] grown to the mid-exponential phase (Section 2.1.3.2) were used in plaque formation assays (Section 2.9.5) with both HeLa and COS-7 cells.

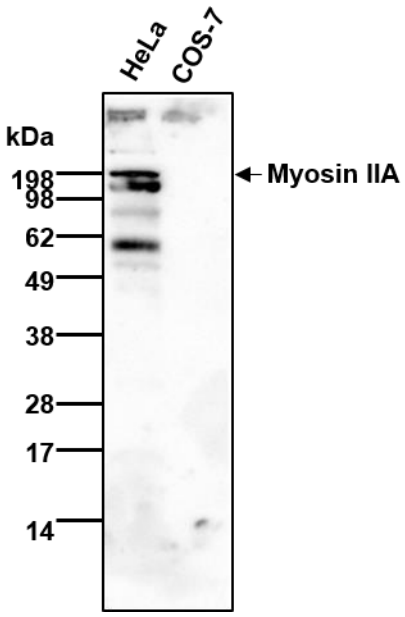

Figure 5.3. Western immunoblotting confirming the absence of Myosin IIA in COS-7 cells

HeLa cells and COS-7 cells (Section 2.2.1) grown to confluence were recovered by cell scraper and prepared into whole cell lysate sample (Section 2.7.14). Samples were then analysed via SDS-PAGE (Section 2.7.9.1) and Western immunoblotting (Section 2.7.11.3) with anti-Myosin IIA antibody (Section 2.3.1). Full length Myosin IIA (~220 kDa) is indicated with an arrow.

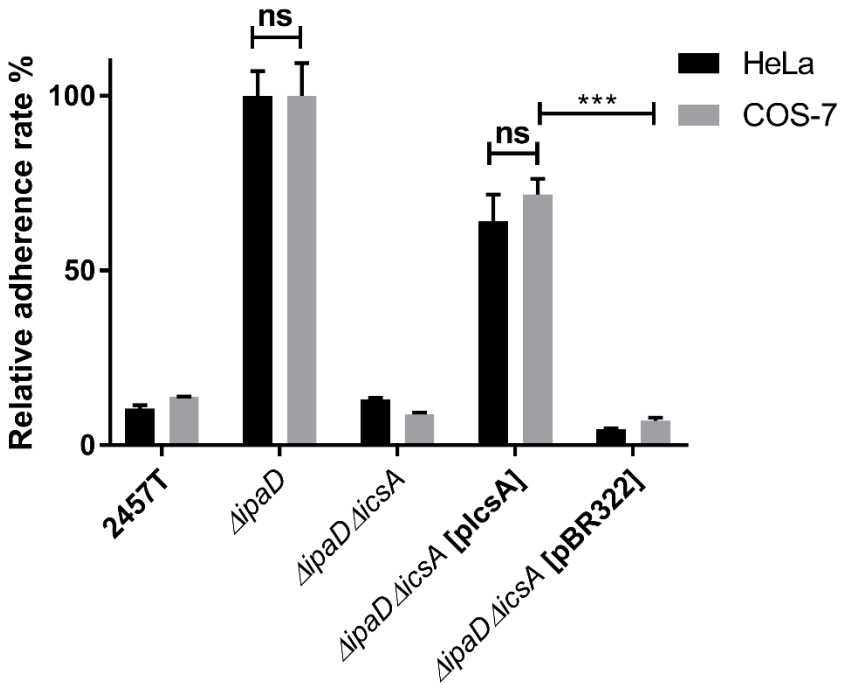

Figure 5.4. Adherence assay of *S. flexneri* with HeLa and COS-7 cells

Shigella grown to an OD_{600} of 0.5 were collected and used to infect HeLa cell monolayer at the MOI of 100 (Section 2.9.1). After 15 min incubation, the cell monolayers were washed and lysed. Lysates were serial diluted before dotting onto agar plates for enumeration (Section 2.9.1). Data is normalised against the mean of *ΔipaD* (defined as 100%) and is the mean with SEM of three independent experiments. Significance was calculated (Section 2.9.4) using a student *t* test, and *p* values are as follows: ****, $p<0.0001$; ns, non-significant.

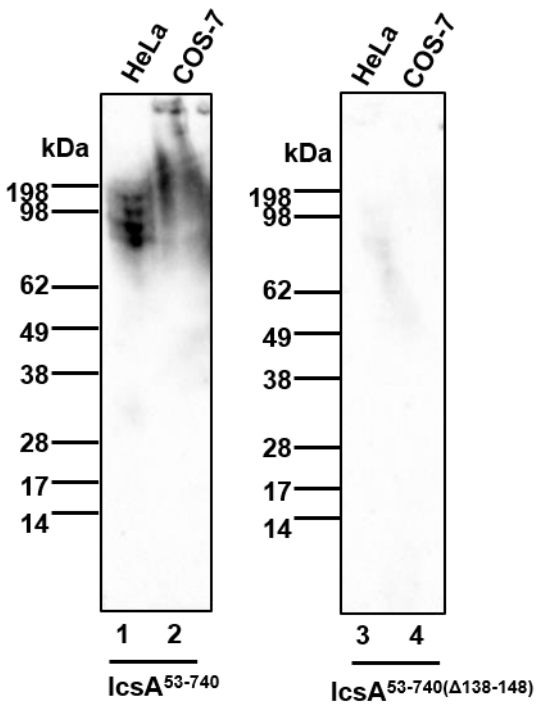

Figure 5.5. Far Western immunoblotting detecting IcsA-interacting molecules from COS-7 cells

HeLa cells and COS-7 cells grown to confluence were recovered either by cell scraper and lysed by RIPA buffer (Section 2.7.14). Lysates were then separated by SDS-PAGE (Section 2.7.9.1), transferred onto a nitrocellulose membrane (Section 2.7.11.1), and probed with $IcsA^{53\text{-}740}$ passenger protein or $IcsA^{53\text{-}740(\Delta 138\text{-}148)}$ as a negative control (Section 2.7.11.5). Membranes were subsequently probed with anti-IcsA antibody (Section 2.7.11.5).

As expected, *S. flexneri ΔicsA* [pIcsA] generated plaques (Figure 5.6 A, upper panel) in a similar size to the WT *S. flexneri* 2457T (Figure 5.6 B) in HeLa cells. However, in COS-7 cells (Figure 5.6 A, lower panel), *S. flexneri ΔicsA* [pIcsA] also generated plaques (Figure 5.6 A, lower panel) as the similar size to the WT *S. flexneri* 2457T (Figure 5.6 B). Interestingly, the size of the plaques on COS-7 cells were significantly larger (~2×) than those generated in HeLa cells (Figure 5.6 B). Together, these data indicated that Myosin IIA is not the limiting factor for IcsA's ABM function in COS-7 cells.

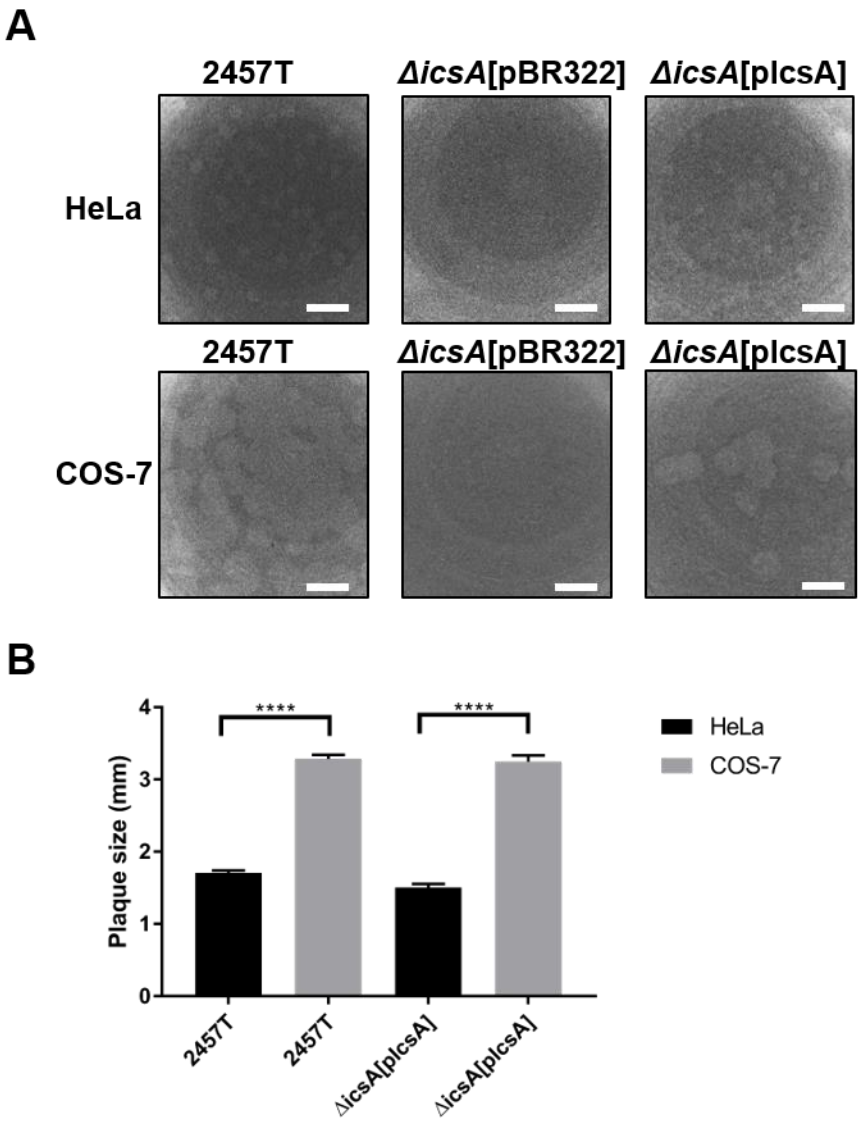

Figure 5.6. Myosin IIA is not essential for intercellular spread in COS-7 cells

(A) Plaque formation assay (Section 2.9.5) using *S. flexneri* WT (2457T), *S. flexneri ΔicsA* [pBR322], and *S. flexneri ΔicsA* [pIcsA] with HeLa cells (upper panel) and COS-7 cells (lower panel). Strains grown to mid-exponential phase were collected and used to infect cell monolayers for 1.5 h. The extracellular bacteria was killed by adding DMEM supplemented with 0.5% (w/v) agar and 40 µg/ml gentamycin. After 24 h post-infection, a second layer of DMEM medium containing 0.5% (w/v) agar and 0.1% (w/v) Neutral Red was added and images were taken after 72 h post-infection. Scale bar represents 5 mm. (**B**) Plaque size measurements for plaques formed in A (Section 2.9.5). Data were acquired at least from 10 plaques for each strain and significant was calculated using a student *t* test (Section 2.9.4), and *p* values are as follow: ****, $p<0.0001$. Note that *S. flexneri ΔicsA* [pBR322] did not form plaques on HeLa and COS-7 cells.

5.4. Discussion

This Chapter attempted to identify the receptors for the *S. flexneri* adhesin IcsA in HeLa cells. Using the purified $IcsA^{53-740}$, several IcsA-interacting molecules from a HeLa whole cell lysate were co-immunoprecipitated with protein A preloaded with either anti-IcsA or anti-His_6 antibodies. The molecules at the molecular sizes corresponding to those trypsin sensitive IcsA-interacting components (~220 kDa) shown by far Western blotting in Chapter 3 (Section 3.5.3) were excised and identified as Myosin IIA and Myosin IIB via mass spectrometry. This implicates these proteins as potential host cell surface displayed receptors for IcsA passenger domain adhesin activity. However, neither anti-Myosin IIA nor anti-Myosin IIB antibody significantly blocked the hyper-adherence of *S. flexneri ΔipaD* to HeLa cells, though anti-Myosin IIA showed slight inhibition at the concentration of 15 µg/ml. The anti-Myosin IIA and anti-Myosin IIB antibodies used in the adherence blocking assay were developed against synthetic peptides corresponding to amino acid residues 1949-1960 of Myosin IIA and 1965-1976 of Myosin IIB, respectively, hence they might have limited ability to block the IcsA interacting sites. In HeLa cells, Myosin IIA might not be the only nor the major receptor for IcsA to target. This is supported by the far Western immunoblotting (Chapter 3, Section 3.5.3), where multiple HeLa cell molecules were recognized by $IcsA^{53-740}$. Hence it might be difficult to validate the role of Myosin IIA in acting as a receptor for IcsA in *S. flexneri* adherence. In addition, Western immunoblotting on the co-IP samples with anti-Myosin IIA antibody failed to detect Myosin IIA. This is likely to due to the low expression level of Myosin IIA on HeLa cell surfaces (Sun *et al.*, 2014).

Although Myosin IIA is not present in COS-7 cells, *S. flexneri ΔipaD* still demonstrated the hyper-adherence phenotype in an IcsA-dependent manner. The adherence level was comparable to that observed with HeLa cells. This data indicated that other cellular molecules may play a role as IcsA receptors. Indeed, using far Western immunoblotting, IcsA-interacting molecules were also detected in COS-7 cell lysates.

Myosin IIA was reported to be essential in *S. flexneri* cell to cell spread in HeLa cells (Lum & Morona, 2014b), yet it was not required for *S. flexneri* to generate plaques in COS-7 monolayers. In fact, *S. flexneri* generated plaques twice the size as those on HeLa

cells. The size of the plaques generated in cell monolayers positively correlated to IcsA's cell to cell spread function. This highlighted an intrinsic difference between cell lines in that *S. flexneri* IcsA could utilise different cellular components and mechanisms in different cells for its cell to cell spread function. This could also be the case in the IcsA mediated hyper-adherence seen in *S. flexneri ΔipaD*, where incubation of IcsA passenger detected different interacting molecules in COS-7 cells compared to HeLa cells.

While Myosin IIA is an intracellular molecule (Shutova & Svitkina, 2018), in the human intestinal mucosa it was found on the villous surface of the epithelial lining and colonic crypt epithelium (Babbin *et al.*, 2009) which are the primary infection sites reported in the Guinea pig and humans (Arena *et al.*, 2015). Myosin IIA has been reported as a receptor for Thrombocytopenia syndrome virus (Sun *et al.*, 2014) and as a cellular entry receptor for herpes simplex virus 1 (HSV-1) (Arii *et al.*, 2010). Currently, it cannot be concluded that interaction between IcsA and myosin IIA is essential for *Shigella* adherence but remains intriguing for future investigation. A cell line with increased surface expression of Myosin IIA would greatly aid the investigation of how Myosin IIA contributes to the IcsA-mediated *S. flexneri* adherence.

Chapter Six

INVESTIGATION OF THE ROLE OF DEOXYCHOLATE IN *SHIGELLA FLEXNERI* HYPER-ADHERENCE

Chapter 6: Investigation of the role of deoxycholate in *Shigella flexneri* hyper-adherence

6.1. Introduction

S. flexneri grown in the presence of deoxycholate (DOC) exhibited a hyper-adherence phenotype (Pope *et al.*, 1995), and this phenotype is depend on the presence of the adhesin IcsA and is controlled by the T3SS (Brotcke-Zumsteg *et al.*, 2014). Incubation of *S. flexneri* WT with DOC at 4 °C did not increase the adherence to HeLa cells (Pope *et al.*, 1995), hence the DOC induction signal cascade is likely to be through the expression of some unknown factors. The molecular mechanism of this induction process remains to be investigated. Similar to this, *S. flexneri ΔipaD* which has a defective T3SS also had increased adherence to host cells compared to that of WT *S. flexneri* (Menard *et al.*, 1993). In a previous study (Brotcke-Zumsteg *et al.*, 2014), it was found that the hNE accessibility of IcsA produced in DOC induced *S. flexneri* WT or *S. flexneri ΔipaD* was altered compared to that produced in *S. flexneri* WT in the absence of DOC, yet the mechanism of how IcsA changed its hNE accessibility remains unclear.

The aim of this Chapter is to characterise the hyper-adherence of *S. flexneri* WT grown in the presence of DOC, and attempt to determine the molecular mechanism of DOC induced IcsA-dependent hyper-adherence.

6.2. DOC triggers the release of IpaD into the culture supernatant

The impact of DOC on the expression and secretion of IpaD in *S. flexneri* WT, and the expression levels of IcsA in both the DOC induced hyper-adherent *S. flexneri* and *S. flexneri ΔipaD* were investigated. Whole cell samples (Section 2.7.1) and corresponding culture supernatant samples (Section 2.7.2) of *S. flexneri* WT and *S. flexneri ΔipaD* grown in the presence and absence of DOC for 2 h were prepared and analysed via SDS-PAGE (Section 2.7.9.1) followed by Western immunoblotting (2.7.11.3) with anti-IcsA and anti-IpaD antibodies (Section 2.3.1).

It was found that the cellular expression level of IcsA was not changed in *S. flexneri ΔipaD* (Figure 6.1, lane 3) compared to the *S. flexneri* WT (Figure 6.1, lane 1). This was in accordance with the results reported by Brotcke-Zumsteg *et al.* (2014).This was also the case for the DOC treated *S. flexneri* WT (Figure 6.1, lane 2). Moreover, the secretion level of the IcsA passenger was also similar in both *S. flexneri* WT (Figure 6.1, lane 5&6) and *S. flexneri ΔipaD* (Figure 6.1, lane 7&8) regardless of DOC treatment. Collectively, these data suggested DOC does not affect the expression and secretion of IcsA.

In contrast to IcsA, the expression level of IpaD in the DOC treated *S. flexneri* WT (Figure 6.1, lane 2) was dramatically decreased compared to that expressed in the untreated *S. flexneri* WT (Figure 6.1, lane 1). It was also found that the level of IpaD in the culture supernatant was increased in the DOC treated *S. flexneri* WT (Figure 6.1, lane 6) compared to the untreated *S. flexneri* WT (Figure 6.1, lane 5). These data suggested that DOC triggers the release of IpaD from bacteria and enhances the secretion of IpaD into the culture supernatant.

6.3. DOC alters the IcsA's hNE accessibility

DOC does not affect the expression of IcsA (Figure 6.1), yet its hyper-adherence phenotype also requires the presence of IcsA (Chapter 3). Therefore, it was hypothesised that the IcsA expressed in the presence of DOC may have an altered hNE proteinase accessibility, which could be attributed to an alternative conformation required for its adhesin activity. To this end, *S. flexneri ΔicsA* [pIcsA^{FLAG}] producing IcsA^{FLAG} in the absence or presence of DOC was digested with hNE (Sectrion 2.7.13), and whole cell samples (Section 2.7.1) were collected at the indicated digestion time points and analysed by SDS-PAGE (Section 2.7.9.1) and Western immunoblotting (Section 2.7.11.3) with anti-FLAG antibodies (Section 2.3.1).

In the absence of DOC, IcsA^{FLAG} was digested into fragments around ~80 kDa, ~50 kDa and ~40 kDa at 90 min post-digestion (Figure 6.2 A), with the ~40 kDa fragment being most resistant to hNE. This was the same as reported in Chapter 4. However, in the presence of DOC, IcsA^{FLAG} was digested into fragments around ~60 kDa and ~50 kDa at 90 min post-digestion (Figure 6.2 B), with a ~50 kDa fragment being the most resistant to

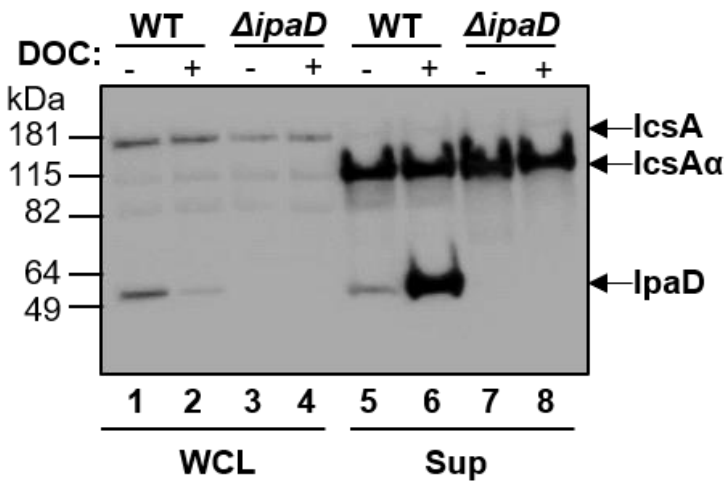

Figure 6.1. DOC triggers the release of IpaD into culture supernatant

Intra- and extra-cellular protein expression of IpaD and IcsA in *S. flexneri* WT and *S. flexneri ΔipaD* grown in the absence (lane 1, 3, 5 and 7) and presence (lane 2, 4, 6 and 8) of 2.5 mM DOC for 2 h. Whole cell protein samples (WCL) (Section 2.7.1) and cultured supernatant protein samples (Sup) (Section 2.7.2) were prepared and analysed via SDS-PAGE (Section 2.7.9.1) followed Western immunoblotting with both anti-IcsA and anti-IpaD antibodies. IcsAα, IcsA passenger domain.

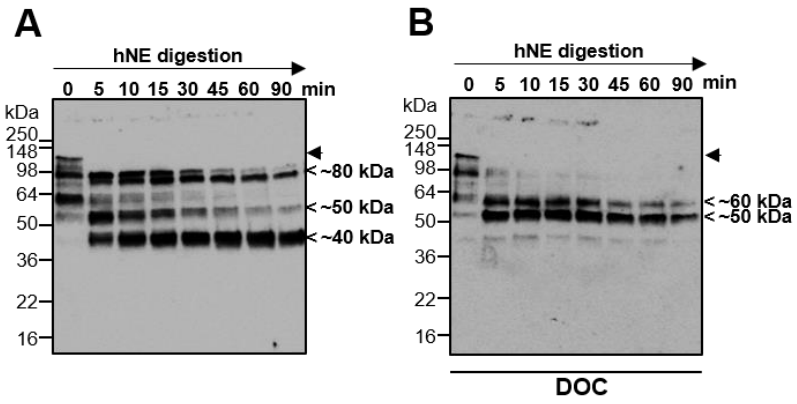

Figure 6.2. DOC alters the hNE accessibility of IcsA

S. flexneri ΔicsA [pIcsA^{FLAG}] grown in the absence (**A**) or presence (**B**) of 2.5 mM DOC were collected and analysed via proteolysis assay by hNE (Section 2.7.13). Digested whole cell samples collected at the indicated time points were analysed via SDS-PAGE (Section 2.7.9.1) and Western immunoblotting (Section 2.7.11.3) with anti-FLAG antibody (Section 2.3.1). Arrow indicates full length IcsA and the apparent molecular sizes of the hNE resistant fragments was as indicated.

hNE. Clearly, the altered hNE accessibility of IcsA produced in the *S. flexneri ΔicsA* [pIcsA^{FLAG}] grown in the presence of DOC is different to that produced in the absence of DOC.

6.4. The adhesin region aa 138-148 does not affect the altered hNE proteinase accessibility of IcsA induced by DOC

It was shown that aa 138-148 was the adhesin region of IcsA and was required for the IcsA-mediated hyper-adherence in the *S. flexneri ΔipaD* (Chapter 3). Furthermore, deletion of this region abolished both the hyper-adherence of *S. flexneri ΔipaD* (Chapter 3) and the altered hNE accessibility (Chapter 4) of IcsA produced in *S. flexneri ΔipaD* background. As the adhesin region aa 138-148 was also found essential for the DOC induced hyper-adherence phenotype of *S. flexneri* WT (Chapter 3), it was therefore decided to assess whether the adhesin region aa 138-148 also affected the altered proteinase accessibility of IcsA in *S. flexneri* WT upon the DOC treatment. To this end, IcsA^{FLAG} and IcsA$^{FLAG/\Delta 138\text{-}148}$ produced in *S. flexneri ΔicsA* [pIcsA^{FLAG}] and *S. flexneri ΔicsA* [IcsA$^{FLAG/\Delta 138\text{-}148}$], respectively, in the absence or presence of DOC were digested with hNE (Sectrion 2.7.13), and whole cell samples (Section 2.7.1) collected at the indicated digestion time points were analysed by SDS-PAGE (Section 2.7.9.1) and Western immunoblotting (Section 2.7.11.3) with anti-FLAG antibodies (Section 2.3.1).

As expected, IcsA^{FLAG} produced from *S. flexneri ΔicsA* [pIcsA^{FLAG}] had an altered hNE proteinase accessibility in the presence of DOC compared to that produced in the absence of DOC (Figure 6.3 A). However, IcsA$^{FLAG/\Delta 138\text{-}148}$ produced from *S. flexneri ΔicsA* [IcsA$^{FLAG/\Delta 138\text{-}148}$] in the presence of DOC also had an altered hNE proteinase accessibility profile (Figure 6.3 B), which was the same to that of IcsA^{FLAG} produced from *S. flexneri ΔicsA* [pIcsA^{FLAG}] grown in the presence of DOC (Figure 6.3 A). This data suggested that the adhesin region aa 138-148 does not affect the altered hNE accessibility profile of IcsA grown in the presence of DOC.

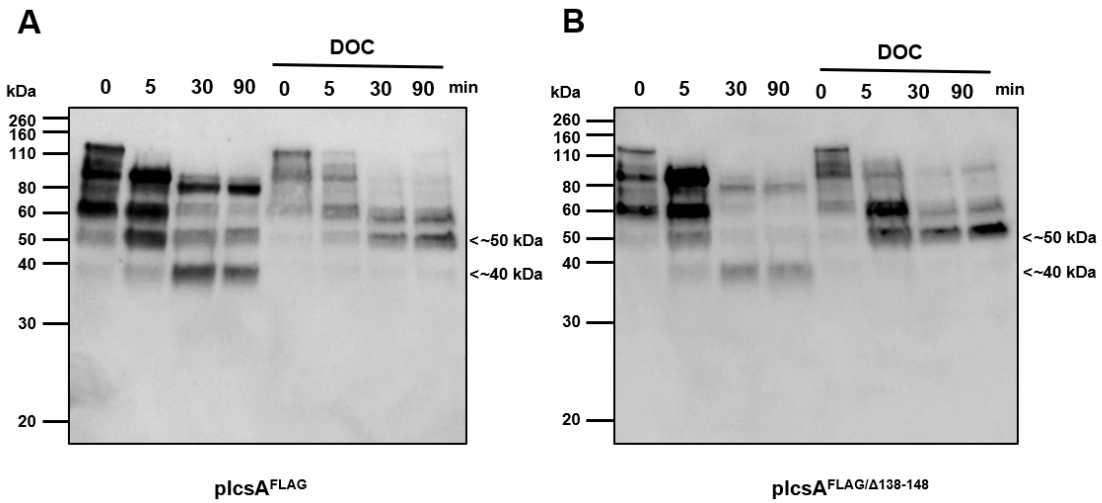

Figure 6.3. The adhesin region aa 138-148 does not affect the altered proteinase accessibility induced by DOC

S. flexneri ΔicsA [pIcsA^{FLAG}] (**A**) and *S. flexneri ΔicsA* [IcsA$^{FLAG/\Delta 138\text{-}148}$] (**B**) grown in the absence or presence of 2.5 mM DOC were collected and analysed via proteolysis assay by hNE (Section 2.7.13). Digested whole cell samples collected at the indicated time points were analysed via SDS-PAGE (Section 2.7.9.1) and Western immunoblotting (Section 2.7.11.3) with anti-FLAG antibody (Section 2.3.1). The apparent molecular size of the hNE resistant fragments was as indicated.

6.5. The C-terminal of IcsA was inaccessible in the presence of DOC

To analyse the origin of the ~50 kDa IcsA fragment with resistance to hNE produced in the presence of DOC, *S. flexneri ΔicsA* [pIcsA^{FLAG}] grown in the presence or absence of DOC were digested with hNE (Section 2.7.13). These digested samples were then separated into whole cell fractions (WCL) and digestion supernatant fractions (Sup) via centrifugation (Section 2.7.13). Samples of both whole cell fractions and digestion supernatant fractions were then analysed via SDS-PAGE (Section 2.7.9.1) and Western immunoblotting (Section 2.7.11.3) with anti-FLAG antibodies (Section 2.3.1).

In the absence of DOC, the ~40 kDa IcsA fragment with resistant to hNE was absent in the digested whole cell fractions (Figure 6.4 A) and appeared in the digested supernatant from 5 min post digestion (Figure 6.4 B), suggesting that the ~40 kDa IcsA fragment was cleaved from the bacteria surface in the first 5 min of digestion and accumulated in the digestion supernatant at 90 min post digestion (Figure 6.4 B). This is in accordance with the results described in Chapter 4, where the ~40 kDa IcsA fragment was predicted to be cleaved at aa 413 and 760 by hNE (Figure 6.4 C). However, when grown in the presence of DOC, the ~50 kDa resistant IcsA fragment was absent in the supernatant of hNE treated cells (Figure 6.4 B), but was present in the whole cell fractions up to 90 min post digestion (Figure 6.4 A). This indicated that the ~50 kDa IcsA fragment remained on the bacteria surface with the IcsA β-barrel domain (aa 759-1102) which is inaccessible to hNE (Figure 6.4 C). Therefore, according to the molecular size of the fragment (~50 kDa), the hNE cleavage site is predicted to be at around aa 667, and the fragment is estimated to be consist of aa 668-1102 (Figure 6.4 C). Unlike the ~40 kDa hNE resistant IcsA fragment digested from IcsA^{FLAG} produced from *S. flexneri ΔicsA* [pIcsA^{FLAG}] in the absence of DOC, the ~50 kDa fragment digested from IcsA^{FLAG} produced from *S. flexneri ΔicsA* [pIcsA^{FLAG}] in the presence of DOC does not contain aa 414-667 (Figure 6.4 C).

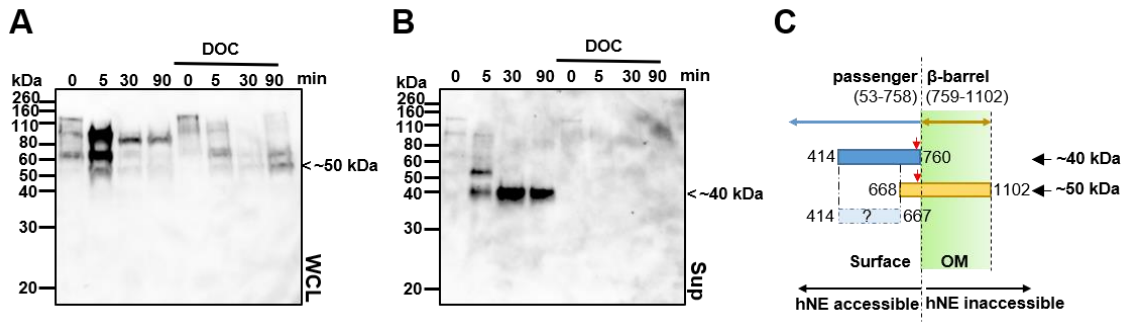

Figure 6.4. The C-terminal of IcsA was inaccessible in the presence of DOC

S. flexneri ΔicsA [pIcsA^{FLAG}] grown in the absence or presence of 2.5 mM DOC were collected and analysed via proteolysis assay by hNE (Section 2.7.13). Digested samples collected at the indicated time points were separated into whole cell fractions (**A**, WCL) and digestion supernatant fractions (**B**, Sup) via centrifugation (Section 2.7.13) and analysed via SDS-PAGE (Section 2.7.9.1) and Western immunoblotting (Section 2.7.11.3) with anti-FLAG antibody (Section 2.3.1). The appeared molecular size of the hNE resistant fragments was as indicated. **(C)** Schemetic representation of the aa prediction on the ~50 kDa and ~40 kDa hNE resistant fragments observed in **A** and **B** respectively. The insertion site of the FLAG×3 tag (aa 737) is indicated by a red arrow.

6.6. The altered hNE proteinase accessibility induced by DOC is independent to bacterial growth

It was reported that the growth of WT *S. flexneri* in the presence of DOC at 4 °C did not activate the hyper-adherence phenotype (Pope *et al.*, 1995), and the authors proposed that the DOC induced hyper-adherence phenotype of *S. flexneri* requires bacterial growth. To examine whether the altered proteinase accessibility induced by DOC also requires bacterial growth, the growth of *S. flexneri ⊿icsA* [pIcsA^{FLAG}] at the mid-exponential phase was inhibited by adding chloramphenicol (Section 2.7.13). The bacterial cultures were then incubated in the presence or absence of DOC for another 2 h before being digested with hNE (Section 2.7.13). Digested samples were then analysed via SDS-PAGE (Section 2.7.9.1) and Western immunoblotting (Section 2.7.11.3) with anti-FLAG antibody (Section 2.3.1).

After the growth inhibition by chloramphenicol in the absence of DOC and following hNE digestion of *S. flexneri ⊿icsA* [pIcsA^{FLAG}], bands of around ~80 kDa, ~50 kDa and ~40 kDa at 90 min post-digestion were detected (Figure 6.5), which is similar as shown in Figure 6.3 (A). Moreover, in the presence of both chloramphenicol and DOC, IcsA^{FLAG} produced from *S. flexneri ⊿icsA* [pIcsA^{FLAG}] was digested into fragments around ~90 kDa, ~60 kDa and ~50 kDa at 90 min post-digestion (Figure 6.5), which is similar as shown in Figure 6.3 (A). These data suggested that inhibition of *S. flexneri* growth by chloramphenicol does not abolish the altered proteinase accessibility of IcsA induced by DOC, and indicating that DOC may act directly on IcsA to affect its conformation.

6.7. DOC promotes the intermolecular interaction of IcsA

IcsA was recently reported to be responsible for the biofilm formation in the presence of DOC (Koseoglu *et al.*, 2019) by promoting cell to cell contacts and aggregative growth. This correlated with the IcsA self-association activity (May *et al.*, 2012). Therefore, it is hypothesised that DOC may have an impact on the IcsA self-association activity. To examine this, and to test whether the adhesin region aa 138-148 is required for the IcsA self-association activity. *S. flexneri ⊿icsA* [pIcsA^{FLAG}] and *S. flexneri ⊿icsA* [IcsA$^{FLAG/\Delta 138\text{-}148}$] were grown in the absence or presence of DOC, and were cross-linked with DSP (Section

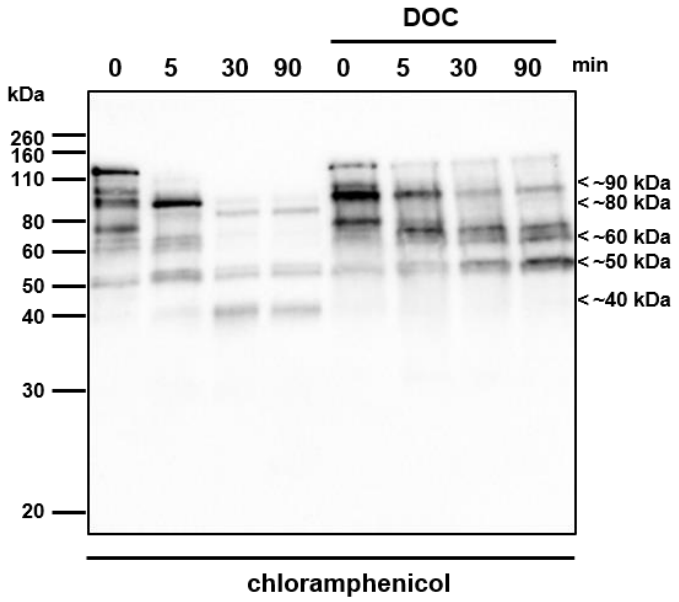

Figure 6.5. Chloramphenicol treatment does not abolish the altered hNE accessibility of IcsA induced by DOC

S. flexneri ΔicsA [pIcsA^{FLAG}] grown to mid-exponential phase were collected via centrifugation, resuspended in LB containing chloramphenicol, and were incubated at 37 °C for 30 min (Section 2.7.13). The bacterial growth inhibition by chloramphenicol was confirmed by measuring the Optical Desntity of cultures at 600 nm (Section 2.7.13). *S. flexneri ΔicsA* [pIcsA^{FLAG}] were then continued to be incubated at 37 °C in the absence or presence of 2.5 mM DOC for 2 h, before being digested with hNE in 1 mL PBS in the presence of chloramphenicol (Section 2.7.13). Digested whole cell samples collected at the indicated time points were analysed via SDS-PAGE (Section 2.7.9.1) and Western immunoblotting (Section 2.7.11.3) with anti-FLAG antibody (Section 2.3.1). The apparent molecular sizes of the hNE resistant fragments are as indicated.

2.7.8.1). Cross-linked samples were collected, solubilised and treated with or without DTT (Section 2.7.8.1) and analysed via SDS-PAGE (Section 2.7.9.1) and Western immunoblotting (Section 2.7.11.3) with anti-IcsA antibody (Section 2.3.1).

When grown in the absence of DOC, both IcsA^{FLAG} and IcsA$^{FLAG/\Delta 138\text{-}148}$ (~120 kDa) produced in *S. flexneri ΔicsA* [pIcsA^{FLAG}] and *S. flexneri ΔicsA* [IcsA$^{FLAG/\Delta 138\text{-}148}$], respectively, were cross-linked to complexes with an apparent molecular size over 260 kDa (Figure 6.6 A, lane 1&3). This is consistent to the results reported by May *et al.* (2012). In addition, cross-linked complexes were detected with apparent molecular sizes of ~90 kDa (Figure 6.6 A, lane 1&3, *), which are smaller than the reduced full-length IcsA (Figure 6.6 A, lane 2&4, arrow). These observations were in accordance with the results described in Chapter 4, where the DSP cross-linked purified IcsA passenger migrated faster than the uncrosslinked IcsA. In the presence of DOC, the quantity of the cross-linked complexes of IcsA^{FLAG} and IcsA$^{FLAG/\Delta 138\text{-}148}$ (~120 kDa) produced in *S. flexneri ΔicsA* [pIcsA^{FLAG}] and *S. flexneri ΔicsA* [IcsA$^{FLAG/\Delta 138\text{-}148}$] with the molecular size around ~90 kDa were dramatically reduced (Figure 6.6 B, lane 1&3, *) compared to samples of cells grown in the absence of DOC (Figure 6.6 A, lane 1&3, *). The quantity of the cross-linked complexes with the apparent molecular size of over 260 kDa were dramatically increased (Figure 6.6 B, lane 1&3), compared to that from cells grown in the absence of DOC (Figure 6.6 A, lane 1&3). There were no detectable differences between the crosslinked IcsA^{FLAG} and IcsA$^{FLAG/\Delta 138\text{-}}$ produced in *S. flexneri ΔicsA* [pIcsA^{FLAG}] and *S. flexneri ΔicsA* [IcsA$^{FLAG/\Delta 138\text{-}148}$] either in the presence or absence of DOC. Together, these data suggested that DOC promotes the intermolecular interaction of IcsA independent of the adhesin region aa 138-148.

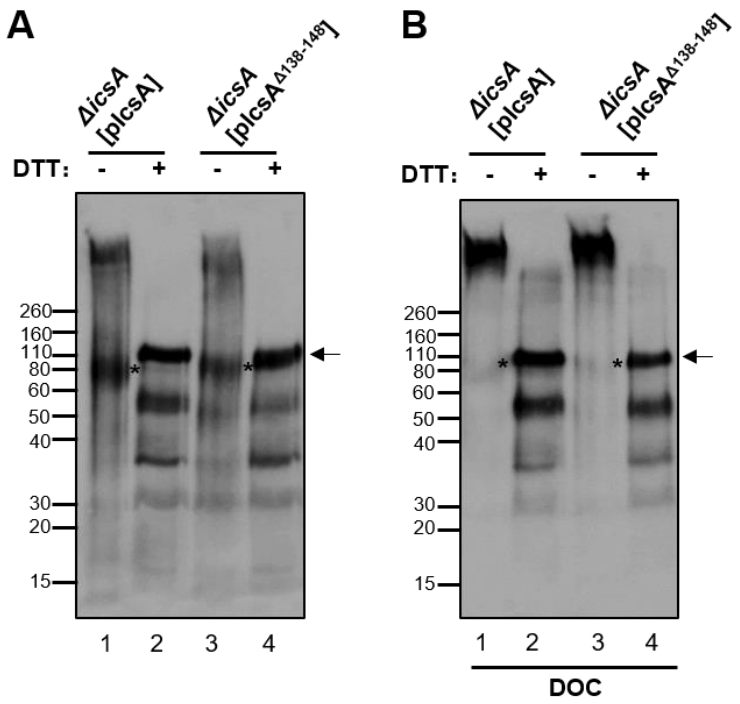

Figure 6.6. DOC promotes the intermolecular interaction of IcsA

S. flexneri ΔicsA [pIcsA^{FLAG}] (lane 1&2) and *S. flexneri ΔicsA* [IcsA$^{FLAG/\Delta 138\text{-}148}$] (lane 3&4) grown in the absence (**A**) or presence (**B**) of 2.5 mM DOC were collected and either left untreated or treated with DSP (Section 2.7.8.1). Cross-linked samples were then treated with or without DTT (Section 2.7.8.1) and analysed via SDS-PAGE (Section 2.7.9.1) and Western immunoblotting (Section 2.7.11.3) with anti-IcsA antibody (Section 2.3.1). Full length IcsA is indicated by an arrow.

6.8. Discussion

It was known that the hyper-adherence phenotype of *S. flexneri* can be experimentally induced either by incubation of *S. flexneri* WT with DOC (Pope *et al.*, 1995) or knocking out *ipaD* (Brotcke-Zumsteg *et al.*, 2014). IpaD has been known to be located at the needle tip of the T3SS extracellularly before DOC induction (Olive *et al.*, 2007, Cheung *et al.*, 2015), and is the protein to sense DOC in the environment (Veenendaal *et al.*, 2007, Barta *et al.*, 2012). Indeed, mutagenesis on the region that is responsible for the conformational change caused by the binding of DOC abolished the hyper-adherence phenotype induced by DOC (Bernard *et al.*, 2017). This chapter showed that DOC reduced the cellular IpaD levels but increased the level of IpaD secretion into culture supernatant. Therefore, it is likely that upon the binding of DOC, IpaD changes its conformation and is destabilised from the T3SS needle tip, thereby being released into culture supernatant. This reaction triggers an unknown signal cascade to activate the hyper-adherence phenotype. The absence of IpaD by mutation could partially mimic this reaction, leading to a hyper-adherence phenotype in *S. flexneri ΔipaD.* These hyper-adherence phenotype depends on the presence of the *S. flexneri* adhesin IcsA (Chapter 3) and was not due to changes in either IcsA expression or secretion level.

In the presence of DOC, IcsA produced from *S. flexneri* WT had an altered hNE accessibility compared to that produced in the absence of DOC. However, unlike the altered hNE accessibility of IcsA produced in *S. flexneri ΔipaD* (Chapter 4), the adhesin region aa 138-148 did not have any effects on the altered hNE accessibility of IcsA produced in *S. flexneri* WT in the presence of DOC. Following the fractionation of digestion samples, it was predicted that the most hNE resistant fragment (~50 kDa) of IcsA produced from *S. flexneri* WT in the presence of DOC consisted of aa 668-1102, which is different to the most resistant fragment (~40 kDa) of IcsA produced from *S. flexneri ΔipaD* (predicted to be consist of aa 414-760) (Chapter 4). However, aa 138-148 of IcsA are required for the hyper-adherence phenotype of *S. flexneri* WT induced by DOC (Chapter 4), hence it is plausible that the altered proteinase accessibility associated with aa 138-148 might be within aa 414-667 of the IcsA passenger. As this region (aa 414-667) does not have a FLAG tag, it was undetectable in the hNE digestions of the $IcsA^{FLAG}$ produced from *S. flexneri* WT grown in

the presence of DOC, hence the hNE digestion of IcsA$^{FLAG/\Delta 138\text{-}148}$ could not show any difference to that of IcsA^{FLAG}.

DOC induces the production and secretion of multiple virulence factors in *S. flexneri* (Faherty *et al.*, 2012). However, the altered hNE accessibility of IcsA is independent of bacterial growth and protein production, as the incubation of *S. flexneri ⊿icsA* [IcsA^{FLAG}] in the presence of chloramphenicol did not abolish the altered hNE accessibility of IcsA^{FLAG} caused by DOC. However, the growth inhibition by incubation of *S. flexneri* with DOC at 4 °C failed to activate the hyper-adherence phenotype (Pope *et al.*, 1995). Therefore, we speculate that the altered hNE accessibility of IcsA induced by DOC and observed in this Chapter is possibly unrelated to the hyper-adherence phenotype.

Through DPS cross-linking, it was found that DOC dramatically promoted the intermolecular interaction of IcsA. This observation supports the results of Koseoglu *et al.* (2019), where IcsA was found to be responsible for *S. flexneri* biofilm formation in the presence of DOC by promoting cell to cell contacts and aggregative growth. Therefore, it is likely that DOC enhances the intermolecular interaction of IcsA, thereby promoting polar aggregation of *S. flexneri* and facilitating biofilm formation. Such intermolecular interaction could have made the C-terminal of IcsA passenger inaccessible to hNE, thereby producing a different hNE digestion pattern.

Chapter Seven

CONCLUSIONS

Chapter 7: Conclusion

7.1. IcsA adhesin region

IcsA was found to be an adhesin in *S. flexneri* (Brotcke-Zumsteg *et al.*, 2014) and *S. sonnei* (Mahmoud *et al.*, 2016) contributing to *Shigella* colonisation of the human colon, thereby facilitating subsequent invasion. The adhesin activity is activated by the growth of *S. flexneri* with DOC, or by knocking out *ipaD* or *ipaB*. What regions are required for IcsA's adhesin activity? Investigation has already been conducted and reported that insertions of 5 aa at sites i148 and i386 affected IcsA's adhesin function (Brotcke-Zumsteg *et al.*, 2014). This was done by screening for invasion defects with *S. flexneri* expressing IcsA 5aa insertion mutants (May & Morona, 2008) grown in the presence of DOC. In Chapter 3, the IcsA 5 aa insertion mutants were expressed in *S. flexneri ΔipaD*, and was screened directly for defects in IcsA adhesin activity. This led to finding of three insertions (i138, i140 and i148), but not the i386, with significant impact on IcsA's adhesin function. By substitutions (I138P, and Q148C/G149N) of amino residues adjacent to these inserted sites, and the deletion of residues from aa 138 to aa 148 in the IcsA passenger domain, the region aa 138-148 was found to be essential for IcsA's adhesin activity. The discrepancy of this work to the previously published data (Brotcke-Zumsteg *et al.*, 2014) is probably due to the screening methods, i.e. adherence defect verses invasion defect. Given that surface localised IcsA passenger on *S. flexneri* remains uncleaved and adapts an elongated shape (Mauricio *et al.*, 2017) with its N-terminal region exposed to the environment for binding to host receptors, it is more likely that the region required for its adhesin activity resides proximal to the N-terminal end. The insertion at i386 might have affected other aspects of IcsA's structure, which will be discussed below. Indeed, in Chapter 3, it was also found that unlike the purified $IcsA^{53\text{-}740}$ passenger, the purified mutant $IcsA^{53\text{-}740(\Delta 138\text{-}148)}$ did not inhibit the hyper-adherence of *S. flexneri ΔipaD* to HeLa cells. Moreover, fluorescently labelled $IcsA^{53\text{-}740(\Delta 138\text{-}148)}$ did not bind to HeLa cell surfaces and had reduced binding affinity to molecules from HeLa cells compared to that of WT $IcsA^{53\text{-}740}$. Overall, these results revealed a subregion (aa 138-148) within IcsA passenger domain important for its adhesin function. In Chapter 3, it was also demonstrated that loss of the adhesin region aa 138-148 in IcsA passenger also

impairs the invasion ability of *S. flexneri*, highlighting the importance of this region and adherence in the early stage of *Shigella* pathogenesis.

It remains to be investigated as to which specific amino residues within this region (aa 138-148) are essential for IcsA's adhesin function. In Chapter 3, the results of alanine scanning on the region aa 138-148 suggested that multiple residues are likely to contribute to IcsA's adhesin function. However, due to the time constraint, this remains to be investigated in the future. The residues required for the adhesin function can be investigated by assessing IcsA mutants with substitutions of more than one residue at a time within this region. Such information will be valuable for understanding the molecular mechanisms of IcsA's adhesin activity and will pave the way for understanding the interactions between IcsA and its receptors. Nevertheless, the work in Chapter 3 has localised the IcsA's adhesin region to aa 138-148.

7.2. The multiple conformations of IcsA

In Chapter 4, the expression level of IcsA was found to be the same in hyper-adherent strains compared to *S. flexneri* WT, yet IcsA's adhesin function is only active in those hyper-adherent strains. How does IcsA function as adhesin in those hyper-adherence strains? By using hNE that targets *Shigella* surface virulence factors (Weinrauch *et al.*, 2002) including IcsA (Brotcke-Zumsteg *et al.*, 2014), the conformations of IcsA produced from non-hyper-adherence *S. flexneri* WT and hyper-adherent *S. flexneri ΔipaD* were revealed to be different (Brotcke-Zumsteg *et al.*, 2014). It was found that the hNE accessibility of $IcsA^{FLAG}$ expressed from *S. flexneri ΔipaD* was altered compared to that produced from WT *S. flexneri*, and this altered hNE accessibility is independent of the presence of LPS O antigen and is depend on the presence of the adhesin region aa 138-148. These data suggested that the adhesin region is also required for IcsA adapting the conformation that is associated with the hyper-adherence of *S. flexneri ΔipaD*. Through the analysis of the hNE digested IcsA fragments using FLAG×3 tagged IcsA reporter, it was found that the adhesin region affected the hNE resistance of a C-terminal region which is estimated to be consists of aa ~414-760. This highlighted a role of IcsA self-association in an alternative conformation. Using the native IcsA purified from the culture supernatant, IcsA was found with two forms. Analysis

of these populations revealed that one form of the purified IcsA was stabilised via an intramolecular disulfide bond. It is likely that the disulfide bond forms between C130 and aa C376 or C380 as a result of the interaction between the N-terminal of IcsA passenger containing the adhesin region aa 138-148 and the C-terminal region of IcsA passenger near aa ~414-760. The previously reported invasion defects caused by the insertion at i386 (Brotcke-Zumsteg *et al.*, 2014) could also be due to the disruption of the spatial localization of C376 and C380 by the 5 aa insertion, which abolished the formation of the disulfide bond. However, the importance of this disulfide bond formation within IcsA passenger to IcsA's function is beyond the scope of this work and remains to be investigated in the future, such as mutation of C130, C376 and C380 and examination of their impact on the IcsA-mediated *S. flexneri* hyper-adherence and subsequent invasion. Nevertheless, this work is the first to describe multiple conformations of IcsA and highlighted a potential self-interaction between the N-terminal region of IcsA to its C-terminal region.

7.3. The interaction between IcsA and host cell surface

What host molecules does IcsA bind to as receptors? In Chapter 3, the purified IcsA was made as a fluorescent probe and revealed to bind to the HeLa cell surfaces. In addition, the purified IcsA also recognised several host molecules sensitive to surface trypsin shaving through indirect probing. These data suggested that the purified IcsA passenger produced form *E. coli* also maintains its adhesin function, similar to when expressed in *E. coli* (Brotcke-Zumsteg *et al.*, 2014). Moreover, this provided a tool to identify the potential receptors of IcsA on HeLa cells. In Chapter 5, the purified IcsA was used as a bait to isolate putative receptors from HeLa cell lysate, and Myosin IIA and Myosin IIB were identified as putative host IcsA-interacting molecules. However, the indirect probing of HeLa lysate with purified IcsA suggested that there might be multiple receptors other than Myosin IIA and Myosin IIB for IcsA on HeLa cells. Therefore, it is difficult to examine the effects of Myosin IIA and Myosin IIB on the IcsA-mediated *Shigella* hyper-adherence at the cellular level. Due to the time constraint, this remains to be investigated in the future. Either a Myosin IIA or Myosin IIB knock-out cell line can be made to examine the effects on the IcsA-mediated *S. flexneri* adherence. Nevertheless, this work has identified Myosin IIA and

Myosin IIB as putative receptor for IcsA and paved way for future IcsA receptor identification studies.

7.4. The effect of DOC on IcsA

How does DOC affect IcsA's adhesin function? In Chapter 6, it was found that DOC does not affect the expression and secretion of IcsA. Growth of *S. flexneri* in the presence of DOC altered the hNE accessibility of IcsA. The altered hNE accessibility profile of IcsA produced from *S. flexneri* in the presence of DOC is different to that of produced from *S. flexneri ΔipaD*, yet IcsA was also found to be essential for the DOC induced hyper-adherence in Chapter 3. The analysis of conformations of IcsA and IcsA$^{\Delta 138\text{-}148}$ produced from *S. flexner*i grown in the presence of DOC revealed no difference. This was probably because that the IcsA C-terminal regions interacting with the adhesin region aa 138-148 shown in *S. flexneri ΔipaD* background were undetectable in the DOC treated *S. flexneri* background. Therefore, it was not possible to completely assess the effect of the adhesin region aa 138-148 had on the DOC induced conformational change in IcsA. Nevertheless, it is likely that the altered hNE accessibility detected in Chapter 6 is independent to IcsA's adhesin function. This is because the incubation of *S. flexneri* in the presence of DOC at 4 °C did not activate the hyper-adherence phenotype (Pope *et al.*, 1995), yet the incubation of *S. flexneri* with the growth inhibition using chloramphenicol in the presence of DOC altered the IcsA's hNE accessibility. The exact effect of DOC on IcsA's conformation might require future re-design of epitopes at other sites within IcsA and/or digestion with different proteinases.

The results in Chapter 6 for the first time reveal that DOC enhances the self-association of IcsA in *S. flexneri*. It has been reported that DOC promotes *Shigella* biofilm formation and aggregative bacterial growth, and this requires the presence of IcsA (Koseoglu *et al.*, 2019). The results in Chapter 6 supports this notion, and highlighted for the first time a molecular mechanism of which DOC enhances the *Shigella* cell to cell contact by promoting IcsA inter-molecular association.

7.5. IcsA as a vaccine potential and therapeutic target

In Chapter 3, it was found that both the purified IcsA passenger and anti-IcsA antibody were able to block the hyper-adherence of *S. flexneri ΔipaD*. This highlighted a vaccine potential for IcsA, in that antibody raised against IcsA might protect against *Shigella* pathogens from the early stage of the infection, i.e. colonisation. For this, IcsA must be purified in its native and functional form with high solubility and stability. However, it is notoriously difficult to purify the full length IcsA passenger in its native form in a large quantity (Kuhnel and Diezmann, 2011, Leupold *et al.*, 2017). Therefore, the work in Chapter 4 developed IcsA purification protocol. Using this protocol, functional IcsA was purified in a high purity and may be of use in vaccine studies. Such a protocol can be also beneficial in determining full length IcsA's structure. It has been determined that by using this protocol, IcsA can be purified and concentrated to ~10 mg/ml, which is the common protein concentration required for primary screening of crysallisation conditions. As this work revealed the adhesin region of IcsA, it is therefore important to include the structure determination of the mutant $IcsA^{\Delta 138\text{-}148}$ in the future. Such information will greatly aid our understanding in not only the IcsA-mediated adherence, but also the overall *Shigella* pathogenesis. Moreover, the knowledge in the molecular basis of IcsA adhesin could also aid the future design of therapeutics targeting IcsA. Such therapeutics would have advantages in avoiding the resistance developed within *Shigella* species, as targeting IcsA's adhesin function does not impact the overall *Shigella* fitness but would disarm the virulence of *Shigella*.

Appendices

BACTERIAL STRAINS

PLASMIDS

OLIGONEUCLEOTIDES

BIBLIOGRAPHY

Appendix A: Bacterial strains

Strains	Notes
Lab strains	
DH5α	F^-, Φ80d*lacZ*△M15, *⊿(lacZYA-argF)*U169, *deoR, recA1, endA1, hsdR17* (rk-,mk+), *phoA*, *supE44*, λ- , *thi*-1, *gyrA*96, *relA*1 (NEB)
TOP10	F^- *mcrA* Δ(*mrr-hsd*RMS-*mcr*BC) φ80*lacZ*ΔM15 *⊿lacX*74 *nupG recA*1 *araD*139 Δ*(ara-leu)7697 galK rpsL(*Str^R*) end*A1 λ^- (ThermoFisher Scientific)
C43(DE3)	F^- *ompT gal dcm hsdSB(*rB^- mB^-*)* λ(DE3) (NEB)
XL10-Gold	*endA1 glnV44 recA1 thi-1 gyrA96 relA1 lac Hte* Δ(*mcrA*)183 Δ(*mcrCB-hsdSMR-mrr*)173 tet^R F'[*proAB lacIqZ*ΔM15 *Tn10*(Tet^R Amy Cml^R)] (Agilent)
2457T	RMA4258, *Shigella flexneri* 2a (Laboratory stock)
2457T*⊿rlmD*	RMA723 (Van Den Bosch *et al.*, 1997)
2457T*⊿icsA*	RMA2041 (Van den Bosch & Morona, 2003)
2457T*⊿icsA⊿rmlD*	RMA2043 (Van den Bosch & Morona, 2003)
MDRM190	TOP10[pMDBAD::$icsA^{his12\text{-}TEV\text{-}52\text{-}740}$] (Dr Matthew Doyle)

Strains	Parent[Plasmids]	Description
Strains generated in this thesis		
JQRM1	2457T[pKD46]	Amp^R, mutagenesis strain, 30 °C
JQRM2	2457T*ΔicsA*[pKD46]	Tet^R, Amp^R, mutagenesis strain, 30 °C
JQRM3	DH5α[pGEM-Teasy::ipaD]	Amp^R, complementation construct storage
JQRM4	DH5α[pGEM-Teasy::*ipaB*]	Amp^R, complementation construct, no expression
JQRM5	2457T*ΔipaD::kan*	Kan^R, *ipaD* knock-out strain, kanamycin cassette
JQRM6	2457T*ΔipaB::kan*	Kan^R, *ipaB* knock-out strain, polar effect
JQRM7	2457T*ΔicsAΔipaD::kan*	Tet^R, Kan^R, *ipaD icsA* knock-out strain
JQRM8	2457T*ΔicsAΔipaB::kan*	Tet^R, Kan^R, *ipaB icsA* knock-out strain, polar
JQRM9	2457T*ΔipaD::frt*	*ipaD* knock-out strain
JQRM10	2457T*ΔipaB::frt*	*ipaB* knock-out strain
JQRM11	2457T*ΔicsAΔipaD::frt*	Tet^R, *ipaD icsA* knock-out strain
JQRM12	2457T*ΔicsAΔipaB::frt*	Tet^R, *ipaB icsA* knock-out strain, polar
JQRM13	2457T*ΔipaD::frt*[pGEM-Teasy::*ipaD*]	Amp^R, IpaD complementation strain
JQRM14	2457T*ΔicsAΔipaD::frt*[pGEM-Teasy::*ipaD*]	Tet^R, Amp^R, IpaD complementation strain
JQRM15	2457T*ΔipaD::frt*[pGEM-Teasy::*90nts*]	Amp^R, vector control.
JQRM16	2457T*ΔicsAΔipaD::frt*[pIcsA]	Tet^R, Amp^R, *icsA* complementation strain
JQRM17	2457T*ΔicsAΔipaD::frt*[pBR322]	Tet^R, Amp^R, vector control
JQRM18	2457T*ΔipaD::frt*[pIcsA^{i148}]	Tet^R, Amp^R, IcsA insertion library
JQRM19	2457T*ΔipaD::frt*[pIcsA^{i386}]	Tet^R, Amp^R, IcsA insertion library
JQRM20	2457T*ΔipaD::frt*[pIcsA$^{i148\text{-}386}$]	Tet^R, Amp^R, IcsA insertion library, combined
JQRM21	2457T*ΔipaD::frt*[pGEM-Teasy::*ipaD*][pIcsA-GFP]	Tet^R, Amp^R, Kan^R, IpaD IcsA complementation
JQRM22	2457T*ΔicsAΔipaD::frt*[pIcsA^{i56}]	Tet^R, Amp^R, IcsA insertion library
JQEM23	2457T*ΔicsAΔipaD::frt*[pIcsA^{i81}]	Tet^R, Amp^R, IcsA insertion library
JQRM24	2457T*ΔicsAΔipaD::frt*[pIcsA^{i87}]	Tet^R, Amp^R, IcsA insertion library
JQRM25	2457T*ΔicsAΔipaD::frt*[pIcsA^{i120}]	Tet^R, Amp^R, IcsA insertion library
JQRM26	2457T*ΔicsAΔipaD::frt*[pIcsA^{i122}]	Tet^R, Amp^R, IcsA insertion library
JQRM27	2457T*ΔicsAΔipaD::frt*[pIcsA^{i128}]	Tet^R, Amp^R, IcsA insertion library
JQRM28	2457T*ΔicsAΔipaD::frt*[pIcsA^{i132}]	Tet^R, Amp^R, IcsA insertion library
JQRM29	2457T*ΔicsAΔipaD::frt*[pIcsA^{i137}]	Tet^R, Amp^R, IcsA insertion library
JQRM30	2457T*ΔicsAΔipaD::frt*[pIcsA^{i138}]	Tet^R, Amp^R, IcsA insertion library
JQRM31	2457T*ΔicsAΔipaD::frt*[pIcsA^{i140}]	Tet^R, Amp^R, IcsA insertion library
JQRM32	2457T*ΔicsAΔipaD::frt*[pIcsA^{i148}]	Tet^R, Amp^R, IcsA insertion library

JQRM33	2457T*ΔicsAΔipaD::frt*[pIcsA^{i185}]	Tet^{R}, Amp^{R}, IcsA insertion library
JQRM34	2457T*ΔicsAΔipaD::frt*[pIcsA^{i193}]	Tet^{R}, Amp^{R}, IcsA insertion library
JQRM35	2457T*ΔicsAΔipaD::frt*[pIcsA^{i219}]	Tet^{R}, Amp^{R}, IcsA insertion library
JQRM36	2457T*ΔicsAΔipaD::frt*[pIcsA^{i226}]	Tet^{R}, Amp^{R}, IcsA insertion library
JQRM37	2457T*ΔicsAΔipaD::frt*[pIcsA^{i228}]	Tet^{R}, Amp^{R}, IcsA insertion library
JQRM38	2457T*ΔicsAΔipaD::frt*[pIcsA^{i230}]	Tet^{R}, Amp^{R}, IcsA insertion library
JQRM39	2457T*ΔicsAΔipaD::frt*[pIcsA^{i244}]	Tet^{R}, Amp^{R}, IcsA insertion library
JQRM40	2457T*ΔicsAΔipaD::frt*[pIcsA^{i248}]	Tet^{R}, Amp^{R}, IcsA insertion library
JQRM41	2457T*ΔicsAΔipaD::frt*[pIcsA^{i268}]	Tet^{R}, Amp^{R}, IcsA insertion library
JQRM42	2457T*ΔicsAΔipaD::frt*[pIcsA^{i271}]	Tet^{R}, Amp^{R}, IcsA insertion library
JQRM43	2457T*ΔicsAΔipaD::frt*[pIcsA^{i288}]	Tet^{R}, Amp^{R}, IcsA insertion library
JQRM44	2457T*ΔicsAΔipaD::frt*[pIcsA^{i292}]	Tet^{R}, Amp^{R}, IcsA insertion library
JQRM45	2457T*ΔicsAΔipaD::frt*[pIcsA^{i297}]	Tet^{R}, Amp^{R}, IcsA insertion library
JQRM46	2457T*ΔicsAΔipaD::frt*[pIcsA^{i312}]	Tet^{R}, Amp^{R}, IcsA insertion library
JQRM47	2457T*ΔicsAΔipaD::frt*[pIcsA^{i314}]	Tet^{R}, Amp^{R}, IcsA insertion library
JQRM48	2457T*ΔicsAΔipaD::frt*[pIcsA^{i322}]	Tet^{R}, Amp^{R}, IcsA insertion library
JQRM49	2457T*ΔicsAΔipaD::frt*[pIcsA^{i324}]	Tet^{R}, Amp^{R}, IcsA insertion library
JQRM50	2457T*ΔicsAΔipaD::frt*[pIcsA^{i326}]	Tet^{R}, Amp^{R}, IcsA insertion library
JQRM51	2457T*ΔicsAΔipaD::frt*[pIcsA^{i330a}]	Tet^{R}, Amp^{R}, IcsA insertion library
JQRM52	2457T*ΔicsAΔipaD::frt*[pIcsA^{i330b}]	Tet^{R}, Amp^{R}, IcsA insertion library
JQRM53	2457T*ΔicsAΔipaD::frt*[pIcsA^{i342}]	Tet^{R}, Amp^{R}, IcsA insertion library
JQRM54	2457T*ΔicsAΔipaD::frt*[pIcsA^{i346}]	Tet^{R}, Amp^{R}, IcsA insertion library
JQRM55	2457T*ΔicsAΔipaD::frt*[pIcsA^{i369}]	Tet^{R}, Amp^{R}, IcsA insertion library
JQRM56	2457T*ΔicsAΔipaD::frt*[pIcsA^{i381}]	Tet^{R}, Amp^{R}, IcsA insertion library
JQRM57	2457T*ΔicsAΔipaD::frt*[pIcsA^{i386}]	Tet^{R}, Amp^{R}, IcsA insertion library
JQRM58	2457T*ΔicsAΔipaD::frt*[pIcsA^{i456}]	Tet^{R}, Amp^{R}, IcsA insertion library
JQRM59	2457T*ΔicsAΔipaD::frt*[pIcsA^{i502}]	Tet^{R}, Amp^{R}, IcsA insertion library
JQRM60	2457T*ΔicsAΔipaD::frt*[pIcsA^{i532}]	Tet^{R}, Amp^{R}, IcsA insertion library
JQRM61	2457T*ΔicsAΔipaD::frt*[pIcsA^{i563}]	Tet^{R}, Amp^{R}, IcsA insertion library
JQRM62	2457T*ΔicsAΔipaD::frt*[pIcsA^{i595}]	Tet^{R}, Amp^{R}, IcsA insertion library
JQRM63	2457T*ΔicsAΔipaD::frt*[pIcsA^{i598}]	Tet^{R}, Amp^{R}, IcsA insertion library
JQRM64	2457T*ΔicsAΔipaD::frt*[pIcsA^{i633}]	Tet^{R}, Amp^{R}, IcsA insertion library
JQRM65	2457T*ΔicsAΔipaD::frt*[pIcsA^{i643}]	Tet^{R}, Amp^{R}, IcsA insertion library
JQRM66	2457T*ΔicsAΔipaD::frt*[pIcsA^{i677}]	Tet^{R}, Amp^{R}, IcsA insertion library
JQRM67	2457T*ΔicsAΔipaD::frt*[pIcsA^{i716}]	Tet^{R}, Amp^{R}, IcsA insertion library
JQRM68	2457T*ΔicsAΔipaD::frt*[pIcsA^{i748}]	Tet^{R}, Amp^{R}, IcsA insertion library

JQRM69	2457T*ΔicsAΔipaD::frt*[pGEM-Teasy::*ipaD*][pSU23::*icsA*]	Tet^R, Amp^R, $Spec^R$, IpaD IcsA complementation
JQRM70	DH5α[$pIcsA^{54::his6}$]	Amp^R, IcsA construct with N terminal tag
JQRM71	DH5α[pCDF-Duet::$IcsA^{54::his6}$]	$Spec^R$, IcsA expression construct
JQRM72	DH5α[pCDF-Duet::$IcsA^{54::his6}$-IcsP]	$Spec^R$, IcsA IcsP co-expression construct
JQRM73	BL21(DE3) Codon plus [pCDF-Duet::$IcsA^{54::his6}$-IcsP]	$Spec^R$, Cml^R, IcsA IcsP co-expression strain
JQRM74	C43(DE3)[pCDF-Duet::$IcsA^{54::his6}$-IcsP]	$Spec^R$, IcsA IcsP co-expression strain
JQRM75	LEMO(DE3) [pCDF-Duet::$IcsA^{54::his6}$-IcsP]	$Spec^R$, Cml^R, IcsA IcsP co-expression strain
JQRM76	DH5α[pGEX-2T::$IcsA^{111-170}$]	Amp^R, IcsA peptide construct
JQRM77	DH5α[pGEX-2T::$IcsA^{351-410}$]	Amp^R, IcsA peptide construct
JQRM78	C43(DE3)[pGEX-2T::$IcsA^{111-170}$]	Amp^R, IcsA peptide expression strain
JQRM79	C43(DE3)[pGEX-2T::$IcsA^{351-410}$]	Amp^R, IcsA peptide expression strain
JQRM80	DH5α[pCDF-Duet::$IcsA^{54::his6-\Delta 138-148}$-IcsP]	$Spec^R$, $IcsA^{\Delta 138-148}$ IcsP construct
JQRM81	DH5α[$pIcsA^{\Delta 138-148}$]	Amp^R, $IcsA^{\Delta 138-148}$ construct
JQRM82	C43(DE3)[pCDF-Duet::$IcsA^{54::his6-\Delta 138-148}$-IcsP]	$Spec^R$, $IcsA^{\Delta 138-148}$ IcsP conexpression strain
JQRM83	2457T*ΔicsA*[$pIcsA^{\Delta 138-148}$]	Tet^R, Amp^R, $IcsA_{\Delta 138-148}$ complementation strain
JQRM84	2457T*ΔicsAΔipaD::frt*[$pIcsA^{\Delta 138-148}$]	Tet^R, Amp^R, $IcsA_{\Delta 138-148}$ complementation strain
JQRM85	2457T*ΔicsAΔipaD::frt*[$pIcsA^{I138R/T139L}$]	Tet^R, Amp^R, IcsA point mutant
JQRM86	2457T*ΔicsAΔipaD::frt*[$pIcsA^{I138P}$]	Tet^R, Amp^R, IcsA point mutant
JQRM87	2457T*ΔicsAΔipaD::frt*[$pIcsA^{m138-139}$-3]	Tet^R, Amp^R, IcsA point mutant
JQRM88	2457T*ΔicsAΔipaD::frt*[pIcsA]	Tet^R, Amp^R, IcsA point mutant
JQRM89	2457T*ΔicsAΔipaD::frt*[$pIcsA^{m138-139}$-5]	Tet^R, Amp^R, IcsA point mutant
JQRM90	2457T*ΔicsAΔipaD::frt*[$pIcsA^{m138-139}$-6]	Tet^R, Amp^R, IcsA point mutant
JQRM91	2457T*ΔicsAΔipaD::frt*[$pIcsA^{m138-139}$-7]	Tet^R, Amp^R, IcsA point mutant
JQRM92	2457T*ΔicsAΔipaD::frt*[$pIcsA^{m138-139}$-8]	Tet^R, Amp^R, IcsA point mutant
JQRM93	2457T*ΔicsAΔipaD::frt*[$pIcsA^{m138-139}$-9]	Tet^R, Amp^R, IcsA point mutant
JQRM94	2457T*ΔicsAΔipaD::frt*[$pIcsA^{I138R/T139T}$]	Tet^R, Amp^R, IcsA point mutant
JQRM95	2457T*ΔicsAΔipaD::frt*[$pIcsA^{m140-141}$-1]	Tet^R, Amp^R, IcsA point mutant
JQRM96	2457T*ΔicsAΔipaD::frt*[$pIcsA^{G140H/S141P}$]	Tet^R, Amp^R, IcsA point mutant
JQRM97	2457T*ΔicsAΔipaD::frt*[$pIcsA^{m140-141}$-3]	Tet^R, Amp^R, IcsA point mutant
JQRM98	2457T*ΔicsAΔipaD::frt*[$pIcsA^{G140L/S141G}$]	Tet^R, Amp^R, IcsA point mutant
JQRM99	2457T*ΔicsAΔipaD::frt*[$pIcsA^{m140-141}$-5]	Tet^R, Amp^R, IcsA point mutant
JQRM100	2457T*ΔicsAΔipaD::frt*[$pIcsA^{m140-141}$-6]	Tet^R, Amp^R, IcsA point mutant
JQRM101	2457T*ΔicsAΔipaD::frt*[$pIcsA^{G140A/S140N}$]	Tet^R, Amp^R, IcsA point mutant

JQRM102	2457T*ΔicsAΔipaD::frt*[pIcsA$^{G140V/S140V}$]	Tet^{R}, Amp^{R}, IcsA point mutant
JQRM103	2457T*ΔicsAΔipaD::frt*[pIcsA$^{m140-141}$-9]	Tet^{R}, Amp^{R}, IcsA point mutant
JQRM104	2457T*ΔicsAΔipaD::frt*[pIcsA$^{m140-141}$-10]	Tet^{R}, Amp^{R}, IcsA point mutant
JQRM105	2457T*ΔicsAΔipaD::frt*[pIcsA$^{m140-141}$-10-2]	Tet^{R}, Amp^{R}, IcsA point mutant
JQRM106	2457T*ΔicsAΔipaD::frt*[pIcsA$^{Q148D/G149S}$]	Tet^{R}, Amp^{R}, IcsA point mutant
JQRM107	2457T*ΔicsAΔipaD::frt*[pIcsA$^{Q148K/G149S}$]	Tet^{R}, Amp^{R}, IcsA point mutant
JQRM108	2457T*ΔicsAΔipaD::frt*[pIcsA$^{m148-149}$-3]	Tet^{R}, Amp^{R}, IcsA point mutant
JQRM109	2457T*ΔicsAΔipaD::frt*[pIcsA$^{Q148F/G149Q}$]	Tet^{R}, Amp^{R}, IcsA point mutant
JQRM110	2457T*ΔicsAΔipaD::frt*[pIcsA$^{m148-149}$-5]	Tet^{R}, Amp^{R}, IcsA point mutant
JQRM111	2457T*ΔicsAΔipaD::frt*[pIcsA$^{Q148C/G149N}$]	Tet^{R}, Amp^{R}, IcsA point mutant
JQRM112	2457T*ΔicsAΔipaD::frt*[pIcsA$^{m148-149}$-7]	Tet^{R}, Amp^{R}, IcsA point mutant
JQRM113	2457T*ΔicsAΔipaD::frt*[pIcsA$^{m148-149}$-8]	Tet^{R}, Amp^{R}, IcsA point mutant
JQRM114	DH5α[pCDF-Duet::IcsA$^{54::FLAG\times3}$-IcsP]	Spec^{R}, IcsA expression construct
JQRM115	C43(DE3)[pCDF-Duet::IcsA$^{54::FLAG\times3}$-IcsP]	Spec^{R}, IcsA expression strain
JQRM116	TOP10[pMDBAD-*icsA*$^{\Delta 138-148}$]	Amp^{R}, IcsA$^{\Delta 138-148}$ expression strain
JQRM117	DH5α[pIcsA$^{737::FLAG\times3}$]	Amp^{R}, IcsA C-terminal tag construct
JQRM118	2457T*ΔicsAΔipaD::frt*[pIcsA$^{737::FLAG\times3}$]	Tet^{R}, Amp^{R}, IcsA$^{\Delta 138-148}$ C-terminal tag complementation
JQRM119	DH5α[pIcsA $^{\Delta 138-148/737::FLAG\times3}$]	Amp^{R}, IcsA$^{\Delta 138-148}$ C-terminal tag construct
JQRM120	2457T*ΔicsA*[pIcsA$^{737::FLAG\times3}$]	Amp^{R}, IcsA C-terminal tag complementation
JQRM121	2457T*ΔicsA*[pIcsA $^{\Delta 138-148/737::FLAG\times3}$]	Amp^{R}, IcsA$^{\Delta 138-148}$ C-terminal tag complementation
JQRM122	2457T*ΔicsAΔipaD::frt*[pIcsA$^{737::FLAG\times3}$]	Tet^{R}, Amp^{R}, IcsA C-terminal tag complementation
JQRM123	2457T*ΔicsAΔipaD::frt*[pIcsA$^{\Delta 138-148/737::FLAG\times3}$]	Tet^{R}, Amp^{R}, IcsA$^{\Delta 138-148}$ C-terminal tag complementation
JQRM124	2457T*ΔicsAΔrmlD*[pIcsA$^{737::FLAG\times3}$]	Amp^{R}, Kan^{R}, IcsA C-terminal tag complementation
JQRM125	2457T*ΔicsAΔrmlD*[pIcsA$^{\Delta 138-148/737::FLAG\times3}$]	Amp^{R}, Kan^{R}, IcsA$_{\Delta 138-148}$ C-terminal tag complementation
JQRM126	2457T(VP^{-})[pIcsA$_{737::FLAG\times3}$]	Amp^{R}, IcsA C-terminal tag complementation
JQRM127	2457T(VP^{-})[pIcsA$^{\Delta 138-148/737::FLAG\times3}$]	Amp^{R}, IcsA$^{\Delta 138-148}$ C-terminal tag complementation
JQRM128	*S. flexneri* Y(VP^{-})[pIcsA$^{737::FLAG\times3]}$	Amp^{R}, IcsA C-terminal tag complementation
JQRM129	*S. flexneri* Y(VP^{-})[pIcsA$^{\Delta 138-148/737::FLAG\times3}$]	Amp^{R}, IcsA$_{\Delta 138-148}$ C-terminal tag complementation
JQRM130	*S. flexneri* Y*ΔicsA*[pIcsA$^{737::FLAG\times3}$]	Amp^{R}, IcsA C-terminal tag complementation
JQRM131	*S. flexneri* Y*ΔicsA*[pIcsA$^{\Delta 138-148/737::FLAG\times3}$]	Amp^{R}, IcsA$^{\Delta 138-148}$ C-terminal tag complementation
JQRM132	2457T*ΔrmlD*[pKD46]	Amp^{R}, Kan^{R}, mutagenesis strain, 30 °C

JQRM133	2457T*ΔicsAΔrmlD*[pKD46]	Amp^R, Kan^R, mutagenesis strain, 30 °C
JQRM134	2457T*ΔgtrII*[pIcsA$^{737::FLAG\times3}$]	Amp^R, IcsA C-terminal tag complementation
JQRM135	2457T*ΔgtrII*[pIcsA$^{\Delta138\text{-}148/737::FLAG\times3}$]	Amp^R, IcsA$^{\Delta138\text{-}148}$ C-terminal tag complementation
JQRM136	2457T*ΔicsAΔipaD::frt*[pIcsA$^{I138P/737::FLAG\times3}$]	Tet^R, Amp^R, IcsA^{I138P} C-terminal tag complementation
JQRM137	2457T*ΔicsAΔipaD::frt*[pIcsA$^{G140G/S141A/737::FLAG\times3}$]	Tet^R, Amp^R, IcsA$^{G140G/S141A}$ C-terminal tag complementation
JQRM138	2457T*ΔicsAΔipaD::frt*[pIcsA$^{Q148C/G149N/737::FLAG\times3}$]	Tet^R, Amp^R, IcsA$^{Q148C/G149N}$ C-terminal tag complementation
JQRM139	BL21[pIcsA]	Amp^R, IcsA expressing strain for glycan array
JQRM140	BL21[pBR322]	Amp^R, Vector contaol strain for glycan array
JQRM141	2457T*ΔicsAΔipaD::frt*[pIcsA^{138A}]	Tet^R, Amp^R, IcsA alanine scanning strain
JQRM142	2457T*ΔicsAΔipaD::frt*[pIcsA^{139A}]	Tet^R, Amp^R, IcsA alanine scanning strain
JQRM143	2457T*ΔicsAΔipaD::frt*[pIcsA^{140A}]	Tet^R, Amp^R, IcsA alanine scanning strain
JQRM144	2457T*ΔicsAΔipaD::frt*[pIcsA^{141A}]	Tet^R, Amp^R, IcsA alanine scanning strain
JQRM145	2457T*ΔicsAΔipaD::frt*[pIcsA^{142A}]	Tet^R, Amp^R, IcsA alanine scanning strain
JQRM146	2457T*ΔicsAΔipaD::frt*[pIcsA^{143A}]	Tet^R, Amp^R, IcsA alanine scanning strain
JQRM147	2457T*ΔicsAΔipaD::frt*[pIcsA^{144A}]	Tet^R, Amp^R, IcsA alanine scanning strain
JQRM148	2457T*ΔicsAΔipaD::frt*[pIcsA^{145A}]	Tet^R, Amp^R, IcsA alanine scanning strain
JQRM149	2457T*ΔicsAΔipaD::frt*[pIcsA^{146A}]	Tet^R, Amp^R, IcsA alanine scanning strain
JQRM150	2457T*ΔicsAΔipaD::frt*[pIcsA^{147A}]	Tet^R, Amp^R, IcsA alanine scanning strain
JQRM151	2457T*ΔicsAΔipaD::frt*[pIcsA^{148A}]	Tet^R, Amp^R, IcsA alanine scanning strain
JQRM152	2457T*ΔicsAΔipaD::frt*[pIcsA^{149A}]	Tet^R, Amp^R, IcsA alanine scanning strain

Appendix B: Plasmids

Plamids	Description
Lab plasmids used in this thesis	
pKD4	Kanamycin cassette for mutagenesis, (Datsenko & Wanner, 2000)
pKD13	Kanamycin cassette for mutagenesis, (Datsenko & Wanner, 2000)
pKD46	Lambda red recombinase construct, (Datsenko & Wanner, 2000)
pCP20	Yeast recombinase recognising *frt* sequences, (Datsenko & Wanner, 2000)
pIcsA	IcsA expression construct, (Morona & Van Den Bosch, 2003)
pBR322	Vector control (Van den Bosch & Morona, 2003)
pSU23::*icsA*	IcsA expression construct, (Teh & Morona, 2013)
pCDF-Duet	Duet expression vector (Novagen)
pGEM-Teasy	Cloning vector for white and blue screening (Promega)
pGEM-Teasy::*90nts*	Vector control with 90 nucleotides insertion, blue colony (Laboratory stock)
pMDBAD::$icsA_{his12\text{-}52\text{-}740}$	IcsA passenger expression construct (Dr Matthew Doyle)
Plasmids generated in this thesis	
pJQ1	pGEM-Teasy::*ipaD*
pJQ2	pGEM-Teasy::*ipaB*
pJQ3	pIcsA$^{54::his6}$
pJQ4	pCDF-Duet::$icsA^{54::his6}$
pJQ5	pCDF-Duet::$icsA^{54::his6}$-*icsP*
pJQ8	pCDF-Duet::$icsA^{54::his6\text{-}\Delta 138\text{-}148}$-*icsP*
pJQ9	pIcsA$^{\Delta 138\text{-}148}$
pJQ10	pCDF-Duet::$icsA^{54::FLAG\times 3}$-*icsP*
pJQ11	pMDBAD::$icsA^{his12\text{-}53\text{-}740(\Delta 138\text{-}148)}$
pJQ12	pIcsA$^{737::FLAG\times 3}$
pJQ13	pIcsA$^{737::FLAG\times 3(\Delta 138\text{-}148)}$

Appendix C: Oligonucleotides

Oligos	Sequences (5'-3')	Description
JQ1	TATATCCAAGAGCCATAATAATATATGGCTCTTCCTGTAAGGAAATAACCGT GTAGGCTGGAGCTGCTTC	Mutagenesis of *ipaD*, pKD4
JQ2	GCCTTATATAAGAATGTTGGCGCTTGAGTATTATTTACATTATGCATGGCGCA CCGCCATGGTCCATATGAATATCCTCC	Mutagenesis of *ipaD*, pKD4
JQ3	AAAGCACAATCATACTTGGACGCAATTCAGGATATCAAGGAGTAATTATTGT GTAGGCTGGAGCTGCTTC	Mutagenesis of *ipaB*, pKD4
JQ4	TATAAAATCTGGGTTGGTTTTGTGTTTTGAATTTCCATAACATTCTCCTTATTT GTAGCCATGGTCCATATGAATATCCTCC	Mutagenesis of *ipaB*, pKD4
JQ5	ATCCCAAGTATCTAAAGAAGCATCCC	Primer amplifying *ipaD*
JQ6	GAAGTTTGCGAACTATGGATATCGG	Primer amplifying *ipaD*
JQ7	AGTTCCAACAAGCAGCAGACC	Primer amplifying *ipaB*
JQ8	GTGGTTGTTAATACGGGATTTTTACCG	Primer amplifying *ipaB*
JQ9	GCCTTATATAAGAATGTTGGCGCTTGAGTATTATTTACATTATGCATGGCGCA CCATGGGAATTAGCCATGGTCC	Replacement of JQ2
JQ10	TATAAAATCTGGGTTGGTTTTGTGTTTTGAATTTCCATAACATTCTCCTTATTT GTAATGGGAATTAGCCATGGTCC	Replacement of JQ4
JQ11	ATCCAAGAGCCATAATAATATATGGCTCTTCCTGTAAGGAAATAACCATGAT TCCGGGGATCCGTCGACC	Mutagenesis of *ipaD*, pKD13
JQ12	AGTATTATTTACATTATGCATGGCGCACCTCAGAAATGGAGAAAAAGTTTTG TAGGCTGGAGCTGCTTCG	Mutagenesis of *ipaD*, pKD13
JQ13	GCACAATCATACTTGGACGCAATTCAGGATATCAAGGAGTAATTATTATGAT TCCGGGGATCCGTCGACC	Mutagenesis of *ipaB*, pKD13
JQ14	GAATTTCCATAACATTCTCCTTATTTGTATCAAGCAGTAGTTTGTTGCAATGT AGGCTGGAGCTGCTTCG	Mutagenesis of *ipaB*, pKD13
JQ15	GGGCCAATAGCTTTTGCTACTCCTCATCACCATCATCACCACC	His_6 insertion in $IcsA_{54}$
JQ16	TCTGAAAAATGAAGTTCTTGAGTACCCGAAAGGTGGTGATGATGGTGATGA	His_6 insertion in $IcsA_{54}$
JQ17	CTACGACCATGGCTATGAATCAAATTCACAAATTTTTTTGTAATATGACCC	NcoI-ATG-IcsA
JQ18	CTACGAGTCGACTCAGAAGGTATATTTCACACCCAAAATACC	IcsA-SalI
JQ19	CTACGACATATGATGAAATTAAAATTCTTTGTACTTGCAC	NdeI-IcsP
JQ20	CTACGAGGTACCTCAAAAAATATACTTTATACCTGCGG	IcsP-KpnI
JQ21	AATCGAGAATTCGCGGGGGCGGTGGAAGCGGCGGGGGTGGGTCTGGGGGCG GTGGAAGCGATATTATGATTAGCGCAGGTCATGG	EcoRI-$IcsA^{111-170}$

JQ22	AATCGAGAATTCAGCGTAATCTGGAACATCGTATGGGTAGCTTCCACCGCCCCCAACAGCCTCACCACCATCAC	IcsA$^{111-170}$-EcoRI
JQ23	AATCGAGAATTCGCGGGGGCGGTGGAAGCGGCGGGGGTGGGTCTGGGGGCGGTGGAAGCAACAATTCATCCATTCTGAAAATTATCAAC	IcsA$^{351-410}$-EcoRI
JQ24	AATCGAGAATTCAGCGTAATCTGGAACATCGTATGGGTAGCTTCCACCGCCCCCACTACTGATTCCAGCTAAATTTAAAGAAC	IcsA$^{351-410}$-EcoRI
JQ25	GGGCTGGCAAGCCACGTTTGGTG	pGEX sequencing primer
JQ26	CCGGGAGCTGCATGTGTCAGAGG	pGEX sequencing primer
JQ27	AATAGTTGTGGCGGTAATGGTGGTGACTCTNNNNNNGGATCTGACTTGTCTATAATCAATCAAGG	Site-directed mutagenesis primer targeting IcsA$_{138-139}$
JQ28	TGTGGCGGTAATGGTGGTGACTCTATTACCNNNNNNGACTTGTCTATAATCAATCAAGGCATG	Site-directed mutagenesis primer targeting IcsA$_{140-141}$
JQ29	CATGCCTTGATTGATTATAGACAAGTC	Reverse primer of JQ27 & JQ28
JQ30	CGCTACCGCCGCTACCACCAAGAATCAT	Reverse primer of mutagenesis primer 148NNS
JQ31	GGAGTCACCACCATTACCG	IcsA$^{\Delta 138-148}$ deletion, alternative codon to have BspEI
JQ32	GGAATGATTCTTGGTGGTAGCG	IcsA$^{\Delta 138-148}$ deletion, alternative codon to have BspEI
JQ33	CTGAATACCAATAAGTGGTATCTAACTAGTGACTACAAAGACCATGACGGTGATTATAAAGATCATGACATCGATTACAAGGATGACGATGACAAGCAGATGGATAATCAAGAATCAAAACAGATG	GBlock Gene for IcsA$^{737::FLAG\times3}$
JQ34	CTGAATACCAATAAGTGGTATCTAACTAGTGACTACAAAGACCATGACGGTGATTATAAAGATCATGACATCGATTACAAGGATGACG	IcsA$^{737::FLAG\times3}$ FLAG tag addition, overlap extension PCR
JQ35	CATCTGTTTTGATTCTTGATTATCCATCTGCTTGTCATCGTCATCCTTGTAATCGATGTCATGATCTTTATAATCACCGTCATGG	IcsA$^{737::FLAG\times3}$ FLAG tag addition, overlap extension PCR
JQ36	CTCGGGGGGCCAATAGCTTTTGCTACTCCTGACTACAAAGACCATGACGGTGATTATAAAGATCATGACATCGATTACAAGGATGACG	IcsA$^{54::FLAG\times3}$ FLAG tag addition, overlap extension PCR
JQ37	TGAAAAATGAAGTTCTTGAGTACCCGAAAGCTTGTCATCGTCATCCTTGTAATCGATGTCATGATCTTTATAATCACCGTCATGG	IcsA$^{54::FLAG\times3}$ FLAG tag addition, overlap extension PCR
JQ38	CATGACATCGATTACAAGGATGACGATGACAAGCTTTCGGGTACTCAAGAACTTC	IcsA$^{54::FLAG\times3}$ FLAG tag addition, reverse PCR
JQ39	ATCTTTATAATCACCGTCATGGTCTTTGTAGTCAGGAGTAGCAAAAGCTATTGG	IcsA$^{54::FLAG\times3}$ FLAG tag addition, reverse PCR
JQ40	CATGACATCGATTACAAGGATGACGATGACAAGCAGATGGATAATCAAGAATCAAAACAG	IcsA$^{737::FLAG\times3}$ FLAG tag addition, reverse PCR
JQ41	ATCTTTATAATCACCGTCATGGTCTTTGTAGTCACTAGTTAGATACCACTTATTGGTATTC	IcsA$^{737::FLAG\times3}$ FLAG tag addition, reverse PCR
JQ43	AGAGTCACCACCATTACCG	Universal primer for alanine scanning aa 138-149
JQ44	GCTACCGGATCTGACTTGTCTATAATC	Mutagenesis primer, I138A
JQ45	ATTGCTGGATCTGACTTGTCTATAATCAATCAAG	Mutagenesis primer, T139A

JQ46	ATTACCGCTTCTGACTTGTCTATAATCAATCAAGG	Mutagenesis primer, G140A
JQ47	ATTACCGGAGCTGACTTGTCTATAATCAATCAAGGCATG	Mutagenesis primer, S141A
JQ48	ATTACCGGATCTGCTTTGTCTATAATCAATCAAGGCATGATTC	Mutagenesis primer, D142A
JQ49	ATTACCGGATCTGACGCTTCTATAATCAATCAAGGCATGATTCTTG	Mutagenesis primer, L143A
JQ50	ATTACCGGATCTGACTTGGCTATAATCAATCAAGGCATGATTCTTGG	Mutagenesis primer, S144A
JQ51	ATTACCGGATCTGACTTGTCTGCTATCAATCAAGGCATGATTCTTGG	Mutagenesis primer, I145A
JQ52	ATTACCGGATCTGACTTGTCTATAGCTAATCAAGGCATGATTCTTGGTG	Mutagenesis primer, I146A
JQ53	ATTACCGGATCTGACTTGTCTATAATCGCTCAAGGCATGATTCTTGGTGG	Mutagenesis primer, N147A
JQ54	ATTACCGGATCTGACTTGTCTATAATCAATGCTGGCATGATTCTTGGTGGTAG	Mutagenesis primer, Q148A
JQ55	ATTACCGGATCTGACTTGTCTATAATCAATCAAGCTATGATTCTTGGTGGTAG CGG	Mutagenesis primer, G149A
148NNS	ATTACCGGATCTGACTTGTCTATAATCAATNNSNNSATGATTCTTGGTGGTAG CGGCGGTAGCG	Site-directed mutagenesis primer targeting IcsA$^{148\text{-}149}$ (Dr Min Teh)
MD80	TTTTTTCTCGAGGACTCCTCTTTCGGGTACTCAAG	XhoI IcsA^{53} Forward (Dr Matthew Doyle)
MD81	TTTTTTGGTACCTTGATCCATCTGACTAGTTAGATACCAC	KpnI IcsA^{740} Reverse (Dr Matthew Doyle)

Thesis Bibliography

Abdul Khalek, F.J., Gallicano, G.I., and Mishra, L. (2010) Colon cancer stem cells. *Gastrointest Cancer Res*: S16-23.

Ambrosi, C., Pompili, M., Scribano, D., Zagaglia, C., Ripa, S., and Nicoletti, M. (2012) Outer membrane protein A (OmpA): a new player in *Shigella flexneri* protrusion formation and inter-cellular spreading. *PloS one* **7**: e49625.

Amerighi, F., Valeri, M., Donnarumma, D., Maccari, S., Moschioni, M., Taddei, A., Lapazio, L., Pansegrau, W., Buccato, S., De Angelis, G., Ruggiero, P., Masignani, V., Soriani, M., and Pezzicoli, A. (2016) Identification of a monoclonal antibody against pneumococcal pilus 1 ancillary protein impairing bacterial adhesion to human epithelial cells. *J Infect Dis* **213**: 516-522.

Anand, B.S., Malhotra, V., Bhattacharya, S.K., Datta, P., Datta, D., Sen, D., Bhattacharya, M.K., Mukherjee, P.P., and Pal, S.C. (1986) Rectal histology in acute bacillary dysentery. *Gastroenterology* **90**: 654-660.

Arena, E.T., Campbell-Valois, F.X., Tinevez, J.Y., Nigro, G., Sachse, M., Moya-Nilges, M., Nothelfer, K., Marteyn, B., Shorte, S.L., and Sansonetti, P.J. (2015) Bioimage analysis of *Shigella* infection reveals targeting of colonic crypts. *Proc Natl Acad Sci U S A* **112**: E3282-3290.

Arii, J., Goto, H., Suenaga, T., Oyama, M., Kozuka-Hata, H., Imai, T., Minowa, A., Akashi, H., Arase, H., Kawaoka, Y., and Kawaguchi, Y. (2010) Non-muscle myosin IIA is a functional entry receptor for herpes simplex virus-1. *Nature* **467**: 859-862.

Arm, H.G., Floyd, T.M., Faber, J.E., and Hayes, J.R. (1965) Use of ligated segments of rabbit small intestine in experimental shigellosis. *J. Bacteriol* **89**: 803- 809.

Babbin, B.A., Koch, S., Bachar, M., Conti, M.A., Parkos, C.A., Adelstein, R.S., Nusrat, A., and Ivanov, A.I. (2009) Non-muscle myosin IIA differentially regulates intestinal epithelial cell restitution and matrix invasion. *Am J Pathol* **174**: 436-448.

Banish, L.D., Sims, R., Sack, D., Montali, R.J., Phillips, L., Jr., and Bush, M. (1993) Prevalence of shigellosis and other enteric pathogens in a zoologic collection of primates. *J Am Vet Med Assoc* **203**: 126-132.

Bao, J., Jana, S.S., and Adelstein, R.S. (2005) Vertebrate nonmuscle myosin II isoforms rescue small interfering RNA-induced defects in COS-7 cell cytokinesis. *J Biol Chem* **280**: 19594-19599.

Barker, N., van Es, J.H., Kuipers, J., Kujala, P., van den Born, M., Cozijnsen, M., Haegebarth, A., Korving, J., Begthel, H., Peters, P.J., and Clevers, H. (2007) Identification of stem cells in small intestine and colon by marker gene Lgr5. *Nature* **449**: 1003-1007.

Barman, S., Saha, D.R., Ramamurthy, T., and Koley, H. (2011) Development of a new Guinea-pig model of shigellosis. *FEMS Immunol Med Mic* **62**: 304-314.

Barry, E.M., Pasetti, M.F., Sztein, M.B., Fasano, A., Kotloff, K.L., and Levine, M.M. (2013) Progress and pitfalls in *Shigella* vaccine research. *Nat Rev Gastroenterol Hepatol1* **10**: 245-255.

Barta, M.L., Guragain, M., Adam, P., Dickenson, N.E., Patil, M., Geisbrecht, B.V., Picking, W.L., and Picking, W.D. (2012) Identification of the bile salt binding site on IpaD from *Shigella flexneri* and the influence of ligand binding on IpaD structure. *Proteins* **80**: 935-945.

Bartfeld, S., Bayram, T., van de Wetering, M., Huch, M., Begthel, H., Kujala, P., Vries, R., Peters, P.J., and Clevers, H. (2015) *In vitro* expansion of human gastric epithelial stem cells and their responses to bacterial infection. *Gastroenterology* **148**: 126-136 e126.

Bartfeld, S., and Clevers, H. (2015) Organoids as model for infectious diseases: culture of human and murine stomach organoids and microinjection of *Helicobacter pylori*. *J Vis Exp* 53359.

Begley, M., Gahan, C.G.M., and Hill, C. (2005) The interaction between bacteria and bile. *FEMS Microbiol Rev* **29**: 625-651.

Belotserkovsky, I., and Sansonetti, P.J. (2018) *Shigella* and Enteroinvasive *Escherichia Coli*. *Curr Top Microbiol Immunol* **416**: 1-26

Bennish, M.L. (1991) Potentially lethal complications of shigellosis. *Rev Infect Dis* **13**: 319-324.

Benz, I., and Schmidt, M.A. (1992) AIDA-I, the adhesin involved in diffuse adherence of the diarrhoeagenic *Escherichia coli* strain 2787 (O126:H27), is synthesized via a precursor molecule. *Mol Microbiol* **6**: 1539-1546.

Bernard, A.R., Jessop, T.C., Kumar, P., and Dickenson, N.E. (2017) Deoxycholate-enhanced *Shigella* virulence is regulated by a rare pi-helix in the type three secretion system tip protein IpaD. *Biochemistry* **56**: 6503-6514.

Bernardini, M.L., Fontaine, A., and Sansonetti, P.J. (1990) The two-component regulatory system ompR-envZ controls the virulence of *Shigella flexneri*. *J Bacteriol* **172**: 6274-6281.

Bernardini, M.L., Mounier, J., Dhauteville, H., Coquisrondon, M., and Sansonetti, P.J. (1989) Identification of IcsA, a plasmid locus of *Shigella flexneri* that governs bacterial intracellular and intercellular spread through interaction with F-actin. *Proc Natl Acad Sci U S A* **86**: 3867-3871.

Bertani, G. (2004) Lysogeny at mid-twentieth century: P1, P2, and other experimental, systems. *J Microbiol* **186**: 595-600.

Blocker, A., Gounon, P., Larquet, E., Niebuhr, K., Cabiaux, V., Parsot, C., and Sansonetti, P. (1999) The tripartite type III secreton of *Shigella flexneri* inserts IpaB and IpaC into host membranes. *J Cell Biol* **147**: 683-693.

Boullier, S., Tanguy, M., Kadaoui, K.A., Caubet, C., Sansonetti, P., Corthesy, B., and Phalipon, A. (2009) Secretory IgA-mediated neutralization of *Shigella flexneri* prevents intestinal tissue destruction by down-regulating inflammatory circuits. *J Immunol* **183**: 5879-5885.

Bourdet-Sicard, R., Rudiger, M., Jockusch, B.M., Gounon, P., Sansonetti, P.J., and Nhieu, G.T. (1999) Binding of the *Shigella* protein IpaA to vinculin induces F-actin depolymerization. *EMBO J* **18**: 5853-5862.

Bowcutt, R., Forman, R., Glymenaki, M., Carding, S.R., Else, K.J., and Cruickshank, S.M. (2014) Heterogeneity across the murine small and large intestine. *World J Gastroentero* **20**: 15216-15232.

Brandon, L.D., and Goldberg, M.B. (2001) Periplasmic transit and disulfide bond formation of the autotransporter *Shigella* protein IcsA. *J Bacteriol* **183**: 951-958.

Brotcke-Zumsteg, A., Goosmann, C., Brinkmann, V., Morona, R., and Zychlinsky, A. (2014) IcsA is a *Shigella flexneri* adhesin regulated by the type III secretion system and required for pathogenesis. *Cell Host Microbe* **15**: 435-445.

Burton, E.A., Pendergast, A.M., and Aballay, A. (2006) The *Caenorhabditis elegans* ABL-1 tyrosine kinase is required for *Shigella flexneti* pathogenesis. *Appl Environ Microb* **72**: 5043-5051.

Butler, T., Speelman, P., Kabir, I., and Banwell, J. (1986) Colonic dysfunction during shigellosis. *J Infect Dis* **154**: 817-824.

Cairnie, A.B. (1970) Renewal of goblet and Paneth cells in the small intestine. *Cell Tissue Kinet* **3**: 35-45.

Carayol, N., and Nhieu, G.T.V. (2013) Tips and tricks about *Shigella* invasion of epithelial cells. *Curr Opin Microbiol* **16**: 32-37.

Chahales, P., and Thanassi, D.G. (2015) Structure, function, and assembly of adhesive organelles by uropathogenic bacteria. *Microbiol Spectr* **3**.

Charbonneau, M.E., Janvore, J., and Mourez, M. (2009) Autoprocessing of the *Escherichia coli* AIDA-I autotransporter: a new mechanism involving acidic residues in the junction region. *J Biol Chem* **284**: 17340-17351.

Charles, M., Perez, M., Kobil, J.H., and Goldberg, M.B. (2001) Polar targeting of *Shigella* virulence factor IcsA in Enterobacteriacae and *Vibrio*. *Proc Natl Acad Sci U S A* **98**: 9871-9876.

Cheng, H., Merzel, J., and Leblond, C.P. (1969) Renewal of Paneth cells in the small intestine of the mouse. *Am J Anat* **126**: 507-525.

Cheung, M., Shen, D.K., Makino, F., Kato, T., Roehrich, A.D., Martinez-Argudo, I., Walker, M.L., Murillo, I., Liu, X., Pain, M., Brown, J., Frazer, G., Mantell, J., Mina, P., Todd, T., Sessions, R.B., Namba, K., and Blocker, A.J. (2015) Three-dimensional electron microscopy reconstruction and cysteine-mediated crosslinking provide a model of the type III secretion system needle tip complex. *Mol Cell Biol* **95**: 31-50.

Chowers, Y., Kirschner, J., Keller, N., Barshack, I., Bar-Meir, S., Ashkenazi, S., Schneerson, R., Robbins, J., and Passwell, J.H. (2007) O-specific polysaccharide conjugate vaccine-induced antibodies prevent invasion of *Shigella* into Caco-2 cells and may be curative. *Proc Natl Acad Sci U S A* **104**: 2396-2401.

Coron, E., Flamant, M., Aubert, P., Wedel, T., Pedron, T., Letessier, E., Galmiche, J.P., Sansonetti, P.J., and Neunlist, M. (2009) Characterisation of early mucosal and neuronal lesions following *Shigella flexneri* infection in human colon. *PLoS One* **4**: e4713.

Cui, X., Wang, J., Yang, C., Liang, B., Ma, Q., Yi, S., Li, H., Liu, H., Li, P., Wu, Z., Xie, J., Jia, L., Hao, R., Wang, L., Hua, Y., Qiu, S., and Song, H. (2015) Prevalence and antimicrobial resistance of *Shigella flexneri* serotype 2 variant in China. *Front Microbiol* **6**: 435.

Datsenko, K.A., and Wanner, B.L. (2000) One-step inactivation of chromosomal genes in *Escherichia coli* K-12 using PCR products. *Proc Natl Acad Sci U S A* **97**: 6640-6645.

Day, C.J., Tran, E.N., Semchenko, E.A., Tram, G., Hartley-Tassell, L.E., Ng, P.S., King, R.M., Ulanovsky, R., McAtamney, S., Apicella, M.A., Tiralongo, J., Morona, R., Korolik, V., and Jennings, M.P. (2015) Glycan:glycan interactions: High affinity biomolecular interactions that can mediate binding of pathogenic bacteria to host cells. *Proc Natl Acad Sci U S A* **112**: E7266-7275.

DeLaine, B.C., Wu, T., Grassel, C.L., Shimanovich, A., Pasetti, M.F., Levine, M.M., and Barry, E.M. (2016) Characterization of a multicomponent live, attenuated *Shigella flexneri* vaccine. *Pathog Dis* **74**.

Deng, W., Marshall, N.C., Rowland, J.L., McCoy, J.M., Worrall, L.J., Santos, A.S., Strynadka, N.C.J., and Finlay, B.B. (2017) Assembly, structure, function and regulation of type III secretion systems. *Nat. Rev. Microbiol* **15**: 323-337.

Dinari, G., Hale, T.L., Washington, O., and Formal, S.B. (1986) Effect of Guinea pig or monkey colonic mucus on *Shigella* aggregation and invasion of HeLa cells by *Shigella flexneri* 1b and 2a. *Infect Immun* **51**: 975-978.

Domingo Meza-Aguilar, J., Fromme, P., Torres-Larios, A., Mendoza-Hernandez, G., Hernandez-Chinas, U., Arreguin-Espinosa de Los Monteros, R.A., Eslava

Campos, C.A., and Fromme, R. (2014) X-ray crystal structure of the passenger domain of plasmid encoded toxin(Pet), an autotransporter enterotoxin from enteroaggregative *Escherichia coli* (EAEC). *Biochem Biophys Res Commun* **445**: 439-444.

Doyle, M.T., Grabowicz, M., and Morona, R. (2015a) A small conserved motif supports polarity augmentation of *Shigella flexneri* IcsA. *Microbiology* **161**: 2087-2097.

Doyle, M.T., Tran, E.N., and Morona, R. (2015b) The passenger-associated transport repeat promotes virulence factor secretion efficiency and delineates a distinct autotransporter subtype. *Mol Microbiol* **97**: 315-329.

Du, J., Reeves, A.Z., Klein, J.A., Twedt, D.J., Knodler, L.A., and Lesser, C.F. (2016) The type III secretion system apparatus determines the intracellular niche of bacterial pathogens. *Proc Natl Acad Sci U S A* **113**: 4794-4799.

Egile, C., Loisel, T.P., Laurent, V., Li, R., Pantaloni, D., Sansonetti, P.J., and Carlier, M.F. (1999) Activation of the CDC42 effector N-WASP by the *Shigella flexneri* IcsA protein promotes actin nucleation by Arp2/3 complex and bacterial actin-based motility. *J Cell Biol* **146**: 1319-1332.

Eilers, B., Mayer-Scholl, A., Walker, T., Tang, C., Weinrauch, Y., and Zychlinsky, A. (2010) Neutrophil antimicrobial proteins enhance *Shigella flexneri* adhesion and invasion. *Cell Microbiol* **12**: 1134-1143.

Emsley, P., Charles, I.G., Fairweather, N.F., and Isaacs, N.W. (1996) Structure of *Bordetella pertussis* virulence factor P.69 pertactin. *Nature* **381**: 90-92.

Etheridge, M.E., Hoque, A.T., and Sack, D.A. (1996) Pathologic study of a rabbit model for shigellosis. *Lab Anim Sci* **46**: 61-66.

Faherty, C.S., Redman, J.C., Rasko, D.A., Barry, E.M., and Nataro, J.P. (2012) *Shigella flexneri* effectors OspE1 and OspE2 mediate induced adherence to the colonic epithelium following bile salts exposure. *Mol Microbiol* **85**: 107-121.

Fernandez, M.I., Regnault, B., Mulet, C., Tanguy, M., Jay, P., Sansonetti, P.J., and Pedron, T. (2008) Maturation of Paneth cells induces the refractory state of newborn mice to *Shigella* infection. *J Immunol* **180**: 4924-4930.

Fernandez, M.I., Thuizat, A., Pedron, T., Neutra, M., Phalipon, A., and Sansonetti, P.J. (2003) A newborn mouse model for the study of intestinal pathogenesis of shigellosis. *Cell Microbiol* **5**: 481-491.

Ferreccio, C., Prado, V., Ojeda, A., Cayyazo, M., Abrego, P., Guers, L., and Levine, M.M. (1991) Epidemiologic patterns of acute diarrhea and endemic *Shigella* infections in children in a poor periurban setting in Santiago, Chile. *Am J Epidemiol* **134**: 614-627.

Fiorentino, M., Levine, M.M., Sztein, M.B., and Fasano, A. (2014) Effect of wild-type *Shigella* species and attenuated *Shigella* vaccine candidates on small intestinal barrier function, antigen trafficking, and cytokine release. *PloS one* **9**: e85211.

Fixen, K.R., Janakiraman, A., Garrity, S., Slade, D.J., Gray, A.N., Karahan, N., Hochschild, A., and Goldberg, M.B. (2012) Genetic reporter system for positioning of proteins at the bacterial pole. *MBio* **3**: e00251-11

Forbester, J.L., Goulding, D., Vallier, L., Hannan, N., Hale, C., Pickard, D., Mukhopadhyay, S., and Dougan, G. (2015) Interaction of *Salmonella enterica* serovar Typhimurium with intestinal organoids derived from human induced pluripotent stem cells. *Infect Immun* **83**: 2926-2934.

Formal, S.B., Dammin, G.J., Labrec, E.H., and Schneider, H. (1958) Experimental *Shigella* infections: characteristics of a fatal infection produced in Guinea pigs. *J Bacteriol* **75**: 604-610.

Formal, S.B., Hale, T.L., Kapfer, C., Cogan, J.P., Snoy, P.J., Chung, R., Wingfield, M.E., Elisberg, B.L., and Baron, L.S. (1984) Oral vaccination of monkeys with an invasive *Escherichia coli* K-12 hybrid expressing *Shigella flexneri* 2a somatic antigen. *Infect Immun* **46**: 465-469.

Formal, S.B., Kent, T.H., Austin, S., and Labrec, E.H. (1966) Fluorescent-antibody and histological study of vaccinated and control monkeys challenged with *Shigella flexneri*. *J Bacteriol* **91**: 2368-2376.

Foster, J.W. (2004) *Escherichia coli* acid resistance: tales of an amateur acidophile. *Nat Rev Microbio* **2**: 898-907.

Fu, Z., Thorpe, M., Akula, S., Chahal, G., and Hellman, L.T. (2018) Extended cleavage specificity of human neutrophil elastase, human proteinase 3, and their distant ortholog clawed frog PR3-three elastases with similar primary but different extended specificities and stability. *Front Immunol* **9**: 2387.

Fujimura, Y., Hosobe, M., and Kihara, T. (1992) Ultrastructural study of M cells from colonic lymphoid nodules obtained by colonoscopic biopsy. *Dig Dis Sci* **37**: 1089-1098.

Fukumatsu, M., Ogawa, M., Arakawa, S., Suzuki, M., Nakayama, K., Shimizu, S., Kim, M., Mimuro, H., and Sasakawa, C. (2012) *Shigella* targets epithelial tricellular junctions and uses a noncanonical clathrin-dependent endocytic pathway to spread between cells. *Cell Host Microbe* **11**: 325-336.

Gangwer, K.A., Mushrush, D.J., Stauff, D.L., Spiller, B., McClain, M.S., Cover, T.L., and Lacy, D.B. (2007) Crystal structure of the *Helicobacter pylori* vacuolating toxin p55 domain. *Proc Natl Acad Sci U S A* **104**: 16293-16298.

Gardner, M.B., and Luciw, P.A. (2008) Macaque models of human infectious disease. *ILAR J* **49**: 220-255.

Gebert, A., Fassbender, S., Werner, K., and Weissferdt, A. (1999) The development of M cells in Peyer's patches is restricted to specialized dome-associated crypts. *Am J Pathol* **154**: 1573-1582.

George, D.T., Behm, C.A., Hall, D.H., Mathesius, U., Rug, M., Nguyen, K.C.Q., and Verma, N.K. (2014) *Shigella flexneri* infection in *Caenorhabditis elegans*: cytopathological examination and identification of host responses. *PloS one* **9**: e106085

Girardin, S.E., Tournebize, R., Mavris, M., Page, A.L., Li, X., Stark, G.R., Bertin, J., DiStefano, P.S., Yaniv, M., Sansonetti, P.J., and Philpott, D.J. (2001) CARD4/Nod1 mediates NF-kappaB and JNK activation by invasive *Shigella flexneri*. *EMBO Rep* **2**: 736-742.

Goldberg, M.B., Barzu, O., Parsot, C., and Sansonetti, P.J. (1993) Unipolar localization and ATPase activity of IcsA, a *Shigella flexneri* protein involved in intracellular movement. *Infect Agents Dis* **2**: 210-211.

Goldberg, M.B., and Theriot, J.A. (1995) *Shigella flexneri* surface protein IcsA is sufficient to direct actin-based motility. *Proc Natl Acad Sci U S A* **92**: 6572-6576.

Good, R.C., May, B.D., and Kawatomari, T. (1969) Enteric pathogens in monkeys. *J Bacteriol* **97**: 1048-1055.

Gorden, J., and Small, P.L. (1993) Acid resistance in enteric bacteria. *Infect Immun* **61**: 364-367.

Gray, A.N., Li, Z.P., Henderson-Frost, J., and Goldberg, M.B. (2014) Biogenesis of YidC cytoplasmic membrane substrates is required for positioning of autotransporter IcsA at future poles. *J Bacteriol* **196**: 624-632.

Gregory, M., Kaminski, R.W., Lugo-Roman, L.A., Galvez Carrillo, H., Tilley, D.H., Baldeviano, C., Simons, M.P., Reynolds, N.D., Ranallo, R.T., Suvarnapunya, A.E., Venkatesan, M.M., and Oaks, E.V. (2014) Development of an Aotus nancymaae model for *Shigella* Vaccine immunogenicity and efficacy studies. *Infect Immun* **82**: 2027-2036.

Gunawardene, A.R., Corfe, B.M., and Staton, C.A. (2011) Classification and functions of enteroendocrine cells of the lower gastrointestinal tract. *Int J Exp Pathol* **92**: 219-231.

Gupta, S., and Chowdhury, R. (1997) Bile affects production of virulence factors and motility of *Vibrio cholerae*. *Infect Immun* **65**: 1131-1134.

Gutierrez-Jimenez, J., Arciniega, I., and Navarro-Garcia, F. (2008) The serine protease motif of Pic mediates a dose-dependent mucolytic activity after binding to sugar constituents of the mucin substrate. *Microb Pathog* **45**: 115-123.

Hagan, C.L., Silhavy, T.J., and Kahne, D. (2011) Beta-Barrel membrane protein assembly by the Bam complex. *Annu Rev Biochem* **80**: 189-210.

Hayward, R.D., Cain, R.J., McGhie, E.J., Phillips, N., Garner, M.J., and Koronakis, V. (2005) Cholesterol binding by the bacterial type III translocon is essential for virulence effector delivery into mammalian cells. *Mol Microbiol* **56**: 590-603.

Headley, V.L., and Payne, S.M. (1990) Differential protein expression by *Shigella flexneri* in intracellular and extracellular environments. *Proc Natl Acad Sci U S A* **87**: 4179-4183.

Henderson, I.R., and Owen, P. (1999) The major phase-variable outer membrane protein of *Escherichia coli* structurally resembles the immunoglobulin A1 protease class of exported protein and is regulated by a novel mechanism involving Dam and oxyR. *J Bacteriol* **181**: 2132-2141.

Heras, B., Totsika, M., Peters, K.M., Paxman, J.J., Gee, C.L., Jarrott, R.J., Perugini, M.A., Whitten, A.E., and Schembri, M.A. (2014) The antigen 43 structure reveals a molecular Velcro-like mechanism of autotransporter-mediated bacterial clumping. *Proc Natl Acad Sci U S A* **111**: 457-462.

High, N., Mounier, J., Prevost, M.C., and Sansonetti, P.J. (1992) Ipab of *Shigella flexneri* causes entry into epithelial cells and escape from the phagocytic vacuole. *EMBO J* **11**: 1991-1999.

Holt, K.E., Thieu Nga, T.V., Thanh, D.P., Vinh, H., Kim, D.W., Vu Tra, M.P., Campbell, J.I., Hoang, N.V., Vinh, N.T., Minh, P.V., Thuy, C.T., Nga, T.T., Thompson, C., Dung, T.T., Nhu, N.T., Vinh, P.V., Tuyet, P.T., Phuc, H.L., Lien, N.T., Phu, B.D., Ai, N.T., Tien, N.M., Dong, N., Parry, C.M., Hien, T.T., Farrar, J.J., Parkhill, J., Dougan, G., Thomson, N.R., and Baker, S. (2013) Tracking the establishment of local endemic populations of an emergent enteric pathogen. *Proc Natl Acad Sci U S A* **110**: 17522-17527.

Inoue, H., Nojima, H., and Okayama, H. (1990) High efficiency transformation of *Escherichia coli* with plasmids. *Gene* **96**: 23-28.

Islam, D., Ruamsap, N., Khantapura, P., Aksomboon, A., Srijan, A., Wongstitwilairoong, B., Bodhidatta, L., Gettayacamin, M., Venkatesan, M.M., and Mason, C.J. (2014) Evaluation of an intragastric challenge model for *Shigella dysenteriae* 1 in rhesus monkeys (Macaca mulatta) for the pre-clinical assessment of *Shigella* vaccine formulations. *APMIS* **122**: 463-475.

Izhar, M., Nuchamowitz, Y., and Mirelman, D. (1982) Adherence of *Shigella flexneri* to Guinea pig intestinal cells is mediated by a mucosal adhesion. *Infect Immun* **35**: 1110-1118.

Jacques, M. (1996) Role of lipo-oligosaccharides and lipopolysaccharides in bacterial adherence. *Trends Microbiol* **4**: 408-409.

Jekow, P., Behlke, J., Tichelaar, W., Lurz, R., Regalla, M., Hinrichs, W., and Tavares, P. (1999) Effect of the ionic environment on the molecular structure of bacteriophage SPP1 portal protein. *Eur J Biochem* **264**: 724-735.

Jennison, A.V., Raqib, R., and Verma, N.K. (2006) Immunoproteome analysis of soluble and membrane proteins of *Shigella flexneri* 2457T. *World J Gastroenterol* **12**: 6683-6688.

Jennison, A.V., and Verma, N.K. (2007) The acid-resistance pathways of *Shigella flexneri* 2457T. *Microbiology* **153**: 2593-2602.

Johnson, T.A., Qiu, J., Plaut, A.G., and Holyoak, T. (2009) Active-site gating regulates substrate selectivity in a chymotrypsin-like serine protease the structure of *Haemophilus influenzae* immunoglobulin A1 protease. *J Mol Biol* **389**: 559-574.

Karnell, A., Cam, P.D., Verma, N., and Lindberg, A.A. (1993) AroD deletion attenuates *Shigella flexneri* strain 2457T and makes it a safe and efficacious oral vaccine in monkeys. *Vaccine* **11**: 830-836.

Kaur, K., Chatterjee, S., and De Guzman, R.N. (2016) Characterization of the *Shigella* and *Salmonella* type III secretion system tip-translocon protein-protein interaction by paramagnetic relaxation enhancement. *Chembiochem* **17**: 745-752.

Kayath, C.A., Hussey, S., El hajjami, N., Nagra, K., Philpott, D., and Allaoui, A. (2010) Escape of intracellular *Shigella* from autophagy requires binding to cholesterol through the type III effector, IcsB. *Microbes Infect* **12**: 956-966.

Kent, T.H., Formal, S.B., LaBrec, E.H., Sprinz, H., and Maenza, R.M. (1967) Gastric shigellosis in rhesus monkeys. *Am J Pathol* **51**: 259-267.

Khaghani, S., Shamsizadeh, A., Nikfar, R., and Hesami, A. (2014) *Shigella flexneri*: a three-year antimicrobial resistance monitoring of isolates in a Children Hospital, Ahvaz, Iran. *Iran J Microbiol* **6**: 225-229.

Khalil, I.A., Troeger, T., and Blacker, B.F. (2018) Morbidity and mortality due to *shigella* and enterotoxigenic *Escherichia coli* diarrhoea: the Global Burden of Disease Study 1990-2016. *Lancet Infect Dis* **18**: 1305-1305.

Koestler, B.J., Fisher, C.R., and Payne, S.M. (2018a) Formate promotes *Shigella* intercellular spread and virulence gene expression. *MBio* **9**: e01777-18.

Koestler, B.J., Ward, C.M., Fisher, C.R., Rajan, A., Maresso, A.W., and Payne, S.M. (2019) Human intestinal enteroids as a model system of *Shigella* pathogenesis. *Infect Immun* **87**: e00733-18.

Koestler, B.J., Ward, C.M., and Payne, S.M. (2018b) *Shigella* pathogenesis modeling with tissue culture assays. *Curr Protoc Microbiol* **50**: e57.

Koseoglu, V.K., and Agaisse, H. (2019) Evolutionary perspectives on the moonlighting functions of bacterial factors that support actin-based motility. *MBio* **10**: e01520-19.

Koseoglu, V.K., Hall, C.P., Rodriguez-Lopez, E.M., and Agaisse, H. (2019) The autotransporter IcsA promotes *Shigella flexneri* biofilm formation in the presence of bile salts. *Infect Immun* **87**: e00861-00818.

Kotloff, K.L., Nataro, J.P., Blackwelder, W.C., Nasrin, D., Farag, T.H., Panchalingam, S., Wu, Y., Sow, S.O., Sur, D., Breiman, R.F., Faruque, A.S., Zaidi, A.K., Saha, D., Alonso, P.L., Tamboura, B., Sanogo, D., Onwuchekwa, U., Manna, B., Ramamurthy, T., Kanungo, S., Ochieng, J.B., Omore, R., Oundo, J.O., Hossain, A., Das, S.K., Ahmed, S., Qureshi, S., Quadri, F., Adegbola, R.A., Antonio, M., Hossain, M.J., Akinsola, A., Mandomando, I., Nhampossa, T., Acacio, S., Biswas, K., O'Reilly, C.E., Mintz, E.D., Berkeley, L.Y., Muhsen, K., Sommerfelt, H., Robins-Browne, R.M., and Levine, M.M. (2013) Burden and aetiology of diarrhoeal disease in infants and young children in developing countries (the Global Enteric Multicenter Study, GEMS): a prospective, case-control study. *Lancet* **382**: 209-222.

Kotloff, K.L., Noriega, F., Losonsky, G.A., Sztein, M.B., Wasserman, S.S., Nataro, J.P., and Levine, M.M. (1996) Safety, immunogenicity, and transmissibility in humans of CVD 1203, a live oral *Shigella flexneri* 2a vaccine candidate attenuated by deletions in aroA and virG. *Infect Immun* **64**: 4542-4548.

Kotloff, K.L., Riddle, M.S., Platts-Mills, J.A., Pavlinac, P., and Zaidi, A.K.M. (2018) Shigellosis. *Lancet* **391**: 801-812.

Kozyreva, V.K., Jospin, G., Greninger, A.L., Watt, J.P., Eisen, J.A., and Chaturvedi, V. (2016) Recent outbreaks of shigellosis in California caused by two distinct populations of *Shigella sonnei* with either increased virulence or fluoroquinolone resistance. *Msphere* **1**: e00344-16.

Krukonis, E.S., and DiRita, V.J. (2003) From motility to virulence: Sensing and responding to environmental signals in *Vibrio cholerae*. *Curr Opin Microbiol* **6**: 186-190.

Kuhnel, K., and Diezmann, D. (2011) Crystal structure of the autochaperone region from the *Shigella flexneri* autotransporter IcsA. *J Bacteriol* **193**: 2042-2045.

Laarmann, S., and Schmidt, M.A. (2003) The *Escherichia coli* AIDA autotransporter adhesin recognizes an integral membrane glycoprotein as receptor. *Microbiology* **149**: 1871-1882.

Labrec, E.H., Schneider, H., Magnani, T.J., and Formal, S.B. (1964) Epithelial cell penetration as an essential step in the pathogenesis of bacillary dysentery. *J Bacteriol* **88**: 1503-1518.

Lafont, F., Tran Van Nhieu, G., Hanada, K., Sansonetti, P., and van der Goot, F.G. (2002) Initial steps of *Shigella* infection depend on the cholesterol/sphingolipid raft-mediated CD44-IpaB interaction. *EMBO J* **21**: 4449-4457.

Lam, P.W., and Bunce, P.E. (2015) A 65-year-old HIV-positive man with acute diarrhea. *CMAJ* **187**: 1153-1154.

Lee, J.L., and Streuli, C.H. (2014) Integrins and epithelial cell polarity. *J Cell Sci* **127**: 3217-3225.

Lett, M.C., Sasakawa, C., Okada, N., Sakai, T., Makino, S., Yamada, M., Komatsu, K., and Yoshikawa, M. (1989) virG, a plasmid-coded virulence gene of *Shigella flexneri*: identification of the virG protein and determination of the complete coding sequence. *J Bacteriol* **171**: 353-359.

Leupold, S., Busing, P., Mas, P.J., Hart, D.J., and Scrima, A. (2017) Structural insights into the architecture of the *Shigella flexneri* virulence factor IcsA/VirG and motifs involved in polar distribution and secretion. *J Struct Biol* **198**: 19-27.

Levine, M.M., DuPont, H.L., Formal, S.B., Hornick, R.B., Takeuchi, A., Gangarosa, E.J., Snyder, M.J., and Libonati, J.P. (1973) Pathogenesis of *Shigella dysenteriae* 1 (Shiga) dysentery. *J Infect Dis* **127**: 261-270.

Levine, M.M., Kotloff, K.L., Barry, E.M., Pasetti, M.F., and Sztein, M.B. (2007) Clinical trials of *Shigella* vaccines: two steps forward and one step back on a long, hard road. *Nat Rev Microbiol* **5**: 540-553.

Leyton, D.L., Rossiter, A.E., and Henderson, I.R. (2012) From self sufficiency to dependence: mechanisms and factors important for autotransporter biogenesis. *Nat Rev Microbiol* **10**: 213-225.

Liechty, K.W., Schibler, K.R., Ohls, R.K., Perkins, S.L., and Christensen, R.D. (1993) The failure of newborn mice infected with *Escherichia coli* to accelerate neutrophil production correlates with their failure to increase transcripts for granulocyte colony-stimulating factor and interleukin-6. *Biol Neonate* **64**: 331-340.

Lievin-Le Moal, V., and Servin, A.L. (2013) Pathogenesis of human enterovirulent bacteria: lessons from cultured, fully differentiated human colon cancer cell lines. *Microbiol Mol Biol Rev* **77**: 380-439.

Lindenthal, C., and Elsinghorst, E.A. (1999) Identification of a glycoprotein produced by enterotoxigenic *Escherichia coli*. *Infect Immun* **67**: 4084-4091.

Longet, S., Vonarburg, C., Lotscher, M., Miescher, S., Zuercher, A., and Corthesy, B. (2014) Reconstituted human polyclonal plasma-derived secretory-like IgM and IgA maintain the barrier function of epithelial cells infected with an enteropathogen. *J Biol Chem* **289**: 21617-21626.

Lu, Q., Yao, Q., Xu, Y., Li, L., Li, S., Liu, Y., Gao, W., Niu, M., Sharon, M., Ben-Nissan, G., Zamyatina, A., Liu, X., Chen, S., and Shao, F. (2014) An iron-containing dodecameric heptosyltransferase family modifies bacterial autotransporters in pathogenesis. *Cell Host Microbe* **16**: 351-363.

Lugtenberg, B., Meijers, J., Peters, R., van der Hoek, P., and van Alphen, L. (1975) Electrophoretic resolution of the ‘major outer membrane protein’ of *Escherichia coli* K12 into four bands. *FEBS Lett* **58**: 254-258.

Lum, M., and Morona, R. (2014a) Dynamin-related protein Drp1 and mitochondria are important for *Shigella flexneri* infection. *Int J Med Microbiol* **304**: 530-541.

Lum, M., and Morona, R. (2014b) Myosin IIA is essential for *Shigella flexneri* cell-to-cell spread. *Pathog Dis* **72**: 174-187.

Mabbott, N.A., Donaldson, D.S., Ohno, H., Williams, I.R., and Mahajan, A. (2013) Microfold (M) cells: important immunosurveillance posts in the intestinal epithelium. *Mucosal Immunol* **6**: 666-677.

Magdalena, J., and Goldberg, M.B. (2002) Quantification of *Shigella* IcsA required for bacterial actin polymerization. *Cell Motil Cytoskel* **51**: 187-196.

Mahmoud, R.Y., Stones, D.H., Li, W.Q., Emara, M., El-Domany, R.A., Wang, D.P., Wang, Y.L., Krachler, A.M., and Yu, J. (2016) The multivalent adhesion molecule SSO1327 plays a key role in *Shigella sonnei* pathogenesis. *Mol Microbiol* **99**: 658-673.

Makino, S., Sasakawa, C., Kamata, K., Kurata, T., and Yoshikawa, M. (1986) A genetic determinant required for continuous reinfection of adjacent cells on large plasmid in *S. flexneri* 2a. *Cell* **46**: 551-555.

Maldonado-Contreras, A., Birtley, J.R., Boll, E., Zhao, Y., Mumy, K.L., Toscano, J., Ayehunie, S., Reinecker, H.C., Stern, L.J., and McCormick, B.A. (2017) *Shigella* depends on SepA to destabilize the intestinal epithelial integrity via cofilin activation. *Gut Microbes* **8:** 544-560.

Mallett, C.P., VanDeVerg, L., Collins, H.H., and Hale, T.L. (1993) Evaluation of *Shigella* vaccine safety and efficacy in an intranasally challenged mouse model. *Vaccine* **11**: 190-196.

Mani, S., Wierzba, T., and Walker, R.I. (2016) Status of vaccine research and development for *Shigella*. *Vaccine* **34**: 2887-2894.

Marteyn, B., West, N.P., Browning, D.F., Cole, J.A., Shaw, J.G., Palm, F., Mounier, J., Prevost, M.C., Sansonetti, P., and Tang, C.M. (2010) Modulation of *Shigella* virulence in response to available oxygen in vivo. *Nature* **465**: 355-358.

Martinic, M., Hoare, A., Contreras, I., and Alvarez, S.A. (2011) Contribution of the lipopolysaccharide to resistance of *Shigella flexneri* 2a to extreme acidity. *PloS one* **6**: e25557.

Mathan, M.M., and Mathan, V.I. (1986) Ultrastructural pathology of the rectal mucosa in *Shigella dysentery*. *Am J Pathol* **123**: 25-38.

Mathias, A., Longet, S., and Corthesy, B. (2013) Agglutinating secretory IgA preserves intestinal epithelial cell integrity during apical infection by *Shigella flexneri*. *Infect Immun* **81**: 3027-3034.

Mattock, E., and Blocker, A.J. (2017) How do the virulence factors of *Shigella* work together to cause disease? *Front Cell Infect Microbiol* **7**: 64.

Maurelli, A.T., Blackmon, B., and Curtiss, R., 3rd (1984) Temperature-dependent expression of virulence genes in *Shigella* species. *Infect Immun* **43**: 195-201.

Maurelli, A.T., Routh, P.R., Dillman, R.C., Ficken, M.D., Weinstock, D.M., Almond, G.W., and Orndorff, P.E. (1998) *Shigella* infection as observed in the experimentally inoculated domestic pig, Sus scrofa domestica. *Microb Pathog* **25**: 189-196.

Mauricio, R.P., Jeffries, C.M., Svergun, D.I., and Deane, J.E. (2017) The *Shigella* virulence factor IcsA relieves N-WASP autoinhibition by displacing the verprolin homology/cofilin/acidic (VCA) domain. *J Biol Chem* **292**: 134-145.

May, K.L., Grabowicz, M., Polyak, S.W., and Morona, R. (2012) Self-association of the *Shigella flexneri* IcsA autotransporter protein. *Microbiology* **158**: 1874-1883.

May, K.L., and Morona, R. (2008) Mutagenesis of the *Shigella flexneri* autotransporter IcsA reveals novel functional regions involved in IcsA biogenesis and recruitment of host neural Wiscott-Aldrich syndrome protein. *J Bacteriol* **190**: 4666-4676.

McCormick, B.A., Siber, A.M., and Maurelli, A.T. (1998) Requirement of the *Shigella flexneri* virulence plasmid in the ability to induce trafficking of neutrophils across polarized monolayers of the intestinal epithelium. *Infect Immun* **66**: 4237-4243.

McCracken, K.W., Cata, E.M., Crawford, C.M., Sinagoga, K.L., Schumacher, M., Rockich, B.E., Tsai, Y.H., Mayhew, C.N., Spence, J.R., Zavros, Y., and Wells, J.M. (2014) Modelling human development and disease in pluripotent stem-cell-derived gastric organoids. *Nature* **516**: 400-404.

McGuckin, M.A., Linden, S.K., Sutton, P., and Florin, T.H. (2011) Mucin dynamics and enteric pathogens. *Nat Rev Microbiol* **9**: 265-278.

Medeiros, P.Q.S., Ledwaba, S.E., Bolick, D.T., Giallourou, N., Yum, L.K., Costa, D.V.S., Oria, R.B., Barry, E.M., Swann, J.R., Lima, A.A.M., Agaisse, H., and Guerrant, R.L. (2019) A murine model of diarrhea, growth impairment and metabolic disturbances with *Shigella flexneri* infection and the role of zinc deficiency. *Gut Microbes* **10**: 615-630.

Menard, R., Sansonetti, P., and Parsot, C. (1994) The secretion of the *Shigella flexneri* Ipa invasins is activated by epithelial cells and controlled by IpaB and IpaD. *The EMBO J* **13**: 5293-5302.

Menard, R., Sansonetti, P.J., and Parsot, C. (1993) Nonpolar mutagenesis of the ipa genes defines IpaB, IpaC, and IpaD as effectors of *Shigella flexneri* entry into epithelial cells. *J Bacteriol* **175**: 5899-5906.

Meng, G., Spahich, N., Kenjale, R., Waksman, G., and St Geme, J.W., 3rd (2011) Crystal structure of the *Haemophilus influenzae* Hap adhesin reveals an intercellular oligomerization mechanism for bacterial aggregation. *EMBO J* **30**: 3864-3874.

Merzel, J., and Leblond, C.P. (1969) Origin and renewal of goblet cells in the epithelium of the mouse small intestine. *Am J Anat* **124**: 281-305.

Mestas, J., and Hughes, C.C. (2004) Of mice and not men: differences between mouse and human immunology. *J Immunol* **172**: 2731-2738.

Morona, R., Daniels, C., and Van Den Bosch, L. (2003) Genetic modulation of *Shigella flexneri* 2a lipopolysaccharide O antigen modal chain length reveals that it has been optimized for virulence. *Microbiology* **149**: 925-939.

Morona, R., and Van Den Bosch, L. (2003) Multicopy icsA is able to suppress the virulence defect caused by wzz(SF) mutation in the *Shigella flexneri*. *FEMS Microbiol Lett* **221**: 213-219.

Mostowy, S., Boucontet, L., Mazon Moya, M.J., Sirianni, A., Boudinot, P., Hollinshead, M., Cossart, P., Herbomel, P., Levraud, J.P., and Colucci-Guyon, E. (2013) The zebrafish as a new model for the in vivo study of *Shigella flexneri* interaction with phagocytes and bacterial autophagy. *PLoS Pathog* **9**: e1003588.

Mounier, J., Vasselon, T., Hellio, R., Lesourd, M., and Sansonetti, P.J. (1992) *Shigella flexneri* enters human colonic Caco-2 epithelial cells through the basolateral pole. *Infect Immun* **60**: 237-248.

Murillo, I., Martinez-Argudo, I., and Blocker, A.J. (2016) Genetic dissection of the signaling cascade that controls activation of the *Shigella* type III secretion system from the needle tip. *Sci Rep* **6**: 27649.

Murray, G.L., Attridge, S.R., and Morona, R. (2003) Regulation of *Salmonella typhimurium* lipopolysaccharide O antigen chain length is required for virulence; identification of FepE as a second Wzz. *Mol Microbiol* **47**: 1395-1406.

Neame, S.J., and Isacke, C.M. (1993) The cytoplasmic tail of CD44 is required for basolateral localization in epithelial MDCK cells but does not mediate association with the detergent-insoluble cytoskeleton of fibroblasts. *J Cell Biol* **121**: 1299-1310.

Niu, C., Yang, J., Liu, H.S., Cui, Y., Xu, H.J., Wang, R.F., Liu, X.K., Feng, E.L., Wang, D.S., Pan, C., Xiao, W., Liu, X.Q., Zhu, L., and Wang, H.L. (2017) Role of the virulence plasmid in acid resistance of *Shigella flexneri*. *Sci Rep* **7**: 46465

Niyogi, S.K. (2005) Shigellosis. *Microbiology* **43**: 133-143.

Nutten, S., Sansonetti, P., Huet, G., Bourdon-Bisiaux, C., Meresse, B., Colombel, J.F., and Desreumaux, P. (2002) Epithelial inflammation response induced by *Shigella flexneri* depends on mucin gene expression. *Microbes Infect* **4**: 1121-1124.

Oaks, E.V., Hale, T.L., and Formal, S.B. (1986) Serum immune response to *Shigella* protein antigens in rhesus monkeys and humans infected with *Shigella spp*. *Infect Immun* **53**: 57-63.

Ogawa, M., Yoshimori, T., Suzuki, T., Sagara, H., Mizushima, N., and Sasakawa, C. (2005) Escape of intracellular *Shigella* from autophagy. *Science* **307**: 727-731.

Olive, A.J., Kenjale, R., Espina, M., Moore, D.S., Picking, W.L., and Picking, W.D. (2007) Bile salts stimulate recruitment of IpaB to the *Shigella flexneri* surface, where it colocalizes with IpaD at the tip of the type III secretion needle. *Infect Immun* **75**: 2626-2629.

Otto, B.R., Sijbrandi, R., Luirink, J., Oudega, B., Heddle, J.G., Mizutani, K., Park, S.Y., and Tame, J.R. (2005) Crystal structure of hemoglobin protease, a heme binding autotransporter protein from pathogenic *Escherichia coli*. *J Biol Chem* **280**: 17339-17345.

Papayannopoulos, V., Co, C., Prehoda, K.E., Snapper, S., Taunton, J., and Lim, W.A. (2005) A polybasic motif allows N-WASP to act as a sensor of PIP(2) density. *Mol Cell* **17**: 181-191.

Perdomo, J.J., Gounon, P., and Sansonetti, P.J. (1994a) Polymorphonuclear leukocyte transmigration promotes invasion of colonic epithelial monolayer by *Shigella flexneri*. *J Clin Invest* **93**: 633-643.

Perdomo, O.J., Cavaillon, J.M., Huerre, M., Ohayon, H., Gounon, P., and Sansonetti, P.J. (1994b) Acute inflammation causes epithelial invasion and mucosal destruction in experimental shigellosis. *J Exp Med* **180**: 1307-1319.

Perez-Zsolt, D., Erkizia, I., Pino, M., Garcia-Gallo, M., Martin, M.T., Benet, S., Chojnacki, J., Fernandez-Figueras, M.T., Guerrero, D., Urrea, V., Muniz-Trabudua, X., Kremer, L., Martinez-Picado, J., and Izquierdo-Useros, N. (2019) Anti-Siglec-1 antibodies block Ebola viral uptake and decrease cytoplasmic viral entry. *Nat Microbiol* **4**: 1558-1570.

Pettersen, E.F., Goddard, T.D., Huang, C.C., Couch, G.S., Greenblatt, D.M., Meng, E.C., and Ferrin, T.E. (2004) UCSF Chimera--a visualization system for exploratory research and analysis. *J Comput Chem* **25**: 1605-1612.

Philpott, D.J., Yamaoka, S.F., Israel, A., and Sansonetti, P.J. (2000) Invasive *Shigella flexneri* activates NF-kappa B through a lipopolysaccharide-dependent innate intracellular response and leads to IL-8 expression in epithelial cells. *J Immunol* **165**: 903-914.

Pieper, R., Fisher, C.R., Suh, M.J., Huang, S.T., Parmar, P., and Payne, S.M. (2013) Analysis of the proteome of intracellular *Shigella flexneri* reveals pathways important for intracellular growth. *Infect Immun* **81**: 4635-4648.

Podolsky, D.K., Fournier, D.A., and Lynch, K.E. (1986) Human colonic goblet cells. Demonstration of distinct subpopulations defined by mucin-specific monoclonal antibodies. *J Clin Invest* **77**: 1263-1271.

Pope, L.M., Reed, K.E., and Payne, S.M. (1995) Increased protein secretion and adherence to HeLa cells by *Shigella spp*. following growth in the presence of bile salts. *Infect Immun* **63**: 3642-3648.

Potten, C.S., and Loeffler, M. (1990) Stem cells: attributes, cycles, spirals, pitfalls and uncertainties. Lessons for and from the crypt. *Development* **110**: 1001-1020.

Prouty, A.M., Brodsky, I.E., Manos, J., Belas, R., Falkow, S., and Gunn, J.S. (2004) Transcriptional regulation of *Salmonella enterica* serovar Typhimurium genes by bile. *FEMS Immunol Med Microbiol* **41**: 177-185.

Prouty, A.M., and Gunn, J.S. (2000) *Salmonella enterica* serovar typhimurium invasion is repressed in the presence of bile. *Infect Immun* **68**: 6763-6769.

Purdy, G.E., Fisher, C.R., and Payne, S.M. (2007) IcsA surface presentation in *Shigella flexneri* requires the periplasmic chaperones DegP, Skp, and SurA. *J Bacteriol* **189**: 5566-5573.

Qiu, S., Xu, X., Yang, C., Wang, J., Liang, B., Li, P., Li, H., Yi, S., Liu, H., Cui, X., Wu, Z., Xie, J., Jia, L., Wang, L., Hao, R., Jin, H., Wang, Y., Sun, Y., and Song, H. (2015) Shift in serotype distribution of *Shigella* species in China, 2003-2013. *Clin Microbiol Infect* **21**: 252 e255-258.

Qu, M., Zhang, X., Liu, G., Huang, Y., Jia, L., Liang, W., Li, X., Wu, X., Li, J., Yan, H., Kan, B., and Wang, Q. (2014) An eight-year study of *Shigella* species in Beijing, China: serodiversity, virulence genes, and antimicrobial resistance. *J Infect Dev Ctries* **8**: 904-908.

Rabbani, G.H., Albert, M.J., Rahman, H., Islam, M., Mahalanabis, D., Kabir, I., Alam, K., and Ansaruzzaman, M. (1995) Development of an improved animal model of shigellosis in the adult rabbit by colonic infection with *Shigella flexneri* 2a. *Infect Immun* **63**: 4350-4357.

Ranganathan, S., Doucet, M., Grassel, C.L., Delaine-Elias, B., Zachos, N.C., and Barry, E.M. (2019) Evaluating *Shigella flexneri* pathogenesis in the human enteroid model. *Infect Immun* **87**: e00740-18.

Rasolofo-Razanamparany, V., Cassel-Beraud, A.M., Roux, J., Sansonetti, P.J., and Phalipon, A. (2001) Predominance of serotype-specific mucosal antibody response in

Shigella flexneri-infected humans living in an area of endemicity. *Infect Immun* **69**: 5230-5234.

Ridlon, J.M., Kang, D.J., and Hylemon, P.B. (2006) Bile salt biotransformations by human intestinal bacteria. *J Lipid Res* **47**: 241-259.

Roehrich, A.D., Guillossou, E., Blocker, A.J., and Martinez-Argudo, I. (2013) *Shigella* IpaD has a dual role: signal transduction from the type III secretion system needle tip and intracellular secretion regulation. *Mol Microbiol* **87**: 690-706.

Rose, L., Shivshankar, P., Hinojosa, E., Rodriguez, A., Sanchez, C.J., and Orihuela, C.J. (2008) Antibodies against PsrP, a novel *Streptococcus pneumoniae* adhesin, block adhesion and protect mice against pneumococcal challenge. *J Infect Dis* **198**: 375-383.

Rossi, R.M., Yum, L., Agaisse, H., and Payne, S.M. (2017) Cardiolipin synthesis and outer membrane localization are required for *Shigella flexneri* virulence. *MBio* **8**: e01199-17.

Rout, W.R., Formal, S.B., Giannella, R.A., and Dammin, G.J. (1975) Pathophysiology of *Shigella* diarrhea in the rhesus monkey: intestinal transport, morphological, and bacteriological studies. *Gastroenterology* **68**: 270-278.

Roy, A., Kucukural, A., and Zhang, Y. (2010) I-TASSER: a unified platform for automated protein structure and function prediction. *Nat Protoc* **5**: 725-738.

Sakaguchi, T., Kohler, H., Gu, X., McCormick, B.A., and Reinecker, H.C. (2002) *Shigella flexneri* regulates tight junction-associated proteins in human intestinal epithelial cells. *Cell Microbiol* **4**: 367-381.

Sambrook, J., and Russell, D.W. (2006) The inoue method for preparation and transformation of competent *E. Coli*: "ultra-competent" cells. *CSH Protoc* **2006**: prot3944

Sansonetti, P.J. (2001) Rupture, invasion and inflammatory destruction of the intestinal barrier by *Shigella*, making sense of prokaryote-eukaryote cross-talks. *FEMS Microbiol Rev* **25**: 3-14.

Sansonetti, P.J., Arondel, J., Cantey, J.R., Prevost, M.C., and Huerre, M. (1996) Infection of rabbit Peyer's patches by *Shigella flexneri*: effect of adhesive or invasive

bacterial phenotypes on follicle-associated epithelium. *Infect Immun* **64**: 2752-2764.

Sansonetti, P.J., Arondel, J., Fontaine, A., d'Hauteville, H., and Bernardini, M.L. (1991) OmpB (osmo-regulation) and icsA (cell-to-cell spread) mutants of *Shigella flexneri*: vaccine candidates and probes to study the pathogenesis of shigellosis. *Vaccine* **9**: 416-422.

Sansonetti, P.J., Arondel, J., Huerre, M., Harada, A., and Matsushima, K. (1999) Interleukin-8 controls bacterial transepithelial translocation at the cost of epithelial destruction in experimental shigellosis. *Infect Immun* **67**: 1471-1480.

Sansonetti, P.J., Hale, T.L., Dammin, G.J., Kapfer, C., Collins, H.H., Jr., and Formal, S.B. (1983) Alterations in the pathogenicity of *Escherichia coli* K-12 after transfer of plasmid and chromosomal genes from *Shigella flexneri*. *Infect Immun* **39**: 1392-1402.

Sansonetti, P.J., Phalipon, A., Arondel, J., Thirumalai, K., Banerjee, S., Akira, S., Takeda, K., and Zychlinsky, A. (2000) Caspase-1 activation of IL-1beta and IL-18 are essential for *Shigella flexneri*-induced inflammation. *Immunity* **12**: 581-590.

Santapaola, D., Del Chierico, F., Petrucca, A., Uzzau, S., Casalino, M., Colonna, B., Sessa, R., Berlutti, F., and Nicoletti, M. (2006) Apyrase, the product of the virulence plasmid-encoded phoN2 (apy) gene of *Shigella flexneri*, is necessary for proper unipolar IcsA localization and for efficient intercellular spread. *J Bacteriol* **188**: 1620-1627.

Schroeder, G.N., and Hilbi, H. (2008) Molecular pathogenesis of *Shigella spp.*: controlling host cell signaling, invasion, and death by type III secretion. *Clin Microbiol Rev* **21**: 134-156.

Schuhmacher, D.A., and Klose, K.E. (1999) Environmental signals modulate ToxT-dependent virulence factor expression in Vibrio cholerae. *J Bacteriol* **181**: 1508-1514.

Scribano, D., Damico, R., Ambrosi, C., Superti, F., Marazzato, M., Conte, M.P., Longhi, C., Palamara, A.T., Zagaglia, C., and Nicoletti, M. (2016) The *Shigella flexneri*

OmpA amino acid residues 188EVQ190 are essential for the interaction with the virulence factor PhoN2. *Biochem Biophys Rep* **8**: 168-173.

Scribano, D., Petrucca, A., Pompili, M., Ambrosi, C., Bruni, E., Zagaglia, C., Prosseda, G., Nencioni, L., Casalino, M., Polticelli, F., and Nicoletti, M. (2014) Polar localization of PhoN2, a periplasmic virulence-associated factor of *Shigella flexneri*, is required for proper IcsA exposition at the old bacterial pole. *PloS one* **9**: e90230.

Senerovic, L., Tsunoda, S.P., Goosmann, C., Brinkmann, V., Zychlinsky, A., Meissner, F., and Kolbe, M. (2012) Spontaneous formation of IpaB ion channels in host cell membranes reveals how *Shigella* induces pyroptosis in macrophages. *Cell Death Dis* **3**: e384.

Sereny, B. (1959) Acquired natural immunity following recovery from keratoconjunctivitis shigellosa. *J Hyg Epidemiol Microbiol Immunol* **3**: 292-305.

Seydel, K.B., Li, E., Swanson, P.E., and Stanley, S.L., Jr. (1997) Human intestinal epithelial cells produce proinflammatory cytokines in response to infection in a SCID mouse-human intestinal xenograft model of amebiasis. *Infect Immun* **65**: 1631-1639.

Shere, K.D., Sallustio, S., Manessis, A., D'Aversa, T.G., and Goldberg, M.B. (1997) Disruption of IcsP, the major *Shigella* protease that cleaves IcsA, accelerates actin-based motility. *Mol Microbiol* **25**: 451-462.

Shi, R., Yang, X., Chen, L., Chang, H.T., Liu, H.Y., Zhao, J., Wang, X.W., and Wang, C.Q. (2014) Pathogenicity of *Shigella* in chickens. *PloS one* **9**: e100264.

Shim, D.H., Suzuki, T., Chang, S.Y., Park, S.M., Sansonetti, P.J., Sasakawa, C., and Kweon, M.N. (2007) New animal model of shigellosis in the Guinea pig: its usefulness for protective efficacy studies. *J Immunol* **178**: 2476-2482.

Shin, K., Fogg, V.C., and Margolis, B. (2006) Tight junctions and cell polarity. *Annu Rev Cell Dev Biol* **22**: 207-235.

Shipley, S.T., Panda, A., Khan, A.Q., Kriel, E.H., Maciel, M., Jr., Livio, S., Nataro, J.P., Levine, M.M., Sztein, M.B., and DeTolla, L.J. (2010) A challenge model for *Shigella dysenteriae* 1 in cynomolgus monkeys (Macaca fascicularis). *Comp Med* **60**: 54-61.

Shutova, M.S., and Svitkina, T.M. (2018) Mammalian nonmuscle myosin II comes in three flavors. *Biochem Biophys Res Commun* **506**: 394-402.

Singer, M., and Sansonetti, P.J. (2004) IL-8 is a key chemokine regulating neutrophil recruitment in a new mouse model of *Shigella*-induced colitis. *J Immunol* **173**: 4197-4206.

Skoudy, A., Mounier, J., Aruffo, A., Ohayon, H., Gounon, P., Sansonetti, P., and Tran Van Nhieu, G. (2000) CD44 binds to the *Shigella* IpaB protein and participates in bacterial invasion of epithelial cells. *Cell Microbiol* **2**: 19-33.

Small, P., Blankenhorn, D., Welty, D., Zinser, E., and Slonczewski, J.L. (1994) Acid and base resistance in *Escherichia coli* and *Shigella flexneri* - role of Rpos and growth pH. *J Bacteriol* **176**: 1729-1737.

Speelman, P., Kabir, I., and Islam, M. (1984) Distribution and spread of colonic lesions in shigellosis: a colonoscopic study. *J Infect Dis* **150**: 899-903.

Sperandio, B., Fischer, N., Joncquel Chevalier-Curt, M., Rossez, Y., Roux, P., Robbe Masselot, C., and Sansonetti, P.J. (2013) Virulent *Shigella flexneri* affects secretion, expression, and glycosylation of gel-forming mucins in mucus-producing cells. *Infect Immun* **81**: 3632-3643.

Stensrud, K.F., Adam, P.R., La Mar, C.D., Olive, A.J., Lushington, G.H., Sudharsan, R., Shelton, N.L., Givens, R.S., Picking, W.L., and Picking, W.D. (2008) Deoxycholate interacts with IpaD of *Shigella flexneri* in inducing the recruitment of IpaB to the type III secretion apparatus needle tip. *J Biol Chem* **283**: 18646-18654.

Sudha, P.S., Devaraj, H., and Devaraj, N. (2001) Adherence of *Shigella dysenteriae* 1 to human colonic mucin. *Curr Microbiol* **42**: 381-387.

Sun, Y., Qi, Y., Liu, C., Gao, W., Chen, P., Fu, L., Peng, B., Wang, H., Jing, Z., Zhong, G., and Li, W. (2014) Nonmuscle myosin heavy chain IIA is a critical factor contributing to the efficiency of early infection of severe fever with thrombocytopenia syndrome virus. *J Virol* **88**: 237-248.

Suzuki, T., Miki, H., Takenawa, T., and Sasakawa, C. (1998) Neural Wiskott-Aldrich syndrome protein is implicated in the actin-based motility of *Shigella flexneri*. *EMBO J* **17**: 2767-2776.

Suzuki, T., Mimuro, H., Suetsugu, S., Miki, H., Takenawa, T., and Sasakawa, C. (2002) Neural Wiskott-Aldrich syndrome protein (N-WASP) is the specific ligand for *Shigella* VirG among the WASP family and determines the host cell type allowing actin-based spreading. *Cell Microbiol* **4**: 223-233.

Suzuki, T., and Sasakawa, C. (1998) N-WASP is an important protein for the actin-based motility of *Shigella flexneri* in the infected epithelial cells. *Jpn J Med Sci Biol* **51 Suppl**: S63-68.

Tahoun, A., Mahajan, S., Paxton, E., Malterer, G., Donaldson, D.S., Wang, D., Tan, A., Gillespie, T.L., O'Shea, M., Roe, A.J., Shaw, D.J., Gally, D.L., Lengeling, A., Mabbott, N.A., Haas, J., and Mahajan, A. (2012) *Salmonella* transforms follicle-associated epithelial cells into M cells to promote intestinal invasion. *Cell Host Microbe* **12**: 645-656.

Takeuchi, A. (1982) Early colonic lesions in experimental *Shigella* infection in rhesus monkeys: revisited. *Vet Pathol Suppl* **7**: 1-8.

Takeuchi, A., Formal, S.B., and Sprinz, H. (1968) Exerimental acute colitis in the Rhesus monkey following peroral infection with *Shigella flexneri*. An electron microscope study. *Am J Pathol* **52**: 503-529.

Takeuchi, A., Jervis, H.R., and Formal, S.B. (1975) Animal model of human disease. Bacillary dysentery, shigellosis, *Shigella dysentery*. Animal model: Monkey shigellosis or dysentery. *Am J Pathol* **81**: 251-254.

Tartoff, K.D., and Hobbs, C.A. (1987) Improved media for growing plasmid and cosmid clones. *Bethesda Research Laboratories Focus* **9**.

Teh, M.Y., and Morona, R. (2013) Identification of *Shigella flexneri* IcsA residues affecting interaction with N-WASP, and evidence for IcsA-IcsA co-operative interaction. *PloS one* **8**: e55152.

Teh, M.Y., Tran, E.N., and Morona, R. (2012) Absence of O antigen suppresses *Shigella flexneri* IcsA autochaperone region mutations. *Microbiology* **158**: 2835-2850.

Tiwari, V., Liu, J., Valyi-Nagy, T., and Shukla, D. (2011) Anti-heparan sulfate peptides that block herpes simplex virus infection *in vivo*. *J Biol Chem* **286**: 25406-25415.

Tran, E.N., Doyle, M.T., and Morona, R. (2013) LPS unmasking of *Shigella flexneri* reveals preferential localisation of tagged outer membrane protease IcsP to septa and new poles. *PloS one* **8**: e70508.

Tran, E.N.H., Attridge, S.R., Teh, M.Y., and Morona, R. (2015) *Shigella flexneri* cell-to-cell spread, and growth and inflammation in mice, is limited by the outer membrane protease IcsP. *FEMS Microbiol Lett* **362**: fnv088

Tran Van Nhieu, G.T., BenZeev, A., and Sansonetti, P.J. (1997) Modulation of bacterial entry into epithelial cells by association between vinculin and the *Shigella* IpaA invasin. *EMBO J* **16**: 2717-2729.

Trent, M.S., Stead, C.M., Tran, A.X., and Hankins, J.V. (2006) Diversity of endotoxin and its impact on pathogenesis. *J Endotoxin Res* **12**: 205-223.

Ud-Din, A., and Wahid, S. (2014) Relationship among *Shigella spp*. and enteroinvasive *Escherichia coli* (EIEC) and their differentiation. *Braz J Microbiol* **45**: 1131-1138.

Valencia-Gallardo, C., Bou-Nader, C., Aguilar-Salvador, D.I., Carayol, N., Quenech'Du, N., Pecqueur, L., Park, H., Fontecave, M., Izard, T., and Tran Van Nhieu, G. (2019) *Shigella* IpaA binding to Talin stimulates filopodial capture and cell adhesion. *Cell Rep* **26**: 921-932 e926.

Van den Beld, M.J., and Reubsaet, F.A. (2012) Differentiation between *Shigella*, enteroinvasive *Escherichia coli* (EIEC) and noninvasive *Escherichia coli*. *Eur J Clin Microbiol Infect Dis* **31**: 899-904.

Van Den Bosch, L., Manning, P.A., and Morona, R. (1997) Regulation of O-antigen chain length is required for *Shigella flexneri* virulence. *Mol Microbiol* **23**: 765-775.

Van den Bosch, L., and Morona, R. (2003) The actin-based motility defect of a *Shigella flexneri rmlD* rough LPS mutant is not due to loss of IcsA polarity. *Microb Pathog* **35**: 11-18.

VanDussen, K.L., Marinshaw, J.M., Shaikh, N., Miyoshi, H., Moon, C., Tarr, P.I., Ciorba, M.A., and Stappenbeck, T.S. (2015) Development of an enhanced human gastrointestinal epithelial culture system to facilitate patient-based assays. *Gut* **64**: 911-920.

Veenendaal, A.K., Hodgkinson, J.L., Schwarzer, L., Stabat, D., Zenk, S.F., and Blocker, A.J. (2007) The type III secretion system needle tip complex mediates host cell sensing and translocon insertion. *Mol microbiol* **63**: 1719-1730.

Voino-Yasenetsky, M.V., and Voino-Yasenetskaya, M.K. (1962) Experimental pneumonia caused by bacteria of the *Shigella* group. *Acta Morphol Acad Sci Hung* **11**: 439-454.

Wassef, J.S., Keren, D.F., and Mailloux, J.L. (1989) Role of M cells in initial antigen uptake and in ulcer formation in the rabbit intestinal loop model of shigellosis. *Infect Immun* **57**: 858-863.

Watarai, M., Funato, S., and Sasakawa, C. (1996) Interaction of Ipa proteins of *Shigella flexneri* with alpha5beta1 integrin promotes entry of the bacteria into mammalian cells. *J Exp Med* **183**: 991-999.

Waterman, S.R., and Small, P.L. (1996) Identification of sigma S-dependent genes associated with the stationary-phase acid-resistance phenotype of *Shigella flexneri*. *Mol Microbiol* **21**: 925-940.

Weinrauch, Y., Drujan, D., Shapiro, S.D., Weiss, J., and Zychlinsky, A. (2002) Neutrophil elastase targets virulence factors of enterobacteria. *Nature* **417**: 91-94.

Wells, C.L., van de Westerlo, E.M., Jechorek, R.P., Haines, H.M., and Erlandsen, S.L. (1998) Cytochalasin-induced actin disruption of polarized enterocytes can augment internalization of bacteria. *Infect Immun* **66**: 2410-2419.

Wells, J.M., and Spence, J.R. (2014) How to make an intestine. *Development* **141**: 752-760.

West, N.P., Sansonetti, P., Mounier, J., Exley, R.M., Parsot, C., Guadagnini, S., Prevost, M.C., Prochnicka-Chalufour, A., Delepierre, M., Tanguy, M., and Tang, C.M. (2005) Optimization of virulence functions through glucosylation of *Shigella* LPS. *Science* **307**: 1313-1317.

Wilson, S.S., Tocchi, A., Holly, M.K., Parks, W.C., and Smith, J.G. (2015) A small intestinal organoid model of non-invasive enteric pathogen-epithelial cell interactions. *Mucosal Immunol* **8**: 352-361.

Xu, D., Liao, C., Zhang, B., Tolbert, W.D., He, W., Dai, Z., Zhang, W., Yuan, W., Pazgier, M., Liu, J., Yu, J., Sansonetti, P.J., Bevins, C.L., Shao, Y., and Lu, W. (2018)

Human enteric alpha-Defensin 5 promotes *Shigella* infection by enhancing bacterial adhesion and invasion. *Immunity* **48**: 1233-1244 e1236.

Yang, G., Wang, L.G., Wang, Y., Li, P., Zhu, J.G., Qiu, S.F., Hao, R.Z., Wu, Z.H., Li, W.J., and Song, H.B. (2015) hfq regulates acid tolerance and virulence by responding to acid stress in *Shigella flexneri*. *Res Microbiol* **166**: 476-485.

Yang, J.Y., Lee, S.N., Chang, S.Y., Ko, H.J., Ryu, S., and Kweon, M.N. (2014) A mouse model of shigellosis by intraperitoneal infection. *J Infect Dis* **209**: 203-215.

Zhang, Y. (2008) I-TASSER server for protein 3D structure prediction. *BMC bioinformatics* **9**: 40.

Zhang, Y.G., Wu, S., Xia, Y., and Sun, J. (2014) *Salmonella*-infected crypt-derived intestinal organoid culture system for host-bacterial interactions. *Physiol Rep* **2**: e12147.

Zhang, Z., Jin, L., Champion, G., Seydel, K.B., and Stanley, S.L., Jr. (2001) *Shigella* infection in a SCID mouse-human intestinal xenograft model: role for neutrophils in containing bacterial dissemination in human intestine. *Infect Immun* **69**: 3240-3247.

Zhao, W.D., Liu, D.X., Wei, J.Y., Miao, Z.W., Zhang, K., Su, Z.K., Zhang, X.W., Li, Q., Fang, W.G., Qin, X.X., Shang, D.S., Li, B., Li, Q.C., Cao, L., Kim, K.S., and Chen, Y.H. (2018) Caspr1 is a host receptor for meningitis-causing *Escherichia coli*. *Nat Commun* **9**: 2296.

Zuo, G., Xu, Z., and Hao, B. (2013) *Shigella* strains are not clones of *Escherichia coli* but sister species in the genus *Escherichia*. *Genom Proteom Bioinf* **11**: 61-65.

Zychlinsky, A., Prevost, M.C., and Sansonetti, P.J. (1992) *Shigella flexneri* induces apoptosis in infected macrophages. *Nature* **358**: 167-169.

Zychlinsky, A., Thirumalai, K., Arondel, J., Cantey, J.R., Aliprantis, A.O., and Sansonetti, P.J. (1996) *In vivo* apoptosis in *Shigella flexneri* infections. *Infect Immun* **64**: 5357-5365.